Caractérisation des phases porteuses: Métaux particulaires en Seine

Cindy R. Priadi

THESE

Présentée pour obtenir le grade de

DOCTEUR de l'Université Paris Sud 11

Ecole Doctorale : Modélisation et Instrumentation en Physique, Energies, Géosciences et Environnement

Présentée et soutenue publiquement par

Cindy Rianti PRIADI

Le 8 décembre 2010

CARACTERISATION DES PHASES PORTEUSES :

METAUX PARTICULAIRES EN SEINE

Composition du jury :

M. Jean-François Gaillard	Rapporteur	Professeur, Northwestern University USA
M.Bruno Lartiges	Rapporteur	Professeur, Université Toulouse-III
Mme.Cécile Quantin	Examinateur	Professeur, Université Paris-Sud 11 Orsay
M.Jean-Marie Mouchel	Examinateur	Professeur, UPMC Paris
Mme. Sophie Ayrault	Co-directrice de thèse	Chercheur CEA, LSCE Gif sur Yvette
M. Philippe Bonté	Directeur de thèse	Chercheur CEA, LSCE Gif sur Yvette

Caractérisation des phases porteuses: Métaux particulaires en Seine

Dans les systèmes aquatiques, les métaux ont des affinités particulières pour la fraction solide. Cette dernière pourrait donc constituer un risque toxique potentiel vers les organismes vivants. Pour une gestion durable du bassin de la Seine, il est nécessaire de caractériser la phase porteuse particulaire de métaux afin de connaître sa géochimie, d'y identifier l'impact de l'urbanisation de la région parisienne et d'en déduire les sources des métaux et leur mobilité. Ce travail de thèse consiste à étudier les métaux particulièrement anthropiques dans la phase particulaire en Seine, en amont et aval de la région parisienne, et les facteurs contrôlant la variabilité temporelle et spatiale des caractéristiques des phases porteuses. Pour ce faire, les matières en suspension (MES) sont étudiées dans leur milieu dans la colonne d'eau et un zoom progressif est effectué sur ces MES jusqu'à étudier l'environnement moléculaire du métal. Alors que le plomb (Pb) a confirmé son affinité pour la phase particulaire et le Ni pour la phase dissoute, les autres métaux tels que le cobalt (Co), le chrome (Cr), le cuivre (Cu), le manganèse (Mn) et le zinc (Zn) semblent avoir une préférence partagée entre la phase solide et la phase dissoute. En aval de la région parisienne, la répartition solide/dissous de Co, Cu et Ni n'a pas seulement diminué, mais la variation temporelle de la répartition a également baissé, indiquant des formes d'association des métaux plus stables. Pour ce qui concerne Cd, Pb et Zn, c'est leur proportion associée à la fraction oxydable des MES, plus particulièrement aux oxydes de fer (Fe_xO_y), qui augmente après le passage de la Seine par la région parisienne. Une source identifiée de ces métaux associés à Fe_xO_y serait le sédiment de fond. Lors d'un épisode du déversement des eaux urbaines non traitées en période d'orage, le sédiment de fond est remis en suspension dans la colonne d'eau. Par un modèle de mélange, le sédiment de fond est estimé contribuer de 30-50% des métaux particulaires dans un panache de déversement, par rapport aux 10-30% des métaux provenant du déversement lui-même. Ensuite, le mélange de ce sédiment de fond avec les eaux d'assainissement pourrait apporter également des sulfures de Zn (ZnS). Ces sulfures ont une forme plutôt amorphe, en particules de quelques centaines de nm, isolées ou en grappes. Cette espèce réduite semble être stable car elle persiste dans la colonne d'eau bien que l'eau de la rivière soit considérée comme un milieu oxique.

Mots clé: répartition solide/solution, extraction séquentielle, urbanisation, mobilité, modèle de mélange, spéciation, rivière, EXAFS, MEB, ICP-MS

∴∴

Identification of particulate metal carriers in the Seine River

In freshwater systems, metals are known to have a particular affinity for the solid fraction. Consequently, the latter may constitute a potential toxic risk for aquatic organisms. Sustainable management in the Seine River Basin requires characterizing particulate carrier phase of metals in order to determine its geochemistry, identify urbanization impact of the Greater Paris Region and deduce the sources of metals and their mobility. To achieve these objectives, suspended particulate matter (SPM) was studied in relative to the water column and zoomed upon until the metal's molecular environment. In agreement to previous studies, lead (Pb) was associated mostly to the solid fraction while nickel (Ni) was found mostly in the dissolved phase. As for the rest of the metals such as cobalt (Co), chrome (Cr), copper (Cu), manganese (Mn) and zinc (Zn), there seems to be a shared preference for the solid and dissolved phase. Downstream Paris, not only did solid/solution partitioning of Co, Cu and Ni decrease, but also temporal variation of the partitioning during monthly observations, indicating more stable forms of carrier phases. As for cadmium (Cd), Pb and Zn, it was their oxidizable fraction in the SPM that increased downstream, particularly associated with iron oxides (FexOy). An identified source of these oxides would be the bed sediment. In the case of intense storm episode, the combined wastewater system would overload and a large volume of direct wastewater would overflow to the Seine River. Calculation using a mixing model suggested that bed sediment contributed from 30-50% of particulate metal found in the overflow plume. This is a relatively high contribution compared to the 10-30% of particulate metal which would originate from the overflow itself. Besides iron oxides, reduced environment in bed sediment and CSO would also contribute to ZnS found in the water column. These ZnS are identified as single or clustered amorphous nanoparticles. This species is rather stable as they are found to persist in oxic environment.

Keywords: Solid/solution partitioning, sequential extraction, urbanization, mobility, mixing model, river EXAFS, scanning electron microscopy, ICP-MS

Remerciements

Ce travail de thèse a été mené depuis Octobre 2007 jusqu'en Décembre 2010 au laboratoire des Sciences du Climat et de l'Environnement, Gif sur Yvette. Elle a été financée par le Programme Interdisciplinnaire de Recheche sur l'Environnment sur la Seine (PIREN Seine), projet Medisis d'EC2CO et le Ministère des Affaires Etrangères.

Cette thèse a été composée d'une multitude de travail analytique, de nombreuses discussions et réunions scientifiques et de plusieurs collaborations. Elle n'aurait jamais été aboutie sans le soutien de nombreuses personnes présentes pendant ces derniers 3 ans. Je tiens à remercier toutes ces personnes qui ont apporté leur pierre et contribuer à bâtir ce travail de leur propre façon.

Mes plus vifs remerciements vont à Dr. Sophie Ayrault (LSCE), co-directrice de thèse, pour simplement tout. Son soutien infini depuis le montage du projet de thèse et la recherche du financement jusqu'à la soutenance hivernale, sa constante disponibilité au long de ce travail, sa patience, ses conseils et ses stratégies face à des nombreuses défis rencontrés au cours de ces 3 derniers ans, de m'avoir fait la confiance et de m'avoir laissé la liberté, son rire et sa présence agréable. J'ai eu la grande chance d'apprendre non seulement les valeurs indispensables pour mener un travail de recherche, mais également la vraie définition de professionnalisme et engagement.

Je remercie également Philippe Bonté (LSCE), d'avoir accepté le rôle du directeur de thèse. Pour son accueil depuis mon arrivée, les nombreuses discussions et conseils, sa curiosité exemplaire, son soutien qui a été toujours puissant et sa présence chaleureuse qui savait très bien soutenir le moral.

Pour Jean-Marie Mouchel (UPMC/Sisyphe), pour son multitude de rôle, depuis professeur au Master SAGE, directeur du PIREN Seine de m'avoir fait la confiance et accorder le financement de ce travail, d'avoir monté et porté le projet Medisis, moteur et acteur (échantillonneur) principale des campagnes du temps de pluie. Ses idées et son intelligence remarquables et sa ténacité et rigeur pour la Seine et la science sont un exemple.

A Cecile Quantin (IDES Orsay), qu'elle accepte mes remerciements pour ses muliples conseils conceptuels et techniques d'un œil critique pendant le long de la thèse et d'avoir accepté le rôle d'examinateur et président du Jury.

Toute ma gratitude va également à Jean-François Gaillard et Bruno Lartiges, qui ont chaleureusement acceptés d'être rapporteurs de cette thèse. Pour leurs idées, commentaires et discussions scientifiques, d'avoir venu du loin et très loin pour juger ce travail.

Je voudrais remercier Guillaume Morin (IMPMC) qui a accepté de collaborer pour ce travail et de m'avoir accueilli dans son laboratoire, d'avoir partagé pédagogiquement ses connaissances, de m'avoir guidé soigneusement pour la réussite des manips, d'interpretation et de rédaction pour le travail EXAFS. Son extraordinaire passion pour la géochimie était un moteur important pendant la thèse.

Cette these a été également le fruit du travail de collaboration avec l'equipe HBAN du Cemagref Antony. Adeline Bourgeault, doctorante, qui a été mon tandem d'échantillonneur Medisis. Son bon humeur, son profesionalisme et son rigueur ont facilité le travail du 12 mois de terrain et tout le reste avant, après et dehors du terrain. A Catherine Gourlay et Marie-Hélène Tusseau-Vuillemin pour leurs conseils précis et précieux, leur regard critique et leur présence très agréable pendant les différentes réunions de travail. A Emmanuelle Uher,

Cécile Mirande-Bret et Aurélie Germain, je remercie également de nous avoir accompagné sur le terrain et d'avoir assuré les manips coté Cemagref.

A Stéphanie Pacini, ancienne stagiaire et CDD qui ont fortement contribué àu réussite du manip d'extraction et d'avoir su impliquer la discipline dans le travail de laboratoire pour son enthousiasme, je tiens à lui remercier.

A Eric Robin (LSCE), je voudrais remercier de m'avoir confié de travailler au MEB, pour son rigueur et sa définition d'une manip correcte, pour les discussion autour du microscope ou comité de pilotage. J'ai pris l'exemple de son enthousiasme qu'il a démonstré pour la micro-analyse.

Je remercie également Eric Douville (LSCE) pour ses conseils sur la bonne utilisation de l'ICP-MS et d'avoir dépanné dans plusieurs occasions afin que je réussisse mes manip. Merci beaucoup à Louise Bordier (LSCE) de m'avoir beaucoup aidé pour finaliser mes derniers manips et organiser les échantillons. Il est vraiment dommage que ton arrivée à l'ICP n'était pas deux ans plus tôt. A Eline Salle d'avoir très soigneusement coordiné les différents utilisateurs de l'ICP.

A toute l'équipe à l'IMPMC, à Georges Ona-Nguema pour ses conseils, sa pédagogié et sa patience sur la bonne pratique de boite à gants et d'avoir aide à passer de nombreuses échantillons à Stanford avec Fabien Maillot. A Farid Juillot pour ses differences spectres de reference d'espèce de Zn à l'EXAFS, à Feriel Skouri d'avoir organisé le calendrier de la boite à gants et son aide en plusieur recours, à Quentin Dermigny pour l'organisation de la DRX et à Agnès Elmaleh et Imene Esteve pour le MEB-FEG. Merci plus particulièrement à Rebecca Hochreutener pour son travail de stage au MEB, RPE et DRX sur les MES, d'avoir contribué à améliorer la connaissance sur la speciation de Zn en Seine.

Je remercie toute l'équipe de FAME à l'ESRF Grenoble de nous avoir chaleureusement accueilli pendant nos deux passages. Tout d'abord à Isabelle Llorens pour son guide, ses explications et son rigueur et son implication personnelle pour la réussite de notre première expérience d'EXAFS. Pour Jean-Louis Hazemann, directeur de la ligne FAME pour ses connaissances pendant la formation et la manip. Pour Denis Testemale de nous avoir guidé et accompagné pendant notre deuxième passage et également pour Olivier Proux.

Je remercie également à tous ceux qui ont aidé à faire avancer le manip EXAFS coté Stanford, surtout John Bargar, Joe Rogers et Samuel Webb. Ma gratitude va à Gordon E.Brown Jr pour ses commentaires pour le papier EXAFS.

Pour Nadine Tisterat-Laborde (LSCE) pour la discussion sur la décarbonatation, pour Caroline Gauthier et Christine Hatté (LSCE) pour l'analyse de carbon particulaire.

Je remercie l'équipe du Jardin Botanique de Marnay de nous avoir assuré l'accès sécurisé au lavoir pour l'échantillonnage, et le SIAAP pour l'accès au site de Bougival. Je remercie Vincent Rocher (SIAAP) et William Thomas (SNS) d'avoir fourni de nombreuses données physico-chimiques de la Seine.

Au laboratoire de CEREVE à Créteil, j'exprime mon gratitude à Gilles Varrault et Yoann Louis pour la collaboration pour le travail de collaboration et également à Benoit Pernet-Coudrier de nous avoir fourni nos premiers échantillons pour le projet ANR de Biomet. Je remercie également Daniel Thévenot pour ses conseils pendant le WWW-YES et ses commentaires pour le papier d'extraction séquentielle.

Je remercie à tous ceux qui ont contribué à la réussite de campagne de temps de pluie et qui a produit une énorme base de données, surtout Karim Bentayeb et l'équipe CEREVE pour leur échantillonneur automatique.

Merci à Fabrice Alliot et Marc Chevreuil à l'EPHE, Sisyphe, de nous avoir fourni des échantillons pour l'axe Seine.

Pour Christine Franke, ancien post-doctorante au LSCE, pour la collaboration au MEB, son aide pour la séparation par densité, et son très bon humeur. Je remercie également Christophe Colin (UPS11) de m'avoir assuré l'accès à la granulométrie à Orsay.

Je remercie toute l'équipe TCO au LSCE de m'avoir accueilli, Jean-Louis Reyys de m'avoir prété ses nombreuses matériels de terrain et de manip, au Christophe Rabouille comme ancien chef d'équipe pour ses conseils techniques et personnels pour la bonne gestion et réussite de la thèse. Pour Bruno Bombled et ses aides logistiques indispendables, Pour Irène Lefèvre d'avoir bien voulu répondre à mes questions administratives avec sa bonne humeur. Pour Matthieu Roy-Barman et ses conseils qui ne sont pas passés inaperçus, Pour Olivier Evrard et ses idées et sa présence agréable.

Cette thèse n'aurait jamais réussi sans le soutien administratif et souriant de Stéphanie Rébélo et Aline Marcinkowski et également assistance informatique de Virginie Metrot et Alain Jegou. A Xavier Quidelleur et Kim-Ngan Ho, je voudrais leur remercier pour la gestion de l'Ecole Doctorale. A Christine Hatté et Elsa Cortijo pour le comité des doctorants. A Rita Aloyol à l'Ambassade de l'Indonésie pour les différentes traductions et à Natalie Gauchy d'avoir assuré mon dossier BGF.

Je remercie Pierre Le-Pape, doctorante au LSCE, pour nos discussions scientifiques mais aussi personnelles et ses différentes questions sur les métaux en Seine qui m'ont fait toujours réfléchir, et surtout pour son aide précieuse pendant le manip de l'EXAFS à Grenoble.

Des soutiens morales m'ont également été indispensableq de la part de collègues au LSCE, des habitants de troisième avec qui j'ai partagé le bonheur de mes journées gifoiseq (et soirées), Les filles: Cécile Cathalot, Claire Treignier, Natalia Vazquez Riveros, Hélène Rebaubier et Eline Salle, à Camille Wandres et Aurélie Van Toer. Egalement François, Romain Coadic et Nicolas Smialkowski.

A ma colocatrice Faradita Safira et amis de l'Asociation des étudiants Indonésiens, surtout Ratna Indira, David Hidayat, Iwan Hermawan et Yuliana Sandy qui ont fait de mon séjour en France beaucoup plus agréable. Terima kasih banyak. A mes easyrideuses, Sandra Marchandise et Isabelle Bierwirth pour les nombreuses sorties et rires.

Je remercie mes amis au pays, et surtout ma profondz gratitude va à mes deux soeurs, Yufi et Deasy Priadi qui comprend très bien le sens du mot soutenir. Dernièrement, je remercie du fond du coeur à mes parents qui m'ont apporté de l'amour et soutien illimité pendant tout le long de ma these et ma vie. C'est grace à eux, qui m'ont toujours encouragé dans tout ce que j'ai fait, que je suis arrivée à ce point. Je leur dédie cette oeuvre en particulière.

Table des matières

Introduction Générale

Dans notre société actuelle, les métaux comme le cuivre (Cu),le nickel (Ni), le plomb (Pb), le zinc (Zn), sont omniprésents dans l'environnement. L'utilisation de ces métaux va des industries les plus variées à des sources liées aux transports, depuis la combustion des énergies fossilesjusqu'aux additifs dans différents produits de moteur et éléments de moteur et de carrosserie. Ils sont également utilisés dansl'agriculture,les matériaux de construction, jusqu'à nos vêtements et produits ménagers ainsi que dans de nombreux médicaments et cosmétiques qui contiennent aussi des métaux (Kevin et al., 2008; Luoma and Rainbow, 2008b; Thévenot et al., 2009; Thorpe and Harrison, 2008).

Alors que ces métaux sont d'origine naturelle, les utilisations anthropiques répandues de ces éléments non-dégradables ont comme conséquences l'accumulation de ces éléments dans certains compartiments de l'environnement. Ces métaux sont connus pour être toxiques au-delà d'un certain seuil de concentration (Förstner and Wittmann, 1983; Nriagu, 1988) ce qui explique le nombre important d'étudessur les métaux dans l'environnement (Chiffoleau et al., 1994; Dupré et al., 1996; Horowitz, 1991; Peltier et al., 2003; Thévenot et al., 2007). Plusieurs milieux sont considérés comme des endroits susceptibles à la perturbation par les contaminations métalliques. Parmi ces milieux, on trouve les rivières situées dans des bassins versants anthropiques. Les zones urbanisées en pays développés sont en grande partie couvertes par les surfaces imperméables des infrastructures urbaines. En conséquence, la plupart de métaux émis dans un bassin versant se trouveront ainsi transportés rapidement vers les fleuves par le ruissellement des pluies sur ces surfaces imperméables. Ces métaux sont pour certains essentiels pour les organismes biologiques à l'état de traces (c'est le cas du zinc) ettous deviennent toxiques au-delà d'une certaine concentration. Du fait de leur nature résistante et non-biodégradable, ils peuvent donc s'accumuler dans les différents

compartiments de l'environnement, dont les êtres vivants dans lesquels ils peuvent également se « magnifier », phénomènes appelés bioaccumulation et biomagnification, respectivement. De nombreuses études sont menées dans le but de mieux comprendre lecomportement de ces métaux dans l'environnement et d'en déduire leur mobilité et toxicité. Les métaux dont les concentrations sont le plus impactées par les activités humaines et en conséquence les plus étudiées sont l'arsenic (As), le cuivre (Cu), le cadmium (Cd), le chrome (Cr), le cobalt (Co), le mercure (Hg), le nickel (Ni), le plomb (Pb) et le zinc (Zn) (Houhou et al., 2009; Le Cloarec et al., In Press; Pernet-Coudrier et al., 2008; Weber et al., 2009). Il existe également des métaux dont l'utilisation a augmenté récemment. Il s'agit de l'antimoine (Sb), l'argent (Ag) et le thallium (Tl) (Blaser et al., 2008; Lanzano et al., 2006j; Rozan et al., 2000; Rubio and Lopez-Sanchez, 2007; Thorpe and Harrison, 2008).

Pour contraindre les dommages subis par l'écosystème, la Directive Cadre Européenne sur l'Eau (DCE) impose un « bon état écologique » pour tous les milieux aquatiques dans les pays membres en 2015. Evidemment, sur la liste des substances prioritaires présentant des risques significatifs, il y a parmi d'autres Ni et Pb. La concentration de ces substances est donc mesurée régulièrement pour identifier le niveau de contamination afin de s'assurer qu'ils ne posent pas de risques pour les êtres vivants.

Néanmoins, la mobilité des métaux dans le cours d'eau et l'accumulation des métaux chez les organismes aquatiques ne dépendent pas seulement de leur concentration totale dans l'eau. Dans un réseau fluvial, les métaux sont introduits dans le système sous plusieurs formes. Ils peuvent exister sous la forme d'ions libres, d'ions associés à des ligands organiques ou inorganiques adsorbés ou non sur une phase porteuse, ou sous la forme précipités ou cristallisés. La nature des associations des métaux avec de nombreux ligands dans la colonne d'eau, appelée la spéciation des métaux, a un rôle important pour évaluer les

risques que posent ces métaux. Alors que seules les concentrations des métaux dissous dans le milieu aquatique sont limitées par la DCE, la phase particulaire a un rôle important dans la géochimie des métaux dans la colonne d'eau. Du fait de la dynamique géochimique et des échanges entre phase dissoute et particulaire, cette dernière est à la fois une source et un puits des métaux pour la phase dissoute (Kalnejais et al.,2007). Selon la nature des liaisons, les métaux particulaires peuvent être plus ou moins mobiles vers la phase dissoute et/ou disponibles pour les êtres vivants. De plus, ces métaux particulaires posent également des risques directs via l'ingestion de particules contaminées par les organismes aquatiques filtreurs (Reeders et al., 1989).

Tous ces enjeux font de la caractérisation des phases porteuses particulaires des métaux dans le cours d'eau une étape indispensable dans l'étude de la contamination métallique. D'autant plus dans un bassin fortement anthropisé où le niveau important de métaux utilisés qui risquent de contaminer l'écosystème est confronté aux enjeux économiques et écologiques du bassin. La Seine, un cours d'eau situé dans le nord-ouest de la France, est un exemple intéressant de cette confrontation d'enjeux. Pour la France, elle est une rivière située dans un bassin sédimentaire traversant Paris et qui accueille 25% de son activité agricole, 30% de ses industrieset 23% de sa population (Thévenot et al., 2007). Des études précédentes ont démontré le niveau important des teneurs en métaux particulaires dans la rivière. Par exemple, pour un niveau de fond de 60 mg/kg en zinc (Thévenot et al., 2002), la teneur en zinc peut aller jusqu'à 1317 mg/kgdans le sédiment déposé lors de crues dans les palines d'inondation (Le Cloarec et al., In Press) et 575 mg/kg dans le sédiment issu de dragage (Meybeck et al., 2007a).De plus, des variations importantes des concentrations en métaux dissous dans la colonne d'eau sont observées, avec plusieurs hypothèses sur les facteurs explicatifs(Elbaz-Poulichet et al., 2006; Pepe et al., 2008; Tusseau-Vuillemin et al., 2007). Au cours de cette thèse, les phases porteuses de métaux particulaires dans la colonne

d'eau de la Seine ont été caractérisées avec pour objectifs de a) définir la spéciation des métaux dans la phase particulaire ; b) mieux comprendre les origines des métaux particulaires et les impacts de sources anthropiques sur la spéciation ; c) comprendre la contribution des métaux particulaires à la variation des concentrations en métaux dissous.

Il existe de nombreuses méthodes d'analyse des métaux dans la phase particulaire applicables pour la gamme de concentrations des métaux dans le bassin de la Seine. En général, les méthodes d'analyses sont divisées en deux grandes catégories. La première, qui est la plus répandue, regroupe les méthodes destructives qui consistent à attaquer la matière solide avec des réactifs adaptés au but de l'analyse. Les attaques peuvent être une attaque sélective de certaines fractions des constituants, une extraction séquentielle (des constituants les plus fragiles au plus réfractaires) ou une extraction totale. L'extrait est ensuite analysé à l'aide d'analyses de techniques généralement basées sur la spectrométrie et la phase porteuse est indirectement déduite des caractéristiques de la solution d'extraction. Une deuxième approche consiste à observer directement les phases porteuses dans leur état solide. Cette dernière approche s'est beaucoup développée ces dernières années grâce à des microscopes puissants à l'échelle micro/nanomètre, et également grâce à des analyses à base de rayonnement synchrotron permettant d'observer l'environnement atomique des éléments étudiés.

Au cours de cette thèse, les deux approches ont été appliquées aux échantillons afin d'arriver aux objectifs. Pendant la période octobre 2008- octobre 2009, des échantillons de matière en suspension ont été collectés chaque mois (pour les échantillonnages ponctuels) et au pas de temps mensuel (échantillonnage continu), sur trois sites différents pour avoir à la fois un site non-impacté par l'urbanisation et deux sites impactés par la région parisienne et d'autres sources significatives. Les impacts du temps de pluie et du déversement de réseau

unitaire dans la rivière ayant été mis en évidence dans plusieurs études antérieures (Estebe, 1998 ; Gromaire 1998 ; Even, 2004), un suivi supplémentaire a été fait au niveau du déversement d'eaux usées non traitées à l'occasion d'un orage d'été concentré sur Paris.

Le document qui suit est divisé en six chapitres. Une brève explication sur le contexte de l'étude et la présentation du site d'étude seront présentés dans le premier chapitre. Ce chapitre a pour but de donner les grandes lignes sur la conclusion de l'étude bibliographique effectuée pendant la thèse et non pas de décrire de façon exhaustive la géochimie des métaux dans les milieux aquatiques. Les détails sur les méthodes analytiques seront exposés en annexe afin d'obtenir une meilleure lisibilité. Les résultats obtenus pendant cette thèse sont présentés dans les chapitres suivants.La stratégie de l'échantillonnage mensuel sera présentée dans le chapitre II.Dans ce deuxième chapitre, nous parlerons également des résultats de l'analyse physico-chimique et l'analyse élémentaire des échantillons ponctuels divisés en phase dissoute (<0.45 mm) et particulaire (>0.45 mm). Par ailleurs, des données des échantillons intégratifs d'un mois ont été présentées. Il s'agit de la phase labile (mesurée par l'échantillonneur passif, DGT (diffusive gel in thin film)) et la phase particulaire (mesurée dans les matières en suspension collectées par trappe à sédiment). Ces données sont présentées en tant que la répartition ponctuelle et intégrative entre la phase particulaire et la phase dissoute ou labile et son évolution spatiale et temporelle. Dans ce chapitre, le rôle de la phase particulaire comme phase porteuse de métaux sera quantifié. De plus, une analyse méthodologique des données de Kd sera discutée dans le but de proposer une méthode alternative dans la surveillance à long terme de contamination métallique dans la colonne d'eau.

Une fois que le rôle de la phase particulaire dans la colonne d'eau sera quantifié, le troisième chapitre discutera de la répartition des métaux dans cette phase particulaire en

utilisant l'extraction séquentielle BCR. Cette méthode a été utilisée car elle donnera une vision globale de la mobilité et les grandes lignes des phases porteuses significatives des métaux. La méthode BCR est choisie car elle est une méthode certifiée et les données pourront être (plus ou moins) comparables avec d'autres études, même s'il y a des limitations, en fonction de caractéristique de l'échantillon étudié. L'évolution spatiale et temporelle de la répartition dans la phase solide seront également étudiées afin de comprendre la clé mécanisme de la dynamique et de comprendre l'impact de l'urbanisation de la région parisienne dans la répartition des métaux dans les différentes fractions.

Le chapitre suivant, le chapitre IV, fera un zoom particulier sur une période critique de la contamination métallique dans le bassin de la Seine. Il s'agit de l'événement du déversement du réseau unitaire d'eaux usées en Seine pendant le temps de pluie, plus précisément pendant l'étiage. Durant cet événement, des eaux usées sont déversées directement dans la Seine sans traitement car les volumes d'eaux usées dépassent les capacités de traitement et de stockage temporaire du réseau. Pendant l'étiage estival, ce déversement aura un impact significatif sur la Seine. Dans ce chapitre, en étudiant le panache de pollution du déversement du réseau, cela nous permettrait de confirmer la (les) source(s) significative(s) de métaux et de comprendre la dynamique du panache au cours de son avancement dans la Seine.

Dans les chapitres II à IV, l'importance de la contamination du Zn sera démontrée, confirmant également les résultats des études précédentes, cette fois-ci plus en détails. Le chapitre V décrira une étude plus approfondie de la phase porteuse de cet élément ubiquiste dans les MES en utilisant la méthode EXAFS. Cette méthode permettra d'étudier l'environnement moléculaire du Zn et de caractériser plus précisément la spéciation du Zn particulaire dans la Seine. Dans le cinquième chapitre, l'existence du sulfure de Zn, jusqu'ici

méconnu dans un milieu oxique, sera mis en évidence. Ce manuscrit sera terminé par la conclusion des cinq chapitres des résultats et également les perspectives concernant l'application de cette étude dans la gestion du bassin de la Seine et les voies potentielles pour la poursuite dans la recherche des métaux particulaire en Seine.

Les données acquises pendant la thèse ont été valorisées dans de nombreuses occasions. Le contenu du Chapitre III a fait l'objet d'un article publié dans « *International Journal of Environmental Science and Technology* ». Le contenu du Chapitre II fait l'objet d'un article en cours de révision pour le *Journal of Environmental Monitoring* et le chapitre IV représente un travail soumis à *Environmental Science and Technology*. D'autres données ont également été utilisées dans deux papiers dont je suis co-auteurs, l'un qui montre l'évolution des concentrations en argent (Ag) et en thallium (Tl) dans le bassin de la Seine de 1930 à 2004 (publié, Annexe 1) et l'autre qui porte sur le rôle de la phase particulaire dans l'accumulation des métaux dans les chaires de *Dressina polymorpha*en collaboration avec le Cemagref (soumis, Annexe 2). Par ailleurs, elles ont été également publiées régulièrement dans le rapport annuel du PIREN Seine et présentées dans plusieurs conférences de grands publics et/ou de publics spécifiques.

Chapitre I – Contexte

1 L'abondance des métaux en phase particulaire

Dans les systèmes aquatiques, les métaux sont présents sous plusieurs formes. Ils peuvent se retrouver dans la phase dissoute sous forme de cations hydratés ou complexés avec des nombreux ligands dissous. Ils peuvent également être dans la phase solide, adsorbés à la surface de particules, ou inclus dans la structure minéralogique de cristaux. Selon les métaux, ils ont plus ou moins une préférence pour une phase spécifique, dissoute ou particulaire. En général, la répartition des métaux entre la phase dissoute et particulaire peut être illustrée par deux valeurs générales, le pourcentage des métaux dans une phase relativement à la quantité totale des métaux présents ou également le ratio entre la concentration dans la phase particulaire et la concentration dans la phase dissoute, connu comme Kd[1]. Il existe relativement plus de données de répartition des métaux entre les deux phases pour les estuaires, les zones côtières et les océans que pour les eaux continentales (Tableau I. 1).

[1] Dans la colonne d'eau, les métaux se repartissent dans tout le continuum de taille de particules et la limite entre la phase dissoute et particulaire est imprécise à cause de la présence de la phase colloïdale qui se situe entre les deux. Pour des raisons pratiques, la limite entre phase dissoute et phase particulaire est opérationnellement définie à 0.22 ou 0.45 µm.

Tableau I. 1a. et I.1b . Quelques valeurs choisies pour représenter les répartitions de métaux dans la colonne d'eau définies par a) le rapport entre la concentration dans la phase particulaire (mg.kg^{-1}) et la concentration dans la phase dissoute (mg.L^{-1}) (Kd, en log L.kg^{-1}) dans plusieurs milieux aquatiques b) le rapport entre la concentration dans la phase particulaire normalisée par la concentration des MES et les métaux totaux dans la phase particulaire et dissoute (en %)

a)

	Cd	Co	Cu	Fe	Mn	Ni	Pb	Zn	Référence(s)
Rivières									
Variées à Auckland, Australie			4.1-6.2	5.2-7	3.6-5.1		5.6-7.3	3.9-6.1	(Bibby and Webster-Brown, 2005)
Humbert, Angleterre		3.6-5.7	3.4-5.5			3.4-5.5	4.5-6.3	3.3-5.7	(Lofts and Tipping, 2000)
Seine, France	3.8-5.4		3.9-5.1			3.6-4.7	4.8-6.0	3.9-5.0	(Tusseau-Vuillemin et al., 2005)
Autres									
L'estuaire de Seine, France	3.9-5.3	5	3.9-5			4.2-4.4	5.7-6.3	3.4-4.7	(Chiffoleau et al., 1994) (Cossa et al., 1994)
Lac Balaton, Hongrie	4.5-5.8	4.5-5.5	4.0-5.7			4.3-5.4	4.8-6.4	4.3-5.5	(Nguyen et al., 2005a)
Côtes et estuaires d'Australie du nord	3.3-6.3		3.7-5.4	5.7-8.8		3.8-5.3	5.5-7.2	4.4-6.7	(Munksgaard and Parry, 2001)

b)

	Cd	Co	Cu	Fe	Mn	Ni	Pb	Zn	Référence(s)
Rivières									
Amazon, Brésil			93	99.4	83				(Koch, 1985)
Etats-Unis			63	98			84	40	(Koch, 1985)
Allemagne	30		55	98	90		98	45	(Koch, 1985)
Autres									
L'estuaire de Seine, France	60	63	40		92	10	80	40	(Chiffoleau et al., 1994)
La Baie de Galvaston, Etats-Unis	24		8	90	59	5	83	44	(Tang et al., 2002)

Pour les métaux tels que le plomb (Pb), le fer (Fe) et le manganèse (Mn), il est évident qu'ils ont une affinité très importante envers la phase particulaire, montrée par leurs valeurs de Kd très élevées (Tableau I. 1a) et également un pourcentage élevé des métaux particulaires dans la colonne d'eau (Tableau I. 1b). Ensuite, viennent le cadmium(Cd) et le cuivre (Cu) qui ont des Kd et un pourcentage de métaux particulaires qui varient beaucoup selon le milieu. Le zinc (Zn) semble d'être en équilibre avec la phase dissoute et particulaire. Seul le nickel (Ni)

a une forte préférence pour la phase dissoute. Finalement, nous pouvons observer qu'une grande partie de la plupart des métaux est portée essentiellement par laphase particulaire.

Néanmoins, les métaux ne restent pas figés dans un compartiment dissous/particulaire. En effet, ils s'échangent entre les deux phases. Dans des conditions physico-chimiques favorables du milieu, les métaux dissous, ayant une affinité élevée pour les matières particulaires, peuvent interagir et seront donc piégés en phase particulaire. Cela diminue leur biodisponibilité, mais inversement, les métaux particulaires peuvent être relargués vers la phase dissoute, prenant une forme plus mobile. La mobilitédes métaux dans la colonne d'eau augmente le risque de disponibilité et toxicité de ces métaux pour les organismes vivants car le modèle des ions libres (FIAM) décrit depuis 1983 (Morel, 1983) explique que la biodisponibilité des métaux est en fonction de leur concentration ionique dans la colonne d'eau. Cependant, la relation entre la disponibilité et la toxicité des métaux est toujours à l'étude, car elles sont fonction de nombreux paramètres spécifiques à l'organisme et également fonction de la spéciation des métaux. Depuis, des études récentes ont montré que les métaux particulaires sont eux aussi une source des métaux pour les organismes aquatiques. Pour certains organismes filtrants, les métaux particulaires pourraient contribuer à la bioaccumulation dans les tissus(Reeders et al., 1989).

En conclusion, il est démontré que des études plus approfondies de la fraction particulaire comme de la phase porteuse de métaux sont alors indispensables pour mieux comprendre leur nature, leur mobilité vers la phase dissoute, leur capacité à porter les métaux et éventuellement la biodisponibilité dans différentes conditions physico-chimiques.

2 Les Métaux dans la phase Solide

Dans la section précédente nous avons montré que la phase particulaire est une fraction très significative dans l'étude de métaux en rivière. La dynamique d'échange entre la phase particulaire et la phase dissoute exige que cette phase fasse l'objet d'une étude détaillée. Pour la suite, nous allons discuter spécifiquement sur les métaux particulaires et la nature des liaisons entre les particules et les métaux.

2.1 Chimie aux interfaces : Propriétés des phases porteuses

La chimie à l'interface métal/particule prend en compte de nombreuses réactions illustrées sur la Figure I. 1. La sorption des métaux dépendra de trois grands paramètres, qui sont la nature des métaux étudiés, les caractéristiques de la surface des phases solides avec lesquels les métaux s'associent, et également les conditions physico-chimiques du milieu. En ce qui concerne la surface de la phase particulaire, la sorption des métaux peut avoir lieu sous deux formes, la première consiste en des liaisons électrostatiques sur la surface de la sphère externe de la particule (la couche de solvatation où l'eau reste intacte) et la deuxième est la formation des liaisons covalentes sur la surface de la sphère interne (la couche de solvatation disparait)(Sigg et al., 2006).

2.1.1 Les phases porteuses

La matrice de la phase particulaire peut consister en de nombreuses particules organiques et inorganiques. Ces particules proviennent de l'altération des roches ou du lessivage du sol (origine allochtone) et peuvent également se former dans les rivières (origine autochtone). Chaque phase particulaire a des propriétés différentes vis-à-vis des deux liaisons citées ci-dessus.

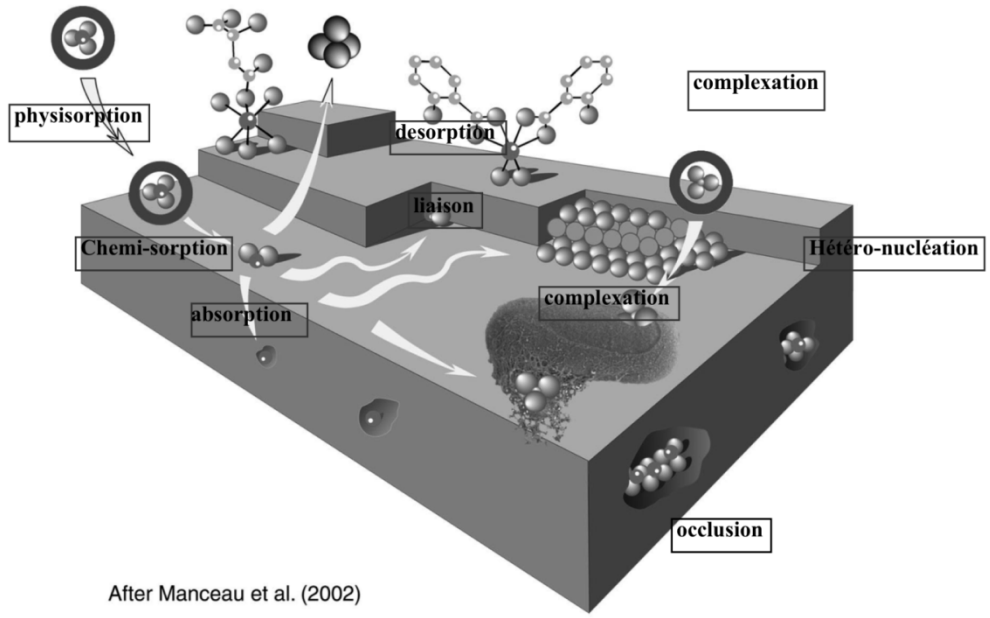

Figure I. 1 - Mécanismes de réaction entre une particule solide et métallique (http://www-lgit.obs.ujf-grenoble.fr/users/manceau/figures_bloc3D.html)

Les phases porteuses dans l'adsorption des métaux sur leurs surfaces sont les suivantes (Horowitz, 1991):

a) *Les argiles*, selon leurs définitions minéralogiques, proviennent de l'altération de la roche lors du lessivage du sol. Elles sont composées par des feuillets de couches Si-O (tétreaèdre) et Al-OH ou Mg-OH (octaèdre) qui se superposent. Les différents types d'argiles dépendent de la variation d'ordre des couches entre les couches tétraédrique et octaédrique. Des substitutions des cations peuvent également avoir lieu avec des nombreux éléments, y compris les métaux qui sont eux aussi des cations. De plus, les argiles ont une surface chargée et seront donc un « fournisseur » de surfaces pour l'adsorption, la co-précipitation et la floculation de matières organiques et minérales secondaires. Les liaisons électrostatiques sur la sphère externe de surface ainsi que les liaisons covalente et

électrostatique avec les complexes de la sphère interne peuvent se former entre les métaux et les particules argileuses.

b) *Les matières organiques*, qui sont des composés hydrocarbonés d'origine naturelle. Leur structure complexe contient des groupes fonctionnels tels que les groupes carboxyliques (C, O et H), des groupes phénoliques (O et H) et des groupes contentant N et S (Sigg et al.2006). Les métaux interagissent avec la matière organique en se complexant avec ces ligands.

c) *Les (hydro)-oxydes métalliques*, notamment de Fe,Mn et Al. Ils précipitent sous formes amorphes ou cristallisées comme des particules individuelles, des colloïdes ou comme une couche sur les surfaces d'autres particules. Ces phases sont des porteuses importantes pour les métaux par les actions des micronodules (Horowitz, 1991).

d) *Sulfures*, les métaux sont souvent associés à des précipités de sulfures (Huerta-Diaz et al., 1998). Quelques métaux comme le nickel et le cobalt pourraient être incorporés dans les pyrites, tandis que d'autres métaux comme Zn, Pb, et Cd se substitueraient au fer, qui donne une forme plus stable de sulfure de métaux (Hochella et White, 1990)

e) *Carbonates*, notamment le carbonate de calcium (calcite) qui est le plus abondant dans le milieu aquatique. Les métaux peuvent se complexer sur la surface de la calcite et éventuellement co-précipiter dans la structure minéralogique (Elzinga et al., 2006)

Il existe d'autres phases dans la matrice particulaire, notamment des particules de silices (souvent des quartz) et des aluminosilicates non-argileux, principalement du feldspath et de l'albite. Néanmoins, ces matrices particulaires ne sont pas significatives comme phases

porteuses (Horowitz, 1991). Ils peuvent être une phase sur lesquelles des dépôts de surface se forment et avec lesquels les métaux vont ensuite s'associer (Ayrault et al., 2008).

L'interaction entre les ligands dissous et les phases porteuses citées ci-dessus dépend de la nature des phases porteuses. Quelques paramètres clés qui contrôlent la capacité de sorption des phases porteuses sont : la capacité d'échange cationique (CEC), la surface de phase, et la charge de la surface en fonction de pH.

2.2 Précipitation et dissolution

L'alternance précipitation/dissolution de la phase solide dans la colonne d'eau est la réaction clé qui contrôle la composition chimique d'un système aquatique. Cela correspond à une réaction acido-basique impliquant les roches du bassin versant. Ces réactions contrôlent également les ions et les minéraux anthropiques qui entrent dans le système. Ils trouveront leur équilibre en fonction de leur solubilité dans la colonne d'eau, la concentration présente et les conditions physico-chimiques du milieu, notamment le pH.

2.3 Réaction d'oxydo-réduction

Une évolution des conditions oxydo-réductrices dans la colonne d'eau peut être le résultat de nombreux phénomènes naturels (volcans, photosynthèse) et également des activités anthropiques (eutrophisation, pluie acide). Elles impliquent notamment les éléments biogènes tels que C, N, H, S, Fe et Mn et également des métaux. Les conditions redox peuvent alors jouer sur la spéciation de certaines phases porteuses telles que les oxydes de fer et de manganèse et également la spéciation et la toxicité éventuelle de certains métaux tels que Cu et Se.

3 Méthodes analytiques des phases porteuses

Nous avons vu dans la section précédente qu'il existe de nombreuses formes et associations des métaux dans la phase particulaire. Du fait de la multiplicité des formes des phases porteuses particulaires de métaux dans la colonne d'eau, il existe plusieurs méthodes de caractérisation. Dans les grandes lignes, les méthodes de caractérisation sont divisées en deux catégories, les méthodes destructives et les méthodes directes.

3.1 Méthodes destructives

Ces méthodes consistent à attaquer la matrice solide par des réactifs choisis pour leur capacité à dissoudre une partie ou la totalité des particules et à transférer la matrice et les métaux de la phase solide vers la phase dissoute. La digestion de la matrice solide peut être totale ou sélective, visant alors une fraction spécifique de la matrice solide. Les solutions utilisées dans la digestion sélective sont alors adaptées aux natures des phases porteuses attaquées. Il peut y avoir plusieurs étapes d'extraction sélective successives sur le même prélèvement, on parlera alors d'extraction séquentielle. Des fractions de métaux sont définies selon leurs solubilités face à certains réactants chimiques. Les métaux dans la phase dissoute sont ensuite plus facilement à analyser par des méthodes classiques telles que l'ICP-MS ou l'ICP-AES.

3.2 Méthodes directes

Ces méthodes sont basées sur des principes physiques d'analyse afin de faire des images de particules ou de conditionner les matrices solides avec des ondes spécifiques selon le besoin analytique. Les différentes interactions électron-matière (diffusion, absorption, transmission,…) sont utilisées dans le but d'identifier directement les formes de particules ou d'obtenir des spectres qui donneront des caractéristiques de la matière et l'association entre les phases porteuses et les métaux. De nombreuses méthodes courantes sont bien expliquées

dans laFigure I. 2. D'une très grande efficacité dans l'identification des phases porteuses, les méthodes directes sont, pour certaines, disponibles uniquement dans des très grandes installations internationales, ce qui limite leur accessibilité.

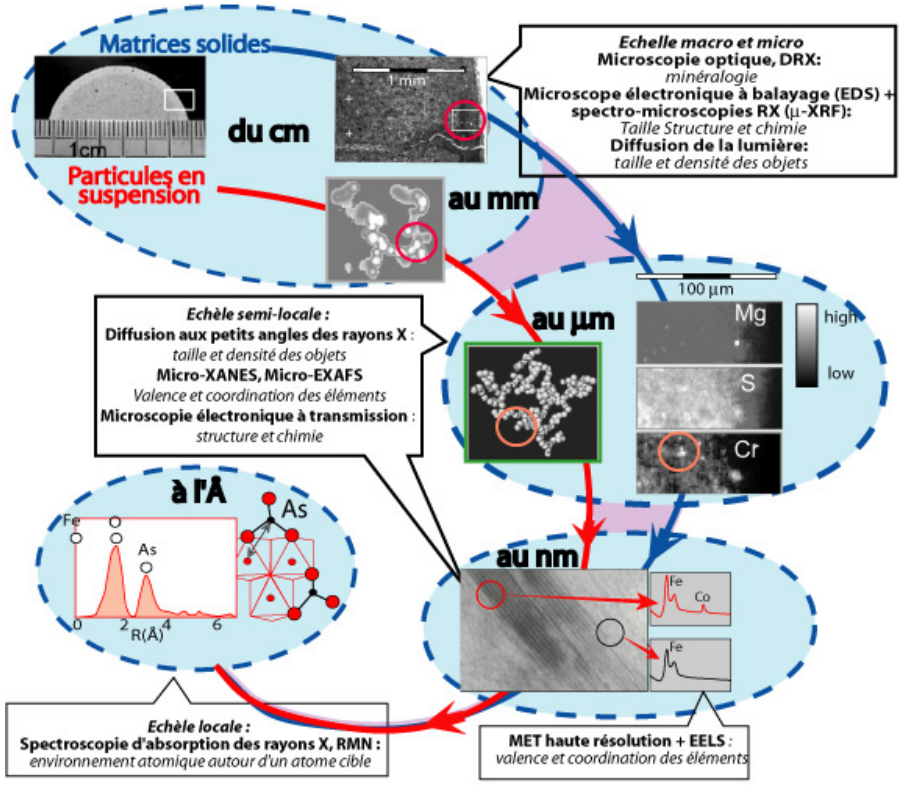

Figure I. 2 - Caractérisation multi-échelles : différentes techniques utilisées (http://www.cerege.fr)

En utilisant les deux types de caractérisations directes et indirectes, il est possible de caractériser l'association entre les métaux et leurs phases particulaires. De nombreuses phases porteuses de métaux dans la phase solide ont été bien identifiées pendant les dernières décennies grâce au développement de méthodes plus pointues dans le domaine de caractérisation des métaux dans les milieux aquatiques. Le Tableau I. 1 donne une illustration non-exhaustive de différentes phases porteuses caractérisées dans les milieux aquatiques.Des résultats préliminaires de caractérisation des phases porteuses en Seine (Priadi and Ayrault,

2007b) ont montré des pistes potentielles pour une étude plus approfondie. En utilisant le MEB-EDS couplé à un système de reconnaissance automatique de particule, certaines phases porteuses de métaux dans le sédiment de fond de la Seine ont pu être identifiées. Le plomb et le nickel sont trouvés préférablement associés aux sulfures de fer. Le quartz et la calcite avec le vanadium, zinc et cuivre. Le zinc se trouve également avec la barytine. Ces particules de barytine seraient issues des freins automobiles (où la barytine entre dans le mélange ayant remplacé l'amiante bannie en 2000) et de la peinture de chaussées (El Samrani et al, 2004). On note également une association particulière entre le vanadium et le calcium. En effet, le vanadium est utilisé dans la production d'acier, le résidu dans une forme de scorie est réutilisé pour les chaussées (Chaurand et al, 2007). Les produits pétroliers contiennent beaucoup de vanadium (essence, asphalte). L'abondance du vanadium avec cette phase porteuse « calcite » indiquerait l'impact du ruissellement sur les surfaces routières sur la rivière.

Tableau I. 2–Phases porteuses particulaires de métaux dans de nombreux milieux anthropiques analysées avec au moins une méthode directe. DRX = Diffraction en Rayon X, SEM-EDS = Microscopie en Balayage couplée à un spectrométrie d'énergie dispersée, EMPA = Analyse microprobe aux électrons, EXAFS = Extended X-ray Absorption Fine Structure, μSXRF = Spectroscopy fluorescence au rayon-X doux

	Activité		Métaux	Méthodes analytiques		Phases porteuses	Référence(s)
Site	minier	urbain		directe	indirecte		
Rivières							
Le Lot, France	x		Cd, Cu, Pb, Zn	DRX, MEB-EDS, EMPA	redox, extraction sélective	spinelles, silicates, sulfates Aval : sulfures,spinelles	(Audry et al.)
La Tyne, Angleterre	x		Cd, Cu, Pb, Zn	MEB-EDX		sulfures, silicate, phosphate, sulfate Aval : carbonate, iron and manganese oxyhydroxides	(Hudson-Edwards et al., 1996)
L'Isle, France	x		As	DRX, MEB-EDS, Mossbaüer	extraction sélective	sulfures détritique, Fe-Mn oxyhydroxydes secondaires, Al-Si	(Grosbois et al., 2007)
Autres							
Sol, Lille, France	x		Zn	EXAFS, □SXRF, DRX	extraction sélective	Zn complexe sphère externe, Zn-MO complexe sphère interne, Zn/Al hydrotalcite, phyllosilicate, magnetite-franklinite	(Juillot et al., 2003)
Décharge, Dolni Chabry, Rep Tcheque		x	Cd, Cu, Ni, Pb, Zn	MEB-EDS, DRX	extraction séquentielle, voltammetrie	calcite (co-precipitation), goethite (Pb, Zn, Cu, Ni), matière organique (Cu)	(Ettler et al., 2006)
Réseau d'assainisMEBent, Nancy, France		x	Cd, Cu, Cr, Ni, Pb, Zn	TEM-EDX, MEB-EDS, DRX		Alliages, morceau de métaux (oxydé ou non-oxydé), sulfures	(El Samrani et al., 2004) (Houhou et al., 2009)
Zones Humides, Chicago, Etats-Unis		x	Zn	XAS		sulfures	(Peltier et al., 2003)
Bassin d'infitration, Nantes, France		x	Cd, Cu, Cr, Ni, Pb, Zn	MEB-EDS, DRX	extraction séquentielle	Alliages, sphérules de fer, verres	(Clozel et al., 2006)

4 Stratégie du suivi du milieu

La Seine est située dans un bassin sédimentaire principalement constitué de calcaire (Figure I. 3). Elle est caractérisée par son taux important de nutriment et une teneur en métaux élevée sur les MES et le sédiment de fond (Grosbois et al., 2006). Alors que l'apport naturel de métaux est très limité à cause de la nature sédimentaire de ce bassin, les apports anthropiques de métaux dans la Seine sont élevés(Meybeck et al., 2007a).

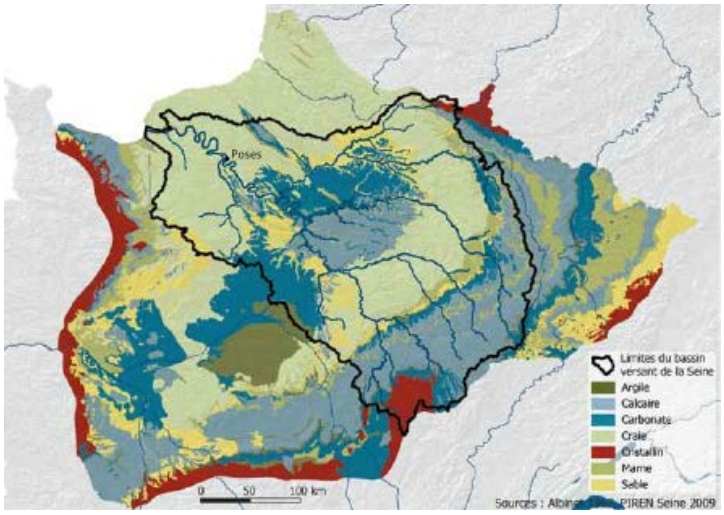

Figure I. 3- Carte lithologique du bassin versant de la Seine (Albinet 1962 de Piren Seine, 2009)

Les apports de métaux viennent en grande partie du ruissellement sur une surface de 78 600 km^2(à l'estuaire) occupée par 16 millions habitants, et également des dépôts atmosphériques urbains et industriels estimées à au moins 30% de la valeur nationale (Thévenot et al., 2007). Cette thèse sera menée dans le bassin de la Seine dans le cadre du Projet Interdisciplinaire de Recherche sur l'Environnement PIREN Seine. Elle fait également partie du projet EC2CO MEDISIS (2007-2010). Le projet MEDISIS a pour objectif de mieux comprendre les mécanismes de variabilité des concentrations des métaux dans la phase dissoute. Ce projet regroupe plusieurs équipes étudiant non seulement la phase dissoute, mais également la phase particulaire (décrite dans cette thèse), et des bioaccumulations sur les

chaires de moules zébrées, et sur les coquilles d'anodontes implantées sur les sites d'étude. Cette thèse est une pièce importante de l'ensemble car en comprenant mieux les associations des métaux sur la phase particulaire, nous pourrons mieux interpréter les fluctuations des métaux dissous dans la Seine, donner des clés de compréhension de la bioaccumulation des métaux par voie trophique dans les organismes modèles, et enfin mieux évaluer les précautions nécessaires à prendre pour la Seine en accord avec la Directive Cadre de l'Eau (DCE).

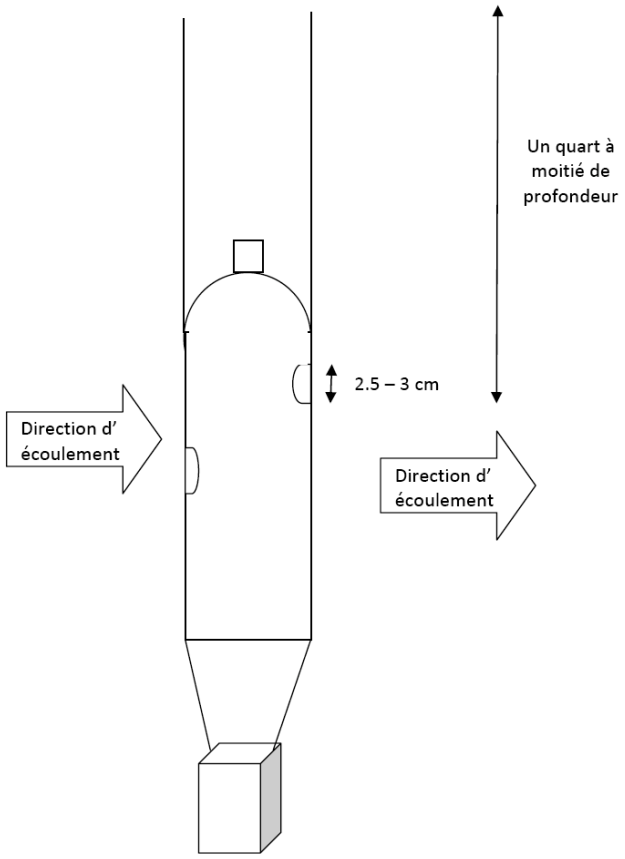

Figure I. 4 Le schéma du trappe à sédiment, à base d'une bouteille PET ayant contenu de l'eau gazeuse du commerce d'une capacité d'un litre, utilisée dans l'étude

La stratégie de suivi dans cette thèse est basée sur des études précédentes sur la variation spatiale et temporelle des concentrations des métaux dans le bassin. Le suivi est fait

pendant une année hydrologique pour pouvoir enregistrer la variation temporelle et également sur trois sites pour étudier la variation spatiale de métaux en Seine. Des échantillonnages mensuels seront faits de façon ponctuelle par filtration de MES et également intégrée par trappes à sédiments (figure 1.4).Les sites d'étude sont situés à trois niveaux de la Seine (Figure I. 5). On étudiera d'abord la Seine en amont avant l'influence de Paris pour connaître son « niveau de fond ». L'échantillonnage se fera au niveau de Marnay-sur-Seine sur un site sécurisé grâce au Jardin Botanique de la commune.

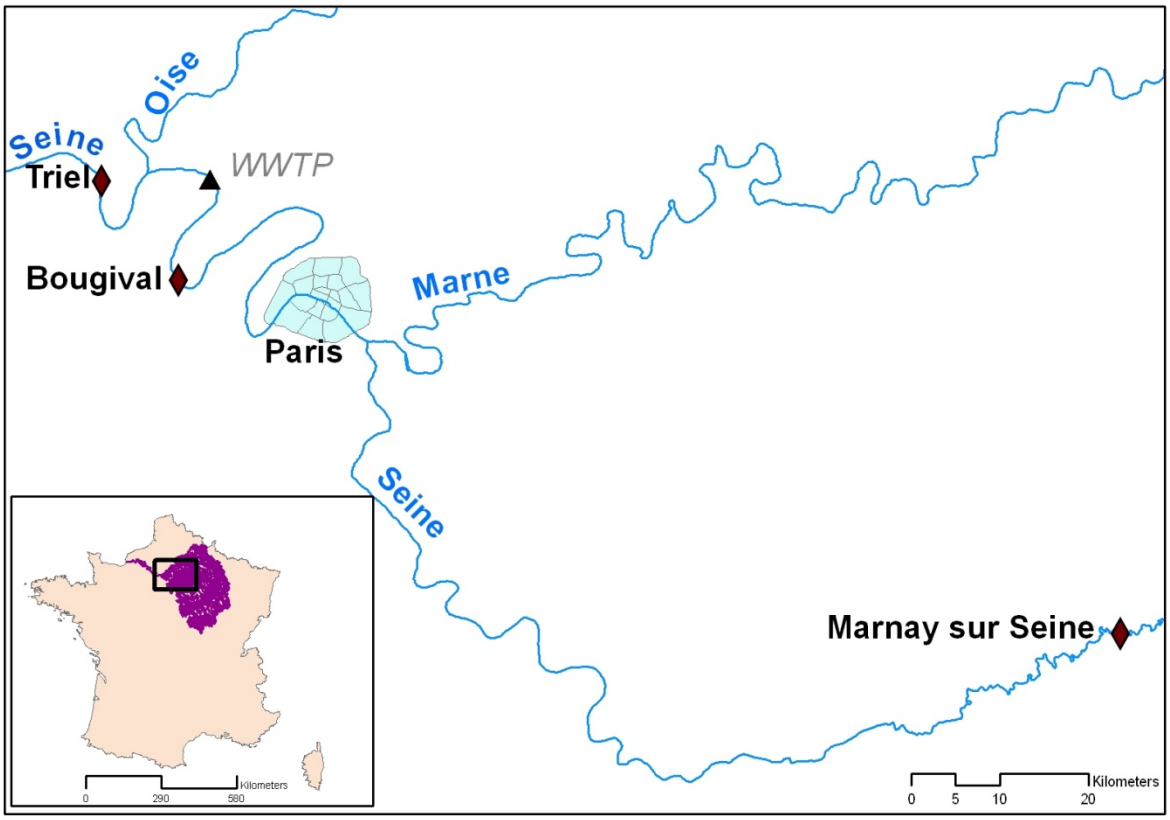

Figure I. 5- Les sites d'étude marqués par les diamants comprenant Marnay sur Seine en amont de la région parisienne, Bougival situé en aval de Paris et Triel situé en aval de Paris et de la station d'épuration des eaux useés (STEP) Seine-Aval, marquée avec le triangle.

Ensuite, on étudiera également la Seine à la sortie de Paris avant (Bougival, site sécurisé du SIAAP[2]) et après (Triel-sur-Seine) la station d'épuration des eaux usées (STEP)

[2] Syndicat Interdépartemental d'Assainissement de l'Agglomération Parisienne (SIAAP) http://www.siaap.fr/le-siaap/missions-du-siaap/presentation/

Seine-Aval gérée par le SIAAP.La STEP Seine-Aval à Achères, traitant les effluents de 6,5 millions de Franciliens, rejette en moyenne 25 $m^3.s^{-1}$d'eau traitée, soit le quart du débit de la Seine à l'étiage après soutien par la vidange des barrages réservoirs. Selon (Thévenot et al., 2007), il faudrait des efficacités d'abattement des métaux de bien plus de 99% pour que cet impact soit négligeable. Les effluents traités pourraient donc être une autre source de métaux. Les rejets en métaux dissous et labiles de la STEP ont été évalués par Tusseau-Vuillemin et al., (2005) et Buzier et al., (2006). Les matières organiques qui sortent depuis la STEP d'Achères ont une forte capacité à retenir les métaux dissous par complexation (Pernet-Coudrier et al., 2008).

En plus du cycle hydrologique annuel typique d'un bassin versant, des événements particuliers sont connus pour bouleverser la spéciation et la répartition des métaux dans la colonne d'eau. Les phénomènes significatifs caractérisés dans des études précédentes sont en général divisés en deux catégories: (1) des phénomènes biologiques, notamment le bloom planctonique, et (2) des phénomènes hydrologiques liés notamment à une augmentation soudaine d'apport d'eaux urbaines par le temps de pluie. Nous avons vu que pour caractériser des phases porteuses de métaux et étudier leur variabilité, il fallait entreprendre une étude globale des différents compartiments de la colonne d'eau. Nous avons donc mis en place une étude de terrain permettant d'acquérir un grand nombre de données physico-chimiques en trois sites de la Seine. Ces résultats sont présentés dans le chapitre II. Les matériels et méthodes utilisés pendant la campagne mensuelle d'échantillonnage sont expliqués brièvement dans le deuxième chapitre. Les données physico-chimiques dans la colonne d'eau pendant la campagne d'échantillonnage ainsi que les mesures chimiques « bulk » des métaux dans les phases dissoute, labile et particulaire sont caractérisées. Les résultats présentés dans ce deuxième chapitre se concentrent sur la répartition et le rôle de la phase particulaire dans la colonne d'eau, relativement aux phases dissoute et labile.

Bibliographie

Audry S, Grosbois C, Bril H, Schäfer J, Kierczak J, Blanc G. Post-depositional redistribution of trace metals in reservoir sediments of a mining/smelting-impacted watershed (the Lot River, SW France). Applied Geochemistry; 25: 778-794.

Ayrault S, Priadi C, Robin E, Bonté P. Méthodologie de caractérisation des phases particulaires porteuses de métaux en Seine et résultats préliminaires. PIREN Seine, Paris, 2008, pp. 17.

Bibby RL, Webster-Brown JG. Characterisation of urban catchment suspended particulate matter (Auckland region, New Zealand); a comparison with non-urban SPM. Science of The Total Environment 2005; 343: 177-197.

Blaser SA, Scheringer M, MacLeod M, Hungerbühler K. Estimation of cumulative aquatic exposure and risk due to silver: Contribution of nano-functionalized plastics and textiles. Science of The Total Environment 2008; 390: 396-409.

Buzier R, Tusseau-Vuillemin M-H, dit Meriadec CM, Rousselot O, Mouchel J-M. Trace metal speciation and fluxes within a major French wastewater treatment plant: Impact of the successive treatments stages. Chemosphere 2006; 65: 2419-2426.

Chiffoleau J-F, Cossa D, Auger D, Truquet I. Trace metal distribution, partition and fluxes in the Seine estuary (France) in low discharge regime. Marine Chemistry 1994; 47: 145-158.

Clozel B, Ruban V, Durand C, Conil P. Origin and mobility of heavy metals in contaminated sediments from retention and infiltration ponds. Applied Geochemistry 2006; 21: 1781-1798.

Cossa D, Meybeck M, Idlafkih Z, Bombled B. Etude pilote des apports en Contaminants par la Seine. In: Ifremer, editor. IFREMER, Nantes, 1994, pp. 154.

Dupré B, Gaillardet J, Rousseau D, Allègre CJ. Major and trace elements of river-borne material: The Congo Basin. Geochimica et Cosmochimica Acta 1996; 60: 1301-1321.

El Samrani AG, Lartiges BS, Ghanbaja J, Yvon J, Kohler A. Trace element carriers in combined sewer during dry and wet weather: an electron microscope investigation. Water Research 2004; 38: 2063-2076.

Elbaz-Poulichet F, Seidel J-L, Casiot C, Tusseau-Vuillemin M-H. Short-term variability of dissolved trace element concentrations in the Marne and Seine Rivers near Paris. Science of The Total Environment 2006; 367: 278-287.

Elzinga EJ, Rouff AA, Reeder RJ. The long-term fate of Cu2+, Zn2+, and Pb2+ adsorption complexes at the calcite surface: An X-ray absorption spectroscopy study. Geochimica et Cosmochimica Acta 2006; 70: 2715-2725.

Ettler Vc, Matura M, MihaljeviÄ M, BezdiÄka P. Metal speciation and attenuation in stream waters and sediments contaminated by landfill leachate. Environmental Geology 2006; 49: 610-619.

Förstner U, Wittmann GTW. Metal pollution in the aquatic environment. Folia Geobotanica 1983; 18: 194-194.

Grosbois C, Courtin-Nomade A, Martin F, Bril H. Transportation and evolution of trace element bearing phases in stream sediments in a mining - Influenced basin (Upper Isle River, France). Applied Geochemistry 2007; 22: 2362-2374.

Hochella, M. F., and A. F. White. Mineral-water interface geochemistry - an overview .Rev. Miner.1990;23: 1-16.

Horowitz AJ. A Primer on Sediment-trace Element Chemistry. MI., USA: Lewis Publishers, 1991.

Houhou J, Lartiges BS, Montarges-Pelletier E, Sieliechi J, Ghanbaja J, Kohler A. Sources, nature, and fate of heavy metal-bearing particles in the sewer system. Science of The Total Environment 2009; In Press, Corrected Proof.

Hudson-Edwards KA, Macklin MG, Curtis CD, Vaughan DJ. Processes of Formation and Distribution of Pb-, Zn-, Cd-, and Cu-Bearing Minerals in the Tyne Basin, Northeast England: Implications for Metal-Contaminated River Systems. Environ. Sci. Technol. 1996; 30: 72-80.

Huerta-Diaz MA, Tessier A, Carignan R. Geochemistry of trace metals associated with reduced sulfur in freshwater sediments. Applied Geochemistry 1998; 13: 213-233.

Juillot F, Morin G, Ildefonse P, Trainor TP, Benedetti M, Galoisy L, et al. Occurrence of Zn/Al hydrotalcite in smelter-impacted soils from northern France: Evidence from EXAFS spectroscopy and chemical extractions. American Mineralogist 2003; 88: 509-526.

Kalnejais LH, Martin WR, Bothner MH. The release of dissolved nutrients and metals from coastal sediments due to resuspension. Marine Chemistry 2007; In Press, Accepted Manuscript.

Kevin GT, Philip NO, Ramon JB, Celso G, Dr. Philip NO. Sediment and contaminant sources and transfers in river basins. Sustainable Management of Sediment Resources. Volume 4. Elsevier, 2008, pp. 83-135.

Koch R. W. Salomons and U. Förstner: Metals in the Hydrocycle. Berlin — Heidelberg — New York — Tokyo: Springer Verlag, 1984, 349 S., 149 Abb., DM 98.—. Acta hydrochimica et hydrobiologica 1985; 13: 267-267.

Lanzano T, Bertram M, De Palo M, Wagner C, Zyla K, Graedel TE. The contemporary European silver cycle. Resources, Conservation and Recycling 2006; 46: 27-43.

Le Cloarec MF, Bonte PH, Lestel L, Lefèvre I, Ayrault S. Sedimentary record of metal contamination in the Seine River during the last century. Physics and Chemistry of the Earth, Parts A/B/C In Press; In Press.

Lofts S, Tipping E. Solid-solution metal partitioning in the Humber rivers: application of WHAM and SCAMP. The Science of The Total Environment 2000; 251-252: 381-399.

Luoma SN, Rainbow PS. Metal Contamination in Aquatic Environments. Cambridge: Cambridge University Press, 2008.

Meybeck M, Lestel L, Bonte P, Moilleron R, Colin JL, Rousselot O, et al. Historical perspective of heavy metals contamination (Cd, Cr, Cu, Hg, Pb, Zn) in the Seine River basin (France) following a DPSIR approach (1950-2005). Science of The Total Environment 2007; 375: 204-231.

Morel FMM. Principles of Aquatic Chemistry. New York: John Wiley and Sons, 1983.

Munksgaard NC, Parry DL. Trace metals, arsenic and lead isotopes in dissolved and particulate phases of North Australian coastal and estuarine seawater. Marine Chemistry 2001; 75: 165-184.

Nguyen HL, Leermakers M, Elskens M, De Ridder F, Doan TH, Baeyens W. Correlations, partitioning and bioaccumulation of heavy metals between different compartments of Lake Balaton. Science of The Total Environment 2005; 341: 211-226.

Nriagu JO. A silent epidemic of environmental metal poisoning? Environmental Pollution 1988; 50: 139-161.

Peltier EF, Webb SM, Gaillard J-F. Zinc and lead sequestration in an impacted wetland system. Advances in Environmental Research2003; 8: 103-112.

Pepe M, Gaillard A, Harrault L, Groleau A, Benedetti MF. Les Métaux dissous en Seine à Paris. PIREN Seine, Paris, 2008.

Pernet-Coudrier B, Clouzot L, Varrault G, Tusseau-Vuillemin MH, Verger A, Mouchel JM. Dissolved organic matter from treated effluent of a major wastewater treatment plant: Characterization and influence on copper toxicity. Chemosphere 2008; 73: 593-599.

Priadi CR, Ayrault S. Caractérisation des phases porteuses de métaux. LSCE, Gif sur Yvette, 2007, pp. 29.

Reeders HH, Devaate AB, Slim FJ. The Filtration-Rate Of Dreissena-Polymorpha (Bivalvia) In 3 Dutch Lakes With Reference To Biological Water-Quality Management. Freshwater Biology 1989; 22: 133-141.Rozan TF, Lassman ME, Ridge DP, Luther GW. Evidence for iron, copper and zinc complexation as multinuclear sulfide clusters in oxic rivers. Nature 2000; 406: 879-882.

Rubio R, Lopez-Sanchez JF. Assessment of inorganic priority pollutants in contaminated soils: Harmonization of analytical protocols for heavy metal extraction: Analytical speciation. In: Simeonov L, editor. NATO Advanced Research Workshop on Soil Chemical Pollution, Risk Assessment, Remediation and Security. Springer, Sofia, BULGARIA, 2007, pp. 95-116.

Sigg L, Behra P, Stumm W. Chimie des milieux aquatiques. Paris: Dunod, 2000.

Sigg L, Stumm W, Behra P. Chimie des milieux aquatiques. Paris: Dunod, 2006.

Tang D, Warnken KW, Santschi PH. Distribution and partitioning of trace metals (Cd, Cu, Ni, Pb, Zn) in Galveston Bay waters. Marine Chemistry 2002; 78: 29-45.

Thévenot D, Lestel L, Tusseau-Vuillemin M-H, Gonzalez JL, Meybeck M. Les Metaux dans le bassin de la Seine. In: Piren-Seine, editor. Eau Seine Normandie. 7, Paris, 2009.

Thévenot D, Meybeck M, Lestel L. Métaux Lords : des bilans en mutation. PIREN Seine, Paris, 2002, pp. 78.

Thévenot DR, Lestel L, Tusseau-Vuillemin M-H, Gonzales J-L, Meybeck M. Plaquette Piren Seine : Les métaux dans le bassin de la Seine. PIREN Seine, Créteil, 2007, pp. 63.

Thorpe A, Harrison RM. Sources and properties of non-exhaust particulate matter from road traffic: A review. Science of The Total Environment 2008; 400: 270-282.

Tusseau-Vuillemin MH, Buzier R, Meriadec Cd, Chardon I, Elbaz-Poulichet F, Seidel J-L, et al. Du réseau à la rivière et de la Marne à Andrésy : métaux labiles, dissous et particulaires. PIREN Seine, Paris, 2005, pp. 17.

Tusseau-Vuillemin MH, Gourlay C, Lorgeoux C, Mouchel JM, Buzier R, Gilbin R, et al. Dissolved and bioavailable contaminants in the Seine river basin. Science of The Total Environment 2007; 375: 244-256.

Weber F-A, Voegelin A, Kretzschmar R. Multi-metal contaminant dynamics in temporarily flooded soil under sulfate limitation. Geochimica et Cosmochimica Acta 2009; 73: 5513-5527.

Chapitre 2 – L’importance des métaux particulaire dans la colonne d’eau de la Seine : Une étude de répartition entre les particules, la fraction « dissous total » et la fraction « dissous labile ».

Avant-Propos

Dans une étude de caractérisation des métaux dans la phase particulaire, il est tout d’abord essentiel de quantifier la part représentée par les métaux particulaires dans la colonne d’eau par rapport aux métaux totaux. Pendant la campagne d’échantillonnage, une vaste gamme de paramètres physico-chimiques et de concentrations de métaux dans de diverses phases a été mesurée afin de bien situer le

rôle des métaux particulaires dans la Seine urbanisée. Plus qu'une présentation des résultats de suivi, les données ont été présentées sous forme de répartition entre les métaux particulaires et dissous afin de donner une vision globale de la colonne d'eau et également une approche méthodologique pour le profit d'un plus grand public scientifique. **Une version modifiée de ce chapitre est en cours de révision au *Journal of Environmental Monitoring* sous le titre "*Spatio-temporal variability of solid, total dissolved and labile metal: passive vs discrete sampling evaluation in river metal monitoring »*"**.

1 Topic introduction

In freshwater systems, metals are found as various forms ranging from cationic, inorganic, organometallic, sorbed on oxides and clay surfaces, metal alloys or incorporated in crystalline structures (Hochella and White, 1990; Luoma and Rainbow, 2006; and Stumm and Morgan, 1981). Defining all the metal forms (i.e. its speciation) in the water column is currently analytically difficult because it involves various forms in multiple pools. Yet, to illustrate and predict the environmental fate and transport of metal contaminants in this dynamic system, there is a need to investigate metal partitioning, and not just isolating specific phases (Lofts and Tipping, 2000; Unsworth et al., 2006; Vignati et al., 2009).

One approach is to define metal partitioning as Kd, a ratio between metal adsorbed in the solid fraction, operationally-defined as the filter-retained fraction (>0.45 μm) and the metal concentration in the dissolved fraction (<0.45 μm). Kd is often used in defining metal partitioning in the river system (Bibby and Webster

Brown, 2005; Lu and Allen, 2001; Nguyen et al., 2005). With relatively simple measurements, it may indicate a useful general view of metal distribution in the water column (Koelmans and Radanovic, 1996; O'Connor et al., 1980)[10, 11] and the ability of the suspended particulate matter (SPM) to bind trace metals [1].

Kd is usually derived from discrete spot measurements. It is a parameter that may vary easily with even a slight fluctuation of dissolved fraction (O'Connor et al., 1980) for which concentrations may oscillate 2-3 folds in urbanized water at the same location and is prone to analytical contamination (Luoma and Rainbow, 2006). Hence, Kd is often considered to have limited predictive capability (Lofts and Tipping, 2000). Alternatively, Kd values can be empirically calculated as a function of water chemistry variables, using metal speciation models such as WHAM, SCAMP or MINTEQ (Koelmans and Radovanovic, 1998; Ng et al., 1996), although significant uncertainties were identified (Lofts and Tipping, 2000).

Consequently, there is a need to explore other possibilities of in-field metal partitioning that depends less on rapidly fluctuating physico-chemical parameters but still responsive to medium and long-term water chemistry evolution and seasonal and spatial evolution.

Discrete sampling-related problems may be solved by calculating partitioning using dissolved and particulate metal concentrations from time-weighted averaged samples. When deployment time is selected correctly, time-averaging samplers are able to measure changes of heavy-metal concentrations related to various physico-chemical parameters (Dunn et al., 2007; Tessier, 2003). In the water column, time-integrated solid fraction may be sampled by sediment trap (Gasperi et al., 2008; Ciffroy et al., 1999;). However, sampling of time-integrated dissolved fraction for

metal analysis is currently difficult in practice. A possible approach is by using in-situ passive samplers. The Diffusion Gradient in Thin Films (DGT) technique was initially developed by Davison and Zhang (1994) to quantitatively measure time-weighted average concentrations of labile metals in water. Tusseau-Vuillemin et al. (2004) and Buzier et al. (2006) then further developed the use of restrictive pore gels in DGTs, measuring labile metals composed of inorganic metals plus a fraction of easily exchangeable organic complexes that correlated with metal toxicity in *Daphnia magna*. With the combination of sediment traps and DGTs, it would then be possible to examine medium-term metal partitioning.

To which extent is metal partitioning obtained from time-averaged samples comparable and representative for spatial and temporal variations as opposed to those calculated from discrete samples? This paper aims to take a closer look on metal partitioning calculated from time-averaged and discrete samples and to evaluate their comparability in the need of robust and representative environmental monitoring parameters. It will also discuss how far these metal partitioning methods allow the study of urbanization impacts on metal behaviour in the water column. For the purpose of this study, suspended sediments are completely digested and thus metal concentration in the solid fraction includes not only adsorbed metals but also incorporated metals. In order to avoid term confusion, this study will use Concentration Index (CI) as a ratio between metal concentration in the solid and metal concentration in the dissolved phase.

2 Methodology

2.1 Study site

For this work, samples are collected along the Seine River, France. The Seine River is located in a sedimentary basin in the north of France (Fig. 1.5), flowing through the Greater Paris Region. Before its estuary, the Seine River drains an area of 64700 km^2 with an average density of 215 people/km^2, an ideal example of an highly anthropized basin as it hosts 25% of French agriculture, 30% of French industry and 23% of French population (Thévenot et al., 2007). Previous studies have indicated a significant metal load within the watershed (Thévenot et al., 2007; Meybeck et al., 2007; Tusseau-Vuillemin et al., 2007), representative of a multi-metal contamination in an urban catchment.

The sampling scheme aims to distinguish the impacts of two sources of anthropogenic influence to the Seine River. The first source is the wastewater treatment plant WWTP Seine-Aval treating around 1.7 million m^3 per day (SIAAP, 2007). The second is the area of Greater Paris, including the most densely urbanized area in the region with more than 3700 inhabitants/km^2 (Billen et al., 2009). Treated municipal wastewater from smaller units and urban runoff are the major identified metal sources to the river in this area. The first sampling site is located at Marnay-sur-Seine, situated far upstream on the Seine River (Figure I.5). It was chosen to represent a site non-affected by the Greater Paris region, where the Seine is a 6 Strahler order river, the population density upstream Marnay is only 15-30 inhabitants/km^2 (Billen et al., 2009). The second site is the Seine at Bougival, situated 40 km downstream of Paris city (Strahler order 7). It was chosen to demonstrate the impact of Greater Paris without the influence of the major WWTP Seine-Aval. Another 40 km further

downstream, Triel-sur-Seine was selected to demonstrate the influence of Greater Paris region including all its inputs to the river. The Triel station is situated downstream of the confluent of the Seine River with one of its major tributaries, the Oise River, making it a Strahler order 8. Sampling was performed from October 2008 to October 2009. Unless mentioned otherwise, samples are collected around the 20th of each month.

2.2 Physico-chemical parameters

pH was measured with either pH meter WTW 330i from VWR or Waterproof pHtestr 20 from Eutech instruments with precision at 0.05. Temperature was continuously monitored with a temperature sensor from Hobo with precision at 0.001°C. Conductivity was measured in the laboratory within 6 hours from field sampling with an Orion conductivity cell from Thermo. Daily discharge values were obtained from www.hydro.eaufrance.fr. Water was collected in plastic bottles for chlorophyll, pheopigment and ion analysis. Water was collected into 1L pre-combusted glass bottles for dissolved organic carbon (DOC), TSS and and particulate organic carbon (POC) analysis (Tusseau-Vuillemin et al., 2003). The absorbance at 254 nm (A254) of the GF-F filtrate was measured and the specific ultra-violet absorbance (SUVA) was calculated as SUVA = A254/DOC in $cm^{-1}.g^{-1}.L$. SUVA can be considered as an indicator of the aromaticity of dissolved organic matter (DOM) (Traina et al., 1990).

2.3 Metal sampling and analysis

Materials and sample handling were done following clean methodologies. All bottles and containers were soaked in 2 N HNO_3 during at least 3 days. Afterwards they were rinsed thoroughly 3 times with de-ionised water. In the field, all bottles,

buckets and containers were rinsed 3 times with river water. Sampling was done from riverbank where a PVC bucket collected water around 3 m from riverbank.

2.3.1 Dissolved fraction sampling

The dissolved 0.45 µm fraction was obtained by filtering on-field with disposable Millex-LH Millipore syringe filters and 20 mL disposable syringe, acidified with pure 200 µl HNO_3 65% (Merck Suprapur) to avoid any precipitation. Sterile disposable 50 ml polyethylene tubes, previously tested for clean handling, were used. All samples are transported and kept in 4°C in the dark before analysis.

2.3.2 Labile fraction sampling

Six diffusive gradient in thin films (DGT) were deployed in each site once a month in order to assess time-weighted average labile metal contamination. Method for assembling DGT is explained thoroughly in Tusseau-Vuillemin et al (2007). In brief, after passing through a 0.45 µm polyethersulfone (PES) filter and a 0.4 polycarbonate filter, labile metals diffuse through a restrictive diffusive gel layer (0.8 mm thickness) and strongly binded by chelex resins. After DGT retrieval, they were brought back to the laboratory and chelex resins were eluted in 1M nitric acid in which the analysis was performed. Labile metal concentrations were calculated according to the method explained in Bourgeault et al [27]. The deployment duration was previously validated by Bourgeault et al to avoid bio-fouling [28].

2.3.3 Suspended Particulate Matter (SPM) sampling

For discrete SPM sampling, water was collected in 2 L polyethylene bottles, kept in the dark at 4°C and filtered in the laboratory in 1-5 days after sampling to

minimize biological activity and SPM accumulation on bottle wall. Only the September sample was filtered 1 month after sampling due to technical reason. Filtration was performed on a 0.45 µm Millipore MF-Millipore cellulose ester filters mounted on the Millipore filtration system diameter 47 mm. Sample bottle was vigorously shaken to ensure all SPM was evacuated during filtration. When possible, filtration was done on one filter, but in extreme cases where turbidity was high, filtration was done on two filters. Filters were weighted before and after filtration after drying at 40°C and stabilizing weight for up to 2 days in a desiccated jar.

A sediment trap was also installed at each site. It consisted of a 2 L polyethylene terephtalate (PET) water bottle hung top-down at least 1 m from the river bank at mid-depth. Two holes (4 cm diameter) were carved on two opposite sides on the upper part of the bottle, and placed in the flow direction. This method was previously successfully used by Tessier (2003) to collect SPM in slow flowing rivers. After sampling, the total sediment trap content (water and SPM) was stored in the dark at 4°C before analysis. Storage duration ranged from 2-5 days for most samples to one month for the September sample. Samples were then centrifuged in the laboratory at 2800 g for 20 mn and SPM was recovered. The SPM was then freeze-dried for at least 48h and homogenized in an agate mortar.

All discrete SPM recovered on filters and 0.1 g of time-integrated SPM from sediment trap were totally digested using a method adapted for the Seine River carbonated SPM (Le Cloarec et al., In Press; Ayrault et al.2010), and allowing total SPM digestion. Details are presented in Supporting Information. All solutions were ultrapure reagents to assure minimum contamination (HNO_3 and HCl Normatom

grade, VWR France, and HF and $HClO_4$ “for trace metal analyses”, Baker, from Sodipro France).

2.3.4 Trace metal analysis

Major and trace metal concentration (Ag, Al, As, Ca, Cd, Cr, Co, Cu, Fe, K, Mg, Mn, Ni, Se, Ti, Pb, V, and Zn) were determined in dissolved fraction and digested SPM fraction using Inductively Coupled Plasma Quadrupolar Mass Spectrometry (ICP-QMS) (XIICCT-Series, ThermoElectron, France). ICP-QMS spectrometer was calibrated using standard solutions and routinely checked with certified river water (SRM 1640, National Institute for Science and Technology, Gaithersburg, USA). Instrumental drifts and plasma fluctuations were corrected using internal standards (Re, Rh, and In (SPEX, SCP Science, France)) for all studied metals, and Ge for major elements including Ca, Al, and Mg. To minimise isobaric interferences, analysis with the Collision Cell Technology (CCT) introducing a supplementary gas mixture of H_2 (7%) and He (93%) was applied for Fe, Mn, and Cd, Cr, Co, Cu, Mn, Ni, Pb, Zn determination.

Overall, sampling representativity and analytical accuracy was satisfactory. Ten dissolved fractions collected at one time in one site showed a standard deviation of 2% or less for Co, Mn, Ni, Pb and Zn, 5% for Cu and 9% for Cr and Cd. Variation of labile metals recovered by DGT depended on time and metals. Standard deviation (SD) of the 6 DGT is displayed as supporting information. Values obtained for the reference sediment SL1 (12 replicates) were compared to certified values, recovery was 90-99% for all analyzed elements except 116% for Cd with a standard deviation

of 10% or less for all elements except Mn with a SD of 18% and Cd with a SD of 24%.

2.4 Two-phase concentration index (CI) calculation

Results and interpretation of two-phase concentration index (CI) was limited to 8 elements, Cd, Cr, Co, Cu, Mn, Ni, Pb and Zn, for which the ability for DGTs to estimate a one-month labile concentration has been validated (Bourgeault et al, 2010)."Discrete" CI (10^3 L/g) was calculated as the concentration ratio between metals in SPM (0.45 µm) to discrete dissolved metals (0.45 µm) both collected by discrete sampling (Eq.II.1). Superscript m refers to the month of sampling.

$$"Discrete"CI = [Me]^{m}_{SolidMeas} / [Me]^{m}_{DissMeas} \quad \text{(Eq.II.1)}$$

"Integrated" CI (10^3 L/g) was calculated as the concentration ratio between metal in SPM collected in sediment trap to labile metal (DGT) both integrating one month of sampling. (Eq.II.2). Integrated CI with superscript m is based on integrated samples deployed between dates m-1 and m.

$$"Integrated"CI = [Me]^{m}_{trap} / [Me]^{m}_{labile} \quad \text{(Eq.II.2)}$$

where $[Me]^{m}_{Trap}$ is the concentration of settleable sediment collected in the sediment trap deployed on month m-1 and collected on month m and $[Me]^{m}_{Labile}$ is the concentration of labile metals measured by the DGT method trap deployed on month m-1 and collected on month m.

2.5 Labile – Inert – Solid Partitioning

Average metal proportion in the three different pools of the water column: labile metals measured by DGT, inert metals as the difference between labile and dissolved metals, and solid metals; were estimated. Due to different sampling methods for each pool (discrete vs integrating) and variable quantification limits (much lower for labile metals via DGT than for total dissolved metals), a specific procedure was set to derive inert (non labile) dissolved metal concentrations.

when $\left(\left[M\right]_{D}^{m-1} + \left[M_s\right]_{D\ s}^{m}\right)/2 > \left[M_{sol}\right]_{l}^{m}$

Inert metal concentrations (Eq.II.3) were calculated as the difference between the averaged dissolved metal concentration (Eq.II.4) and the labile metal concentration.

$$\left[Me\right]_{Inert}^{m} = \left[Me\right]_{DissAvg}^{m} - \left[Me\right]_{Labile}^{m} \quad \text{(Eq.II.3)}$$

where for month m, discrete dissolved metal concentration were averaged between measurements taken on month m and the month before (m-1).

$$\left[Me\right]_{DissAvg}^{m} = \left[Me\right]_{DissMeas}^{m-1} + \left[Me\right]_{DissMeas}^{m} / 2 \quad \text{(Eq.II.4)}$$

When dissolved concentrations were lower than quantification limit (QL) and average dissolved concentration calculated from Eq.II.3 became lower than labile concentration, inert metals were considered as negligible in the balance and integrated labile metals were considered as a relevant proxy for integrated total dissolved metals (Eq.II.5).

$$\left[Me\right]_{DisAvg}^{m} = \left[Me\right]_{labile}^{m} \text{(Eq.II.5)} \quad \text{when} \quad \left(\left[Me\right]_{DissMeas}^{m-1} + \left[Me\right]_{DissMeas}^{m}\right)/2 < \left[Me\right]_{labile}^{m}$$

Total solid metal, defined as total solid metal per liter of water, was obtained by multiplying metal content (μg/g) of each month with SPM concentration (g/L). Average solid metal (μg/L) for month m ($[Me]^{m}_{SolidAvg}$) was then calculated similarly to the calculation of the average dissolved concentration in Eq.II.3.

Total metal (μg/L) was calculated as a sum between the average solid metal and dissolved metal concentration, both in μg/L (Eq.II.6).

$$[Me]^{m}_{Total} = [Me]^{m}_{DisAvg} + [Me]^{m}_{SolidAvg} \quad \text{(Eq.II.6)}$$

Distribution of metal in each phase (labile, inert and solid) was then calculated using the total metal calculated using Eq.II.6.

3 Results

In order to optimally present data of monthly variation, median values were used. Comparison between samples was performed using Mann-Whitney ranked test (p = 0.01).

3.1 River Chemistry

Table II.1 Summary of measured physico-chemical parameters during 13 months of sampling between 2008-2009 indicating minimum-maximum values with 1st quartile – median – 3rd quartile in parenthesis; Q: discharge; DOC: dissolved organic carbon; SPM: suspended particulate matter; POC: particulate organic carbon (n=13)

	Marnay	Bougival	Triel
Q (m3/s)	25 - 89 (37 - 50 - 54)	92 - 324 (116 - 184 - 215)	198 - 550 (225 - 340 - 384)
pH	8.06 - 8.32 (8.14 - 8.18 - 8.28)	7.20 - 8.24 (7.76 - 7.91 - 8.09)	7.10 - 8.01 (7.58 - 7.73 - 7.85)
Alkalinity (mg/L)	152 - 287 (218 - 238 - 262)	182 - 281 (224 - 244 - 259)	189 - 281 (236 - 253 - 264)
Conductivity (µS/cm)	268 - 526 (387 - 479 - 499)	449 - 611 (490 - 527 - 570)	506 - 668 (588 - 619 - 655)
Temperature (°C)	5.6 - 23 (7 - 13.1 - 17.1)	4.5 - 22.8 (8.5 - 15.2 - 19.9)	4.9 - 22 (8.9 - 14.4 - 19.2)
Chlorophyll (µg/L)	0.5 - 3.5 (0.7 - 1.0 - 1.7)	0.4 - 15.1 (2.7 - 3.7 - 8.1)	0.3 - 16.4 (2.1 - 2.5 - 7.9)
Dissolved fraction			
DOC (mg/L)	1.62 - 2.68 (1.83 - 2.05 - 2.38)	2.56 - 4.34 (2.77 - 2.94 - 3.25)	3.42 - 5.45 (3.72 - 3.87 - 3.97)
Ca^{2+} (mg/L)	58 - 105 (72 - 88 - 93)	73 - 100 (80 - 95 - 98)	77 - 109 (89 - 99 - 102)
Mg^{2+} (mg/L)	0.54 - 8.93 (3.28 - 3.97 - 4.66)	0.64 - 10.3 (3.45 - 6.4 - 7.03)	0.68 - 8.63 (5.79 - 7.34 - 8.12)
K^{+} (mg/L)	1.55 - 6.26 (1.93 - 2.06 - 3.28)	0.42 - 4.61 (2.49 - 3.36 - 4.19)	1.54 - 9.18 (3.79 - 4.32 - 5.55)
Na^{+} (mg/L)	3 - 20 (6 - 8 - 9)	6.7 - 17.7 (12.6 - 14.9 - 16.1)	10.4 - 27.5 (15.3 - 19.5 - 22.2)
Cl^{-} (mg/L)	11 - 27 (13 - 14 - 20)	17.4 - 34.2 (23.9 - 26.6 - 30.1)	19.9 - 41.9 (34 - 37 - 41.2)
NH_4^{+} (mg/L)	0.3 - 1.4 (0.4 - 0.6 - 1)	0.09 - 2.92 (0.17 - 0.41 - 0.74)	0.23 - 4.28 (0.38 - 0.51 - 1.39)
NO_3^{-} (mg/L)	7.8 - 26 (11.3 - 18 - 24.9)	13.2 - 26.7 (15.1 - 21.3 - 25)	20.2 - 35.2 (27.9 - 28.5 - 31.3)
SO_4^{2-} (mg/L)	13.7 - 22.4 (14.3 - 17.3 - 18.8)	24.4 - 44.6 (31.1 - 36.1 - 38.4)	28 - 51.5 (43.6 - 46.4 - 49.5)
Particulate fraction			
SPM (mg/L)	3.1 - 96.9 (4.0 - 8.5 - 13.1)	3.4 - 20.3 (7.7 - 8.9 - 16.2)	3.1 - 82.4 (6.7 - 9.5 - 11.3)
POC (mg/L)	0.05 - 1.9 (0.42 - 0.56 - 0.9)	0.38 - 3.92 (0.69 - 0.88 - 1.03)	0.04 - 2.47 (0.72 - 0.89 - 1.08)
Ca (%)	13.9 - 44.2 (17.0 - 17.8 - 18.7)	7.2 - 15.5 (11.6 - 12.1 - 12.7)	4.0 - 30.8 (9.1 - 9.7 - 10.1)
Fe (%)	0.65 - 2.87 (1.53 - 1.84 - 2.20)	1.42 - 3.26 (2.35 - 2.62 - 2.91)	0.29 - 5.17 (2.40 - 2.78 - 3.09)
Al (%)	0.4 - 4.77 (2.22 - 3.10 - 3.41)	1.19 - 5.30 (2.69 - 4.06 - 4.55)	0.25 - 8.47 (3.02 - 3.80 - 3.94)
Mg (mg/kg)	158 - 12227 (2661 - 3382 - 3970)	3515 - 19076 (4429 - 5766 - 8270)	1397 - 8815 (4965 - 5462 - 7656)
K (mg/kg)	183 - 9478 (5288 - 7306 - 8088)	2726 - 11946 (7317 - 8883 - 10320)	1446 - 17945 (7944 - 9052 - 9885)

Most water quality parameters measured throughout the campaign displayed a Marnay - Bougival - Triel gradient indicating evident evolution in water chemistry (Table II.1). pH in upstream site is relatively more basic,8.20±0.04, where the river drains calcareous rocks. As the catchment becomes more urbanized, pH drops to 7.91±0.04 and 7.73±0.04 downstream at Bougival and Triel, respectively. Downstream sites had significantly higher values of DOC and POC and higher photosynthetic activities indicated by higher chlorophyll concentration. Major ions showed two different trends; Ca and NH_4^{+} concentrations remained constant at the 3 sites, while the others increased downstream. From upstream to downstream, median

of magnesium and potassium ion concentration doubled, while chloride and sulfate multiplied by 2.5.

Median metal concentrations in different pools in the water column showed an evident upstream-downstream increasing trend from Marnay to Bougival and Triel, although in general, Bougival displays higher metal content than Triel for all except for Co and Mn (Table II.2). The dilution effect of the confluence between the Seine and the Oise River (25 km downstream Bougival and 15 km upstream Triel-sur-Seine) may be the cause of the decrease of metal concentration in Triel.

Dissolved metal concentrations compared with other rivers with strong urban influence (Luoma and Rainbow, 2008) showed that the Seine River dissolved concentrations (Table II.2) are higher but are still in the same order of magnitude. Data found during this campaign were also comparable to other dissolved metal concentration earlier reported in the Seine River (Elbaz-Poulichet et al. 2006). Labile metal concentrations of Co, Cu, Mn and Ni were within the range of those measured by (Tusseau-Vuillemin et al., 2007) in the Seine River basin. Concentration of metals in SPM collected by discrete sampling were much more variable than those measured in SPM collected with the sediment trap on a monthly basis. Median values between the two sets were comparable. When metal concentration in SPM was normalized by background geological values obtained from numerous sites in the Seine River basin (Thévenot et al., 2009), SPM collected downstream at Bougival and Triel showed an average enrichment of 2-3 times for Ni, Cr and Co, 7-8 times for Pb, Cu and Zn, and 15-18 times for Cd.

Table II.2 Summary of metal concentration at the three studied sites in four measured phases indicating minimum-maximum values with 1st quartile – median – 3rd quartile in parenthesis (n=13)

			Marnay	Bougival	Triel
Cd	Grab	<0.45µm (µg.L-1)	<LQ	0 - 0.015 (0 - 0 - 0.013)	0 - 0.019 (0.012 - 0.013 - 0.014)
		>0.45µm (µg.g-1)	0 - 4.42 (0.43 - 0.54 - 1.05)	0.77 - 20.53 (1.69 - 2.47 - 4.05)	0.44 - 2.29 (0.88 - 1.41 - 2.06)
	time integrated	Labile DGT (µg.L^{-1})	0 - 0.002 (0.001 - 0.001 - 0.001)	0 - 0.007 (0.002 - 0.003 - 0.005)	0 - 0.005 (0.003 - 0.004 - 0.005)
		sed.trap (µg.g-1)	0.269 - 0.444 (0.294 - 0.309 - 0.332)	1.53 - 8.07 (1.73 - 2.65 - 3.57)	0.35 - 3.03 (0.85 - 1.23 - 1.86)
Cr	Grab	<0.45µm (µg.L-1)	0 - 1.086 (<LQ)	0 - 1.041 (0 - 0 - 0.508)	0 - 1.235 (0 - 0.212 - 0.324)
		>0.45µm (µg.g-1)	7.7 - 101.7 (41.9 - 53.6 - 64.8)	46.3 - 102.4 (73 - 84.2 - 88.9)	35.9 - 121.9 (58.1 - 69.1 - 88.1)
	time integrated	Labile DGT (µg.L-1)	0 - 0.035 (0.018 - 0.02 - 0.025)	0 - 0.093 (0.024 - 0.028 - 0.035)	0 - 0.086 (0.025 - 0.031 - 0.037)
		sed.trap (µg.g-1)	42.1 - 54.2 (50 - 50.5 - 51.4)	69.2 - 109.3 (71.3 - 85.4 - 96.4)	56.4 - 86.7 (65 - 73.5 - 80.9)
Co	Grab	<0.45µm (µg.L-1)	0.04 - 0.18 (0.09 - 0.12 - 0.16)	0.13 - 0.25 (0.17 - 0.21 - 0.23)	0.2 - 0.39 (0.26 - 0.3 - 0.32)
		>0.45µm (µg.g-1)	2.48 - 9.17 (6.49 - 7.59 - 8.52)	6.42 - 38.4 (10.75 - 11.51 - 12.7)	5.9 - 25.2 (10.9 - 14 - 17.5)
	time integrated	Labile DGT (µg.L-1)	0 - 0.022 (0.006 - 0.012 - 0.019)	0 - 0.051 (0.016 - 0.023 - 0.042)	0 - 0.078 (0.029 - 0.038 - 0.057)
		sed.trap (µg.g-1)	5.76 - 7.13 (6.44 - 6.68 - 6.87)	8.25 - 11.81 (9.1 - 9.79 - 11.2)	7.69 - 13.04 (9 - 10.33 - 11.76)
Cu	Grab	<0.45µm (µg.L-1)	0.27 - 0.67 (0.35 - 0.37 - 0.46)	0.77 - 1.76 (1.02 - 1.12 - 1.27)	0.8 - 1.56 (1.07 - 1.22 - 1.45)
		>0.45µm (µg.g-1)	5.7 - 95.5 (18.7 - 19.4 - 28)	44.7 - 169.3 (67.9 - 103.9 - 147)	21.1 - 130.3 (56.2 - 72.2 - 93.6)
	time integrated	Labile DGT (µg.L-1)	0 - 0.104 (0.062 - 0.074 - 0.085)	0 - 0.481 (0.172 - 0.253 - 0.298)	0 - 0.388 (0.21 - 0.251 - 0.307)
		sed.trap (µg.g-1)	13.5 - 18.1 (15.3 - 16.1 - 17.2)	78.8 - 185.3 (90.2 - 121.7 - 150.1)	53.4 - 96.8 (56 - 81.8 - 88.9)
Mn	Grab	<0.45µm (µg.L-1)	1.44 - 3.19 (1.81 - 2.43 - 2.6)	3.07 - 17.39 (7.01 - 8.3 - 10.75)	4.37 - 27.63 (11.62 - 15.38 - 17.67)
		>0.45µm (µg.g-1)	130 - 910 (394 - 444 - 761)	514 - 1762 (817 - 1035 - 1186)	484 - 2314 (1097 - 1428 - 1911)
	time integrated	Labile DGT (µg.L-1)	0 - 3.21 (0.41 - 1.13 - 2.24)	0 - 8.38 (2.27 - 3.72 - 7.18)	0 - 10.23 (4.45 - 4.71 - 9.65)
		sed.trap (µg.g-1)	268 - 527 (317 - 431 - 452)	281 - 1825 (492 - 637 - 653)	414 - 966 (502 - 594 - 872)
Ni	Grab	<0.45µm (µg.L-1)	0.48 - 1.93 (0.8 - 1.45 - 1.59)	0.94 - 2.25 (1.48 - 1.76 - 1.98)	1.49 - 2.74 (1.96 - 2.17 - 2.36)
		>0.45µm (µg.g-1)	9.1 - 83.5 (20.5 - 25.4 - 32)	20.9 - 40.5 (26.3 - 32.1 - 36)	0 - 59.5 (21.5 - 30.1 - 39.5)
	time integrated	Labile DGT (µg.L-1)	0 - 0.212 (0.135 - 0.173 - 0.202)	0 - 0.47 (0.228 - 0.322 - 0.419)	0 - 0.796 (0.443 - 0.543 - 0.578)
		sed.trap (µg.g-1)	20.5 - 26.2 (20.6 - 21.3 - 21.6)	26.2 - 40.2 (28.4 - 31.3 - 37.4)	21.2 - 30.7 (25.2 - 27.7 - 29.3)
Pb	Grab	<0.45µm (µg.L-1)	0 - 0.071 (<LQ)	079 - 0.255 (0.152 - 0.195 - 0.23	0 - 0.327 (0.145 - 0.162 - 0.204)
		>0.45µm (µg.g-1)	1 - 69 (29 - 36 - 47)	71 - 307 (118 - 139 - 161)	34 - 145 (82 - 109 - 115)
	time integrated	Labile DGT (µg.L-1)	0 - 0.031 (0.004 - 0.007 - 0.011)	0 - 0.161 (0.024 - 0.032 - 0.058)	0 - 0.039 (0.018 - 0.019 - 0.023)
		sed.trap (µg.g-1)	18.7 - 23.5 (19.7 - 20.2 - 21.7)	80 - 245.2 (93.3 - 123 - 155.2)	50.7 - 98.5 (58.7 - 81.8 - 84.1)
Zn	Grab	<0.45µm (µg.L-1)	0 - 9.768 (0 - 2.257 - 2.611)	3.28 - 24.11 (4.39 - 6.22 - 7.35)	3.47 - 14.6 (4.53 - 6.72 - 9)
		>0.45µm (µg.g-1)	45 - 713 (134 - 185 - 395)	336 - 671 (383 - 480 - 567)	43 - 1402 (256 - 351 - 434)
	time integrated	Labile DGT (µg.L-1)	0 - 1.488 (0.159 - 0.444 - 0.756)	0 - 3.13 (1.51 - 1.83 - 2.47)	0 - 3.74 (1.55 - 2.68 - 3.06)
		sed.trap (µg.g-1)	106 - 149 (110 - 120 - 126)	307 - 694 (406 - 506 - 544)	225 - 415 (249 - 342 - 395)

3.2 Labile – Inert – Solid Partitioning

Partitioning of each metal in the defined phases varied according to metals and sites (Fig.II.1). The approach described in Eq.II.2-II.4 consisted in averaging discrete total metal for the dissolved and solid phases causing the total median values of the three phases displayed in Fig. II.1 to be occasionally less or more than 100% of the total metal calculated through Eq.II.6. This is mainly true for Cd, Mn and Zn that displayed high variation of discrete concentration to which this averaging method may constitute incertitude of total partitioning of around 5-10%. Nevertheless,

averaged median values were considered representative because Co, Cr, Cu, Ni and Pb showed total averages close to 100%.

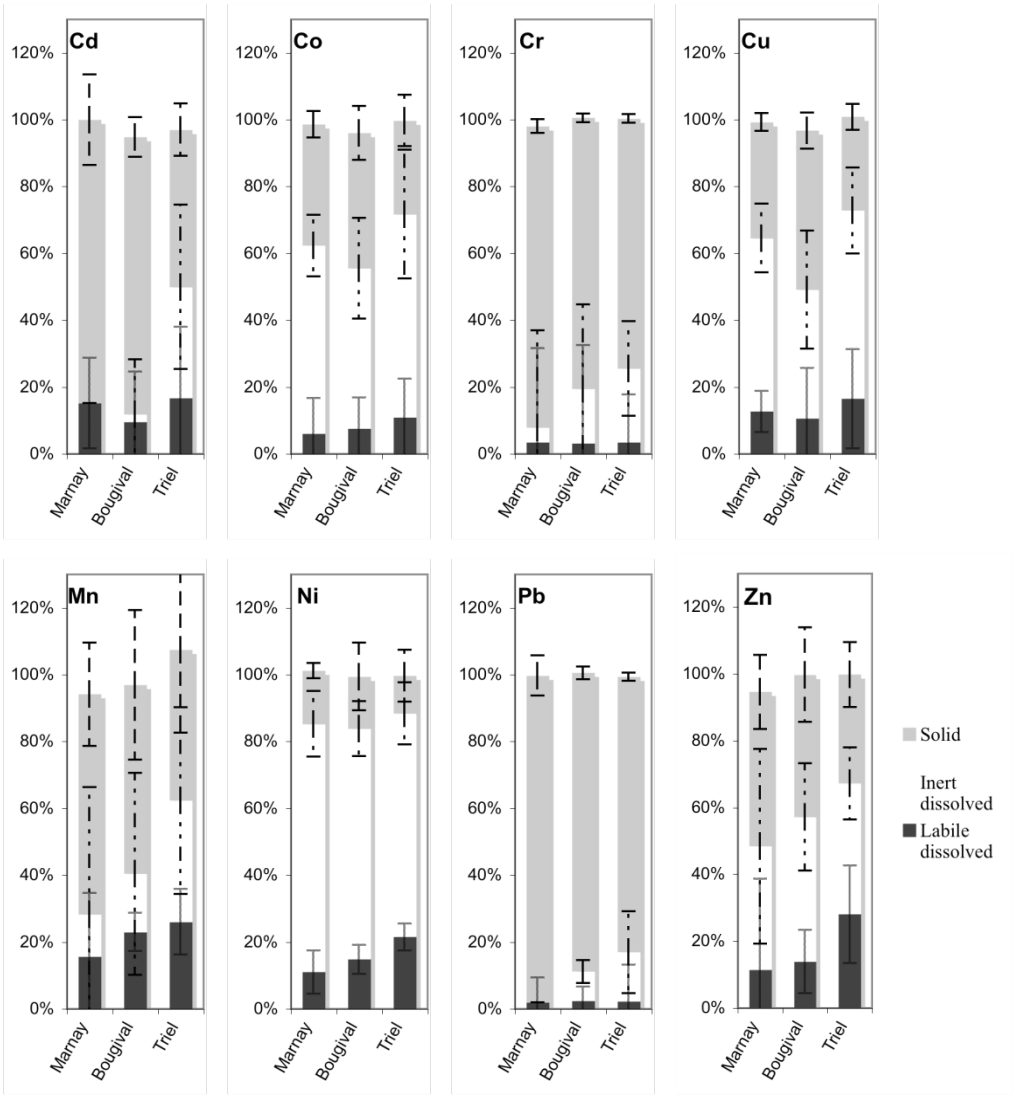

Figure II.1. Bar charts represent average proportion of metal in each pool relative to the total of metal in the three defined pools. Individual labile dissolved metals were measured by DGT. Discrete inert dissolved metals were calculated from the average of dissolved metals for two months between the deployment and the collection of DGT subtracted by the labile metal pool. When labile metals were larger than the average dissolved metals, the dissolved metal pool was represented by concentration in the labile pool. Individual solid metals were calculated from the average of dissolved metals for two months between the deployment and the collection of DGT (n=12).

Despite complete digestion of particulate metals, proportion of dissolved metals in these samples was relatively high compared to literature data. Our data showed that for most metals, median proportion of dissolved metal in the water

column exceeded more than 50%. Nguyen et al (2005) found Zn, Co, Cd and Pb in a contaminated lake highly associated to the solid phase (for about 70% of the total metal load). Previous metal partitioning values on the Seine River accounted for higher solid fraction (70 to 90%) mostly due to relatively high approximation of SPM concentration used to theoretically calculate total solid metal (Thevenot et al.,2007). Nevertheless, our dissolved and particulate metal data were in agreement with other Seine references (Chiffoleau et al., 1994, Elbaz-Poulichet et al., 2006), indicating that calculated CI was fairly accurate despite differences with other water bodies.

3.3 Two-phase Concentration Index (CI)

Average Concentration Index (CI) for a given metal were ranked by their preference to the solid phase, indicated with a high discrete CI where Pb > Cr > Mn ~ Cd > Zn > Cu ~ Co > Ni (Table II.3). When time-integrated CI is compared, a similar order is observed for most of the metals, except for Co and Cu that went up the rank: Pb > Cr> Cd > Co> Cu>Zn > Mn > Ni. Most studies display logarithmic CI values but for this study, basic CI was chosen to better observe the fluctuations in metal partitioning.

CI for each month in three sites was also individually compared in order to evaluate spatial evolution (Figure 3). Discrete CI at Bougival was found to be significantly higher than at Triel ($p = 0.011$) for all metals except for Cd, Cr and Pb which were excluded from the comparison because many dissolved concentration values at Marnay were lower than the quantification limit (QL). Nevertheless, no difference was found between discrete metal partitioning at Marnay when compared to Bougival and Triel ($p > 0.05$) because CI variation at Marnay was very high.

Table II.3 Summary of metal partitioning at the three studied sites (in $L.g^{-1}$), "discrete CI" is the ratio between concentration of a given metal in the solid fraction to the dissolved fraction (water collected by discrete sampling and filtered at 0.45 μm) and "time-integrated CI" is the ratio between concentration of a given metal in the settleable suspended particles collected by a sediment trap to the labile fraction measured with the Diffusive Gradient Thin (DGT) films. Indicated values correspond to minimum-maximum values with 1st quartile – median – 3rd quartile in parenthesis (n=13 for "discrete CI" and n=10 for "Time-integrated CI). QL: quantification limit.

		Marnay	Bougival	Triel
Cd	"Discrete" CI	<QL	118 - 590 (196 - 284 - 339)	64 - 169 (83 - 116 - 145)
	"Time-integrated" CI	236 - 936 (316 - 364 - 522)	497 - 3591 (647 - 859 - 1160)	131 - 595 (168 - 414 - 567)
Cr	"Discrete" CI	28 - 301 (80 - 132 - 216)	70 - 325 (167 - 186 - 240)	47 - 415 (131 - 230 - 276)
	"Time-integrated" CI	1422 - 3256 (1687 - 2334 - 2868)	1425 - 4461 (2292 - 2914 - 3628)	712 - 9420 (1565 - 2586 - 3326)
Co	"Discrete" CI	26 - 204 (43 - 52 - 87)	31 - 224 (48 - 51 - 78)	23 - 129 (39 - 45 - 50)
	"Time-integrated" CI	302 - 1766 (345 - 532 - 1028)	222 - 760 (336 - 519 - 703)	99 - 452 (132 - 252 - 376)
Cu	"Discrete" CI	16 - 269 (41 - 52 - 103)	52 - 166 (58 - 102 - 115)	21 - 103 (42 - 52 - 85)
	"Time-integrated" CI	153 - 277 (174 - 202 - 241)	349 - 831 (473 - 513 - 567)	223 - 469 (242 - 258 - 300)
Mn	"Discrete" CI	79 - 553 (163 - 189 - 345)	49 - 337 (62 - 133 - 189)	37 - 505 (61 - 93 - 114)
	"Time-integrated" CI	132 - 1665 (158 - 331 - 973)	74 - 887 (97 - 164 - 249)	49 - 208 (60 - 96 - 128)
Ni	"Discrete" CI	6 - 73 (13 - 18 - 42)	11 - 43 (13 - 19 - 22)	0 - 30 (11 - 14 - 20)
	"Time-integrated" CI	97 - 221 (110 - 121 - 147)	75 - 218 (87 - 113 - 128)	41 - 66 (48 - 51 - 55)
Pb	"Discrete" CI	654 - 654 (654 - 654 - 654)	424 - 1325 (701 - 881 - 945)	217 - 749 (483 - 563 - 634)
	"Time-integrated" CI	718 - 5644 (1577 - 2543 - 4023)	2698 - 9863 (3992 - 4459 - 5044)	1494 - 9509 (2803 - 4593 - 5593)
Zn	"Discrete" CI	19 - 577 (53 - 100 - 171)	17 - 165 (46 - 94 - 109)	5 - 360 (29 - 50 - 71)
	"Time-integrated" CI	100 - 1064 (143 - 158 - 413)	205 - 872 (250 - 291 - 536)	60 - 172 (119 - 144 - 156)

When the same test was applied to time-integrated CI, values at Bougival were also found to be significantly higher than at Triel ($p<0.0001$). Moreover, CI at Marnay was also found to be significantly higher than CI at Triel ($p<0.0002$), which was not observed for discrete CI values. As time-integrated CI had lower detection limits, CI for Cd, Cr and Pb were better defined for Marnay. When this statistical comparison was performed on all elements without excluding Cd, Cr and Pb, similar conclusion was obtained.

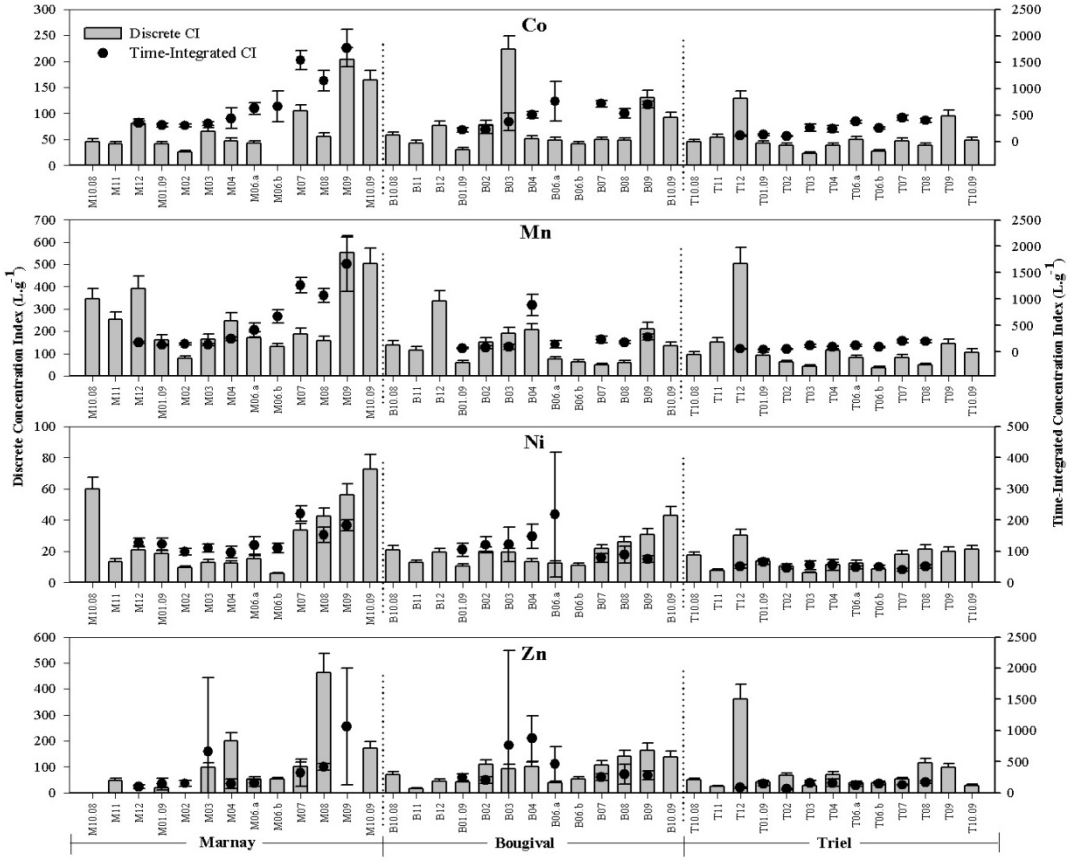
Discrete CI
Time-Integrated CI
Co
Mn
Ni
Zn
Discrete Concentration Index (L.g-1)
Time-Integrated Concentration Index (L.g-1)
Marnay
Bougival
Triel

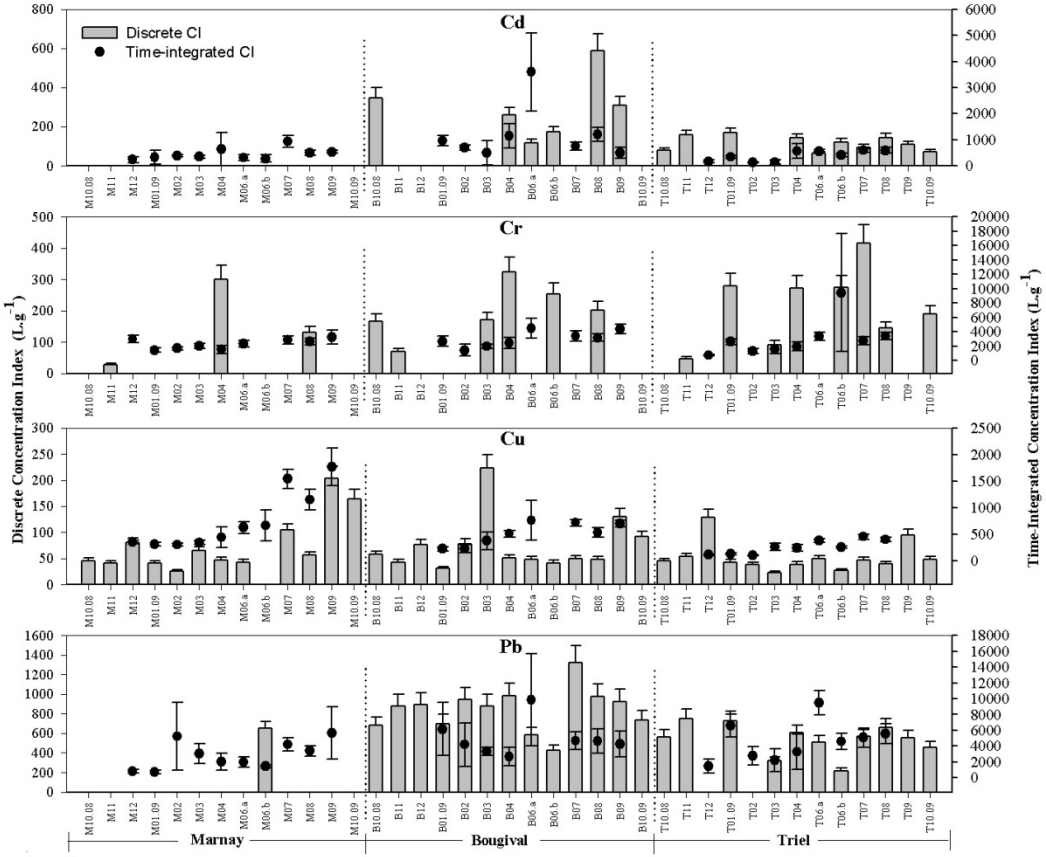

Figure II.2. "Discrete" CI (concentration ratio of metals in SPM (>0.45 µm) to dissolved metals (<0.45 µm) both collected by discrete sampling) (L/g) are presented as bars, indicating "discrete" CI from Marnay, Bougival and Triel from left to right from October 2008 to October 2009. "Time - Integrated" CI (concentration ratio of metals in SPM collected in sediment trap to labile metals measured by DGT) (L/g) are presented as dotted line indicating "time-integrated" CI from Marnay, Bougival and Triel for each month during sampling from December 2008 – September 2009 (Indicated month corresponding to collection time with deployment time the month befor

Individual CI values were also compared in order to identify temporal variation during the one-year campaign (Figure II.3). ln general, temporal variations were higher at Marnay than at Bougival and Triel, except for a few extreme events where CI values increased dramatically at the two downstream sites. Indeed, there was a high variation of discreteCI values for five elements, Co, Cu, Mn, Ni and Zn at Marnay that wassignificantly less visible at Triel: at Marnay, relative standard deviations for discreteCI were 69%, 84% and 73% for Co, Cu and Ni, respectively whereas at Triel, RSD for discreteCI were 54%, 44% and 51% and for Co, Cu and Ni, respectively. These higher variations of discrete CI values at Marnay compared to Triel were also observed for time-integratedCI for Cu and Ni. RSD for time-integrated CI at Marnay were 102%, 29% for Co and Ni, respectively and at Triel, RSD for time-integrated CI at Triel were 51%, 12% for Co andNi, respectively. In addition to Co, Cu and Ni, Mn and Zn average values of time-integrated CI decreased at Triel compared to those at Marnay. This evolution was not observed on average values of discrete CI for Mn and Zn. Cr, Cd and Pb were not compared because most of their discrete CI at Marnay was lower than QL.

Observing the different trends on temporal variation of CI, it was possible to divide the metals in two groups. The first group consisted of Co, Mn, Ni, and Zn with a significantly higher discrete and time-integrated CI at Marnay than at Triel notably for the summer months going from July to October. The second group included Cd, Cr, Cu and Pb. Due to discrete CI at Marnay below quantification limits for these metals, observations are made on time-integrated CI. These metals have relatively comparable CI values between Marnay and Triel both in low and high flows, with higher CI at Bougival during certain periods. The only period where Cd displayed discrete CI at Marnay higher than at Triel was on the month of October 2008. Discrete CI of Cr multiplied up to six to ten folds in one site between two different periods. Values increased from 27±3.9, 70±9.9, and 47±6.7 at Marnay, Bougival and

Triel, respectively on the month of November 2008 to 301±42.8, 325±46.3 and 272±38.8 on April 2009, an increase of 11, 5 and 6 times at Marnay, Bougival and Triel, respectively.

4 Discussion

4.1 Discrete vs time-integrated concentration indexes

The comparison between discrete and time-integrated metal concentration index (CI) originated from the need of an environmental indicator representative of the medium and long-term trend in the milieu. As frequency of discrete sampling for metal monitoring is often limited by labor factors, this study was aimed at considering time-integrated metal concentration index as an option. Difficulties faced in measuring CI for Cd, Pb and Cr due to low dissolved concentrations was overcome by using DGT that concentrates labile metals over a period of time. Passive and time-integrated samplers also hold great potential in the cross-validation of biological accumulation under field condition (Vignati et al., 2009; Bourgeault et al, submitted). Nevertheless, the relatively high variability using the DGT method (supporting information) must be that causes integrative CI values to have large uncertainty levels must be kept in mind.

The authors are aware that the two CI values do not represent the same partitioning, mostly because dissolved metals do not coincide with labile metals. Some inert dissolved metal complexes are not sampled by DGT. Consequently, time-integrated CI calculated using labile metals measured by DGT would result in higher values CI than discrete CI, and the difference is amplified for metals with a low lability in water. This would be the reason why Cu, Zn and Co ranked differently between discrete and time-integrated CI.

In order to further investigate whether time-integrated CI could be representative as an environmental indicator, partitioning evolution between sites and along the year was investigated. Statistical tests performed previously in section 3.3 showed that time-integrated metal partitioning is more effective in differentiating spatial evolution. As physico-chemical parameters between the three sites are significantly different, metal partitioning at the three sites are also expected to vary. Differences in CI values between Marnay and Triel were not significant when evaluated with discrete values whereas it was considered different when comparing time-integrated values. Regarding temporal variation, Co, Mn and Ni had significantly higher discrete and time-integrated CI at Marnay than at Triel notably for the summer months going from July to October. On the other hand, Cr and Cu showed relatively stable discrete and time-integrated CI values between Marnay and Triel both in low and high flows, with possible higher CI at Bougival during certain periods. This similarity of temporal variation between discrete and time-integrated CI means that to a certain extent, one month time-integrated CI is capable of illustrating temporal variation of metal partitioning in the water column.

The biggest challenge in performing environmental monitoring is the representativity of samples in respect with spatial and temporal evolution. Collected samples are expected to represent the water column without being over or under-magnified by extreme events or sudden variations. Although discrete CI captures instant variations that may be significantly different, variations are irregular depending on sampling period and thus general trend is hardly observable. The difference observed when comparing discrete and time-integrated CI in this study suggest that although time-averaged CI gives averaged and consequently "buffered" values,it averages short-term variation and enhances sustainable and medium to long-term variation in a given site.

4.2 Urbanization impacts observed by time-integrated CI

Recent studies showed that metal speciation in the solid phase (Priadi et al., 2011) and furthermore metal accumulation in aquatic species (Bourgeault et al., submitted) were modified downstream of the urbanized Greater Paris Region. With this study, change in land use not only affects metal speciation but also partitioning between the solid and the dissolved phase of urban-enriched metals. Previously discussed results demonstrated difference of temporal variation between upstream and downstream (smaller standard variation for the upstream Marnay data set compared to the Triel data set for Co, Cu and Ni) and higher discrete and time-integrated CI at Marnay from July to October for Co, Mn, Ni, and Zn. Urbanization was likely to affect metal partitioning in the Seine River. This impact is evidenced by time-integrated CI differences between upstream and downstream of the Greater Paris Region observed for enriched metals above. In opposite, such difference was not observed for Cr, a non-enriched metal in the Seine River despite the physico-chemical evolution on a given period from Marnay to Triel.

The behavior of metals enriched by anthropogenic activities downstream seems to be controlled by different parameters compared to metal behavior at upstream site. This is seen both through statistical differences between CI at Marnay and Triel and the higher fluctuating CI at Marnay compared to Triel. Spearman correlation test (significancy level $p<0.05$) were performed separately between Marnay representing the non-urban site, and Bougival and Triel, representing the anthropogenic sites to further investigate key factors affecting metal behavior in the water column. No significant direct correlation between CI and the measured physico-chemical parameters was found. This would be due to differences in governing processes and response level between metal concentration in the solid and the dissolved fraction. While no significant correlation was either found between solid metals and physico-chemical parameters, dissolved metals appeared to be correlated to some water parameters.

Higher temporal variation in Marnay compared to Triel would likely be due to dissolved metal concentration at Marnay being more correlated with flow-related parameters which can fluctuate significantly. Upstream, correlations of some dissolved metals with conductivity were relatively high (Cu r^2=0.657; Mn r^2=0.699; Ni r^2=0.804) while being negatively correlated with discharge (Cu r^2=-0.736; Mn r^2 =-0.813; Zn r^2=-0.688). Downstream, dissolved metal concentrations were less correlated with fluctuating flow-related parameters and were more correlated with redox-related parameters such as DOC (Co r^2=0.655; Cu r^2=0.469; Mn r^2= 0.507; Ni r^2= 0.574) and temperature (Cd r^2=0.531; Cu r^2=0.523; Mn r^2=0.602; Pb r^2=0.724) while displaying negative correlation with pH (Cd r^2=-0.608; Co r^2=-0.552; Cu r^2= -0.805; Mn r^2= -0.697; Pb r^2= -0.501). Higher temporal fluctuations of CI at Marnay compared to Triel may be explained by correlation of metal concentrations with these different water parameters. As discharge varies considerably compared to DOC, temperature and pH, metal concentration at Marnay would also vary in a higher extent than at Bougival and Triel. Downstream, dissolved metal concentrations seemed more affected with sorption process. Their concentrations are more correlated with DOC, temperature and pH than at Marnay. These three parameters are known to control adsorption and desorption reactions on surfaces. Temperature and pH are known to control point zero charge (PZC) of adsorption on many mineral surfaces (Dong et al., 2007; Li et al., 2009) and DOC is known to form complexes with available dissolved metals (Pernet-Coudrier et al., 2008). Adsorption to solid phase may likely be an important process controlling fluctuation of metal partitioning and mobility in the water column downstream.

5 Conclusion

Comparison of discrete and time-integrated metal partitioning in the water column of the Seine River demonstrated the capability of time-integrated CI to represent spatial and temporal variation of metal variation trend. Although it is recognized that time-integrated CI does not measure the exact same pool as discrete CI, time-integrated CI could be useful to study medium and long-term trend of metal partitioning in river systems related to urbanization, reducing the labor costs needed to obtain representative discrete metal sampling. It could also be related to bioaccumulation, which is also a time-integrated phenomenon. Further investigation of time-integrated CI should be performed on other watersheds to study the effectiveness of this method on other water systems.

References

Ayrault S., Priadi C., O. Evrard, Lefèvre I., and Bonté P, Silver and thallium historical trends in the Seine River basin. Journal of environmental monitoring : JEM 2010; 12(11), 2177-85

Bibby RL, Webster-Brown JG. Characterisation of urban catchment suspended particulate matter (Auckland region, New Zealand); a comparison with non-urban SPM. Science of The Total Environment 2005; 343: 177-197.

Billen G., Silvestre M., Barles S., J. M. Mouchel, J. Garnier, F. Curie and P. Boët, in Eau Seine Normandie, ed. Piren-Seine, Paris, Editon edn., 2009, vol. 7.

Bourgeault A., C. Gourlay-Francé and M. H. Tusseau-Vuillemin, Modeling the effect of water chemistry on the bioaccumulation of waterborne cadmium in zebra mussels. Water Research 2010; 29, 2182-2189

Bourgeault A., C. Gourlay-Francé, C. Priadi, S. Ayrault and M.-H. Tusseau-Vuillemin, Bioavailability of particulate metal to zebra mussels: Biodynamic modeling shows that assimilation efficiencies are site-specific. Aquatic Toxicology, submitted.

Bourgeault A, Gourlay-Francé C, Vincent-Hubert F, Palais F, Geffard A, Biagianti-Risbourg S, et al. Lessons from a transplantation of zebra mussels into a small urban river: An integrated ecotoxicological assessment. Environmental Toxicology 2010; 25: 468-478.

Buzier, R., M.-H. Tusseau-Vuillemin, and J.-M. Mouchel. Evaluation of DGT as a metal speciation tool in wastewater, Science of The Total Environment, 2006; 358: 277-285.

Chiffoleau J-F, Cossa D, Auger D, Truquet I. Trace metal distribution, partition and fluxes in the Seine estuary (France) in low discharge regime. Marine Chemistry 1994; 47: 145-158.

Davison W, Zhang H. In-situ speciation measurements of trace components in natural waters using thin-film gels. Nature 1994; 367: 546-548.

Dong D-m, Zhao X-m, Hua X-y, Zhang J-j, Wu S-m. Lead and Cadmium Adsorption onto Iron Oxides and Manganese Oxides in the Natural Surface Coatings Collected on Natural Substances in the Songhua River of China. Chemical Research in Chinese Universities 2007; 23: 659-664.

Dunn RJK, Teasdale PR, Warnken J, Arthur JM. Evaluation of the in situ, time-integrated DGT technique by monitoring changes in heavy metal concentrations in estuarine waters. Environmental Pollution 2007; 148: 213-220.

Elbaz-Poulichet F, Seidel J-L, Casiot C, Tusseau-Vuillemin M-H. Short-term variability of dissolved trace element concentrations in the Marne and Seine Rivers near Paris. Science of The Total Environment 2006; 367: 278-287.

Gasperi J, Garnaud S, Rocher V, Moilleron R. Priority pollutants in wastewater and combined sewer overflow. Science of The Total Environment 2008; 407: 263-272.

Hochella MF, White AF. Mineral-water interface geochemistry - an overview. Reviews in Mineralogy 1990; 23: 1-16.

Koelmans AA, Radovanovic H. Prediction of trace metal distribution coefficients (K-D) for aerobic sediments. Water Science and Technology 1998; 37: 71-78

Le Cloarec, M.F.; Bonte, P.H.; Lestel, L.; Lefèvre, I.;Ayrault, S., Sedimentary record of metal contamination in the Seine River during the last century. Physics and Chemistry of the Earth, Parts A/B/C, doi:10.1016/j.pce.2009.02.003.

Li Y, Wang XL, Huang GH, Zhang BY, Guo SH. Adsorption of Cu and Zn onto Mn/Fe Oxides and Organic Materials in the Extractable Fractions of River Surficial Sediments. Soil and Sediment Contamination: An International Journal 2009; 18: 87 - 101.

Lofts S, Tipping E. Solid-solution metal partitioning in the Humber rivers: application of WHAM and SCAMP. The Science of The Total Environment 2000; 251-252: 381-399.

Luoma SN, Rainbow PS. Metal Contamination in Aquatic Environments. Cambridge: Cambridge University Press, 2008.

Meybeck M, Lestel L, Bonte P, Moilleron R, Colin JL, Rousselot O, et al. Historical perspective of heavy metals contamination (Cd, Cr, Cu, Hg, Pb, Zn) in the Seine River basin (France) following a DPSIR approach (1950-2005). Science of The Total Environment 2007a; 375: 204-231.

Ng B, Turner A, Tyler AO, Falconer RA, Millward GE. Modelling contaminant geochemistry in estuaries. Water Research 1996; 30: 63-74.

Nguyen HL, Leermakers M, Osán J, Török S, Baeyens W. Heavy metals in Lake Balaton: water column, suspended matter, sediment and biota. Science of The Total Environment 2005b; 340: 213-230.

O'Connor DJ, Connolly JP. The effect of concentration of adsorbing solids on the partition coefficient. Water Research 1980; 14: 1517-1523.

Ciffroy P., V. Mataix, J. Taconnet, A. Estèbe, D. Thévenot, O. Bourguignon, Z. ldlafkih, M. Meybeck, . Intercomparaison de méthodes d'échantillonnage des matières en suspension en milieu fluvial : application à la mesure de la concentration en micropolluants métallique, Comparison of methods for sampling suspended matter in rivers: application to measurement of particulate metals Hydroécol. Appl. 1999; 11: 71-102.

Pernet-Coudrier B, Clouzot L, Varrault G, Tusseau-Vuillemin MH, Verger A, Mouchel JM. Dissolved organic matter from treated effluent of a major wastewater treatment plant: Characterization and influence on copper toxicity. Chemosphere 2008; 73: 593-599

Priadi C., S. Ayrault, S. Pacini, P. Bonte. Urbanization impact of the Greater Paris Region on metal mobility in suspended sediments in the Seine River, France: Role of iron oxides. International Journal of Environmental Science and Technology. 2011; 8 (1), 1-18.

Siaap, Dossier du maitre d'ouvrage [online]. http://www.debatpublic-station-epuration-seineaval.org/docs/pdf/dossier-mo/doc-synthese-2.pdf [Accessed Access Date 2010]

Stumm W, Morgan JJ. Aquatic Chemistry. Toronto: Wiley-Interscience, 1981.

Tessier L. Transport et Caracterisation des Matières en Suspension dans le bassin versant de la Seine: Identification de signatures naturelles et anthropiques. Ecole Nationale des Ponts et Chaussées, Marne la Vallée, 2003, pp. 245.

Thévenot D, Lestel L, Tusseau-Vuillemin M-H, Gonzalez JL, Meybeck M. Les Metaux dans le bassin de la Seine. In: Piren-Seine, editor. Eau Seine Normandie. 7, Paris, 2009.

Thévenot D, Moilleron R, Lestel L, Gromaire M-C, Rocher V, Cambier P, et al. Critical budget of metal sources and pathways in the Seine River basin (1994-2003) for Cd, Cr, Cu, Hg, Ni, Pb and Zn. Science of The Total Environment 2007; 375: 180-203.

Traina, S.J., J. Novak, and N.E. Smeck. An ultraviolet absorbance method of estimating the percent aromatic carbon content of humic acids. J. Environ. Qual.1990; 19:151–153

Tusseau-Vuillemin, M.-H., Dispan, J., Mouchel, J.-M., Servais, P.(2003). Biodegradable fraction of organic carbon estimated in oxic and anoxic conditions. Water Research. 37(9), 5.

Tusseau-Vuillemin, M. H., R. Gilbin, E. Bakkaus, and J. Garric. Performance of diffusion gradient in thin films to evaluate the toxic fraction of copper to Daphnia magna, Environmental Toxicology and Chemistry 2004; 23: 2154-2161.

Tusseau-Vuillemin MH, Gourlay C, Lorgeoux C, Mouchel JM, Buzier R, Gilbin R, et al. Dissolved and bioavailable contaminants in the Seine river basin. Science of The Total Environment 2007; 375: 244-256.

Unsworth ER, Warnken KW, Zhang H, Davison W, Black F, Buffle J, et al. Model predictions of metal speciation in freshwaters compared to measurements by in situ techniques. Environmental Science & Technology 2006; 40: 1942-1949.

Vignati DAL, Valsecchi S, Polesello S, Patrolecco L, Dominik J. Pollutant partitioning for monitoring surface waters. TrAC Trends in Analytical Chemistry 2009; 28: 159-169.

Zwolsman JJG, van Eck GTM. Geochemistry of major elements and trace metals in suspended matter of the Scheldt estuary, southwest Netherlands. Marine Chemistry 1999; 66: 91-111.

Chapitre 3 – L'impact de l'urbanisation sur la mobilité des métaux dans la matière en suspension fluviale: Rôle des oxydes

Avant-Propos

Dans le chapitre précédent, nous avons observé que pour les métaux d'origine surtout anthropique, les métaux particulaires représentent 40-95% des métaux dans la colonne d'eau. Dans ce chapitre, l'évolution spatiale et temporelle de la répartition des métaux dans les matières en suspension (MES) collectées dans les trappes sera étudiée de plus près en utilisant la méthode d'extraction séquentielle certifiée par la méthode certifiée par le Bureau Communautaire des Références (BCR). Le BCR définit leurs fractions extraites comme étant la fraction échangeable, la fraction réductible, la fraction oxydable et la fraction résiduelle (Pueyo et al., 2001). Dans cette étude, les résultats des métaux extraits (Cd, Cr, Cu, Ni, Pb, Zn) dans chaque étape sont accompagnés avec les éléments majeurs de la matrice (Al, Ca, Fe,

Mg, Mn). L'impact de l'urbanisation sur la répartition des métaux sera mis en évidence ainsi que la préférence des métaux dans une ou plusieurs phases opérationnellement définies. **Une version révisée de ce chapitre a été publiée à *International Journal of Environmental Science and Technology* sous le titre « *Urbanization impact on metal mobility in riverine suspendedsediment: Role of metal oxides*» (Priadi et al. 2011, 8(1), 1-18)**.

1 Introduction

In the last decade, metal contamination in urban continental aquatic system has been a growing concern. Impacts of anthropogenic activities on metal contamination in a watershed are far from being insignificant (Horowitz et al., 1999; Davis et al., 2001; Taylor and Owens, 2009). They are known to generate a considerable amount of metal to the environment through various pathways including atmospheric particles (Azimi et al., 2005), urban runoff (Gromaire-Mertz et al., 1999), industrial and wastewater effluents (Buzier et al., 2006) and urbanization impacts on metal contamination concern watersheds inhabiting more than 50% of the world population (Meybeck, 2003).

The Seine River watershed is home to 25-30% of French industries, 23% of French constantly increasing urban and agricultural activities contribute to metallic aquatic contamination. In the last two decades, many institutions carried out actions in the Seine River to understand pollutant behaviour with parallel decontamination. Since then, the concentration of trace elements such as the Cd, Cr, Cu, Ni, Pb, and Zn showed a significant decline measured in dated sediment cores (Le Cloarec et al., In Press). Nevertheless, due to very high anthropogenic pressures and very limited dilution power, the Seine River downstream of Greater Paris is still among the world's most contaminated rivers (Meybeck et al., 2007). Despite the decreasing concentrations in the solid phases, Elbaz-Poulichet et al.

(2006) still found moderate contamination of dissolved metals in the water column of the Marne and Seine Rivers.

Various studies contributed to the understanding of metal behaviour in different compartments due to the dynamic metal distribution between different phases in the water column. In the Seine River, the value and dynamics of dissolved Mn, Cu, Cd and Mo were partly attributed to variation in redox condition (Elbaz-Poulichet et al., 2006). Short-time extreme variation of dissolved Zn is also observed using high-definition sampling (Pepe et al., 2008). Depending on the element, the solid fraction holds 50-90% of the anthropogenic metal stock (Cd, Cu, Cr, Zn, and Pb) in the Seine River water column (Thévenot et al., 2007). Furthermore, floodplain and bed sediments contain a large stock of historical deposit and contamination. Therefore, this solid fraction plays an important role in metal contamination as it may release heavy metal to the water column, as well as scavenging them. It is then necessary to understand the behaviour and distribution of trace elements in the different solid phases and their mobility towards the dissolved fraction. The latter, more specifically the labile fraction, represent the bio-available fraction. Moreover, the solid fraction may hold evidences of metal sources and formation processes. The study of metal speciation in the solid fraction may therefore help us understand the contribution of different sources and biogeochemical processes in the formation and mobility of metal in the solid phase.

Metal speciation studies such as the sequential extraction are often performed on mining-impacted rivers (da Silva et al., 2002; Galan et al., 2003; Audry et al., 2006; Lesven et al., 2009) but rarely on non-mining urban watershed even though urban anthropogenic activities can generate a specific characteristic of metal speciation in a water course (Garnaud, 1999; Dali-Youcef et al., 2004; Carter et al., 2006; Sutherland and Tack, 2007). Interpretation are also rarely compared by simultaneous extraction of major elements originating from the

metal-bearing particles including Ca, Fe, Mn, and Mg, except for a few studies (Gagnon et al., 2009; Li et al., 2009; Vieira et al., 2009). Tongtavee et al. (2005) have shown that the analysis of extracted major elements is of great interest to understand lead speciation in soils affected by mining activities.

Despite the Seine River basin great economic importance and the many articles published on contents and behaviour in dissolved and labile fraction of trace metals in the Seine River (Elbaz-Poulichet et al., 2006; Tusseau-Vuillemin et al., 2007; Chen et al., 2009; Jouvin et al., 2009), trace metal speciation on solid fraction were only conducted on average suspended matter from 3 sites (Taconet, 1996) and urban source-related samples (Garnaud, 1999). According to these studies, metal mobility can be ranked as follows: Cu<<Cd<Pb<Zn. Nevertheless, these studies do not detail the temporal variation of the metal distribution, and spatial variation was concluded from only one sampling in three sites.

This study is therefore aimed to investigate anthropogenic impact on the temporal and spatial variability of metal speciation and understand heavy metal mobility in the Seine River suspended particulate matter (SPM) through the BCR sequential extraction with preliminary study focusing on efforts on reducing working weight. A one-year study was conducted in three characteristic sites of the Seine River. The solid speciation of six metals (Cd, Cr, Cu, Ni, Pb and Zn) along with nine major elements was determined.

2 Materials and methods

2.1 Location

Seven monthly samplings from December 2008-August 2009 were conducted in the 3 study sites along the Seine River at Marnay, Bougival and Triel (Figure I. 5).

2.2 Sampling and sample treatment

Materials and sample handling were done in a systematic clean method with details in Chapter II, section 2.

2.3 Solid phase analyses

2.3.1 Bulk digestion

Metal contents were obtained through total chemical digestion with details in Chapter II, section 2.

2.3.2 BCR sequential extraction

Each BCR sequential extraction was performed on duplicates of 0.25 g of sediment following Revised BCR (Pueyo et al, 2001) with extra rinsing to overcome the difficulty due to the smaller amount of extracting solution used. Extraction protocol is summarized in Table III. 1.

Due to a lack of end-to-end shaker, shaking was performed using platform orbital shaker during 16 h at 300 rpm (Heidolph vibramax 100). The speed was chosen to keep the samples well in suspension without shaking excessively to avoid over-extraction. Due to the relatively low quantity of samples used, separating the extracted solution without removing the sample was a difficult task. A second rinsing was applied using half the normal volume of the same extracting solution before rinsing samples with water. Each extraction batch was accompanied by a duplicate of the BCR 701 (Bureau Communautaire de Recherches, Gent, Belgium), a certified lake sediment for sequential extraction.

Table III. 1 - Summary of the BCR sequential extraction protocol after Pueyo et al. (2001) except step 4 with aqua regia, added to complete protocol

	Reagent	Operationally defined fraction	Nominal target phase	experimental condition
step 1	0.11 mol l^{-1} CH_3COOH	exchangeable	soluble and exchangeable cations and carbonates	room temperature, constant shaking 16 h
step 2	0.5 mol l^{-1} $NH_2OH.HCl$ at pH 1.5	reducible	Fe-Mn oxyhydroxides	room temperature, constant shaking 16 h
step 3	H_2O_2 (85°C) then 1.0 mol l^{-1}	oxidisable	organic matter and sulfides	room temperature 1h, occasional shaking, then agitation 85°C, 1h (two times)
	CH_3COONH_4			room temperature, constant shaking 16 h
step 4	aqua regia	residual		room temperature, constant shaking 16 h

2.4 Analytical procedure

Major and trace metal concentration were determined in total and sequential extraction samples using Inductively Coupled Plasma Quadrupolar Mass Spectrometry (ICP-QMS) with details in Chapter 2, section 2.

Major elemental bulk analysis including Ca, Si, Al, Fe, Mg, S, K, P, and Ti were performed with micro (50 µm) X-ray fluorescence (XRF) (Microfocus x-ray source IFG X-1) through measurements of pressed pellets (diameter 0.5 cm, average weight 0.02 g). Measurements were calibrated with at least 5 reference materials (USGS Mn Nodule A1, USGS Marine mud MAG-1, USGS jasperoid GXR-1, IAEA lake sediment SL1 and IAEA Soil-7) and sample analysis was done in duplicate to compensate for possible sample heterogeneity.

Particulate organic carbon (POC) and nitrogen (PON) contents were measured in 0.25 mg samples previously decarbonated by 3.4 ml of 1 N HCl. Decarbonation comprises of 4 cycles of addition of HCl solution, 20 mn of 300 rpm orbital shaking, 3000 rpm centrifugation, solution separation. Samples were weighed precisely and analysed through a Carbon Hydrogen and Nitrogen (CHN) analyser (Thermoflash EA 1112 series).

2.5 Enrichment factors

Enrichment factors (EF) were calculated bynormalizing concentrations to Al and using localbackground values established for the Seine river watershed by (Thévenot et al., 2002) throughmeasurements of selected river mouth values based onan Al content of 33000 mg/kg. Assembled backgroundvalues are shown on Table 2 and formula is shown in Equation 1. The EF values should be evaluated keepingin mind the shortcomings of this approach (Reimannand de Caritat, 2005; Karbassi et al., 2008). Here, localbackground values were preferred to continental crustconcentrations, due to the specificity of thecarbonaceous Seine River basin geology.

Table III.2 - Background concentration (mg.kg-1) in selected river mouth values (Poses estuary) established by Thévenot et al. (2002)

	Zn	Cd	Pb	Cr	Ni	Cu	Fe	Al
Background in Poses ($mg.kg^{-1}$)	60 ± 10	0.22 ± 0.55	20 ± 3	40 ± 5	16 ± 2	15 ± 5	15000	33000

Assembled background values are shown on Enrichment factors (EF) were calculated bynormalizing concentrations to Al and using localbackground values established for the Seine river watershed by (Thévenot et al., 2002) throughmeasurements of selected river mouth values based onan Al content of 33000 mg/kg. Assembled backgroundvalues are shown on Table 2 and formula is shown in Equation 1. The EF values should be evaluated keepingin mind the shortcomings of this approach (Reimannand de Caritat, 2005; Karbassi et al., 2008). Here, localbackground values were preferred to continental crustconcentrations, due to the specificity of thecarbonaceous Seine River basin geology.

Table III.2 and formulae is shown in Equation 1. The EF values should be evaluated keeping in mind the shortcomings of this approach (Reimann and de Caritat, 2005; Karbassi

et al., 2008). Here, local background values were preferred to continental crust concentrations, due to the specificity of the carbonaceous Seine River basin geology.

$$EF = \frac{[Me]_{sample} / [Al]_{sample}}{[Me]_{background} / [Al]_{background}}$$

Equation III. 1 - Enrichment factor (EF) where [Me]sample = metal concentration in sample, [Al]sample = aluminum concentration in sample, [Me] background = metal concentration in background value and [Al] background = aluminum concentration in sample

2.6 Scanning electron microscopy analyses

Cartography of suspended sediment were collected at 6-7 kV using in backscattered electrons imaging mode on a Zeiss ULTRA scanning electron microscopy (SEM) coupled with field emission gun (FEG) at the IMPMC, Paris, France. Energy Dispersive X-ray Spectroscopy (EDXS) data were collected at the same electron beam-voltage using a BRUKER AXS Si-drift detector. A supplementary image coupled with its EDS spectrum is also demonstrated. This latter image was obtained with JEOL JSM 840 SEM coupled to an X-ray microanalysis system from Princeton Gamma Tech (PGT) at LSCE.

3 Results and Discussion

3.1 Extraction recoveries, analytical uncertainties and limit of detection

Extraction and analytical processes were validated using various standard materials. Extraction recovery (recovery in Table III. 3) was calculated by comparing the average concentration of our BCR sequential extraction on 0.25 g (n=4) with the BCR certified values comprising of Zn, Cd, Pb, Cr, Ni and Cu in the exchangeable, reducible and oxidisable fraction. Recovery value is accompanied with standard deviation (SD in Table III. 3).

Analytical detection limits (DL in Table III. 3) are two times the blank value of sample that went to the same preparation, extraction, and analytical treatment.

For the trace elements, SDvalues showed that Cd and Cu shows a lowreproducibility with SD ranging from 13-19 % for Cdand 13-16 % for Cu. Cd concentrations are relativelylow, which may be prone to contamination during theextraction. This is reflected in our recovery levels whichare higher than total digestion values in downstreamsites, 99+12 and 93+19 at Bougival and Triel,respectively. Ca presented difficulties as it is presentin extremely high quantity in the exchangeable fractionand may often pose difficult analytical problems.

Table III. 3 - Average recovery and its standard deviation (Recovery and SD in %) of BCR sequential extraction in this study performed on the BCR-701 sediment compared with concentration of trace elements, certified by the BCR (n=4). Analytical detection limits (DL in mg.kg^{-1}) are calculated through 2 times the average blank values.

	Zn			Cd			Pb			Cr			Ni			Cu		
	recovery	±	SD	DL	recovery	±	SD	DL	recovery	±	SD	DL	recovery	±	SD	DL	recovery	±	SD	DL
Exchangeable fraction	98	±	3	0.5	104	±	6	53	121	±	7	3.7	118	±	9	32	95	±	9	0.5	115	±	5	20
Reducible fraction	93	±	8	904	82	±	9	26	99	±	2	46	91	±	6	394	96	±	7	208	92	±	7	149
Oxidisable fraction	82	±	11	368	86	±	26	185	58	±	23	53	90	±	4	115	81	±	10	100	81	±	7	56

Table III. 4 - Average recovery and standard deviation (Recovery SD in %). Recovery compares the total extracted metals in the four fractions with the BCR sequential extraction procedure compared to metal concentration obtained by total digestion (n=7)

	Zn			Cd			Pb			Cr			Ni			Cu			Mn			Fe			Ca			Mg			Al		
	recovery	±	SD	recovery	±	SD	recovery	±	SD	recovery	±	SD	recovery	±	SD	recovery	±	SD	recovery	±	SD	recovery	±	SD	recovery	±	SD	recovery	±	SD	recovery	±	SD
Marnay	65	±	6	98	±	13	79	±	8	29	±	4	51	±	2	88	±	13	60	±	9	46	±	10	81	±	8	25	±	4	9	±	3
Bougival	84	±	10	99	±	12	103	±	10	41	±	5	62	±	6	97	±	11	87	±	17	70	±	23	86	±	8	41	±	6	15	±	1
Triel	77	±	13	93	±	19	104	±	12	36	±	3	58	±	6	40	±	5	91	±	21	72	±	13	119	±	30	35	±	4	14	±	1

Nevertheless, the recovery level between the 4 extraction phases of the BCR and our total bulk extraction depends on the metal's properties and the site's location. For most cases, more than 90 % of Cd and Pb are extracted by the BCR extraction, except for Pb in Marnay which has a slightly lower recovery, at 79±7 %. More than 80% of Cu, Zn, and Ca are extracted with the BCR sequential extraction except for Zn at Marnay where recovery compared to the total digestion is relatively lower, 65±6 %. Zn, Pb, Cr, Ni and Al extracted by the BCR are significantly higher at Bougival than at Marnay. This shows that Zn, Pb, Cr, and Ni could be from natural sources, associated to Al which would be more resistant to chemical extraction. Cr and Ni are probably found in the crystalline phases because only half are extracted by the BCR extraction, 52±2, 62±6, 58±5 for Ni, and even lower for Cr 29±3 41±5 37±3 at Marnay, Bougival and Triel, respectively. For Cd, Cr, Cu, Ni, Pb and Zn, these results agree with most studies using the BCR sequential extraction, although none specified the uncertainty and detection limits for each extraction phase and each element. Larner et al. (2008) stated an extraction efficiency of 70-115%. Nevertheless, these values were incomparable with those from other studies because our total digestion protocol attacks almost 100% of the bulk sediment. Our recovery would then be underestimated compared to recoveries values in other studies where pseudo-total digestion was performed (i.e. Larner et al., 2008). The major elements showed different extractability by the BCR extraction compared to the total bulk digestion, reflecting the different mineral forms in which the major element takes form. The order of extractability from the element less extracted by the BCR to the most extracted is Al< Mg < Fe < Mn < Ca.

3.2 Enrichment Factors

Enrichment factors (EF) of the 7 values at each site were averaged and shown on Figure III. 1. Values showed significant increase in downstream samples for Zn, Cd, Pb and Cu. On the other hand, Cr and Ni show no spatial increase in EF, keeping a relatively steady

value of around 2 from Marnay to Bougival and Triel. These two elements represent metals with the solid phase non-enriched by urban activities. In the case of the Seine River, the evolution of the concentration of the trace elements is also accompanied by an increase in most of the major elements (Table III. 5).

The trend of metal enrichment in suspended sediments is similar with recent studies of metals in the Seine River through analysis of sediment cores and estuarine mussels (Meybeck et al., 2007; Le Cloarec et al., In Press). This shows that SPM collected in this study are representative to the Seine watershed and that these four metals represent metals affected by anthropogenic sources. Urban activities may increase EF in two or even seven folds in the downstream sites, depending on the metals. In average, Cd is the metal most enriched while Zn, Pb and Cu present EF of 6-7.

Metal concentrations at Bougival were not found to be lower than at Triel (Mann-Whitney, $p = 0.983$), despite of the Seine Aval WWTP outlet situated between the two sites. Considering the possible contribution of the WWTP outgoing flow to the metal contamination in the water column, one could have expected that metal concentrations in SPM would be higher at Triel than at Bougival. In 2002, Thévenot et al. (2002) calculated that particulate flux of Cd, Cu and Pb from the Seine-Aval

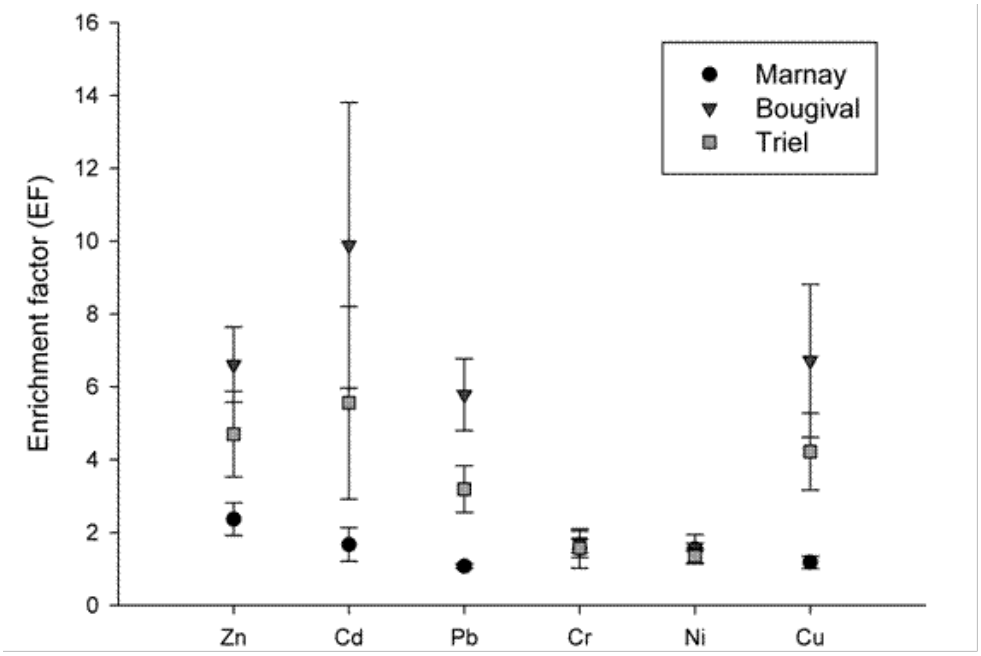

Figure III. 1 - Average enrichment factors during December 2008 until August 2009 for six metals (Cd, Cu, Cr, Ni, Pb, Zn) at the 3 studied sites (Marnay, Bougival, Triel) n=7

WWTP contributed from 2-6% in the river mouth despite of the relatively low SPM concentration in the WWTP outlet water of 28-49 mg/L (Estebe et al., 1998; Meybeck et al., 1998; Thévenot et al., 2007). Through calculations of influx, WWTP treatment efficiency and sludge recovery, Thévenot et al. (2007) established an outflux of 26, 25.5 and 90 $t.y^{-1}$ for Cu, Pb, and Zn respectively. Buzier et al., (2006) also found that WWTP outflux may have a significant impact on the labile metal flux downstream of the outlet in low flow conditions. Ever since these studies were published, an effort was made through construction of numerous WWTP to distribute and relieve the wastewater load of Seine Aval. This finding indicates that improved WWTP are efficient in reducing incoming metal load to the Seine River.

The analysis of the major elements is an important aspect in the interpretation of sequential extraction data as these major phases are likely to be the carrier phase of the trace elements. In order to confirm whether our extraction corresponds to the operationally-defined fraction, the extracted major elements for each step are presented (Fig. 2).

At Bougival and Triel, Ca is more than 90% extracted on the exchangeable fraction, leaving less than 10% extracted in the reducible step and almost no Ca is found in the oxidisable and residual phase. Upstream, the Seine shows a slightly different behaviour where more Ca is found in the reducible fraction.

Unlike Ca, Fe and Al that varies between the three sites, there is no significant difference in the distribution of Mg and Mn at the three sites. Mn takes on a slightly similar behaviour to Ca where around 70% are found in the exchangeable form while Mg contains more oxidisable and residual form. Even though Fe and Mn exist as oxides, the distribution of the two elements is significantly different. Fe is not released in the exchangeable fraction but rather during reducible and residual extraction for Bougival and Triel and mostly in the residual fraction for Marnay.

Table III. 5 - Concentration of average major element contents of suspended particulate matter collected monthly in the sediment trap from December 2008 to August 2009 (n=7)

	POC (%)		PON (%)		Ca (%)		Si (%)		Al (%)		Fe(%)	
Marnay	7.6	± 0.9	0.8	± 0.1	26.5	± 1.0	10.9	± 0.7	3.4	± 0.2	2.1	± 0.2
Bougival	10.0	± 1.9	0.9	± 0.2	18.5	± 1.4	17.4	± 0.8	4.8	± 0.5	3.3	± 0.7
Triel	7.7	± 1.7	0.9	± 0.2	15.4	± 1.7	20.6	± 1.5	4.9	± 0.4	3.4	± 0.5
	Mg ($mg.kg^{-1}$)		P ($mg.kg^{-1}$)		S ($mg.kg^{-1}$)		Mn ($mg.kg^{-1}$)		K ($mg.kg^{-1}$)		Ti ($mg.kg^{-1}$)	
Marnay	5845	± 1288	1582	± 340	1337	± 328	442	± 70.7	8300	± 643	1696	± 299
Bougival	10506	± 1877	4071	± 723	4148	± 798	609	± 133	12040	± 1278	3923	± 1048
Triel	10771	± 2097	4790	± 901	3966	± 1094	721	± 172	13311	± 1565	3378	± 1926

The domination of Ca at Marnay with an average of 26.5% reflects the geological condition of the Seine watershed where 95% being underlain by carbonate rocks (Meybeck et al., 1999). Further downstream, Ca concentration decreases to an average of 18.5% and 15.4% for Bougival and Triel, respectively, and replaced by the general increase of other major elements such as Si, Fe, Mg, P, S, Mn, K and Ti. For example, Si concentration increases from 10.9% at Marnay to 17.4% and 20.6%, Fe average concentration increases from 2.1% to 3.3% in the downstream sites.

A dramatic increase is observed for P and S concentrations at Bougival and Triel compared to Marnay. The impacts of anthropogenic activities on P and S are less well documented but some studies mentioned sources mostly coming from wastewater (Houhou et al., 2009). The increase of P and S may be due to the increase of organic matter. Even though on the average, there is no significant difference between POC at Marnay, Bougival and Triel, but on a monthly basis, Bougival contains higher POC than Marnay and Triel (Mann Whitney Test for 7 months of samples $\alpha = 0.05$). Nevertheless, it is also possible that P and S increase is due to increasing phosphate, sulfate or sulfide species. The increasing Al concentrations downstream underlines the importance of interpreting metal concentration as enrichment factor bynormalization with Al.

3.3 Speciation

Before interpreting extraction results, it is important to note that sediment traps integrate one month of SPM during which the sample may be subjected to evolution of speciation. In the course of a month, SPM sedimenting on the bottom of sediment trap may create reducing conditions, favourizing the formation of reduced forms. This possibility is to be taken into account during the lecture and interpretation of data.

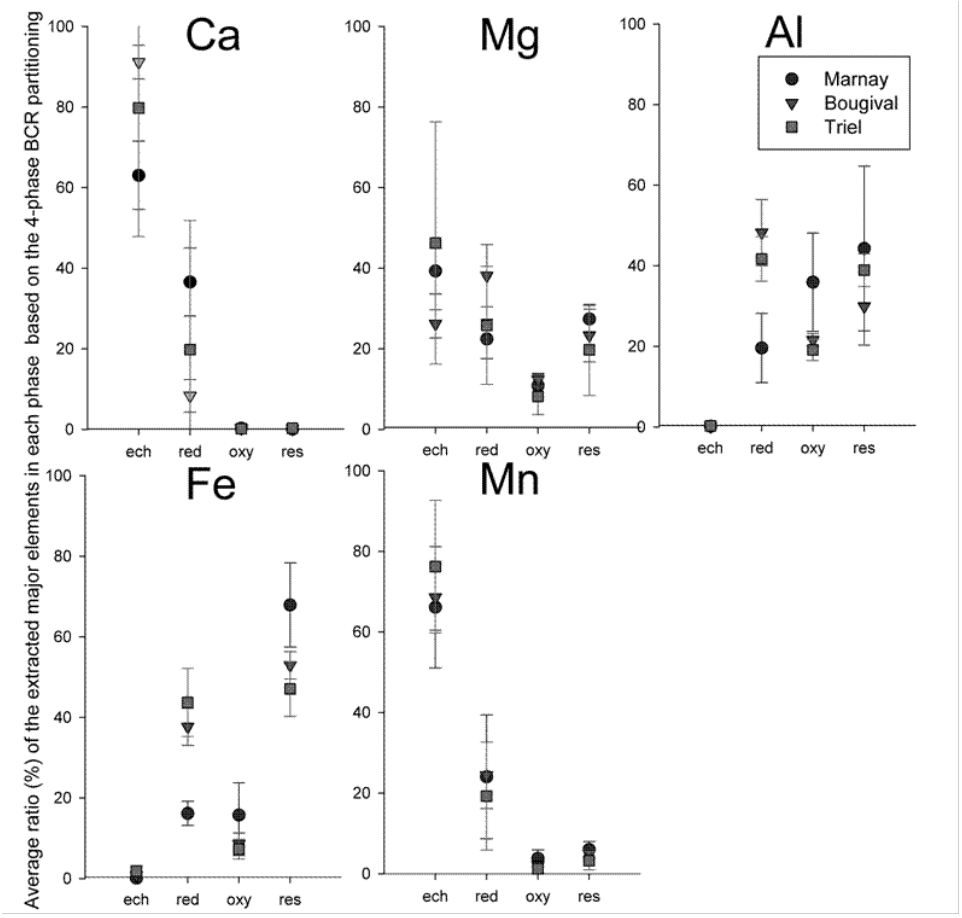

Figure III. 2 - Average ratios of extracted major elements for each BCR sequential extraction phase at the 3 sites (Marnay, Bougival, Triel) (n=7)

First of all, extraction of major elements is interpreted in order to confront operationally-defined phases for each extraction step and extraction reality. A spatial evolution in the Al speciation is observable mostly for the reducible phase (Figure III. 2). This evolution of Al would mean that there is an increase of allochthonous Al coming from the Greater Paris Region. This is also the case for Fe where the reducible proportion increases in the downstream sites. The similarity of Fe and Al where both elements tend to be present mostly in the reducible fraction at Bougival and Triel may mean a similar anthropogenic source. Indeed, Fe and Al are the two most abundant metals (Luoma and Rainbow, 2008) thus becoming the two mostly utilized metals worldwide (USGS, 2010). In 2004, 1370 kt of Al were used in France, mostly in the transportation, construction and packaging sector (AFA).

Nevertheless, this anthropogenic Al possibly present in the reducible fraction only accounts for 30-40% of total BCR extractable Al (Figure III. 2), which in turn only contributes to 14-15% of the total Al in Seine SPM (Annexe 5). This small proportion of reducible and possibly anthropogenic Al would only be around 6% of the total Al and with this uncertainty it is still considered safe to calculate enrichment factors through normalization by Al.

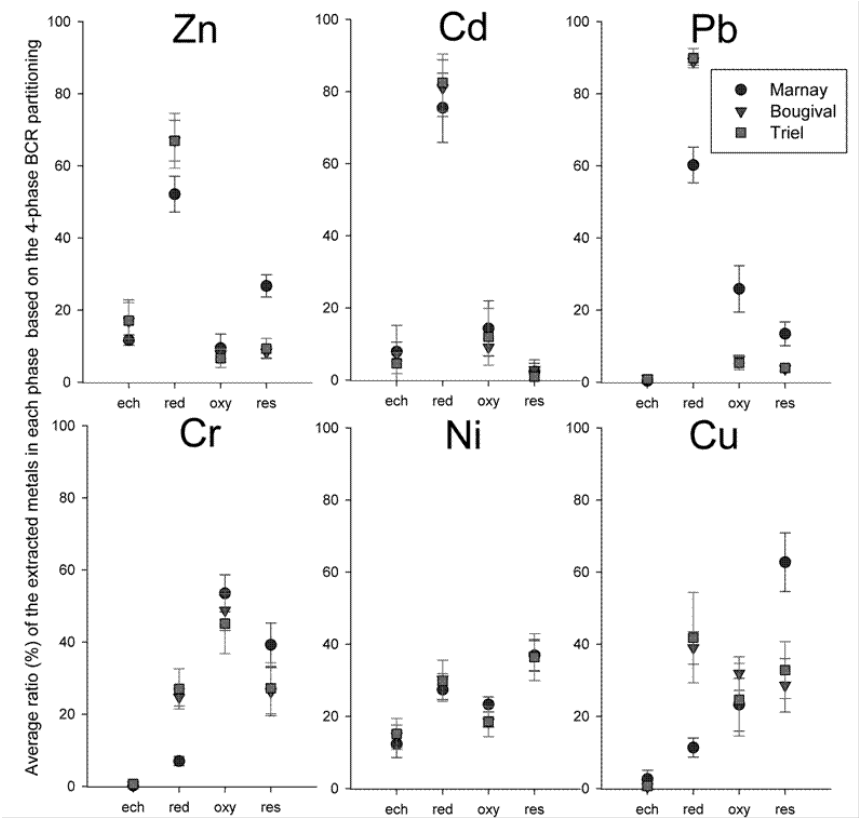

Figure III. 3 - Average ratios of extracted trace elements for each BCR sequential extraction phase of the 3 sites (Marnay, Bougival, Triel) (n=7)

The average distribution of the 6 metals for the 7 monthly sampling is shown in Figure III. 3. As a whole, an evolution from upstream to downstream is significant enough while the difference between Bougival and Triel is less pronounced (Mann Whitney, p= 59%, 49% 85% between Marnay to Bougival, Marnay to Triel and Bougival and Triel, respectively, with H_0 hypothesis is proportion $_{site\ 1}$ = proportion $_{site\ 2}$). Regarding temporal variation, the distribution

at a given site is relatively stable with deviation of around 5% for most metal in certain fractions (n=7), and with a maximum of 10-15% for some metals.

Speciation evolution from Marnay to Bougival and Triel was observed for Zn, Cd, Pb and Cu but not for Cr and Ni. Moreover, these four metals are those demonstrating a significantly higher EF downstream. This implicates that anthropogenic contamination is likely to bring in material with different metal distribution and that variation in the physico-chemical condition downstream leads to a different type of speciation.

The general observation allows us to divide the six metals into 2 distinct groups. The first group constituting of Zn, Cd, and Pb, averages more than 60% in the reducible fraction and even reaching up to 90%. The reducible fraction for these three elements is always significantly higher than the 3 other fractions (t test, α=0.05). These metals are known to be preferably associated with iron oxy-hydroxides (Luoma and Bryan, 1981) which would explain the high proportion found in the reducible fraction. The increasing proportion of these reducible metals rises significantly from upstream to downstream, marking a possible anthropogenic impact. This idea is also supported with the increasing EF as the water reaches Bougival and Triel. The increase in EF is accompanied with the increase in the reducible fraction for Zn, Pb and Cu but in a lesser extent for Cd which shows that for this metal, the metal physico-chemical properties also play an important role in determining the distribution.

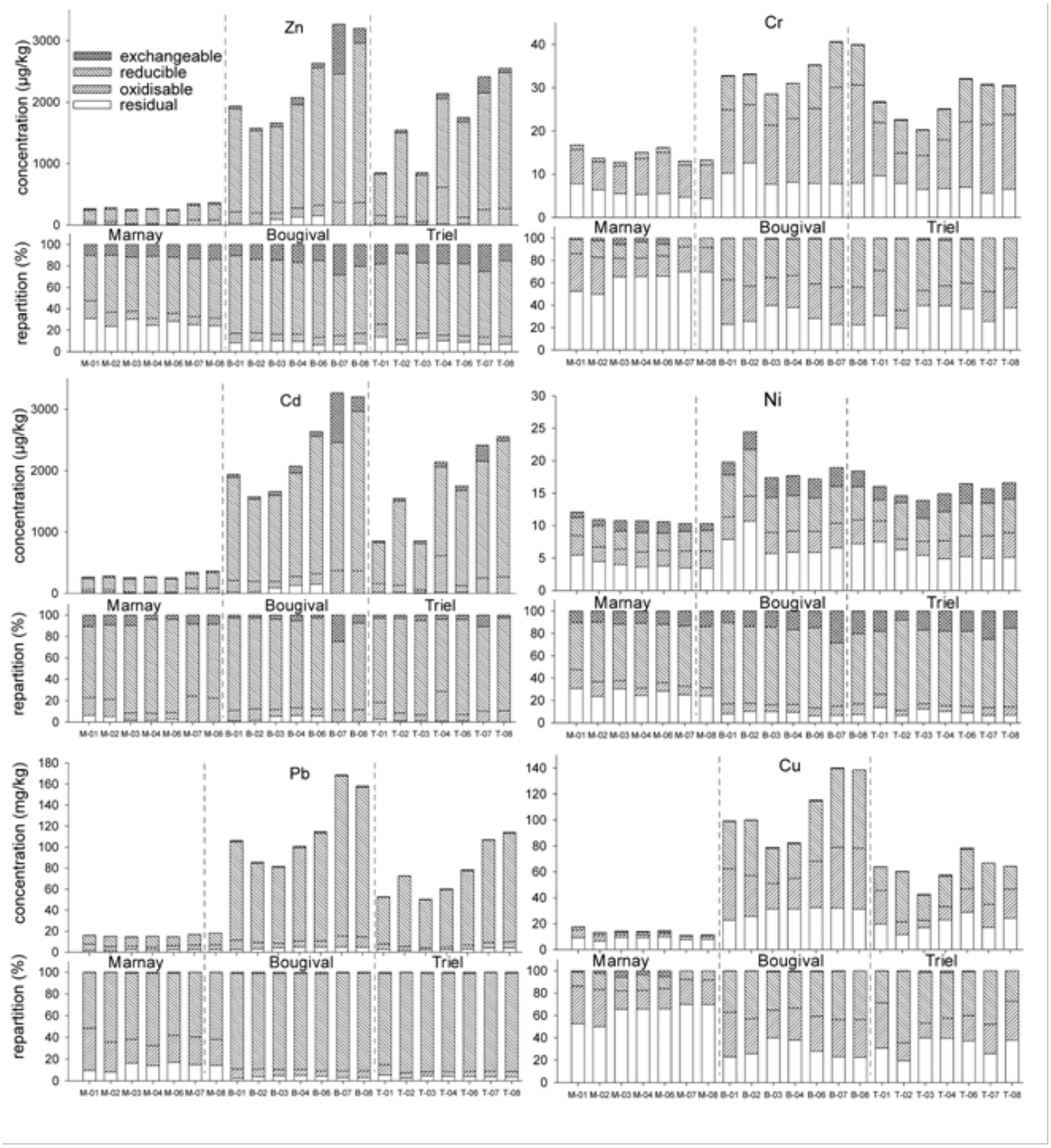

Figure III. 4 - Distribution of Zn, Cd, Pb, Cr, Ni, and Cu in the 4 different fractions of the BCR defined phases both in concentration (mg/kg) and relative concentration (%) with axis X indicating M for Marnay, B for Bougival and T for Triel sites accompanied by numbers representing the month when the sediment trap was collected (01 = January 2009 until 08 (August 2009)).

The second group consists of Cr, Ni, and Cu with higher fractions of the residual phase than the first group, averaging around 35%. Compared to the first group, the metals in the second group are distributed relatively equal where no fraction holds more than 60% for a given metal, except for residual Cu at Marnay.

While in a first approach, the metals can be divided into two groups, each metal shows a typically different behaviour and it will be interesting to discuss the distribution of each particular metal. From the first group, Zn seems to stand out from Cd and Pb in terms of association to the exchangeable fraction. The proportion of Zn associated to this phase remains around 20% from Marnay to Triel. Despite the stability in its proportion, this means an increase of 4-6 folds in concentration going from an average of 9 $mg.kg^{-1}$ at Marnayto an average of 63 and 45 $mg.kg^{-1}$ at Bougival and Triel respectively. Moreover, the relative stability of the proportion of Zn associated to the exchangeable phase is seen in a smaller proportion for oxidisable Zn. The proportion remains around 10% while the concentration increases 2-4 folds in most cases.

Except for July 2009, the average proportion of exchangeable and oxidisable fraction of Zn is relatively stable from Marnay to Triel. Distinct changes are observable with Zn associated to the reducible phase (student test confidence interval 99% between Marnay and the two downstream sites). Average reducible fraction Zn increased from upstream to downstream with $52\pm9\%$ at Marnay to $67\pm6\%$ at Bougival and $67\pm8\%$ at Triel. This is the result of a 4 to 7 time increase of concentration from Marnay to Bougival and Triel. Consequently, the reducible fraction accounts for at least 50% of BCR extractable Zn at Marnay and up to 75% for Bougival and Triel. Garnaud et al. (1999) also found a majority of reducible and exchangeable Zn particularly in SPM sampled during a rain period in the le Marais catchment outlet of the Seine River. A weak increase of Zn in the residual form from upstream to downstream also marks a relatively steady amount of residual fraction of Zn transported in the Seine River which could originate from the Seine's geological background.

It is difficult to compare Seine Zn distribution with other urban river studies because Zn in the Seine river watershed is particular compared to other urban rivers in the world.

Unlike most watersheds, roof runoff constitutes one of the major sources of Zn contamination in the Greater Paris Region, where it reaches roughly 40% of all roofing surfaces (Robert-Sainte et al., 2009). 85-100% of Zn washed from roof surfaces are in its ionic form (Heijerick et al., 2002). Zn has a high affinity for solid particles and so it is easily adsorbed mostly to carbonates, hydrous iron oxide and silicate minerals (Fujiyoshi et al., 1994). Nevertheless, these Zn-bearing particles undergo physico-chemical evolution and once found in the sewer system, 70% of Zn is found to be associated with organic matter and biofilm (Rocher et al., 2004). However, our analysis showed that Zn in the SPM is far more likely to be associated with the reducible form, with an average of more than two thirds of the total BCR extractable Zn for Bougival and Triel. This means that the sediment undergoes further transformation until reaching the water body. Our result is comparable to the lower median percentage of acid-soluble Zn found in the urban streams of Prague (Hnatukova et al., 2009).

The dominating reducible phase of Zn is to a further extent similar for Cd. Cd is found to be associated up to 80% with the reducible phase increasing the concentration to 10 folds going from 200 µg/kg of Cd to around 2000 µg/kg from upstream to downstream.

Although the relative distribution of the 4 phases remains relatively stable, the absolute concentration increases to 4-6 times from Marnay to Triel, and increasing more labile Cd in the exchangeable and reducible fraction simultaneously. The exchangeable proportion is higher in Bougival and Triel, in the 5-10% range. Nevertheless, along with Zn and Ni, Cd still represents one of the metals with the highest proportion associated to the exchangeable phase making it relatively more mobile to the environment than other metals, because the exchangeable phase is the phase most likely to go into the dissolved phase thus becoming more available to the environment.

The high proportion of reducible fraction of Cd and Zn in the Seine River SPM differs from previous urban river studies which showed mostly acid-soluble fraction. Hnatukova et al., (2009) found 38-64 and 15-43% acid-soluble Cd and Zn, respectively, in the urban streams of Prague as opposed to the acid-soluble Cd and Zn in Seine measuring at 3-11% and 8-28% respectively. This makes Cd one of the most mobile element compared to the 6 studied elements showing the highest proportion associated to the mobile phase (exchangeable+ reducible+ oxidisable), with an average of 2% associated to the residual phase.

Comparing the six studied metals, Cd shows the highest EF increase from upstream to downstream, increasing 3 to 5 folds compared to an average EF increase of 2 to 3 folds for Zn and Pb in the downstream sites. This significant Cd increase in the bulk concentration is not accompanied with an evolution of the average distribution from upstream to downstream (Figure III.4). This is not the case for two urban watersheds, the St Lawrence River, Canada (Gagnon et al., 2009) and the Loura River, Spain (Filgueiras et al., 2004) which exhibited significant spatial variation of Cd solid speciation. Evolution for the Seine River solid SPM is only observable once comparing monthly variations when the proportion of exchangeable Cd along with exchangeable Zn increases in July 2009. This phenomenon could be attributed to the low flow occurring during the SPM accumulation for this sample (22 June to 22 July, 2009), but also the transport of first flush runoff from the storm rain taking place between the 16 and 17 July increasing the river flow rate from 126 to 189 $m^3.s^{-1}$. This runoff discharge may consist of particles with different speciation as opposed to the low flow-particles which would explain the abrupt increase of exchangeable Cd and Zn.

The high EF of Cd and the relatively high proportion of Cd in the mobile fraction make Cd an important element to monitor in the environment. Nevertheless, despite of this high enrichment of the Cd downstream of the Seine River, Cd shows a stable distribution in

the 4 fractions from upstream to downstream. The speciation of Cd found downstream is not similar to Cd speciation of solid matters collected in the basin such as traffic aerosols containing 75% of exchangeable Cd (Lebreton and Thevenot, 1992) or road dusts containing more than 30% of Cd associated with the oxidisable fraction (Thévenot et al., 2002). This implies that urban Cd would be mobile and solid Cd entering the river would be directly remobilized to its preferable fractions in the solid phase, despite of its original form. This would make speciation-based source tracing in the solid form unadoptable for Cd in the Seine River.

Pb showed the highest increase of the reducible fraction relative content from upstream to downstream (20-30%) and a 10-15 fold the concentration increase. This is by far the highest spatial increase of the reducible fraction compared to Zn and Cd. Compared to Zn and Cd, there does not seem to be a significant proportion of exchangeable Pb compared to the four other fractions. In the downstream sites, the three remaining fractions, exchangeable, oxidisable and residual only makes up 10% of the total extractable Pb. This means that further studies on Pb contamination has to be focused on the reducible fraction, containing mostly Pb associated with iron and manganese oxides.

Nevertheless, our results remain similar to other studies of metal fractionation in urban watersheds. The preference of Pb for the reducible phase is also observed by Sutherland and Tack (2007) and Carter et al.(2006). They found a high association of Pb with the Mn oxide and to a lesser extent with the Fe oxide. Hnatukova et al. (2009) also found Pb to be mainly bound to the reducible fraction. Jain et al. (2008) also found only 1-3% of exchangeable Pb in the sediments of the River Narmada, India. The weak association of Pb with the exchangeable fraction is equally observed in the study by Carter et al. (2006). Nevertheless, the Seine oxidisable Pb proportion seems to be underestimated compared to their study as fractionation

of Pb is mainly dominated by the reducible fraction. The study of Hassellov and von der Kammer (2008) strongly suggests that iron-oxide Pb bearing particles are in the form of nano-colloids. Consequently, Pb may be efficiently transported to the estuary.

The Seine River is located in a carbonated basin. Consequently, SPM contains abundant carbonates onto which the metals could be adsorbed. Nevertheless, this is not the case for the Seine River where the absence of exchangeable Cu, along with Cr and Pb, is notably similar to the distribution in the Aire River (Carter et al., 2006). The predominant species in the range of pH of the Seine River measured during the campaign (between 7.5-8.3) would be $CuCO_3(aq)$ and $Cu(CO_3)_2^{2-}$ (Stumm and Morgan, 1981) which means that $CuCO_3(s)$ is not present even with abundant $CaCO_3$ in the system.

Along with Zn, Cu seems to be the element with a mobile phase evolving considerably from upstream to downstream, where its proportion could reduce 20% the proportion of the residual phase. This would mean a higher mobility downstream, and it would also mean a high anthropogenic contribution.

Similar to Cd, Ni is distributed steadily from Marnay to Triel, around 15, 20, 30, and 40% for the exchangeable, oxidisable, reducible and residual phases respectively. Ni displays a minimum spatial increase in absolute concentration from upstream to downstream, reflected by the values of Ni EF. These two evidences may mean that Ni sources mostly originate from lithogenic sources rather than anthropogenic contamination. Ni seems to be the metal containing in average the highest metal proportion in the residual fraction ranging around 31-47%. The relatively steady proportion of the residual Ni from upstream to downstream would signify the steady contribution of lithogenic background, reflected by the steady values of enrichment factor from upstream to downstream.

The relatively high exchangeable Ni is somehow comparable to that of Zn but while reducible and residual fraction of Zn varies considerably from upstream to downstream, reducible and residual Ni remain stable and do not show significant spatial variation. Therefore, the high exchangeable Ni cannot be contributed to anthropogenic sources, but more to the typical geochemistry of Ni to the solid phase

Among the elements found in the second group, Ni shows the highest exchangeable phase, which is not the case for other fractions. Similarly to Cd and Zn, Ni is found to be already significantly associated with the exchangeable phase beginning from the upstream site. The presence of a significant exchangeable phase in Ni, Cd and Zn is not at all apparent in Pb, Cr, and Cu. The grouping of Ni, Cd, and Zn was observed by (Tusseau-Vuillemin et al., 2005) on Seine River SPM. Based on a multi-elementary study, they found a correlation between the ratio of the dissolved and solid fraction (K_d) of Ni, Cd and Zn. This would indicate similar adsorption-desorption behaviour for Ni, Cd and Zn. As mentioned above, a recent study observed a high variation of dissolved Zn in the Seine. Zn similar behaviour with Ni and Cd would imply that pulsating concentration of dissolved Ni and Cd could also be a problem in the Seine River. This should be further investigated as Cd and Ni are considered even a more toxic element and regulated by the European Water Directive.

Similar to Ni, Cr displays a constant EF for the 3 sites. Nevertheless, what distinguishes Cr from Ni is that Cr seems to even be less mobile with relatively no exchangeable phase present. This is also supported by the low BCR-extractability of Cr, representing more than 60% associated with the non-extractable phase indicated by the difference of the total Cr of the four BCR extracted fractions and the total Cr obtained by the bulk extraction. This would indicate as Cr being mostly incorporated in mineral particles, relatively difficult to extract. Chromite is regularly found in the Seine SPM through analysis

by Scanning Electron Microscopy (SEM) (unpublished work) and this may be a possible mineral form of Cr. This is an evidence of the importance of completing total digestion with metal speciation study to understand its mobility to the environment.

Compared to the 5 other elements, Cr seems to be an element that is mostly associated with the oxidisable phase, averaging about 40-50%. The strong preference of Cr with organic matter was mostly observed in an anoxic estuary (Du Laing et al. 2009). The high capacity of Cr complexation with the organic matter is also observed in bed sediments (Lin and Chen, 1998). This would mean that Cr could be ingested by organisms consuming the organic matter.

Despite the stable enrichment factor from upstream to downstream indicating possible lithogenic origin of Cr, a shift of distribution, is apparent from Marnay towards Bougival and Triel. There is a 10% decrease of Cr in the residual phase, replaced by an increase in the reducible form. This shows that Cr evolves more considerably than Ni inside the solid phase and is more labile to physico-chemical changes.

The abundance in the oxidisable phase is also apparent at a lesser extent for Cu. The oxidisable Cu represents 30% as compared to Cr going up to 50%. A concentration increase of 5-20 times is observed, the highest upstream-downstream increase of oxidisable Cu compared to other metals. Luoma and Rainbow (2008) noted the strong affinity of Cu to organic ligands. More recently, various studies in the Seine River also noted this characteristic, which would be due to the presence of urban dissolved organic matter. It presents different complexing capacity as compared to the natural organic matter, thus creating a higher affinity for the dissolved copper (Pernet-Coudrier et al., 2008). Such colloidal organic matters could possibly be collected in a monthly trap. The formation of bio-film inside the trap could also be an equally important Cu-collecting mechanism.

As for Zn and Pb, reducible Cu also shows an increase in proportion going from 12% at Marnay to 30-40% at Bougival and Triel. This abrupt apparition of reducible Cu could be attributed to a source related phenomenon where average EF increases 3-5 folds from Marnay to Bougival and Triel. Cu introduced to the river could be associated with the reducible fraction, especially the iron and Mn oxides. Luoma and Bryan (1981) noted Cu preference to iron oxy-hydroxides, although in our cases, the proportion of reducible Cu is relatively low as compared to reducible Zn, Cd and Pb ranging about 40%. A higher reducible fraction is observed at Triel on February 2009 where it reaches up to 70%. This sudden increase of reducible Cu on February 2009 coincides with the increase of reducible Zn, Cd, and Pb for the same period. During this period, the Seine River flow rate at Bougival more than tripled in 11 days from 157 to 528 $m^3.s^{-1}$. The flow decreased by an average of 200 $m^3.s^{-1}$ during the next 9 days and re-increased to 505 $m^3.s^{-1}$ in 7 days. These increasing flow rate episodes due to rain runoff would include urban runoff with specific source-related characteristics. As during this period, a significant increase in reducible Zn, Cd, Pb and Cu is observed, the 2 rain episodes were likely to transport urban pollutants associated in the reducible fraction, mostly iron oxides.

Images of the Triel August 2008 suspended sediment sample using the SEM-FEG demonstrated iron oxide as a cluster with a geometrical crystal structure (Figure III. 5inset). The Ca detected behind the iron oxide cluster could indicate a calcite-hosted iron-oxide growth as suggested by the elemental cartography (Figure III. 5a). The similar composition of iron oxide with Ca was also observed by SEM-EDS on bed sediment collected on 2001 (Tessier and Bonté, 2002). Iron oxide particles were found as cohesive particles and proved to be an effective metal scavenger (Hochella and White, 1990; Morin et al., 2009; Sekabira et al., 2010) found to be associated with Cu, Pb, Sb and Zn.

3.4 Sulfidic species

The grouping of Zn, Cd, and Pb along with relatively mobile Cu would support the hypothesis of possible sulfidic forms in the samples. These four elements are known as chalcophile elements in the Geochemical Classification of Goldschmidt and preferably bond with sulphur rather than oxygen.

Indeed, according to Larner et al. (2008), sequential extraction of samples containing sulfidic phases in oxic conditions would lead to redistribution of Cd, Zn, Cu and Pb to a lesser extent from the oxidisable to the reducible phase. This study explained that during the exchangeable extraction, sulfidic phases may be oxidised and redistributed to the reducible phase.

No previous studies showed a significant amount of sulfidic phases in oxic riverine SPM non-affected by mining activities (Taylor and Owens, 2009). Therefore no special care was taken in preserving oxidation state during the sequential extraction procedure. This study showed that with the minor oxidisable phase, and the extremely high reducible fraction, a considerable amount of the studied metals could be associated with the sulfidic phases.

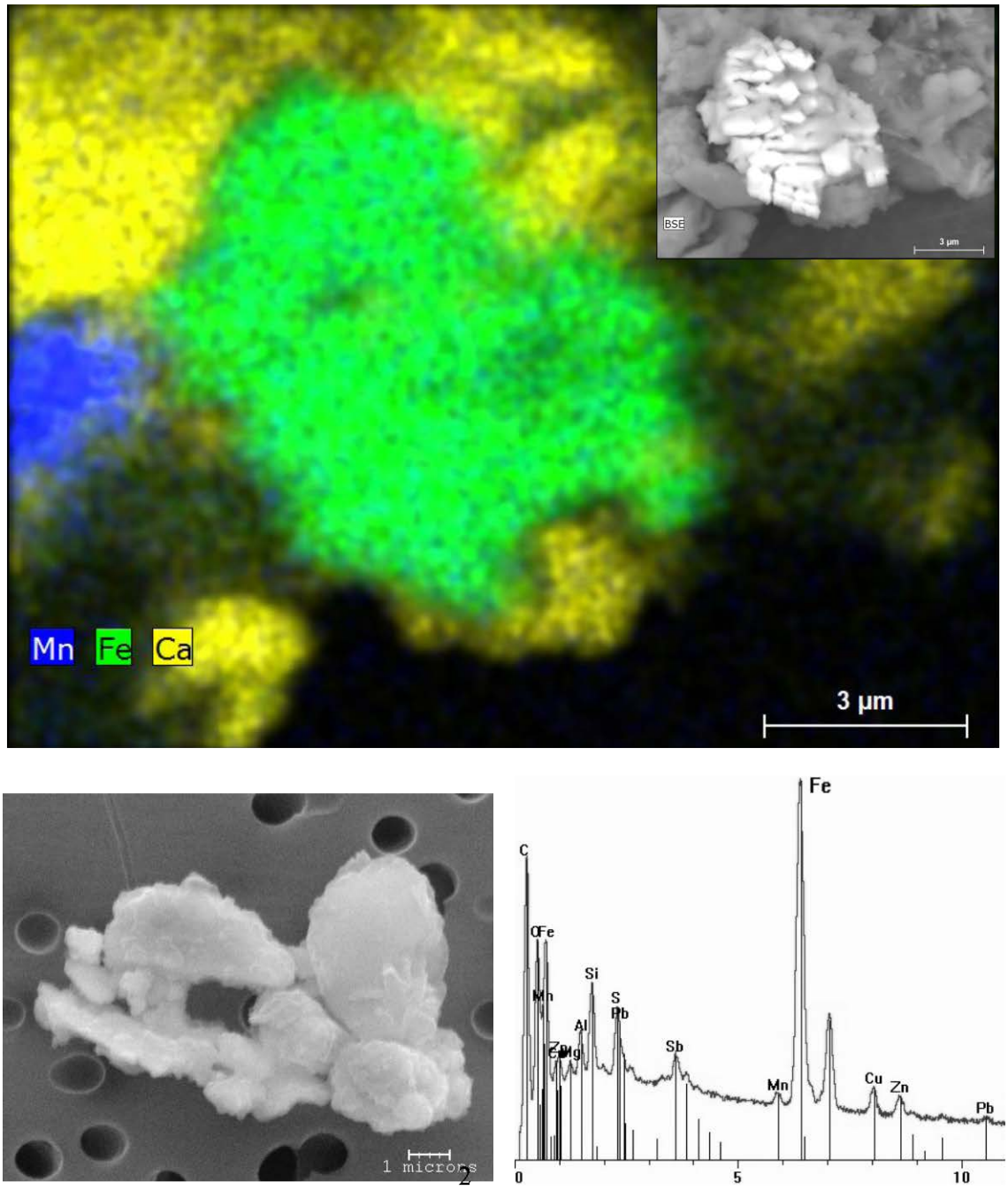

Figure III. 5 - Top: Cartography from energy dispersive spectroscopy (EDS) and Scanning electron microscopic image (inset) and of iron-manganese oxide growth on calcium carbonate mineral analyzed with MEB-FEG at IMPMC, Paris ; Bottom : SEM image (left) and EDS spectrum (right) of a cluster of particles indication metal bearing iron oxide associated with antimony, copper, lead, and zinc analyzed with MEB-EDS at LSCE, Gif sur Yvette

3.5 Urban impacts on metal speciation

The proportion of the reducible fraction seems to reflect the enrichment factor of the metal. Metals affected by anthropogenic activities having a relatively high enrichment factor (EF>3), seems to prefer association with the reducible form. Obviously, the proportion of the residual fraction reflects the contribution of the background. The oxidisable fraction also seems to show, to a lesser extent, contribution by natural sources as it is exceptionally high for Cr, reaching up to 50% compared to the other fractions. Ni, a non-enriched metal in the Seine River, also contains a relatively high oxidisable fraction, ranging around 23% at Marnay, and 11-23% at the downstream sites. It seems that the immediate mobility is minimized for most of the metals, reflected by their small proportion in the exchangeable form.

Two downstream sites were chosen in order to measure impacts of Greater Paris at Bougival and of the wastewater treatment plant (WWTP) Seine Aval at Triel. Even though at Bougival the metal concentrations are significantly higher than at Triel, no significant difference is remarkable in their distribution between the four phases for any of the six metals. The addition of numerous WWTP and the redistribution of incoming wastewater to other plants in the course of the Seine River may prove to be effective in reducing the metal load flowing in the Seine River at Bougival. Nevertheless, the issue of reducing the metal load is still important for Greater Paris where enrichment from Marnay to Bougival remains considerably high.

4 Conclusion

In this study, applying the BCR sequential extraction to suspended particulate matter sampled monthly in the Seine River, a river impacted by human activities, the highly urban

Greater Paris Region is found to modify not only metal concentration but also metal speciation as observed in speciation evolution between Marnay vs Bougival and Triel. As Cd, Cu, Pb and Zn are enriched in the suspended matter, their proportion associated with the reducible fraction is found to greatly increase. Based on the speciation behaviour, the analysed metals can be divided into two groups; the first group contains the anthropogenic metals, Cd, Pb, and Zn, in which the reducible fraction accounts for more than 60% of the total BCR extractable metals for the downstream Paris sites. The second group includes Cr, Cu, and Ni that are associated with at least 15% in three of the four defined BCR fraction in the downstream Paris sites. Exchangeable fraction is only significant for Cd, Ni and Zn while those associated with the oxidisable fraction accounts for less than 20% for the anthropogenic metals downstream except for Cu. The enrichment of Zn, Pb and Cu by the Greater Paris Region seen at Bougival and Triel is accompanied by the increasing distribution of metals on more mobile phases including the exchangeable and reducible phases. This fraction is more mobile as the metals can be released to the dissolved phase easily with pH variation, thus making the metal more bio-available. Temporal variation in the speciation is found to be related with discharge variations. No impact form the wastewater treatment plant was observed, neither on the trace metal concentration, enrichment factors nor speciation. This study suggests that a considerable amount of the metal studied could be associated with sulfidic phases which will be investigated in further studies. Nevertheless, the possible formation of sulfidic phases in the SPM accumulating during one month in the trap must be considered.

References

Afa, A.F.D.L.A., Les utilisations: Les marchés; http://www.Aluminium-info.Com/fr/utilisations/marches.Html [online]. [Accessed 27-Apr 2010].

Audry, S.; Blanc, G.;Schäfer, J., (2006). Solid state partitioning of trace metals in suspended particulate matter from a river system affected by smelting-waste drainage. Science of The Total Environment, 363 (1-3), 216-236.

Azimi, S.; Rocher, V.; Garnaud, S.; Varrault, G.;Thevenot, D.R., (2005). Decrease of atmospheric deposition of heavy metals in an urban area from 1994 to 2002 (Paris, France). Chemosphere, 61 (5), 645-651.

Buzier, R.; Tusseau-Vuillemin, M.-H.; Dit Meriadec, C.M.; Rousselot, O.;Mouchel, J.-M., (2006). Trace metal speciation and fluxes within a major French wastewater treatment plant: Impact of the successive treatments stages. Chemosphere, 65 (11), 2419-2426.

Carter, J.; Walling, D.E.; Owens, D.P.N.;Leeks, G.J.L., (2006). Spatial and temporal variability in the concentration and speciation of metals in suspended sediment transported by the River Aire, Yorkshire, UK. Hydrological Processes, 20, 3007-3027.

Chen, J.; Gaillardet, J.; Louvat, P.;Huon, S., (2009). Zn isotopes in the suspended load of the Seine River, France: Isotopic variations and source determination. Geochimica et Cosmochimica Acta, 73 (14), 4060-4076.

Da Silva, I.S.; Abate, G.; Lichtig, J.;Masini, J.C., (2002). Heavy metal distribution in recent sediments of the Tietê-Pinheiros river system in São Paulo state, Brazil. Applied Geochemistry, 17 (2), 105-116.

Dali-Youcef, N.; Ouddane, B.;Derriche, Z., (2004). Metal partitioning in calcareous sediment of the Tafna River and its estuary (Algeria). Fresenius Environmental Bulletin, 13 (12B), 1500-1508.

Davis, A.P.; Shokouhian, M.;Ni, S., (2001). Loading estimates of lead, copper, cadmium, and zinc in urban runoff from specific sources. Chemosphere, 44 (5), 997-1009.

Elbaz-Poulichet, F.; Seidel, J.-L.; Casiot, C.;Tusseau-Vuillemin, M.-H., (2006). Short-term variability of dissolved trace element concentrations in the Marne and Seine rivers near Paris. Science of The Total Environment, 367 (1), 278-287.

Estebe, A.; Mouchel, J.M.;Thevenot, D.R., (1998). Urban runoff impacts on particulate metal concentrations in River Seine. Water Air and Soil Pollution, 108 (1-2), 83-105.

Filgueiras, A.V.; Lavilla, I.;Bendicho, C., (2004). Evaluation of distribution, mobility and binding behaviour of heavy metals in surficial sediments of Louro River (Galicia, Spain) using chemometric analysis: A case study. Science of The Total Environment, 330 (1-3), 115-129.

Fujiyoshi, R.; Okamoto, T.;Katayama, M., (1994). Behavior of radionuclides in the environment .2. Application of sequential extraction to Zn(II) sorption studies. Applied Radiation and Isotopes, 45 (2), 165-170.

Gagnon, C.; Turcotte, P.;Vigneault, B., (2009). Comparative study of the fate and mobility of metals discharged in mining and urban effluents using sequential extractions on suspended solids. Environmental Geochemistry and Health, 31 (6), 657-671.

Galan, E.; Gomez-Ariza, J.L.; Gonzalez, I.; Fernandez-Caliani, J.C.; Morales, E.;Giraldez, I., (2003). Heavy metal partitioning in river sediments severely polluted by acid mine drainage in the Iberian Pyrite Belt. Applied Geochemistry, 18 (3), 409-421.

Garnaud, S., (1999). Transfert et évolution géochimique de la pollution métallique en bassin versant urbain. Université Paris XII-Val de Marne, Créteil.

Gromaire-Mertz, M.C.; Garnaud, S.; Gonzalez, A.;Chebbo, G., (1999). Characterisation of urban runoff pollution in Paris. Water Science and Technology, 39, 1-8.

Hassellov, M.;Von Der Kammer, F., (2008). Iron oxides as geochemical nanovectors for metal transport in soil-river systems. Elements, 4 (6), 401-406.

Heijerick, D.G.; Janssen, C.R.; Karlen, C.; Wallinder, I.O.;Leygraf, C., (2002). Bioavailability of zinc in runoff water from roofing materials. Chemosphere, 47 (10), 1073-1080.

Hnatukova, P.; Benesova, L.;Kominkova, D., (2009). Impact of urban drainage on metal distribution in sediments of urban streams. Water Science and Technology, 59 (6), 1237-1246.

Hochella, M.F.;White, A.F., (1990). Mineral-water interface geochemistry - an overview. Reviews in Mineralogy, 23, 1-16.

Horowitz, A.J.; Meybeck, M.; Idlafkih, Z.;Biger, E., (1999). Variations in trace element geochemistry in the Seine River basin based on floodplain deposits and bed sediments. Hydrological Processes, 13 (9), 1329-1340.

Houhou, J.; Lartiges, B.S.; Hofmann, A.; Frappier, G.; Ghanbaja, J.;Temgoua, A., (2009). Phosphate dynamics in an urban sewer: A case study of Nancy, France. Water Research, 43 (4), 1088-1100.

Jain, C.K.; Gupta, H.;Chakrapani, G.J., (2008). Enrichment and fractionation of heavy metals in bed sediments of River Narmada, India. Environmental Monitoring and Assessment, 141 (1-3), 35-47.

Jouvin, D.; Louvat, P.; Juillot, F.; Marechal, C.N.;Benedetti, M.F., (2009). Zinc isotopic fractionation: Why organic matters. Environmental Science & Technology, 43 (15), 5747-5754.

Karbassi, A.R.; Monavari, S.M.; Bidhendi, G.R.N.; Nouri, J.;Nematpour, K., (2008). Metal pollution assessment of sediment and water in the Shur River. Environmental Monitoring and Assessment, 147 (1-3), 107-116.

Larner, B.L.; Palmer, A.S.; Seen, A.J.;Townsend, A.T., (2008). A comparison of an optimised sequential extraction procedure and dilute acid leaching of elements in anoxic sediments, including the effects of oxidation on sediment metal partitioning. Analytica Chimica Acta, 608 (2), 147-157.

Le Cloarec, M.F.; Bonte, P.H.; Lestel, L.; Lefèvre, I.;Ayrault, S., (2009). Sedimentary record of metal contamination in the Seine River during the last century. Physics and Chemistry of the Earth, Parts A/B/C, doi:10.1016/j.pce.2009.02.003.

Lebreton, L.;Thevenot, D.R., (1992). Metal pollution release by road aerosols. Environmental Technology, 13 (1), 35-44.

Lesven, L.; Lourino-Cabana, B.; Billon, G.; Proix, N.; Recourt, P.; Ouddane, B.; Fischer, J.;Boughriet, A., (2009). Water-quality diagnosis and metal distribution in a strongly polluted zone of Deûle River (Northern France). Water, Air, & Soil Pollution, 198 (1), 31-44.

Li, Y.; Wang, X.L.; Huang, G.H.; Zhang, B.Y.;Guo, S.H., (2009). Adsorption of Cu and Zn onto Mn/Fe oxides and organic materials in the extractable fractions of river surficial sediments. Soil and Sediment Contamination: An International Journal, 18 (1), 87 - 101.

Lin, J.G.;Chen, S.Y., (1998). The relationship between adsorption of heavy metal and organic matter in river sediments. Environment International, 24 (3), 345-352.

Luoma, S.N.;Bryan, G.W., (1981). A statistical assessment of the form of trace-metals in oxidized estuarine sediments employing chemical extractants. Science of The Total Environment, 17 (2), 165-196.

Luoma, S.N.;Rainbow, P.S., (2008). Metal Contamination in Aquatic Environments. Cambridge: Cambridge University Press.573

Meybeck, A., (2003). Global analysis of river systems: From earth system controls to anthropocene syndromes. Philos Trans R Soc Lond B Biol Sci, 358 (1440), 1935-1955.

Meybeck, M.; De Marsily, G.;Fustec, E., (1998). La Seine en Son Bassin : Fonctionnement Ecologique d'un Système Fluvial Anthropisé. Elsevier.752

Meybeck, M.; Idlafkih, Z.; Fauchon, N.;Andreassian, V., (1999). Spatial and temporal variability of total suspended solids in the Seine basin. Hydrobiologia, 410, 295-306.

Meybeck, M.; Lestel, L.; Bonte, P.; Moilleron, R.; Colin, J.L.; Rousselot, O.; Herve, D.; De Ponteves, C.; Grosbois, C.;Thevenot, D.R., (2007). Historical perspective of heavy metals contamination (Cd, Cr, Cu, Hg, Pb, Zn) in the Seine River basin (France) following a DPSIR approach (1950-2005). Science of The Total Environment, 375 (1-3), 204-231.

Morin, G.; Wang, Y.H.; Ona-Nguema, G.; Juillot, F.; Calas, G.; Menguy, N.; Aubry, E.; Bargar, J.R.;Brown, G.E., (2009). EXAFS and HRTEM evidence for As(III)-containing surface precipitates on nanocrystalline magnetite: Implications for as sequestration. Langmuir, 25 (16), 9119-9128.

Pepe, M.; Gaillard, A.; Harrault, L.; Groleau, A.;Benedetti, M.F., (2008). Les métaux dissous en Seine à paris. Paris.

Pernet-Coudrier, B.; Clouzot, L.; Varrault, G.; Tusseau-Vuillemin, M.H.; Verger, A.;Mouchel, J.M., (2008). Dissolved organic matter from treated effluent of a major wastewater treatment plant: Characterization and influence on copper toxicity. Chemosphere, 73 (4), 593-599.

Reimann, C.;De Caritat, P., (2005). Distinguishing between natural and anthropogenic sources for elements in the environment: Regional geochemical surveys versus enrichment factors. Science of The Total Environment, 337 (1-3), 91-107.

Robert-Sainte, P.; Gromaire, M.C.; De Gouvello, B.; Saad, M.;Chebbo, G., (2009). Annual metallic flows in roof runoff from different materials: Test-bed scale in Paris conurbation. Environmental Science & Technology, 43 (15), 5612-5618.

Rocher, V.; Azimi, S.; Moilleron, R.;Chebbo, G., (2004). Hydrocarbons and heavy metals in the different sewer deposits in the `Le Marais' catchment (Paris, France): Stocks, distributions and origins. Science of The Total Environment, 323 (1-3), 107-122.

Sekabira, K.; Oryem Origa, H.; Basamba, T.A.; Mutumba, G.;E., K., (2010). Assessment of heavy metal pollution in the urban stream sediments and its tributaries. International Journal of Environmental Science and Technology, 7 (3), 435-446.

Siaap, (2007). Dossier du maitre d'ouvrage [online]. http://www.debatpublic-station-epuration-seineaval.org/docs/pdf/dossier-mo/doc-synthese-2.pdf [Accessed Access Date 2010].

Stumm, W.;Morgan, J.J., (1981). Aquatic Chemistry, 2 ed. Toronto: Wiley-Interscience.780

Sutherland, R.;Tack, F., (2007). Sequential extraction of lead from grain size fractionated river sediments using the optimized BCR procedure. Water, Air, & Soil Pollution, 184 (1), 269-284.

Taconet, J., (1996). Métaux fixés sur les matières en suspension dans le bassin de la Seine : Évolution des teneurs et des mobilités. DEA Sciences et Techniques de l'Environnement. MSc. Thesis Université Paris XII: Val de Marne Créteil.

Taylor, K.G.;Owens, P.N., (2009). Sediments in urban river basins: A review of sediment-contaminant dynamics in an environmental system conditioned by human activities. Journal of Soils and Sediments, 9 (4), 281-303.

Tessier, L.;Bonté, P., (2002). Suspended sediment transfer in Seine River watershed, France: A strategy using fingerprinting from trace elements. Science for Water Policy: the implications of the Water Framework Directive, Norwich, 79-99.

Thévenot, D.; Meybeck, M.;Lestel, L., (2002). Métaux lords : Des bilans en mutation. Paris.

Thévenot, D.R.; Moilleron, R.; Lestel, L.; Gromaire, M.-C.; Rocher, V.; Cambier, P.; Bonté, P.; Colin, J.-L.; De Pontevès, C.;Meybeck, M., (2007). Critical budget of metal sources and pathways in the Seine River basin (1994-2003) for Cd, Cr, Cu, Hg, Ni, Pb and Zn. Science of The Total Environment, 375 (1-3), 180-203.

Tongtavee, N.; Shiowatana, J.;Mclaren, R.G., (2005). Fractionation of lead in soils affected by smelter activities using a continuous-flow sequential extraction system. International Journal of Environmental Analytical Chemistry, 85 (8), 567-583.

Tusseau-Vuillemin, M.H.; Buzier, R.; Meriadec, C.D.; Chardon, I.; Elbaz-Poulichet, F.; Seidel, J.-L.; Mouchel, J.M.;Varrault, G., (2005). Du réseau à la rivière et de la Marne à Andrésy : Métaux labiles, dissous et particulaires. Paris.

Tusseau-Vuillemin, M.H.; Gourlay, C.; Lorgeoux, C.; Mouchel, J.M.; Buzier, R.; Gilbin, R.; Seidel, J.L.;Elbaz-Poulichet, F., (2007). Dissolved and bioavailable contaminants in the Seine River basin. Science of The Total Environment, 375 (1-3), 244-256.

USGS, (2010). Aluminum : Statistics and information http://minerals.Usgs.Gov/minerals/pubs/commodity/aluminum/ last update : 26-mar-2010 [online]. USGS. Available from: http://minerals.usgs.gov/minerals/pubs/commodity/aluminum/ [Accessed Access Date 2010].

Vieira, J.S.; Botelho, C.L.M.S.;Boaventura, R.A.R., (2009). Trace metal fractionation by the sequential extraction method in sediments from the Lis River (portugal). Soil and Sediment Contamination: An International Journal, 18 (1), 102 - 119.

Chapitre IV – Contribution du sédiment du fond et du déversoir du réseau unitaire d'assainissement aux métaux particulaires en Seine pendant le temps de pluie

Avant propos

Dans les chapitres précédents, une contamination élevée et mobile par le Cd, Cu, Pb et Zn a été mise en évidence dans la colonne d'eau. Des études menées dans le bassin de la Seine et dans d'autres bassins urbanisés ont mis en évidence une source particulière de la contamination élevée de ces métaux : le lessivage des surfaces urbaines. Le temps de pluie apporterait une grande quantité des métaux dans la Seine (en particulier après une période sèche), et particulièrement pendant un déversement du réseau unitaire d'assainissement

directement dans la rivière. Ce phénomène arrive dans le cas où la capacité de stockage du réseau est dépassée par le volume d'effluents produits pendant le temps de pluie. Alors que plusieurs études ont précisé les concentrations élevées des métaux dans les réseaux d'assainissement, le mécanisme de mélange entre les différentes sources (rivière, déversoir, sédiment de fond) pendant l'épisode du déversement reste méconnu. Dans ce chapitre, nous tenterons d'identifier la contribution de chaque source pendant le temps de pluie dans l'augmentation de la concentration métallique dans la rivière. En utilisant différents traceurs discriminants dans la phase solide, ce chapitre aura pour objectif de quantifier la contribution du déversoir et du sédiment du fond pendant un épisode du déversement du réseau unitaire afin de comprendre le mécanisme de mélange pendant les 36 heures suivant l'événement. **Une version révisée de ce chapitre est en cours de préparation pour une soumission au journal *Water Research* intitulé *"Contamination input to water column during a rain event : sediment resuspension vs combined sewer overflow"***.

1 Introduction

Runoff waters have been a subject of many studies due to their capacity of transporting contaminants in an urban watershed (Chebbo et al., 2001; Gromaire-Mertz et al., 1999; Lee and Bang, 2000; Neal et al., 2006). Basin equipped with combined sewer systems (CSS) where domestic wastewater and urban runoff are both collected and channelled together, are most concerned with these runoff waters. In cases of high rain intensity, generated wastewater may exceed sewer capacity and would flow directly to receiving water body through combined sewer overflow (CSO) construction, with or without being previously retained in interceptor basins. Metal concentration in overflow waters are known to be significantly high compared to the receiving water body (Gasperi et al., 2008; Houhou et al., 2009). With the European Water

Framework Directive (EWFD) and sediment quality guidelines (SQG) imposing water quality to water bodies, the impact of this overflow episode to a water body must be reduced. To achieve this, decision-maker and water basin agencies must fully understand the processes taking place during an overflow episode. Numerous studies have been conducted in the understanding of an overflow episode. During an overflow event, the water column becomes a mixing box of influx including the CSO itself, river water coming upstream of the CSO outlet, and also bed sediments resuspended into the water column with the mechanical agitation caused by the overflow episode(Old et al., 2003). Knowledge about the process taking place and the impact of CSO on organic carbon and oxygen level has been investigated thoroughly during the last decade (Even et al., 2007a; Seidl et al., 1998). It is now accepted that CSO episodes are responsible for a long period of anoxic in the river systems (Even et al., 2004). Few studies also observed the impact of CSO on metal contamination directly in the river system (Estebe et al., 1998; Weyrauch et al., 2010). Nevertheless, no attempt has been made on quantifying the impact of these overflow episodes toward the overall metal pollution in the receiving dynamic water system. Overflow events have been simulated in laboratory experiments mostly to study impact of sediment resuspension to the water column (Caetano et al., 2003; Eggleton and Thomas, 2004; Simpson et al., 1998) but no field experiment have been conducted to confirm laboratory findings. Moreover, physico-chemical parameters during a rain event with an overflow episode would have a complex dynamic and this would be difficult to mimic in the laboratory. By using various tracers in both dissolved and solid phases, this paper will attempt to quantify contribution of different sources to the metal flux in the water column during an overflow episode. Moreover, this paper will also discuss the temporal dynamic of an overflow plume in a river system.

2 Materials and Methods

2.1 Study Site

This study was conducted in the downstream area of the Seine River Basin. Wastewater evacuation in this region combines the use of separated system and combined system. Within the combined sewer system, interceptors and around 200 overflows were constructed in order to withhold wastewater in case of overcapacity during rain episodes in order to regulate inflow to the four major wastewater treatment plants (WWTP) operated by the SIAAP (SIAAP, 2007). Two notable interceptors and overflow are the Clichy CSO and the La Briche CSO, both located downstream of the Paris Region before the Seine Aval WWTP.

This study will focus on the Clichy downstream interceptor. This overflow is a part of the wastewater network, draining 2581 ha with a population density of 268 hab ha^{-1}. This interceptor has a hydraulic length of 12.5 km and a runoff coefficient of 67% (Kafi et al., 2008). Overflow events in the Clichy interceptor may generate as high as 40 $m^3.s^{-1}$ of wastewater produced by the urban population of the Greater Paris Region to the Seine River (an average of five times per year) with average overflow discharge of 20 $m^3.s^{-1}$ (Even et al. 2007). Anoxic episodes have been identified (Seidl et al., 1998) and the PROSE model have been created (Even et al., 2004) for the use of local basin management agencies such as SIAAP and Seine Normandy watershed agency to simulate aquatic impact using continuous physico-chemical data. Metal pollution in the combined sewer system has also been previously identified (Gasperi et al., 2008; Gromaire-Mertz et al., 1999) with high definition monitoring. Nevertheless, the impact of the metal contamination by the CSO is still unknown.

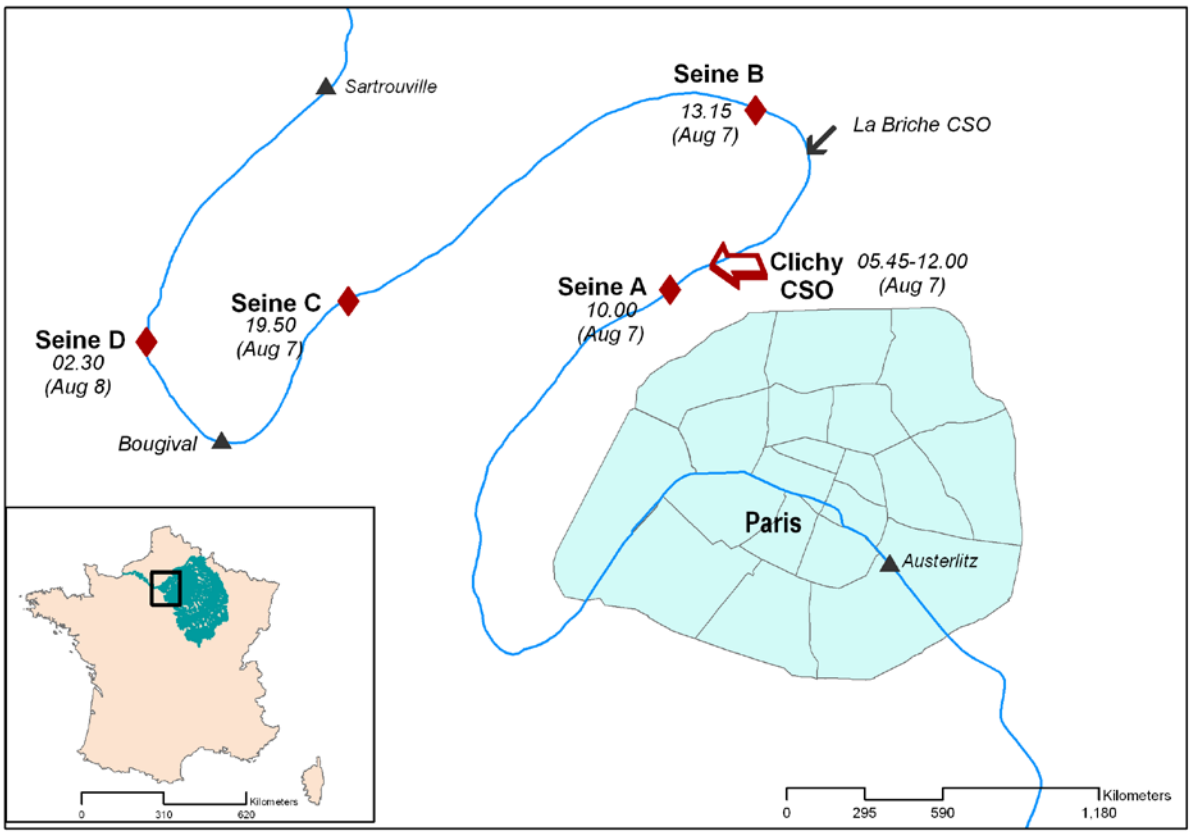

Figure IV. 1 - Sampling location in the Seine River, France downstream of Paris. Clichy combined sewer overflow (CSO) is marked by red arrow. Overflow time is indicated on its right. Diamonds from Seine A-D indicate overflow plume sampling sites with sampling time. Bed sediments were collected from Austerlitz to Sartrouville and Seine River reference was collected at Bougival.

2.2 Plume monitoring in the water body

A warning system was established between collaborating laboratories under the Interdisciplinary Environmental Research Program on the Seine River (PIREN Seine) and the Interdepartmental Association for Sewage Disposal in the Paris Conurbation (SIAAP) when the overflow system would potentially occur. This warning system emitted alerts when the Seine River discharge at the Seine River when it enters Paris in Austerlitz reaches a low level of 200 $m^3.s^{-1}$ and when a relatively high storm is announced through the national weather company. During this period, an overflow episode would have a relatively high impact due to a low dilution capacity of the Seine River.

When wastewater overflows to the receiving waters, a physical mixing occurs between wastewater, river water and bed sediment creating an overflow pollution plume. As this plume

advances, its composition evolves due to physico-chemical processes taking place in the plume. During this campaign, sampling was aimed to observe the temporal dynamic of the overflow plume in the receiving water body. Sampling was conducted in the centre of the CSO pollution plume in the Seine River as the plume advances from the Clichy CSO facility until the Chatou isle. This end point was chosen because the transit time of the Seine River between the left and right branch of the isle is different and overflow plume would be expected to evolve beyond this point.

Continuous conductivity measurements were performed from a small motorboat to locate the center of the overflow plume where conductivity was expected to be at its lowest since rainwater demonstrates significantly lower conductivity level compared to river water. For each given site, samples were collected at the surface and at the bottom. Parallel to sampling for metal analysis, other samples were collected for a wide range of biological and chemical parameters. Thus, two return trips were needed to complete necessary sampling for each given site. For one given plume center, the time needed to collect necessary samples was around 4-5 hours.

3 Source Sampling

3.1 Combined Sewer

Overflow water was collected by vacuometric samplers installed by the OPUR (Observatory of Urban Pollutants research program) at the Clichy overflow facility. Mechanism of sampling was previously described and validated by (Kafi-Benyahia et al., 2005). In brief, automated wet weather sampling was initiated once a maximum water level in the interceptor facility is reached just before an overflow episode takes place. Samples were taken at a fixed

span from 3-6 minutes every 30 minutes. Twelve sampling bottles were installed to monitor a maximum of 6 hour of overflow.

During this overflow episode, all 12 sampling bottles were filled. Average CSO sample was manually assembled a few hours after CSO samples arrived at the field laboratory. The average flow-weighted composite sample consisted of water from each of the 12 bottles in proportion to discharge (Kafi et al., 2008). A theoretical average was also calculated from the 12 individually analyzed samples. Theoretical average value for each element as the sum of each the twelve samples normalized by discharge (Eq.IV.1).

$$\overline{[Me]} = \frac{\sum_{n=1}^{12}([Me]_n * Q_n)}{\sum_{n=1}^{12} Q_n} \quad \text{Equation IV. 1}$$

3.2 Seine River Reference

To fully understand the impact of an overflow episode to the Seine River, it was important to compare impacted waters to a reference of the river condition prior to the overflow episode. For this study, the Seine River reference was evaluated with two sets of samples. The first one consists of the Seine River sampled during the beginning of the overflow episode approximately 1 km upstream of the CSO outlet (sample Seine A). A second set of samples consisted of Seine River samples collected during a monthly sampling conducted between October 2008 - October 2009 (Chapter II). These two sets of values will be compared in order to obtain a representative value for the Seine River dry weather reference.

3.3 Bed sediment resuspension

During an overflow event, a physical mixing occurs, and bed sediment may be resuspended and feed the water column with metal pollution (Caetano et al., 2003; Eggleton and Thomas, 2004; Simpson et al., 1998). To take into account of this potentially significant

source, analyzed bed sediment of the Seine River was kindly provided by the Seine Navigation Service (SNS) from numerous sites between Austerlitz and Sartrouville during 2007 to 2009.

4 Analytical Method

Sampling of overflow plume, CSO and the Seine River reference were performed with clean method. All sample containers and filtration system were polyethylene bottles and acid soaked in 2N HNO_3 during at least 24 hours and then rinsed thoroughly with deionized water.

Filtration of overflow plume was performed within three hours of sampling in the field laboratory in the SIAAP facility. Average CSO sample was composed 24 hours after the end of the overflow episode and filtration of composed average and individual composite samples were performed in laboratory a few days after overflow episode.

Filtration was performed using quartz filter 0.45 µm mounted on a Millipore filtration system. Between 100-250 mL of water were filtered using 1-2 filters depending on suspended particulate matter (SPM) concentration. Once finished, filters with recovered SPM were stocked and filtered water was stocked in polyethylene bottles, acidified to around pH 2 and stored in 4°C in the dark before analysis. Between filtration of different samples, filtration system was thoroughly rinsed with tap water, followed by deionized water, and completed with ethanol. Digestion of solid metal and trace metal analysis were explained in Chapter II.

5 Overflow modelling

5.1 Hypothesis 1: Combined sewer + Dry weather = plume

The mixing system was modelled based on a three-source contribution involving the CSO, the Seine River, and the bed sediment (Figure IV. 2). Before quantifying the contribution of each source in the overflow plume, it was important to identify concentration, conservativity

and evolution of various trace elements and physico-chemical parameters in the different pools. Investigation of geochemistry in the water column would also be useful to identify conservative elements that could be used to discriminate each of the three sources. This step of elemental identification was performed using a preliminary hypothesis of two sources. The first hypothesis explains the plume as a simple combination of two sources; the combined sewer and the Seine River prior to the introduction of the CSO (Hypothesis 1, Figure IV. 2). Dissolved and solid elemental concentrations of the samples collected in the Seine River (overflow plume and Seine River reference) were plotted against a conservative parameter. By commencing with this hypothesis, it was possible to obtain an illustration of the behaviour of numerous elements in the Seine River. Moreover, it was possible to estimate the gain or loss of metal when wastewater enters the river (see results section). This estimation was used afterwards to calculate a preliminary mass balance during the overflow episode and have an used to evaluate the potential of bed sediment as a source of contamination.

5.2 Hypothesis 2: Combined sewer + Dry weather + Bed Sediment = plume

This hypothesis focuses on the solid phase and takes into account the two sources of CSO and Seine River used in the first hypothesis while adding a third source which is the contribution of bed sediment resuspension. A simple 3-source mixing model for the solid phase was developed applying the least square fitting (LSF) on the R statistical computing (see Annexe 6 for complete programming). Conservative elements identified from the results of the first hypothesis were used to run the model in order to minimize possible error caused by adsorption/desorption process which was not calculated in this model. Moreover, the conservative elements must also demonstrate significantly different concentration in the three sources for the model to discriminate the three sources. The model was expected to quantify the contribution of each of the three sources in the overflow plume.

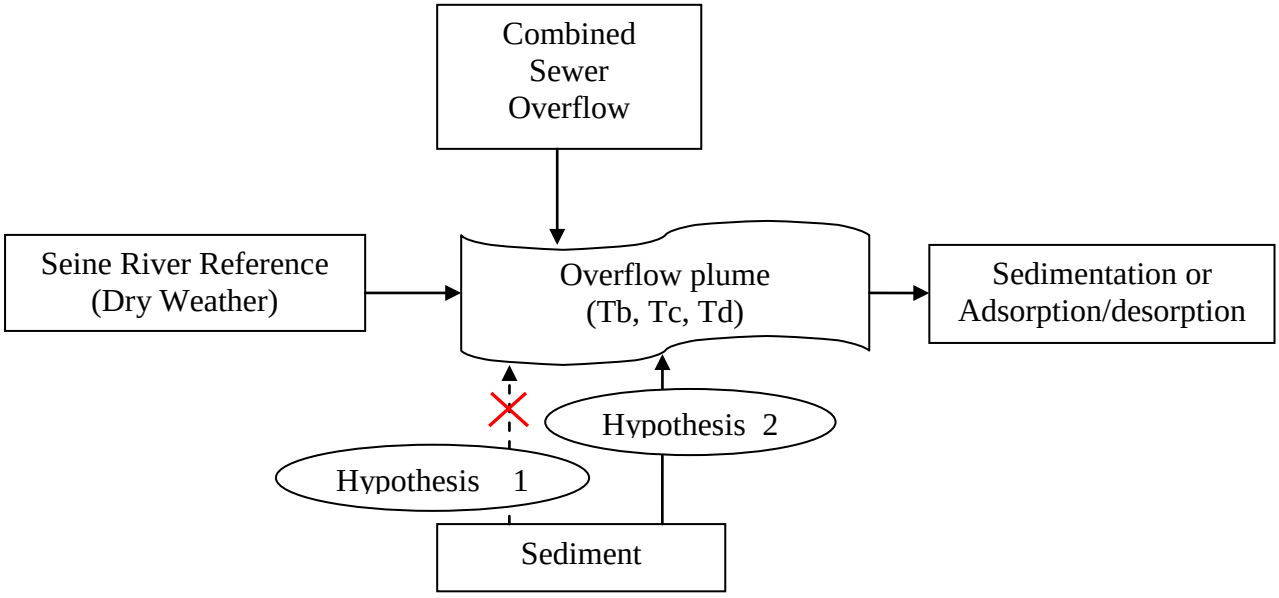

Figure IV. 2- Source modelling of overflow pollution plume. Calculation was performed with a preliminary hypothesis (Hypothesis 1) with only overflow and the Seine River as sources and a second hypothesis (Hypothesis 2) with bed sediment as a third source

6 Field Measurement Results

6.1 Overflow event

On August 7th 2008, an overflow episode in the Clichy sector took place starting at 5.45 AM and ending approximately at noon. This overflow episode was a result of a storm crossing France from southwest to the northeast direction. The storm area was 200 km wide with the intense storm centered with a diameter of around 100 km. The rainfall height during the overflow episode was a 10-year return period. During this overflow episode, the Seine River discharge at Austerlitz increased dramatically from less than 157 $m^3.s^{-1}$ at 6 am to around 356 $m^3.s^{-1}$ at 09.00 (SIAAP). An estimated volume of 577 000 m^3 of untreated waste water overflowed from the Clichy interceptor to the Seine River with a peak discharge of around 40 $m^3.s^{-1}$ (Figure IV. 3). This overflow episode had one of the highest volume measured during 2008.

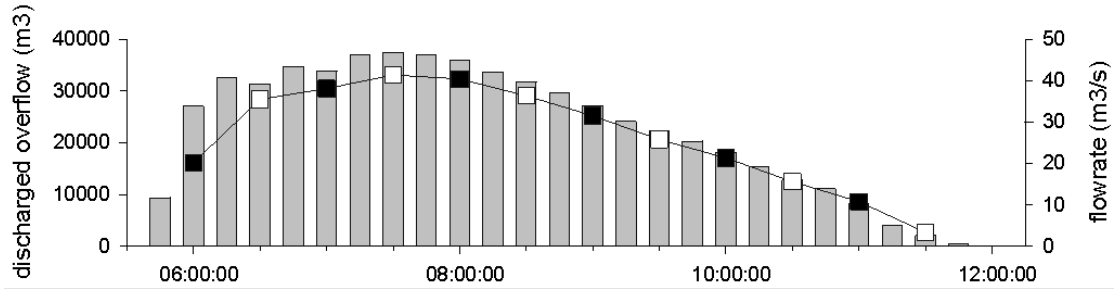

Figure IV. 3 - Combined sewer overflow volume with a 15-minute step representated as histograms (left axis) and average 30-minute flowrate representated as connected squares (right axis) (SIAAP)

6.2 Overflow plume

The overflow plume was collected at three zones over the 28 km target study site expected for sampling. This was less than expected, because sampling time were 4-5 hours per site and Seine River discharge was higher than predicted, due to the large storm, causing the plume to advance faster with the water body. Collected samples were named Seine B, Seine C and Seine D, each with surface (surf) and bottom (bot) water samples (Figure IV.1). Conductivity measurements performed before sampling Seine B indicated two centers in the overflow plume. Sampling was finally performed in the second plume center further downstream because the first plume center upstream was estimated to be caused by another overflow structure, La Briche, situated between the Clichy overflow and the Seine B point. Although contamination by the La Briche overflow was avoided, impact was expected to be observable in results.

Overflow plume behaviour in the water body was in agreement with conservative water mass evolution. Conductivity was correlated with dissolved oxygen, indicating a continuous degradation of organic carbon brought in by the overflow pollution with high level organic matter. Nevertheless, temporal evolution of dissolved oxygen was also present due to the relative level of available organic matter and bacterial population. For a conductivity reference

of 440 µS.cm^{-1}, dissolved oxygen went from 7.2 mg/L for the B series, 5.6 mg/L for the C series and a reoxygenation to 6.8 mg.L by the Chatou weir for the D series.

6.3 Combined sewer

12 CSO samples were collected, accompanied by an analyzed reconstituted average CSO and also a theoretical average CSO both normalized by discharge. During average sample reconstitution, precise discharge was not available and thus estimations were made by using estimated discharge from field facility. Comparison of the two data sets of discharge, field and validated discharge, demonstrated an overrepresentation of the last hour of CSO. Nevertheless, this error was considered non-significant since the last hour consisted of 3% of sample.

6.4 Seine River water reference

A sample was acquired as a reference of the Seine River before impact of the overflow event, called Seine A surface and bottom. Nevertheless, this reference sample seemed to have been significantly contaminated by other overflow facilities upstream. This was observed to the high concentration of anthropogenic contaminants in the Seine A sample and lower conductivity compared to dry weather samples collected previously (Table 1). Consequently, Ta would not be representative of the dry weather and another sample must be considered to substitute this value. Samples collected in the Seine River during a monthly campaign were then used to represent the Seine River reference. Among the two downstream sites collected for this campaign (Priadi et al., in preparation), the Bougival point was chosen as it is located around 30 km after the Clichy overflow before any other significant point sources. Out of 13 samples measured throughout 2008-2009, the sample collected on June 22nd was chosen to represent the Seine River during low flow. During this period, flow rate was very low while conductivity was high (indicating no recent contamination by rainwater), and suspended matter concentration was also relatively low (Table 1).

Table IV. 1 - Two sets of Seine River dry weather reference. The first pre-overflow plume set was collected during the plume sampling campaign and the second Bougival set was collected during a yearly campaign of the Seine River (*Flowrate measured at Austerlitz at 5.45 on August 7th)

	Flowrate (m^3/s)	Conductivity (µS/cm)	[SPM] (mg/L)
Pre-overflow plume			
Seine A surface	157*	498	16.6
Seine A bottom	157*	496	18.6
Bougival			
22/04/09	184	611	7.7
09/06/09	167	606	16.8
22/06/09	116	609	6.4
22/07/09	148	550	10.9
19/08/09	97	527	7.9
29/09/09	92	474	9.7
22/10/09	112	498	8.5

7 Modelling results

7.1 Hypothesis 1: Tracer determination

7.1.1 Dissolved metal tracers and mixing line

Conductivity is often used as a conservativity parameter of dissolved elements in a water system. For this campaign, conductivity values from CSO samples and CSO plume were plotted against Na which is representative of the pollution in a sewer system, and Ca which exists in the Seine River from the carbonate geological background (Figure IV.4).

The overflow plume and CSO samples demonstrated two separate pools indicating that the mixing process from the two pools was observable. Mixing lines demonstrated uncertainties, but for both Na and Ca samples, the theoretical average sample seemed to be comprised in the uncertainty of the mixing line. Taking into consideration the large range of Na and Ca concentration in the CSO, the theoretical average CSO will be used as a source reference for this first hypothesis. In these figures, Seine B points demonstrated anomaly and should be discussed and correlated with attention because their behaviour does not conform to the Na and Ca conservativity of the two sources. Indeed, this anomaly would indicate that the

La Briche overflow, and not only the Clichy overflow, may be highly influential to the Tb points.

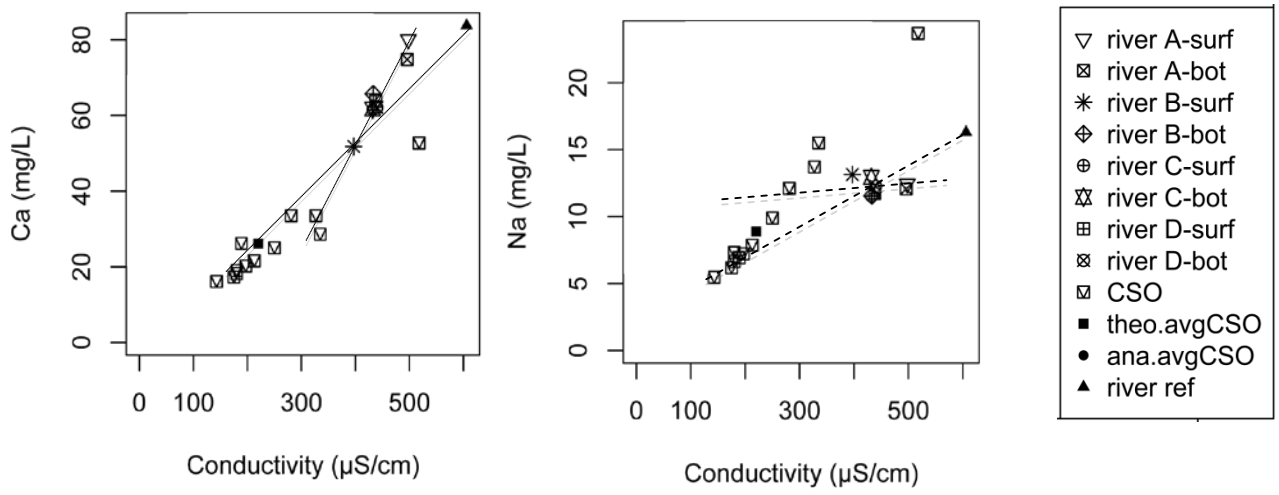

Figure IV. 4 – Identification of conductivity as a potential tracer by mixing line of calcium and sodium ions plotted against conductivity

When conductivity was plotted against dissolved metal concentration, itwas possible to distinguish mobile metals with preference to the dissolved fraction (Figure IV. 5) including Co and Ni demonstrated dissolved metal concentration that did not correlate with conductivity. Ba and Zn are two elements which are known to have a relative preference for the solid fraction (Chapter II). During this campaign, dissolved Ba and Zn in the Seine River did not display a conservative behaviour which could indicate that the CSO could be an input of contamination. Dissolved Ba and Zn from the CSO would therefore require a longer mixing time, more than the 24 hours of plume sampling in the case for this campaign. For metals with a higher affinity to the solid fraction such as Cu and Pb, dissolved metal concentration was more aligned with conductivity. Complete correlation coefficients of the dissolved metals in the plume are presented in Table II.2.

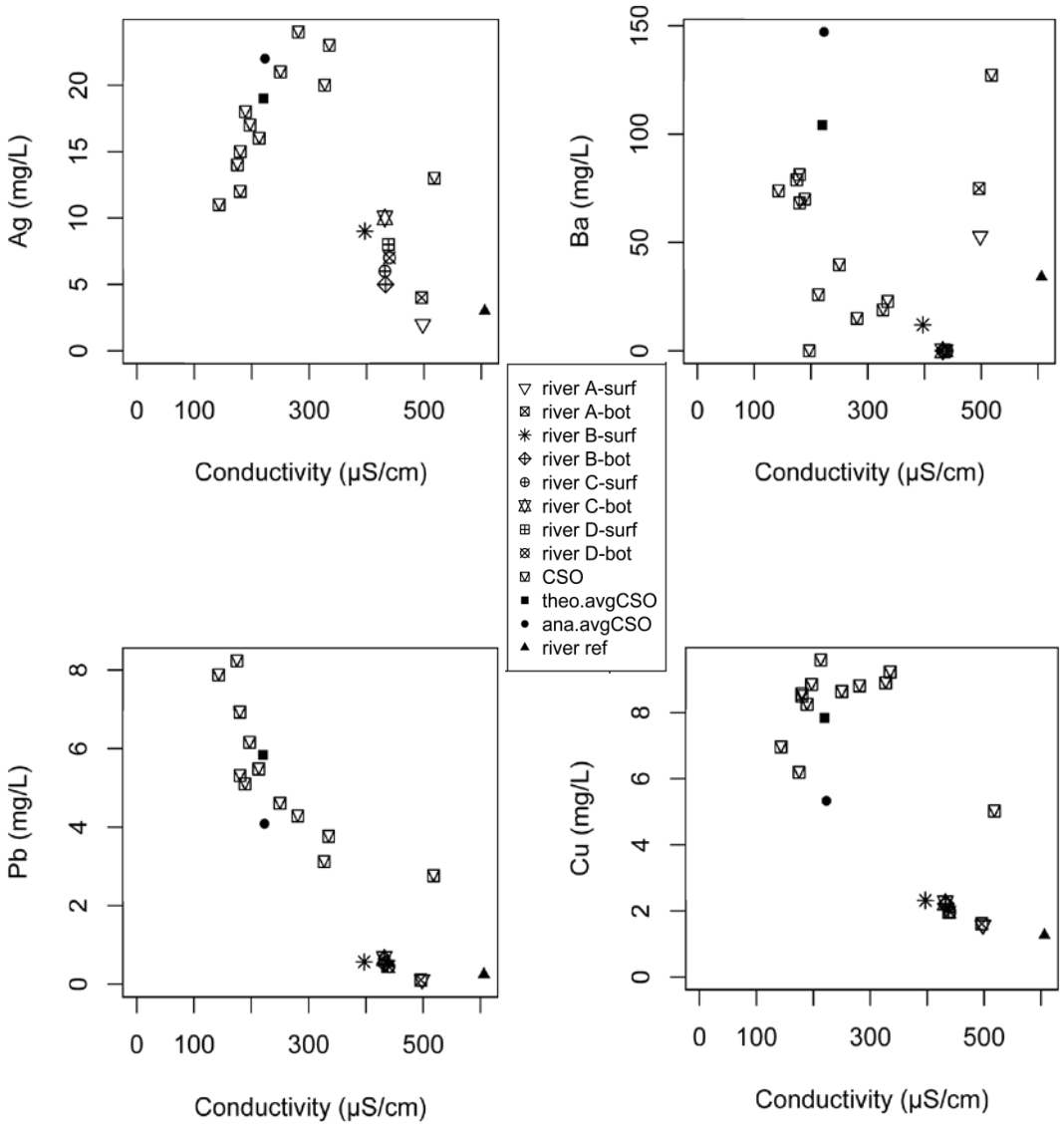
Ag (mg/L)
Ba (mg/L)
Pb (mg/L)
Cu (mg/L)
Conductivity (µS/cm)
river A-surf
river A-bot
river B-surf
river B-bot
river C-surf
river C-bot
river D-surf
river D-bot
CSO
theo.avgCSO
ana.avgCSO
river ref

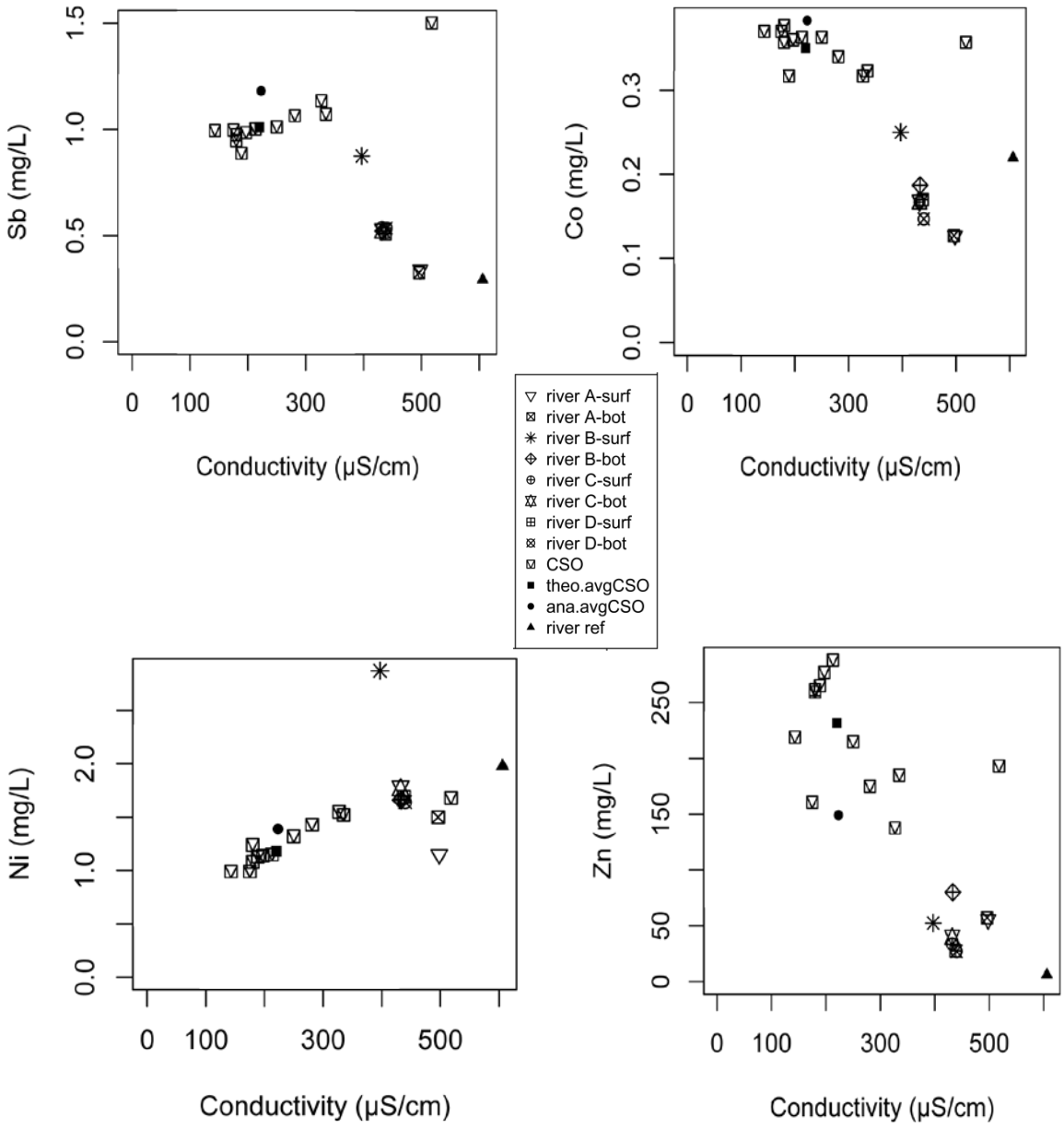

Figure IV. 5 - Dissolved metal concentrations in combine sewer overflow (CSO) and overflow plume used to calculate metal excess or deficiency during an overflow episode for Table II. 2

7.1.2 . Particulate metal tracers and mixing line

Unlike conductivity for the dissolved pool, a common elemental tracer for the solid pool does not exist because each watershed has a different geological background. Therefore, an attempt to identify particulate tracers was performed by plotting solid elemental contents in

samples against Al. Potential tracers among the numerous analyzed elements were Ba, Pb and Ti (Figure IV. 6). Considering the uncertainties in the mixing line, all three elements pointed towards theoretical average CSO sample as a representative sample of the overflow source.

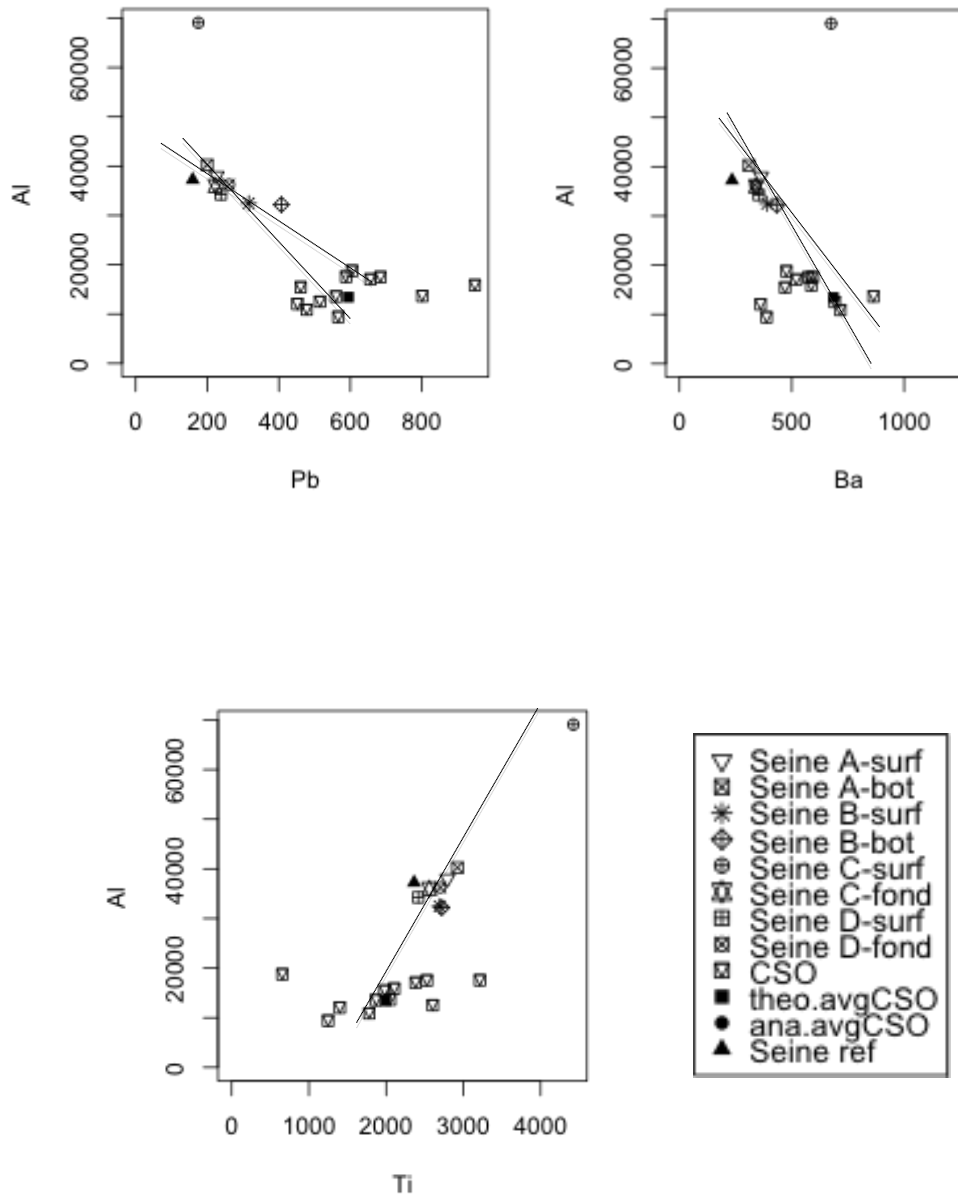

Figure IV. 6 - Identification of potential particulate tracer in the Seine River during an overflow episode with element concentration in µg.g^{-1}both in x and y axis

Among the three elements titanium (Ti) was finally selected because its concentration normalized by Al was discriminative. There was limited potential bias by dissolved Ti compared to dissolved Ba. Moreover, Ti could be used as a natural tracer for the Seine River basin as opposed to Pb that is highly impacted by urban activities. Indeed, Ti is often used as a lithogenic tracer found in most minerals including the heavy mineral, rutile. Ti/Al values were then used to continue with hypothesis 1 for the particulate fraction (Figure IV. 7).

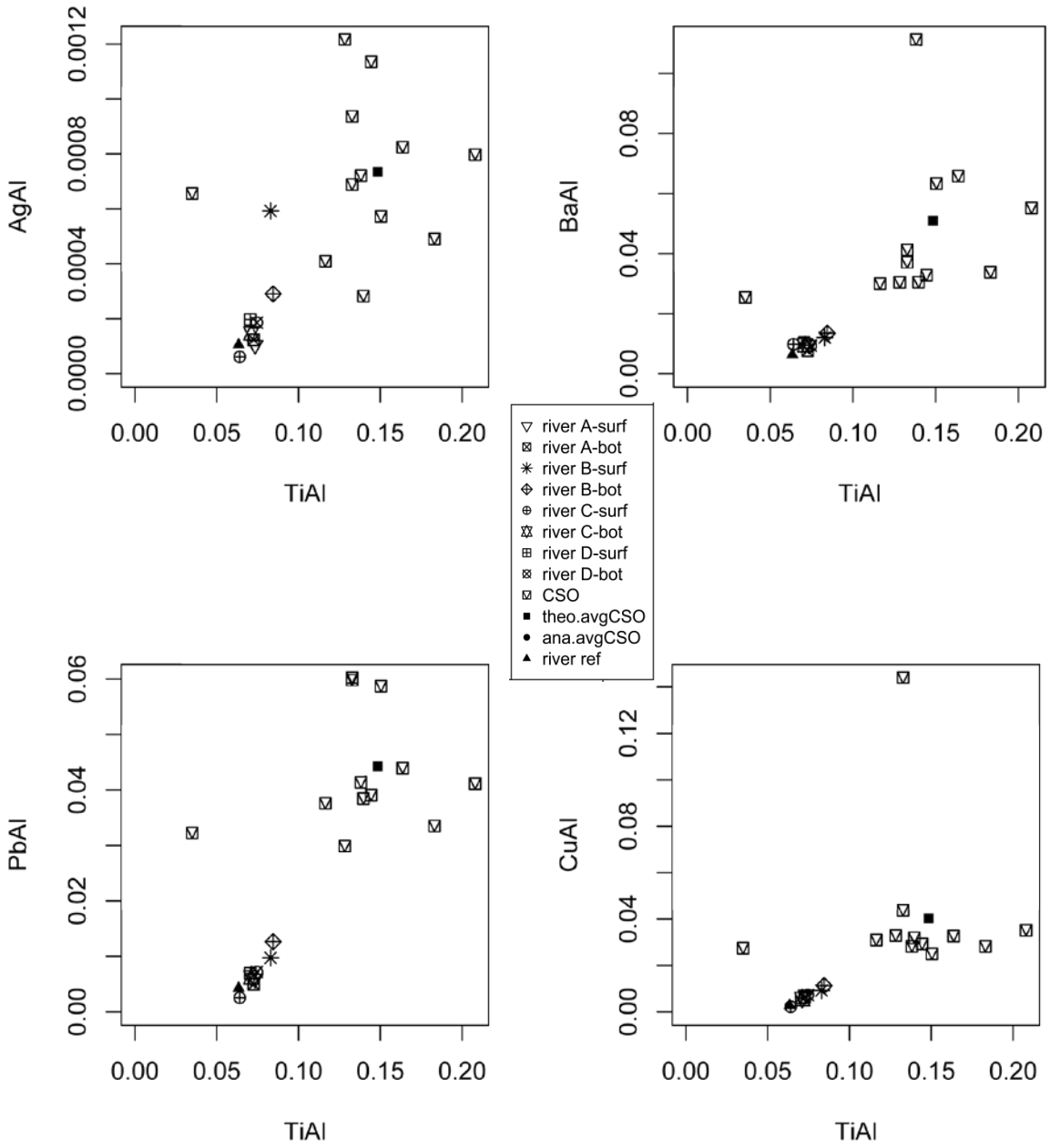
AgAl
0.0000
0.0004
0.0008
0.0012
0.00
0.05
0.10
0.15
0.20
TiAl
BaAl
0.00
0.04
0.08
PbAl
0.02
0.06
CuAl
0.12
river A-surf
river A-bot
river B-surf
river B-bot
river C-surf
river C-bot
river D-surf
river D-bot
CSO
theo.avgCSO
ana.avgCSO
river ref

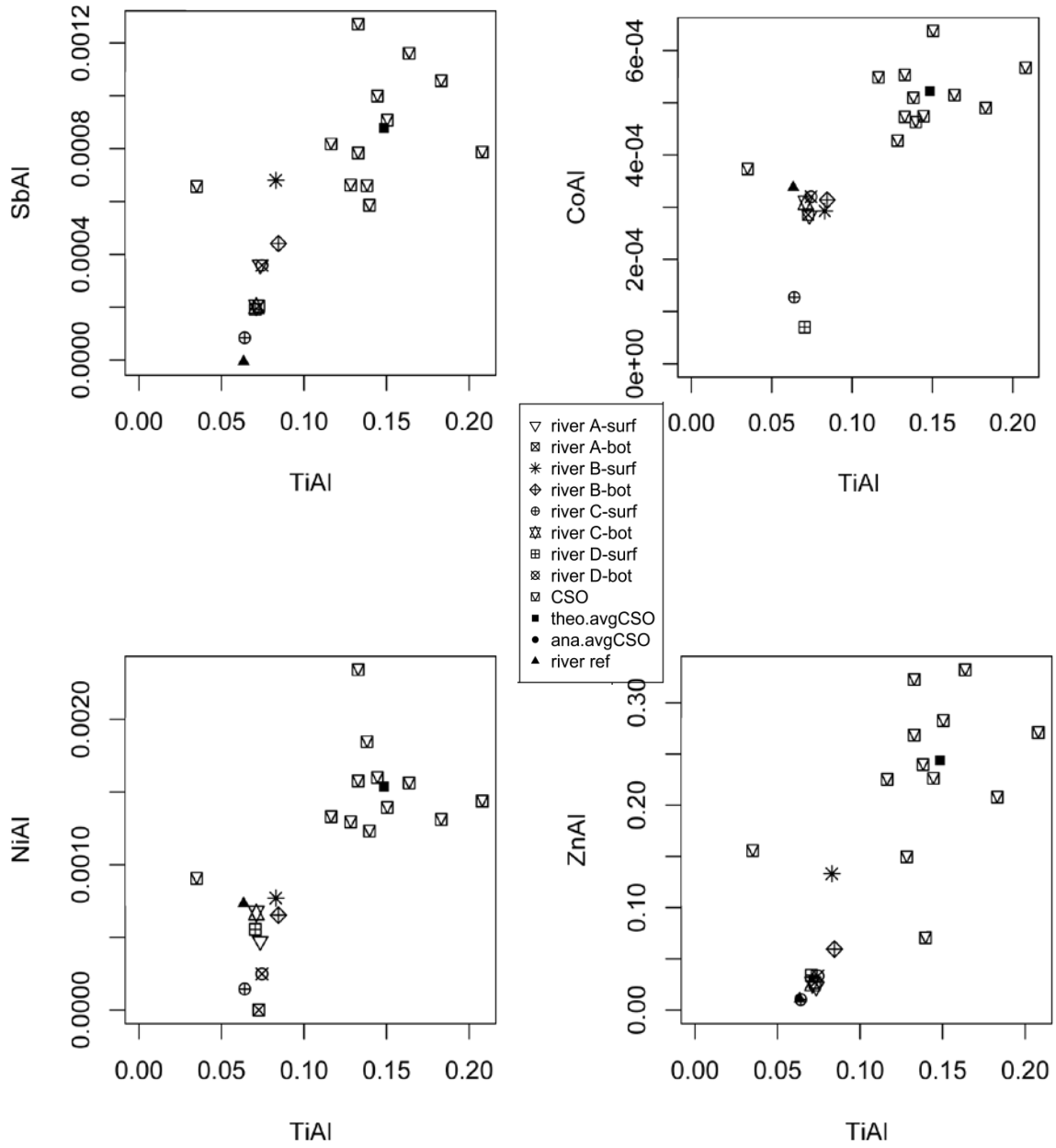

Figure IV. 7 – Particulate metal concentrations normalized by Al in combined sewer overflow (CSO) and overflow plume plotted against Ti normalized by Al. These plots were used to calculate metal excess or deficiency during an overflow episode for Table IV. 2

Similar to plots in Figure IV.4 for dissolved concentration, plots in Figure IV. 6 showed a general trend of Co and Ni that were not conservative. Correlations of Pb/Al and Cu/Al with Ti/Al were satisfactory and displayed a high level of conservativity. As mentioned previously, Ba and Zn showed conservative behaviour in the solid fraction.

An example of CSO mixing calculation for copper (Cu) in the dissolved fraction is illustrated in figure 8. In this case, vertical distance from the mixing line indicates an excess of the dissolved Cu from CSO point of -4.3 $mg.L^{-1}$ and -4.8.10-3 $Cu.Al^{-1}$ equal to -65 $\mu g.g^{-1}$excess of solid Cu from CSO. When this is calculated as flux (multiplied by average discharge of the overflow, 26.4 $m^3.s^{-1}$), estimated total excess in the dissolved and solid fraction can be calculated (Table IV. 2).

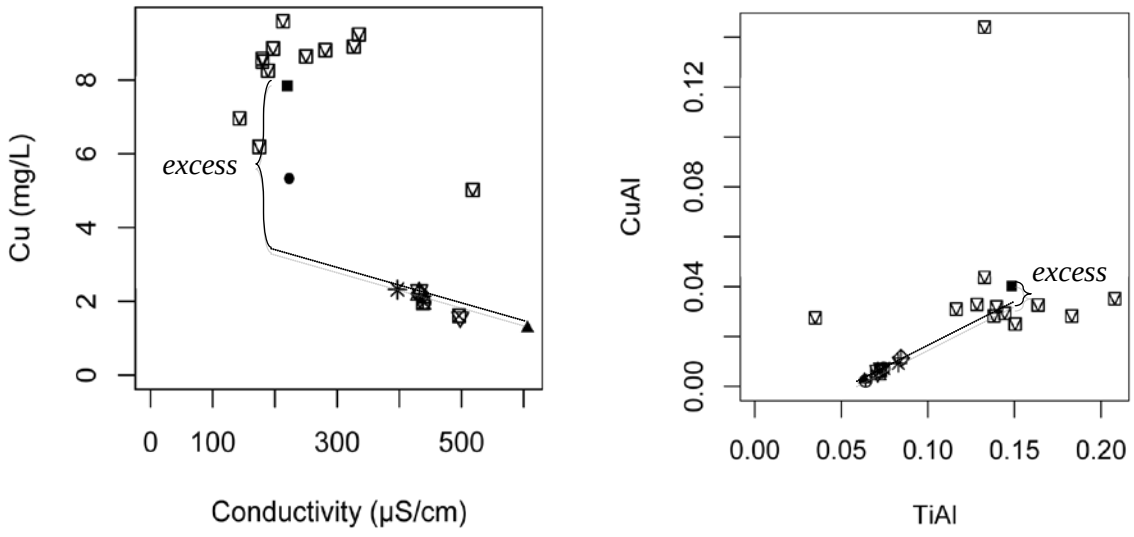

Figure IV. 8 - Example of excess calculation of the overflow wastewater in solid and dissolved phase for copper when entering the Seine River.

For most metals enriched by anthropogenic activities in the Seine River such as Cu and Zn (Priadi et al. 2010), a net deficiency of dissolved and solid metals are demonstrated (negative total excess Table 2). Pb also demonstrated to a lesser extent a net deficiency. This would indicate that other metal sources do exist and is needed in order to compensate for the metal deficiency between the CSO and the Seine River mixing line. This would confirm that the bed sediment is indeed a potential source of metals to the water column as stated in Hypothesis 2.

Table IV. 2 - Preliminary excess calculation of metals in solid and dissolved phase during overflow episode into the Seine River

	dissolved			solid			Total excess ($mg.s^{-1}$)
	r^2 mixing line	excess ($\mu g.L^{-1}$)	excess ($mg.s^{-1}$)	r^2 mixing line	excess ($\mu g.g^{-1}$)	excess ($mg.s^{-1}$)	
Ag	0.69	-0.09	-2.4	0,71	1,6	8,7	-72
Ba	0.44	-170	-4489	0,64	-320	-1804	-3543
Ca	0.98	5828	154041	0,16	-13281	-74767	154041
Cd	0.34	-0.04	-1.1	0,61	0,42	2,4	-22
Co	<0.15	IC	IC	0,02	-1,7	-9,5	-28
Cr	0.50	-0.45	-12	0,35	5,4	30	-317
Cu	0.94	-4.3	-112	0,96	-65	-364	-3339
Fe	<LQ	IC	IC	0,88	-525	-2957	-890
Ni	<0.15	IC	IC	0,09	-2,87	-16	-95
Pb	0.70	-4.6	-121	0,86	-116	-651	-3622
Sb	0.82	0.26	6.9	0,85	13	72	-82
Tl	0.13	0.02	0.54	0,50	0,32	1,8	-1.5
Zn	0.16	-150	-3965	0,89	-624	-3510	-26408

For Ag and Cd, the excess in the solid fraction was notcompensated by the deficiency in the dissolved fraction. This would signify that desorption of Ag and Cd from the solid fraction to the dissolved fraction could have occurred, but extra excess in the solid fraction would be transferred to another pool, in which case would be a potential process would be sedimentation of suspended matter towards the bed sediment. Fluxes for other metals such as Co, Ni, and Ca were incalculable because mixing line in the dissolved fraction was difficult to define (regression coefficient for regression line (r^2) <0.25, Table IV. 2, illustrations in Figure

IV. 5). This seems to be the case for metals with low solubility and with a preference to the dissolved fraction (Chapter II). Nevertheless, this preliminary two-source method has proven useful to estimate the importance of other source and sink involved during a process for most conservative metals which would help further interpretation of results in the Hypothesis 2.

7.2 Hypothesis 2

Elements identified as conservative and discriminates the three different sources were chosen as input for the least square fitting calculation (see supporting information for fitting language in R). Numerous elements among K, Mg, Ca, Ti, Fe, Pb and POC were used to find the best fit. These elements were chosen due to their potential ability to trace natural or anthropogenic sources. Among various combinations, the use of Pb and K as fitting elements seems to give satisfactory fit (error in Annexe 6 Table S2). Pb was previously identified as a potential conservative discriminator between the different sources (Figure IV. 6). As for K, it was chosen not only for its discriminative nature between the three sources, but also for its importance in representing the natural geological background. While Pb was chosen to be the anthropogenic tracer, K was chosen to be the natural tracer. Fit results using these two elements are shown on Figure IV. 9. Results demonstrate a satisfactory fit for relatively conservative elements such as Ag, Cu and Zn except for Seine B-surf samples which would confirm once again the possible contamination from the La Briche overflow. Metals with a preference to the dissolved fraction, in this case Co and Ni, demonstrated poor fit. The model tends to overestimate solid Co and Ni concentration. Due to their preference to the dissolved fraction (Chapter II), this could signify the possible loss through desorption of Co and Ni from the solid fraction to the dissolved fraction. For their case, the dissolved fraction would have a higher role in controlling metal concentration in the water column and further attempt of modeling should be continued. Sb demonstrated that the model systematically underestimated measured concentrations. Opposite to the possible desorption phenomenon for

Co and Ni, Sb may have a higher preference for the solid fraction. Due to a significant excess of dissolved Sb measured through hypothesis 1 (Table IV. 2), a significant adsorption phenomenon may take place during the overflow episode. In general, surface samples were observed to be more difficult to fit than bottom samples.

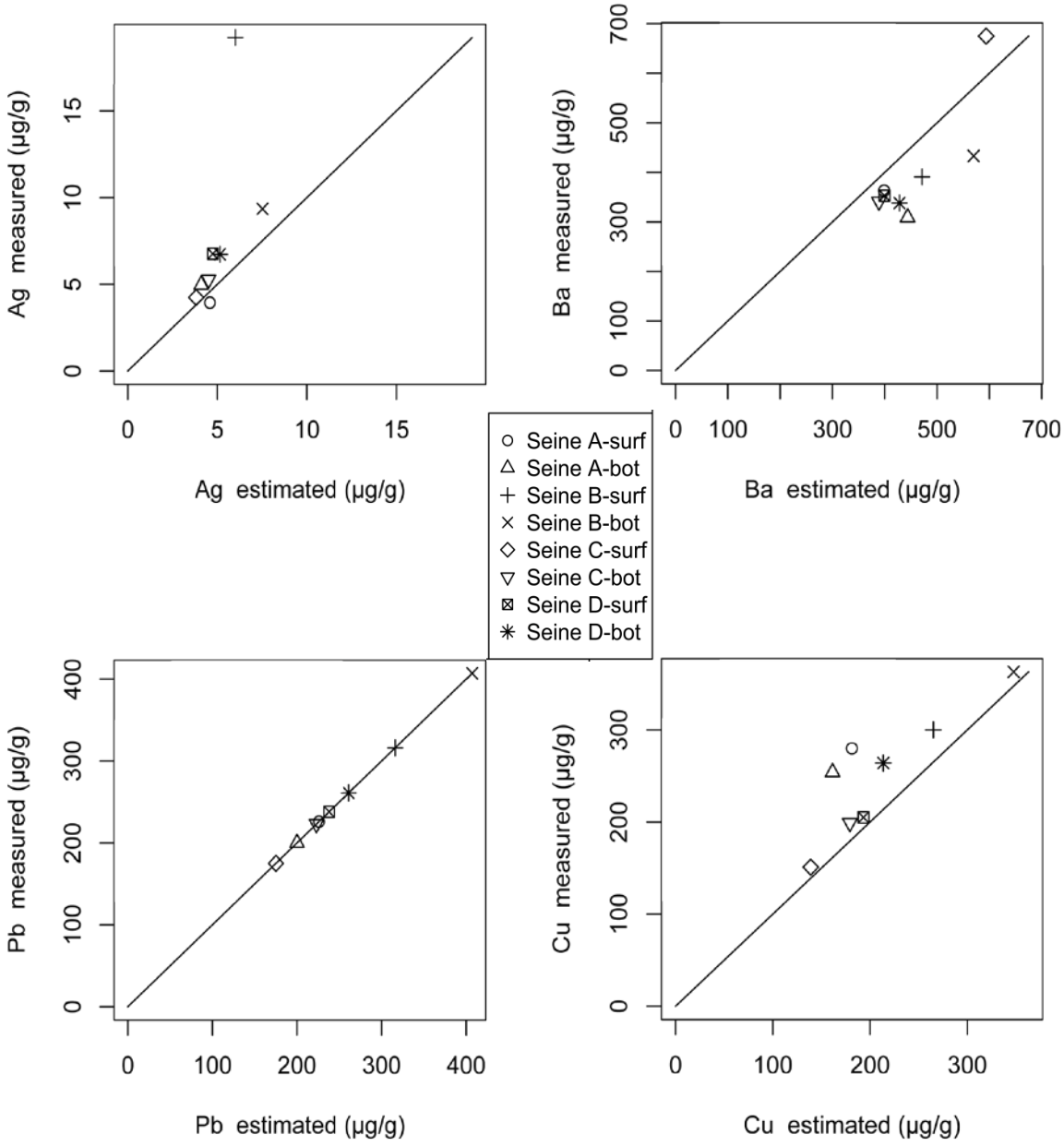

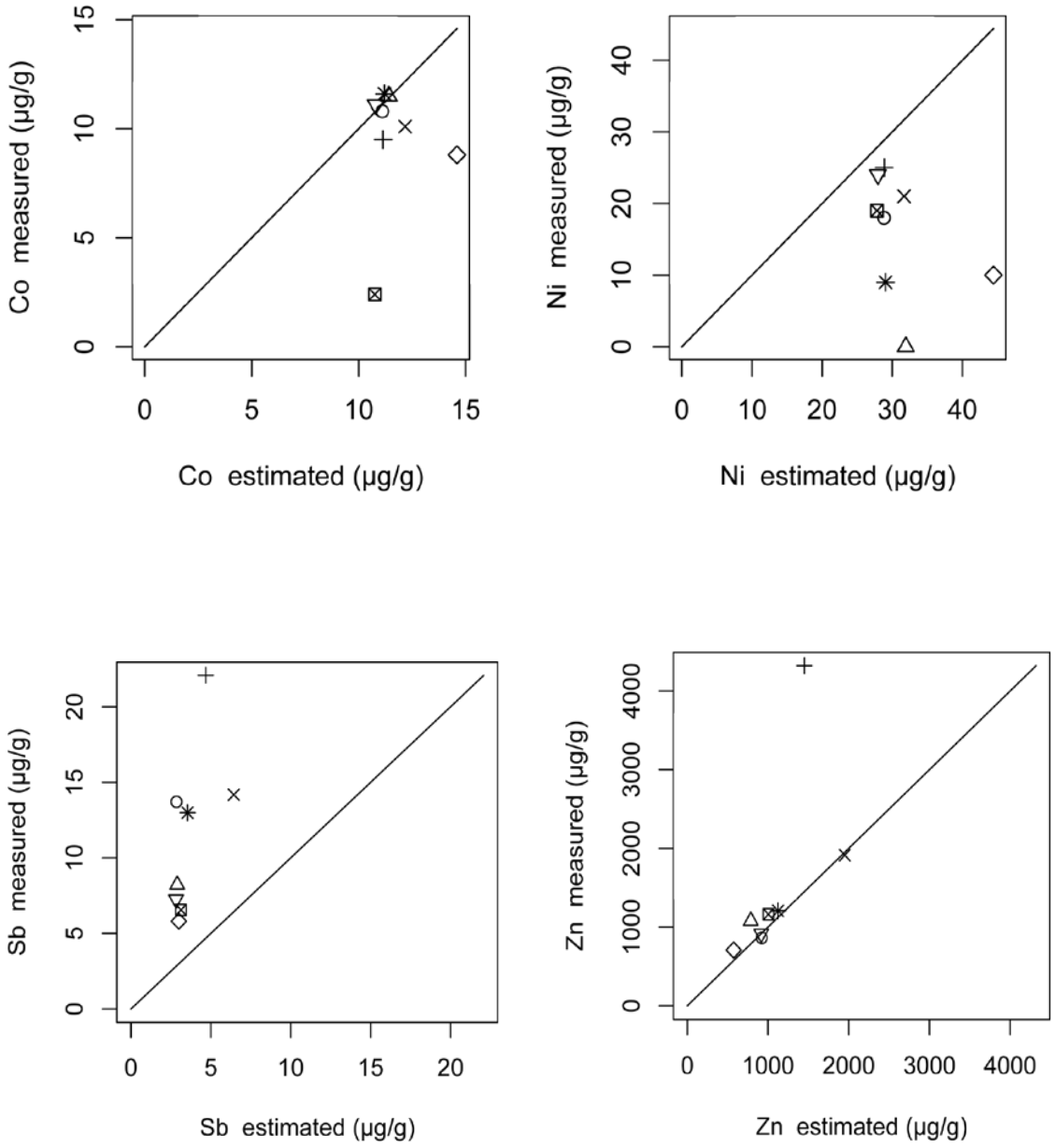

Figure IV. 9 - Least square fitting results of metal concentration in the overflow plume estimated using Pb and K to quantify contribution of combined sewer overflow, bed sediment and the Seine River during an overflow episode

Calculation of source contribution is represented by bar graphs in Figure IV. 10. Although fit results in Figure IV. 9 displayed satisfactory results for most metals, source estimation for surface samples demonstrated questionable results, especially for Seine C-surf for which the model detected 100% of contribution by the bed sediment. Indeed, fit results in Figure IV. 9 demonstrated a general difficulty to fit surface samples with the model. This estimation seems to work better for bottom water samples, shown by fewer unfitted results and also contribution percentage that are more acceptable. As described in section 6.4 in this chapter, the Seine A-samples were already contaminated with other sources upstream. River body arriving at the overflow already displayed a significant proportion of bed sediment, caused by the river discharge that doubled which created shear forces against the bed sediment.

As wastewater from the Clichy combined sewer overflow entered the Seine River, an increase in metal concentrations were observed in the Seine B samples. At this stage, contribution of overflow to the pollution plume in the Seine River was estimated to be around 35% at the Seine B samples. This was relatively equal to the metals transported by the Seine River. Although the CSO was known to contain a high level of suspended matter, around 30% of suspended matter actually originated from bed sediment. The overflow phenomenon was not only a source of chemical contamination, but also a source of physical force provoking sediment resuspension.

CSO particles seem to suspend relatively rapid because Seine C samples seem to have 50% less samples from CSO than B samples. Suspended matter could have stabilized on the Seine C point, because contribution of each source was similar in Seine C and D points. Fitting procedure demonstrated satisfactory results for bottom samples.

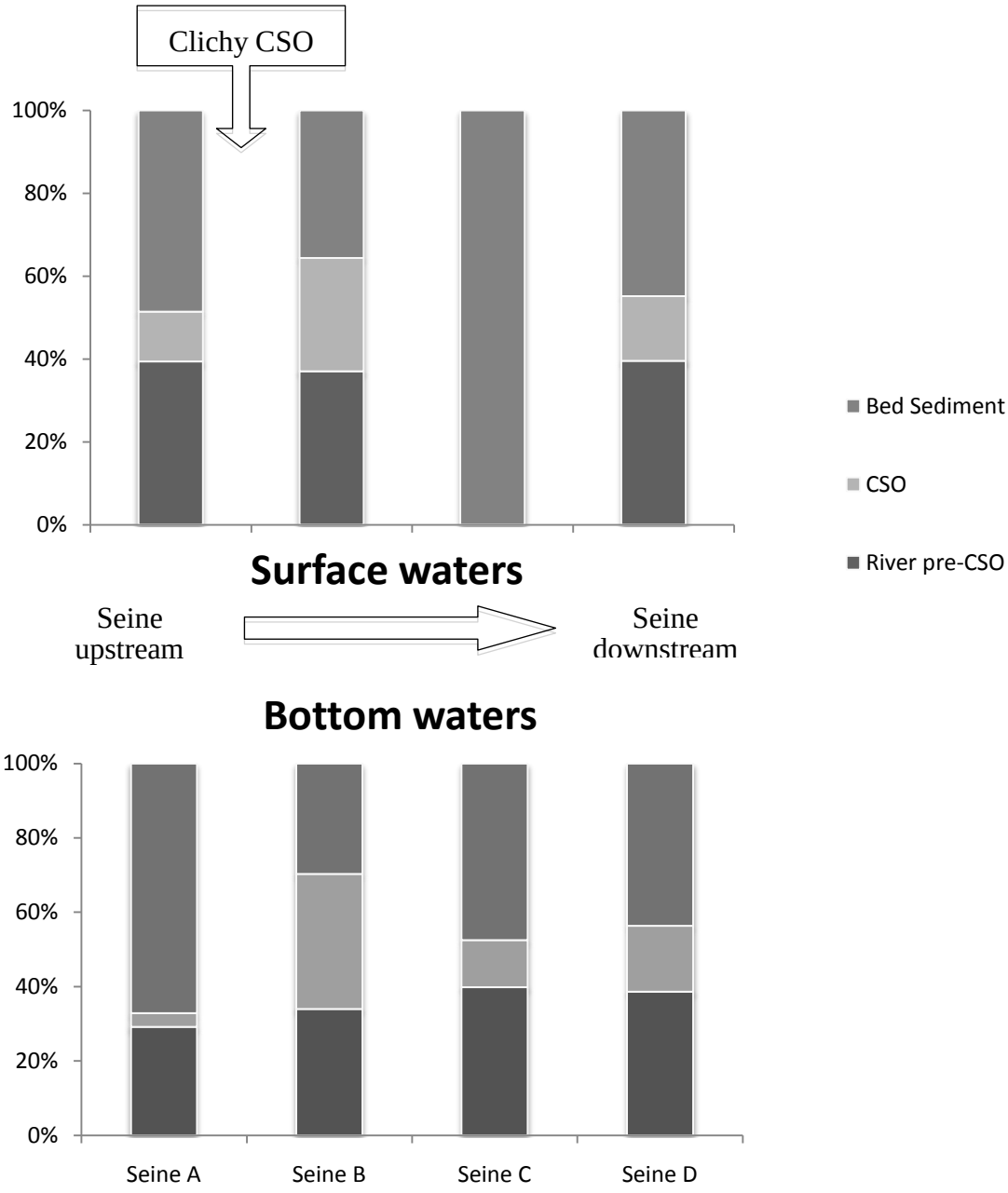

Figure IV. 10 – Percentage of contribution of each identified source (CSO, Seine River and bed sediment) to the metal contamination in suspended matter in the river during an overflow episode

Surface samples may be difficult to model because one particular phenomenon may affect the surface samples which is the oxidation of reduced species. Indeed, surface samples are more in contact with atmosphere and are more susceptible to aeration compared to bottom

samples. As CSO and bed sediment samples are known to contain reduced species such as sulfides, surface samples are prone to oxidation and therefore metal conservativity is not assured. Therefore, a further attempt to key processes of exchange between solid and dissolved fractions must be made for surface samples.

8 Conclusion

High definition sampling conducted during an overflow event indicated a significant contribution of bed sediment, as well as the overflow itself, to the increase of metal concentration in the water column. Wastewater from the overflow structure impacted metal concentration in the solid fraction, although not as significant as expected. Each identified sources including overflow water, river water and bed sediment contributed equally to elemental content in the solid fraction after the first hours of overflow episode. Nevertheless, sediments originating from overflow rapidly settled and proportion of suspended matter originating from bed sediment dominated the water column once more. Sample surfaces displayed a high variation in the dissolved fraction. As surface water are aerated, this could indicate a possible oxydation of reduced species into the dissolved phase. Further investigations are needed to identify particular behaviour of thèse surface samples and specifically characterize their spéciation.

References

Caetano M, Madureira MJ, Vale C. Metal remobilisation during resuspension of anoxic contaminated sediment: short-term laboratory study. Water Air and Soil Pollution 2003; 143: 23-40.

Chebbo G, Gromaire MC, Ahyerre M, Garnaud S. Production and transport of urban wet weather pollution in combined sewer systems: the "Marais" experimental urban catchment in Paris. Urban Water 2001; 3: 3-15.

Eggleton J, Thomas KV. A review of factors affecting the release and bioavailability of contaminants during sediment disturbance events. Environment International 2004; 30: 973-980.

Estebe A, Mouchel JM, Thevenot DR. Urban runoff impacts on particulate metal concentrations in river Seine. Water Air and Soil Pollution 1998; 108: 83-105.

Even S, Mouchel JM, Servais P, Flipo N, Poulin M, Blanc S, et al. Modelling the impacts of Combined Sewer Overflows on the river Seine water quality. Science of The Total Environment 2007a; 375: 140-151.

Even S, Poulin M, Mouchel JM, Seidl M, Servais P. Modelling oxygen deficits in the Seine River downstream of combined sewer overflows. Ecological Modelling 2004; 173: 177-196.

Even S, Thouvenin B, Bacq N, Billen G, Garnier J, Guezennec L, et al. An integrated modelling approach to forecast the impact of human pressure in the Seine estuary. Hydrobiologia 2007b; 588: 13-29.

Gasperi J, Garnaud S, Rocher V, Moilleron R. Priority pollutants in wastewater and combined sewer overflow. Science of The Total Environment 2008; 407: 263-272.

Gromaire-Mertz MC, Garnaud S, Gonzalez A, Chebbo G. Characterisation of urban runoff pollution in Paris. Water Science and Technology 1999; 39: 1-8.

Houhou J, Lartiges BS, Montarges-Pelletier E, Sieliechi J, Ghanbaja J, Kohler A. Sources, nature, and fate of heavy metal-bearing particles in the sewer system. Science of The Total Environment 2009; In Press, Corrected Proof.

Kafi-Benyahia M, Gromaire MG, Chebbo G. Spatial variability of characteristics and origins of urban wet weather pollution in combined sewers. Water Science & Technology 2005; 52.

Kafi M, Gasperi J, Moilleron R, Gromaire MC, Chebbo G. Spatial variability of the characteristics of combined wet weather pollutant loads in Paris. Water Research 2008; 42: 539-549.

Lee JH, Bang KW. Characterization of urban stormwater runoff. Water Research 2000; 34: 1773-1780.

Neal C, Neal M, Hill L, Wickham H. The water quality of the River Thame in the Thames Basin of south/south-eastern England. Science of The Total Environment

Urban Environmental Research in the UK: The Urban Regeneration and the Environment (NERC URGENT) Programme and associated studies. 2006; 360: 254-271.

Old GH, Leeks GJL, Packman JC, Smith BPG, Lewis S, Hewitt EJ, et al. The impact of a convectional summer rainfall event on river flow and fine sediment transport in a highly

urbanised catchment: Bradford, West Yorkshire. The Science of The Total Environment 2003; 314-316: 495-512.

Seidl M, Huang V, Mouchel JM. Toxicity of combined sewer overflows on river phytoplankton: the role of heavy metals. Environmental Pollution 1998; 101: 107-116.

SIAAP. Dossier du maitre d'ouvrage. In: SIAAP, editor. Débat Public Refonte de la Station d'Epuration Seine Aval. 2010, 2007.

Simpson SL, Apte SC, Batley GE. Effect of short term resuspension events on trace metal speciation in polluted anoxic sediments. Environmental Science & Technology 1998; 32: 620-625.

Weyrauch P, Matzinger A, Pawlowsky-Reusing E, Plume S, von Seggern D, Heinzmann B, et al. Contribution of combined sewer overflows to trace contaminant loads in urban streams. Water Research 2010; 44: 4451-4462.

Chapitre V – Mise en évidencede sulfure de zinc dans les matières en suspension fluviales par EXAFS et MEB

Avant-Propos

Les chapitres précédents ont démontré que le Zn est parmi les métaux les plus mobilesn'ayant pas de préférence particulière ni pour la phase dissoute ni pour la phase particulaire. Sa mobilité est encore plus marquée dans le pourcentage significatif dans de présence dans la phase échangeable et le niveau important du Zn dans la phase dissoute pendant les premières heures suivant un rejet d'eaux urbaines non traitées. Dans ce chapitre, nous allons donc exposer une spéciation plus détaillée du Zn dans les matières en suspension enutilisant la méthode EXAFS couplée par la microscopie électronique à balayage. Pendant l'expérience, l'état d'oxydation des échantillons a été conservé afin de préserver toutes les

espèces telles quelles, notamment les espèces réduites. Les résultats montrent qu'il existe en effet des espèces réduites qui sont des porteurs significatifs du Zn dans la phase particulaire. **Une version révisée de ce chapitre est soumise au journal *Environmental Science and Technology* sous le titre « *EXAFS and SEM evidence for zinc sulfide solid phases insuspended matter from the Seine River, France*».**

1 Introduction

Determining the solid state speciation of trace metal elements (TME) in impacted natural systems is potentially useful for distinguishing between natural vs. anthropogenic sources and is required for evaluating the impact of these elements on ecosystems. Indeed, the oxidation states of TME, their mode of association (surface-complexation, incorporation in mineral structures) with mineral or organic host phases, and the stability of these phases are key parameters that directly influence their solubility, bioavailability, and toxicity. The speciation of TME depends on physicochemical parameters of the medium, such as pH and redox conditions, that can also be significantly modified by biological activity. Although determining molecular-level speciation is generally accepted as an essential step in building reliable biogeochemical models, it is often a difficult task when considering compositionally and structurally heterogeneous samples from soils and sediments. For the two last decades, synchrotron-based spectroscopic methods, especially Extended X-ray Absorption Fine Structure (EXAFS) spectroscopy, have been developed and used to overcome these difficulties. EXAFS spectroscopy, in particular, has been shown to be an efficient analytical tool for quantifying the various chemical forms of dilute metals or metalloids in complex natural solid samples (e.g., Brown and Sturchio, 2002).

Speciation of TME in riverine suspended matter is especially difficult to determine accurately because these solids occur at very low concentration in rivers (typically a few mg/L) and their speciation can be potentially sensitive to changes in redox conditions during sampling and analysis (Borch et al.2009). In addition, distinguishing between soluble TME and TME associated with particulate matter is difficult because mineral and organic colloidal materials often occur in natural waters and may bind or incorporate TME. For instance, Rozan et al.(2000) showed that Cu, Zn, Fe, and polysulfide complexes in the dissolved fraction (<0.2 µm) of river water from an urbanized area might explain the increase of sulfide-associated metals. Kramer et al. (2007) also noted a significant increase of chromium reducible sulfides (CRS) from pristine waters to urban impacted waters. More generally, group B metals such as Fe, Cu, Zn, Hg, and Pb are known to bind strongly to reduced inorganic and organic sulfides (S^{2-} or S_2^{2-}) ligands (Sigg et al., 2006), which partly explains the ubiquity of metal sulfides in reducing environments. Accordingly, several studies have underlined the importance of sulfide phases as TME hosts in anoxic river and estuarine bottom sediments (Lewis et al., 2007; Sigg et al., 2006; Weber et al., 2009). Although these sulfide phases are expected to be sensitive to oxidation, thermodynamic and kinetic studies have shown that this process may be relatively slow in oxic waters (8), which suggests that Fe, Cu and Zn sulfides may account for a significant fraction of the total metal load in oxic waters.

This study presents mineralogical and spectroscopic evidence for the occurrence of significant quantities of zinc sulfide in suspended matter from the Seine River downstream of the Paris conurbation. Our results emphasize the importance of preserving redox conditions during sampling and drying of solid suspended matter in oxic rivers and provide new perspectives on metal speciation in oxic rivers, knowledge of which is essential for establishing reliable water monitoring methods.

2 Material and Methods

2.1 Sampling

Water samples were collected in the downstream section of the Seine River watershed after flowing through the Paris region. This river section is strongly affected by urbanization, which has led to high levels of Zn contamination of the Seine sediments downstream from Paris (Meybeck et al., 2007). Indeed, while the average natural background concentration of Zn in the basin is 60 mg/kg (Thévenot et al., 2007), Zn concentrations can be as high as 1317 mg/kg in archive sediments from the Lower Seine (Le Cloarec et al., In Press) and can reach up to 1402 mg/kg in recent suspended particulate matter (SPM) samples (see Results and Discussion section). A particular source of Zn contamination of this watershed is zinc roofing that prevails in the Paris conurbation. Consequently, the zinc concentration in the Seine River is among the highest when compared with other large urban rivers (Robert-Sainte et al., 2009). In order to take into account the influence of the Paris region on Zn speciation in the Seine River, the water sampling site was chosen in Triel sur Seine, which is located 80 km after the Seine River flows out of Paris in the southwest.

The set of samples used in the present study were chosen for their high Zn concentrations and the unusual nature of the hydrological regime during sampling. SPM samples were collected in December 2008 (referred to as 'winter') and in February 2009 (referred to as 'winter+rain') and correspond to regular winter flow and storm-affected winter flow, respectively. Another SPM sample was collected on August 2009 (referred to as 'summer') and corresponds to low summer flow (Table V. 1). Water was collected using a PVC bucket at ~ 3 m from riverbank and 1 m beneath the water surface. Before sampling, all bottles and containers were soaked in 2 N HNO_3 for at least 3 days and were rinsed thoroughly three times with deionised water. In the field, all bottles, buckets, and containers

were rinsed three times with river water before sampling. SPM was recovered by filtration of a 20 L volume of Seine water through 0.45 μm Millipore cellulose filters. This filtration was done at our laboratory in Paris, France within 1-2 days after the water sampling, except for the winter sample, which was stored at 4°C for 1 month in air before filtration in a glove box.

For both the 'winter' and the 'winter+rain' samples, two types of protocols were used to recover the SPM. The first type, referred to as 'O_2', consisted of filtration under an ambient atmosphere and air-drying. SPM were recovered by scraping them from filters. The second type, referred to as 'N_2', filtration was performed under an ambient atmosphere until a water layer of at least 2 mm thickness was maintained above the filter to avoid exposing filtered SPM directly to air. Filtration of the remaining overlying water layer was achieved in a glove box under an N_2 atmosphere (< 50 ppm O_2) to avoid direct exposure of SPM to atmospheric O_2. Afterwards, the wet SPM paste was scraped from the filter and vacuum dried inside the glove box. For EXAFS analyses, samples were prepared as pure pellets of 5-7 mm in diameter in the glove box. Following our usual sample preparation procedures (Morin et al., 2009; Wang et al., 2008; Wang et al., 2009), samples were sealed in anoxic containers for shipping and transfer into a glove-box at the Stanford Synchrotron Radiation Lightsource (SSRL) in Stanford, CA, USA or the European Synchrotron Radiation Facility (ESRF) in Grenoble, France. Samples were transferred from the glove box to the beamline at SSRL in a liquid nitrogen bath and quickly introduced into a cryostat where they were analyzed under He atmosphere. Due to the limited weight of SPM samples collected from water filtration, SPM samples were also collected in a sediment trap emptied on the same dates and at the same location as the filtered SPM samples after one month of sediment trap deployment at 1 m depth. SPM samples collected in the sediment trap may display different oxidation level compared to grab SPM samples due to the nature of the sediment trap collection method.

Nevertheless, the latter was considered adequate to confirm Zn speciation in grab samples due to the similar metal concentrations and general Zn speciation in both samples.

SEM images were collected on these later samples at 6-7 kV using the backscattered electron imaging mode on a Zeiss ULTRA SEM-FEG microscope. Energy Dispersive X-ray Spectroscopy (EDXS) data were collected at the same electron beam-voltage using a BRUKER AXS Si-drift detector.

2.2 Model compounds

Two types of Zn sulfide model compound samples were used in the present study: amorphous ZnS prepared by neutralizing a Zn(II) salt solution with a basic Na_2S solution, following the procedure reported by (Helz et al., 1993) and a natural sphalerite (ZnS) from Franklin, New Jersey, USA, kindly provided by J.C. Boulliard from the French Mineral Collection of UPMC, Jussieu, France. A Zn/Al layered double hydroxide (Zn/AL-LDH) sample, $(Zn_2Al)(OH)_2Cl$, was used as a model compound for Zn^{2+} octahedrally coordinated by oxygen. This sample was synthesized and previously analyzed using EXAFS spectroscopy (Juillot et al., 2003) using the protocols of Trainor et al.(2000).

2.3 Extended X-ray Absorption Fine Structure (EXAFS) data collection and analysis

Zn K-edge EXAFS spectra were recorded at a temperature below 20K under He atmosphere in order to minimize thermal dampening of the EXAFS signal and to preserve the oxidation state of the sample during the measurement. Sphalerite, ZnS and Zn/Al-LDH data were recorded in transmission detection mode at SSRL on wiggler beamlines IV-1 and IV-3, respectively. Data for the 'winter+rain' SPM sample were recorded on the high-flux wiggler beam line 11-2 at SSRL in fluorescence detection mode using a CANBERRA high-throughput 30-element Ge array detector (Proux et al.,2005) and thin Al foils to attenuate the

iron fluorescence signal. EXAFS spectra of the 'winter' and 'summer' SPM samples were recorded on the FAME-BM30B bending magnet beamline at ESRF in fluorescence detection mode using a CANBERRA high-throughput 30-element Ge array detector. Amorphous ZnS data were collected in transmission detection mode at the SAMBA beamline at the SOLEIL synchrotron, Saclay, France. For the three experiments, energy was calibrated with a metal Zn foil with the first inflexion point set at 9659 eV.

EXAFS χ(k) functions were extracted using the XAFS program (Winterer, 1996). Fast Fourier transforms of the k^3-weighted χ(k) functions were calculated over the 2-10.5 $Å^{-1}$*k*-range. The first-neighbour contribution to the EXAFS was then obtained by back-Fourier transformation over the 0.6 – 2.4 Å range. This Fourier-filtered signal was then fit using the plane-wave formalism and a non-linear Levenberger-Marquard minimization algorithm. Phase shift and amplitude functions used in this fitting procedure were calculated using curved-wave theory as incorporated in the *ab initio* FEFF8 code (Zabinsky et al., 1995) and based on the zincite (ZnO) and sphalerite (ZnS) structures (*22*) for Zn-O and Zn-S pairs, respectively. The fit quality was estimated using a reduced χ^2 of the following form:

$$\chi^2_{FT} = \frac{N_{ind}}{(N_{ind} - p).n} \sum_{i=1}^{n} \left(\|FT\|_{\exp_i} - \|FT\|_{\mathrm{calc}_i} \right)^2$$

with $N_{ind} = (2\Delta k \Delta R)/\pi$) = the number of independent parameters, *p* the number of free fit parameters, *n* the number of data points fitted, and $\|FT\|_{\exp}$ and $\|FT\|_{\mathrm{calc}}$ the experimental and theoretical Fourier transform magnitudes over the 0.6-2.4 Å *R*-range of the Fourier Transform (Morin et al., 2009).

2.4 Chemical analysis of water and SPM samples

The results of standard physico-chemical measurements as well as multi-elemental analysis by ICP-MS of dissolved metals and of chemically-digested suspended matter (SPM)

are reported in Table V. 1. Details about the analytical procedures used are reported in Priadi et al. (2011). In summary, suspended matter was digested using *aqua regia*, HF and then $HClO_4$ and analyzed with ICP-QMS (X-Series, CCT II+ThermoElectron, France) in a 0.5N HNO_3 matrix.

3 Results and Discussion

3.1 Zn Concentrations and pH

Bulk Zn concentrations (Table V.1) in the three SPM samples range from 232 to 1402 mg/kg. Dissolved oxygen concentrations indicate significant oxic conditions, with all samples containing > 6 mg/L of O_2. pH values are slightly alkaline, which is consistent with buffering by the dominant carbonate rocks comprising the Seine sedimentary basin (Meybeck et al., 1999) as well as the high concentration of Ca both in the dissolved and solid fractions.

3.2 Evidence for ZnS mineral phases

Raw experimental Zn K-edge $k^3\chi(k)$ spectra for the three SPM samples are displayed in Figure V.1a. They clearly indicate significant differences in Zn speciation between samples dried under N_2 vs. O_2 atmospheres. Accordingly, fast Fourier transform of the data (Figure V.1b) show large differences in first-shell contributions to the EXAFS. For both the winter and summer N_2 samples, the first-neighbor peak is observed at a longer distance and has a higher intensity than that of the corresponding O_2 samples. Comparison with modelcompound data indicates a strong similarity between the spectra of these N_2samples

Table V. 1 - Physico-chemical characteristics of dissolved and particulate phases of the Seine River samples

	High water	High water+rain	Low water
pH	8.01	7.93	7.85

Temperature (°C)	5.2	6.90	19.6
Conductivity (µS/cm)	513	-	604
Dissolved Oxygen (mg/s)	12.46	12.04	6.25
Discharge (m^3/s)	495	550	211
SPM (>0.45 µm)			
[MES] (mg/L)	9.5	16.3	3.1
COP (mg/L)	0.93	1.46	0.73
Zn (mg/kg)	1402	232	522
Mg (%)	0.79	0.40	0.56
Ca (%)	19.4	6.69	9.26
K (%)	1.79	0.70	0.92
Fe (%)	5.17	2.09	2.93
Al (%)	8.47	3.02	3.88
Dissolved (<0.45 µm)			
COD (mg/L)	4.14	3.42	3.54
Sodium (mg/L)	10.9	10.4	5.71
Ammonium (mg/L)	0.52	0.50	nd
Potassium (mg/L)	n.d	3.16	1.88
Magnesium (mg/L)	0.68	7.02	8.93
Calcium (mg/L)	98.6	108.8	64.8
Chloride (mg/L)	19.9	25.7	12.0
Nitrite (mg/L)	n.d	0.79	nd
Nitrate (mg/L)	28.5	28.3	8.8
Sulfate (mg/L)	28.0	35.4	14.2
Zn labile (mg/L)	2.79	1.44	2.42
Zn dissolved (mg/L)	3.90	3.47	4.53

and that of the amorphous ZnS model compound. The similarity between the ZnS model EXAFS data and that for the N_2 and O_2 'winter+rain' samples was much less marked, and the EXAFS data for these two SPM samples are similar.

Fourier-filtered first-neighbor contributions to the EXAFS were adjusted using either Zn-O or Zn-S single scattering paths, or a combination of both, depending on the samples studied. Results of this fitting procedure are given in Table V. 2 and are plotted as dotted lines in Figures V. 1b and V. 1c for all samples studied. Varying the ΔE_0 values by ±3 eV yielded variations of ±0.05 Å in the Zn-S and Zn-O distances. Because these variations in ΔE_0 values did not affect the fit quality, i.e. the χ^2_{FT} value, the corresponding distance range was taken as an estimate of the standard deviation for the fit Zn-S and Zn-O distances. Such a large standard deviation (±0.05 Å) is related to the short usable *k*-range (2 - 10.5 $Å^{-1}$) of the data,

which is a result of the dilute character of the natural samples studied. Although good quality data were recorded over a larger *k*-range for the model compounds, these data were fitted over the same *k*-range as the natural samples in order to yield consistent fitting results and error estimates.

First-neighbor Fourier-filtered data for amorphous ZnS and crystalline ZnS (sphalerite) were fit with a single Zn-S path, and the data for Zn/Al-LDH were fit with a single Zn-O path. The Zn-S distance values obtained for amorphous ZnS and crystalline ZnS (sphalerite) are similar and equal to 2.34 ± 0.05 Å with observed coordination numbers *N*= 3.7 and 3.8, respectively (Table V.2). These distance and *N* values are consistent with Zn^{2+} being four-coordinated by sulfur in sphalerite (Zabinsky et al., 1995) as well as in our amorphous ZnS model compound. The Zn-O distance for Zn/Al-LDH, where Zn is six-coordinated by oxygen, was 2.07±0.05 Å, in agreement with Juillot et al. (2003).

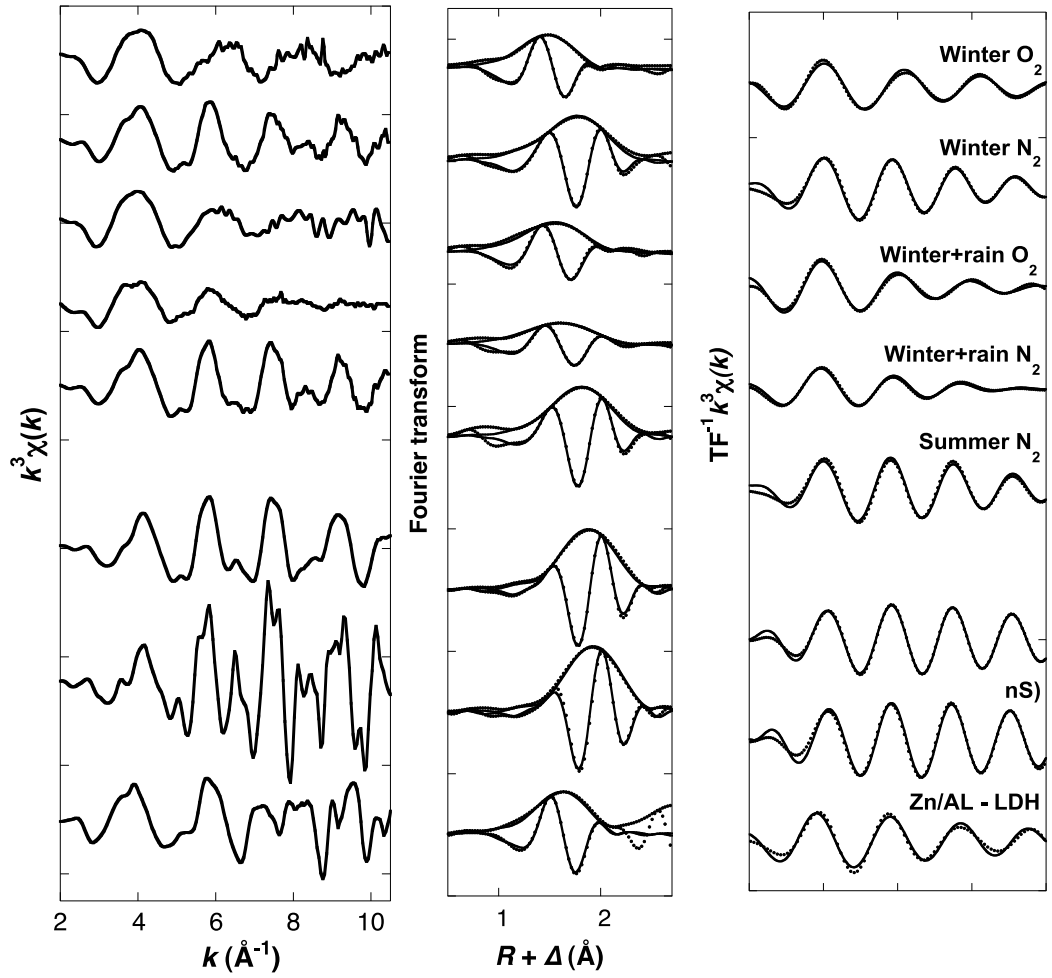

Figure V. 1 - Zn-K edge EXAFS data of the samples studied. Experimental unfiltered $k^3\chi(k)$ spectra (solid lines, left). Fourier-filtered experimental data (dotted lines) within the 0.6-2.4 Å *R*-range and the corresponding fits in *k*-space (solid lines, right). Corresponding Fourier transforms are also reported (middle); For comparison, experimental data of amorphous ZnS, crystalline ZnS and Zn/Al-LDH are reported, as references for Zn-S and Zn-O first shell coordination.

For the 'O_2' SPM samples, best fits were obtained using a single Zn-O path, while a combination of Zn-O and Zn-S paths were necessary for the 'N_2' samples, which confirms the differences observed between the 'N_2' and 'O_2' sample EXAFS data (Figure V.1). Adding a Zn-S path in fitting the 'O_2' samples systematically increased the goodness of fit estimator (χ^2_{FT} value) and led to unstable fits, with unrealistic Zn-S distances and *N* values. The Zn-O distance fit for the 'O_2 winter' sample (1.95 ± 0.05Å) indicates that a significant proportion of Zn^{2+} is tetrahedrally coordinated by oxygen in this sample (e.g., Juillot et al., 2008). In contrast, the Zn-O distance obtained for the 'N_2 summer' sample (2.03 ± 0.05 Å) is

similar to that of Zn^{2+} octahedrally coordinated by oxygen as in the Zn-LDH model compound (2.07 ± 0.05 Å). Zn-O distances determined for the other samples (2.01 ± 0.05 Å) are intermediate between those for octahedral (six-fold) and tetrahedral coordination (four-fold) by oxygen, suggesting a mixture of both, although the presence of five-fold coordination to oxygen as in some zinc phosphate minerals (Sarret et al., 2004) cannot be excluded.

The Zn-S distances obtained for all the 'N_2' samples (2.30–2.33 ± 0.05 Å) are similar to that observed for the ZnS model compounds (2.34 ± 0.05 Å), which shows that a significant fraction of Zn^{2+} is tetrahedrally coordinated to sulfur in these samples (Table V. 2). This Zn-S path is absent in the corresponding 'O_2' samples, which indicates significant oxidation of the sulfide Zn-host phase during air-drying. However, EXAFS data suggest a lower proportion of sulfide Zn-host phases in the 'winter+rain' sample (Table V.2, Figure V.1).

Table V. 2 - Fitting results for the Fourier Filtered $k^3\chi(k)$ first coordination shell. Standard deviations on the inter-atomic distances R(Å) were estimated to ±0.05Å from the fit of the model compounds by varying the energy shift ΔE_0(eV) of ±3eV. Other fitting parameters, N, σ(Å), and χ^2_{FT} correspond to number of neighbors, Debye-Waller parameter, goodness of fit (see text).

	Zn-O			Zn-S				
	R(Å)	N	σ(Å)	R(Å)	N	σ(Å)	ΔE_0(eV)	χ^2_{FT}
Winter O_2	1.95	3.6	0.09	-	-	-	3.9	0.25
Winter N_2	2.03	2.2	0.13	2.30	3.0	0.09	5.1	0.64
Winter + Rain O_2	2.01	4.8	0.12	-	-	-	7.5	0.27
Winter + Rain N_2	2.02	3.4	0.14	2.30	0.8	0.11	5.3	0.32
Summer N_2	2.07	2.0	0.09	2.33	2.3	0.07	7.5	1.39
Amorphous ZnS	-	-		2.33	3.7	0.07	7.5	0.13
Sphalerite (ZnS)	-	-		2.35	3.8	0.07	10.5	0.01
Zn-LDH	2.07	4.2	0.07	-	-	-	6.5	0.30

The similarity between the spectra of amorphous ZnS and the N_2 'winter' and 'summer' SPM samples suggests that the Zn-S pair correlations determined from EXAFS data fitting (Figure V.1, Table V.2) may be dominantly related to this mineral component, although the presence of a minor amount of crystalline ZnS can not be excluded. SEM observations of SPM collected in sediment traps during the same sampling period yield

further information on the nature of the Zn-bearing sulfide phase. Indeed, they revealed the presence of sub-micron ZnS mineral phases (Figure V.2a), often forming aggregates of ~ 100-200 μm in size (Figure V.2b).

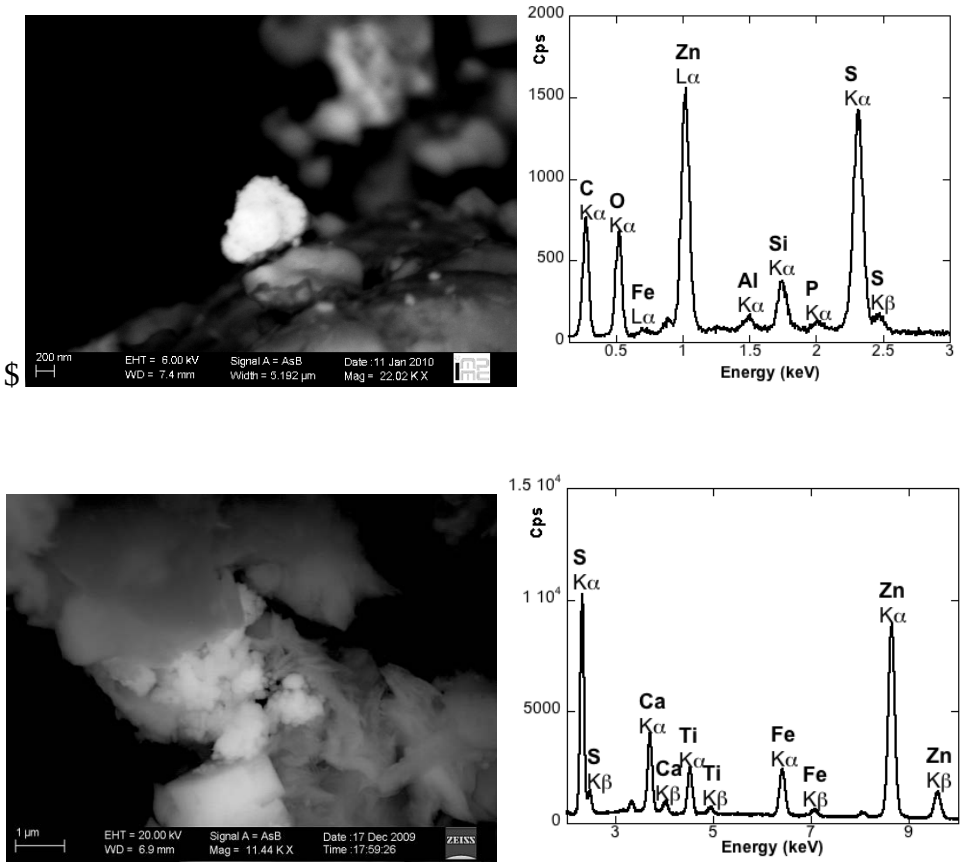

Figure V. 2Backscattered electrons SEM images of zinc sulfide particles in suspended particulate matter (SPM) sampled from sediment trap in the Seine River downstream the Paris region on winter (December 23) 2008 (top) and summer (June 9) 2009 (bottom). Energy Dispersive X-ray Spectra of the bright ZnS particles are reported on the right.

Representative micrographs of these ZnS solid phases are displayed in Figures V.2a and V.2b. The results of EDXS analyses unambiguously indicate that these samples consist of pure ZnS (Figures 2c, 2d). Accordingly, clear evidence of dominant Zn-S bonding is provided by the Zn K-EXAFS analysis of these samples (see Figure S1 and Table S1 in Annexe 10). In contrast, Zn was not detected in pyrite framboids (FeS_2) (data not shown) that are relatively abundant in the SPM samples, indicating that Zn concentration in pyrite is lower than 1%. Further EXAFS analysis using an extensive set of model compounds will be required to

identify other Zn-bearing species that are present in these complex samples, and which may account for the fraction of Zn coordinated to oxygen atoms revealed by our EXAFS data (Table V.2).

3.3 Environmental significance of ZnS mineral phases in the oxic water column

EXAFS and SEM results from the present study highlight the occurrence of sub-micron ZnS solid phases in the SPM of the oxic Seine River water. Although the exact nature of these phases is not yet elucidated, comparison of SPM Zn-EXAFS data with Zn-EXAFS data of amorphous and crystalline ZnS strongly suggest that they consist of amorphous ZnS. As demonstrated by EXAFS analysis, the absence of sulfur neighbors around Zn in the air-dried samples ('O_2'), in contrast with the samples dried under nitrogen atmosphere ('N_2'), suggests that these sub-micron ZnS particles are rapidly oxidized upon drying in air through a thin water film during filtration. Although the dissolved oxygen level in the water column indicates relatively oxic conditions, oxygen diffusion is expected to be much slower in the water column, thus liming the extent of oxidation of such particles in the Seine River. In addition, previous studies by Luther and Rickard (2005) and Rozan et al.(2003) also showed the presence of nm-sized polynuclear Zn_xS and Cu_xS phases and aggregates of these phases in the dissolved fraction of the oxic column of the Thames River. The present finding suggests that such soluble polynuclear ZnS species could be in equilibrium with sub-micron-sized ZnS particles that we found in the particulate fraction of the Seine River water. Persistence of such ZnS solid phases could also be related to the high stability of dissolved ZnS clusters that are known to be resistant to oxidation (Rozan et al.(2000) and references herein). Alternatively, Kramer et al. (2007) hypothesized that particulate Cu_xS would persist in oxic environments through the formation of a "rind" of sulfates formed on the surface that

acts as a passivation barrier with respect to oxidation. Although such rinds were not detected in the present study, rinds of Zn sulfate can not be ruled out on the basis of our data.

Interestingly, ZnS is considered to be the one of the most soluble metal sulfides. Indeed, Rozan et al. (2000) stated that the formation of ZnS is less favorable than of Cu, Ag, Cd, or Pb sulfides. Similarly, Luther and Rickard (2005) and Weber et al. (2009) reported that metal sulfide formation follows the "sulfide ladder", i.e. from the most insoluble to more soluble metal sulfide. The occurrence of ZnS particles in the Seine River, instead of sulfides such as Cu_xS or Fe_xS that incorporated Zn, is consistent with the high concentration of Zn in this urban catchment. Although the origin of these particles is still undetermined, one may infer that they formed under anoxic conditions, as in bottom sediments or in the urban sewage network. Indeed, CuS and PbS were regularly observed in bottom sediments in the downstream area of the Seine River catchment. Although ZnS has not been previously reported in the Seine catchment, ZnS particles were recently reported in the sewage network of Nancy, Moselle, France (Houhou et al., 2009).

The present study reports for the first time particulate ZnS in the suspended matter of an oxic river and found that these phases are unstable upon air-drying. These results underline the importance of preserving the oxidation state of solid samples using appropriate filtration and drying procedures under an inert atmosphere. Our results also suggest that systematic use of such sampling procedures could reveal the presence of reduced solid phases that might have been overlooked in previous studies in the oxic water columns of surface waters

References

Borch, T.; Kretzschmar, R.; Kappler, A.; Cappellen, P. V.; Ginder-Vogel, M.; Voegelin, A.; et al. Biogeochemical redox processes and their impact on contaminant dynamics. Environ. Sci. Technol. 2009 44: 15-23.

Brown Jr., G. E.; Sturchio, N. C. An overview of synchrotron radiation applications to low temperature geochemistry and environmental science. Rev. Mineral. Geochem. 2002, 49, 1-115.

Helz, G. R.; Charnock, J. M.; Vaughan, D. J.; Garner, C. D. Multinuclearity of aqueous copper and zinc bisulfide complexes - an EXAFS investigation. Geochim. Cosmochim. Acta 1993, 57, 15-25.

Houhou, J.; Lartiges, B. S.; Montarges-Pelletier, E.; Sieliechi, J.; Ghanbaja, J.; Kohler, A. Sources, nature, and fate of heavy metal-bearing particles in the sewer system. Sci. Total Environ. 2009, In Press.

Juillot, F.; Marechal, C.; Ponthieu, M.; Cacaly, S.; Morin, G.; Benedetti, M.; , Hazemann, J. L.; Proux, O.; Guyot, F. Zn isotopic fractionation caused by sorption on goethite and 2-Lines ferrihydrite. Geochim. Cosmochim. Acta 2008, 72 (19), 4886-4900.

Juillot, F.; Morin, G.; Ildefonse, P.; Trainor, T. P.; Benedetti, M.; Galoisy, L.; et al. Occurrence of Zn/Al hydrotalcite in smelter-impacted soils from northern France: Evidence from EXAFS spectroscopy and chemical extractions. Am. Mineral. 2003, 88, 509-526.

Kramer, J. R.; Bell, R. A.; Smith, D.S. Determination of sulfide ligands and association with natural organic matter. Appl. Geochem. 2007, 22, 1606-1611.

Le Cloarec, M. F.; Bonte, P. H.; Lestel, L.; Lefèvre, I.; Ayrault, S. Sedimentary record of metal contamination in the Seine River during the last century. Phys. Chem. Earth, Parts A/B/C, In Press.

Lewis, B. L.; Glazer, B. T.; Montbriand, P. J.; Luther III, G. W.; Nuzzio, D. B.; Deering, T.; et al. Short-term and interannual variability of redox-sensitive chemical parameters in hypoxic/anoxic bottom waters of the Chesapeake Bay. Mar. Chem. 2007, 105, 296-308.

Luther, G. W.; Rickard, D. T. Metal sulfide cluster complexes and their biogeochemical importance in the environment. J. Nanopart. Res. 2005, 7, 389-407.

Meybeck, M.; Idlafkih, Z.; Fauchon, N.; Andreassian, V. Spatial and temporal variability of total suspended solids in the Seine basin. Hydrobiologia 1999, 410, 295-306.

Meybeck, M.; Lestel, L.; Bonté, P.; Moilleron, R.; Colin, J. L.; Rousselot, O.; et al. Historical perspective of heavy metals contamination (Cd, Cr, Cu, Hg, Pb, Zn) in the Seine River basin (France) following a DPSIR approach (1950-2005). Sci. Total Environ. 2007, 375, 204-231.

Morin, G.; Wang, Y. H.; Ona-Nguema, G.; Juillot, F.; Calas, G.; Menguy, N. et al. EXAFS and HRTEM evidence for As(III)-containing surface precipitates on nanocrystalline magnetite: Implications for As sequestration. Langmuir 2009, 25, 9119-9128.

Priadi, C.; Pacini, S.; Ayrault, S.; Bonté, P. Urbanization impact of the Greater Paris Region on metal mobility in suspended sediments in the Seine River, France: Role of iron oxides. Internat. J. Environ. Sci. Technol.,2011, 8(1), 1-18

Proux O.; Biquard X.; Lahera E.; Menthonnex J.-J.; Prat A.; Ulrich O. et al FAME: A new beamline for X-ray absorption investigations of very-diluted systems of environmental, material and biological interests. Physica Scripta 2005, 115, 970-973.

Robert-Sainte, P.; Gromaire, M. C.; De Gouvello, B.; Saad, M.; Chebbo, G. Annual metallic flows in roof runoff from different materials: test-bed scale in Paris conurbation. Environ. Sci. Technol. 2009, 43, 5612-5618.

Rozan, T.F.; Lassman, M.E.; Ridge, D.P.; Luther III, G.W. Evidence for iron, copper and zinc complexation as multinuclear sulfide clusters in oxic rivers. Nature. 2000, 406, 879-882

Sarret, G.; Balesdent, J.; Bouziri, L.; Garnier, J. M.; Marcus, M. A.; Geoffroy, N.; et al. Zn speciation in the organic horizon of a contaminated soil by micro-x-ray fluorescence, micro- and powder-EXAFS spectroscopy, and isotopic dilution. Environ. Sci. Technol. 2004, 38, 2792-2801.

Sigg, L.; Stumm, W.; Behra, P. Chimie des milieux aquatiques. Paris: Dunod, 2006.

Thévenot, D.R.; Moilleron, R.: Lestel, L.; Gromaire, M.C.; Rocher, V.; Cambier, P.; et al. Critical budget of metal sources and pathways in the Seine River basin (1994–2003) for Cd, Cr, Cu, Hg, Ni, Pb and Zn. Sci. Total Environ. 2007, 375, 204-231

Trainor, T. P.; Brown Jr., G. E.; Parks, G. A. Adsorption and precipitation of aqueous Zn(II) on alumina powders. J. Colloid Interface Sci. 2000, 231, 359-372.

Wang, Y. H.; Morin, G.; Ona-Nguema, G.; Menguy, N.; Juillot, F.; Aubry, E.; et al. Arsenite sorption at the magnetite-water interface during aqueous precipitation of magnetite: EXAFS evidence for a new arsenite surface complex. Geochim. Cosmochim. Acta 2008, 72, 2573-2586.

Wang, Y.; Morin, G.; Ona-Nguema, G.; Juillot, F.; Guyot, F.; Calas, G.; et al. Evidence for different surface speciation of arsenite and arsenate on green rust: An EXAFS and XANES study. Environ. Sci. Technol. 2009, 44, 109-115.

Weber, F.-A.; Voegelin, A.; Kretzschmar, R. Multi-metal contaminant dynamics in temporarily flooded soil under sulfate limitation. Geochim. Cosmochim. Acta 2009, 73, 5513-5527.

Winterer, M. XAFS—a data analysis program for materials science. J. Phys. IV France 1996, 7, C2-243 - C2-244.

Wyckoff, R. W. G. Crystal Structures. New York: John Wiley & Sons, 1963.

Zabinsky, S. I.; Rehr, J. J;, Ankudinov, A.; Albers, R. C.; Eller, M. J. Multiple-scattering calculations of x-ray-absorption spectra. Phys. Rev. B 1995, 52, 2995.

Conclusions et Perspectives

Les rivières dans les bassins versants urbanisés sont soumises à de nombreuses pollutions, y compris métalliques. La fraction particulaire joue un rôle important en ce qui concerne le transport des métaux puisqu'elle constitue une phase porteuse importante de métaux dans la colonne d'eau et également une source potentielle de métaux mobiles et éventuellement toxiques pour l'écosystème. Cette thèse avait comme objectifs de caractériser la phase porteuse particulaire de métaux dans la Seine afin de connaître sa géochimie, d'identifier l'impact de l'urbanisation de la région parisienne et d'en déduire les sources et la mobilité pour une gamme de métaux la plus large possible.

Pour arriver aux objectifs, la stratégie d'analyse était d'étudier la phase particulaire dans l'ensemble de la colonne d'eau et de faire un zoom de cette phase particulaire au fur et à mesure. Ce stratégie a été choisie car il est aussi fondamental de quantifier le rôle de la phase particulaire dans la colonne d'eau que d'étudier la phase particulaire isolée. A partir des échantillonnages mensuels entre octobre 2008 - octobre 2009, une image globale dela proportion de la phase particulaire s'est dessinée à partir de l'analyse élémentaire de la phase dissoute (<0.45 µm), de la phase labile (DGT) et de la phase particulaire (>0.45 µm). L'affinité importante du plomb et du chrome pour la phase particulaire a été confirmée, avec une proportion de la phase particulaire à 94 % et 80 % respectivement à Marnay, et à 83 % et 71 % respectivement à Triel. Dans l'autre coté de la tendance, le nickel a démontré une affinité exceptionnelle pour la phase dissoute à 84 % à Marnay et 81% à Triel. Le Cd, Cu, Co, Mn, et Zn, quant à eux, semblent de ne pas avoir des préférences très marquées. L'urbanisation entre la partie amont et aval n'a pas seulement affecté les concentrations dissoutes et a, au contraire, enrichi les métaux dans la phase particulaire. Surtout, l'urbanisation modifie la préférence des métaux pour la fraction plus labile et dissoute en

aval. Ceci est observable surtout pour le Cd, Pb et Zn, qui sont les trois métaux les plus affectés dans la phase particulaire et sont encore plus affectés dans la phase dissoute.

Cette augmentation de la proportion des métaux dans les fractions labiles et dissoutes en aval de la région parisienne est, en fait, accompagnée de l'augmentation de la proportion des métaux dans la phase oxydable des métaux particulaires. L 'enrichissement des concentrations sédimentaires de 3-12 fois pour le Cd, Pb et Zn par rapport au fond géologique a également été accompagné par l'augmentation de la fraction des métaux liés aux oxydes de manganèse mais surtout aux oxydes de fer dans les zones urbanisées. L'observation au microscope électronique à balayage a montré que ces oxydes de fer sont associés avec d'autres particules porteuses, possiblement de la calcite et ou du quartz, comme indiqué par les spectres EDX. Ces matrices de calcite et de quartz sont abondantes et ont une surface importante sur laquelle les couches d'oxydes de fer se forment. Ensuite ces oxydes de fer auront des charges importantes sur lesquels les métaux s'associent. La phase échangeable (celle très mobile), quant à elle, n'est significative (plus de 2%) que pour le Cd, Ni, et Zn.

Les résultats ont montré l'augmentation des concentrations métalliques suivant des pluies, que ce soit en période hivernale ou estivale. Une augmentation de la proportion des métaux dissous par rapport aux métaux solides été également observée après les pluies. Les échantillonnages de haute définition pendantun déversement d'eaux usées vers la Seine suite à un épisode d'orage ont indiqué que les concentrations en métaux dans le panache de mélange du déversement avec l'eau de la Seine ne sont pas expliquées par un simple mélange binaire de l'eau du déversement et la Seine. En utilisant un modèle à trois sources, Seine + déversoir + sédiment de fond, il est calculé que le sédiment de fond resuspendu serait une source significative et aurait un impact très significatif dans l'augmentation des concentrations de métaux dans le panache du rejet.

Ce sédiment de fond et le réseau d'assainissement sont connus pour être des milieux réduits, des réacteurs chimiques dans lesquels les processus redox sont dominants. Ce sédiment du fond et/ou l'eau du déversement auraient pu contribuer aux espèces réduites identifiées en Seine, notamment les sulfures. Cette espèce a été observée avec l'EXAFS sur des matières en suspension dont l'état d'oxydation a été préservé depuis la filtration jusqu'à l'analyse. Le sulfure de zinc serait une espèce significative dans la colonne d'eau puisque les sulfures auraient un nombre de coordination2.3-3 du premier voisin du Zn, par rapport à 2-2.2 de l'oxygène pendant des périodes plutôt réduites. La remise en suspension du sédiment de fond et l'apport par les déversoirs d'orage sont deux sources possibles de sulfures. Ce sulfure de zinc serait sous forme amorphe en particules isolées ou en grappes de petites particules (<100 nm).

Pendant cette thèse, plusieurs progrès sensibles ont été également réalisés sur la méthodologie des études des phases porteuses. La comparaison de Kd, le ratio entre la teneur particulaire et la concentration dissoute, à partir des données ponctuelles et intégratives des métaux a montré que le Kd intégratif pourrait être un indicateur potentiel de l'impact biologique de l'urbanisation dans le bassin de la Seine. Ces Kd « intégratifs » ont été obtenus par le rapport entre la teneur particulaire des matières en suspension (MES) collectées dans les trappes à sédiment et la concentration labile des métaux mesurés par l'échantillonnage intégratif (DGT= diffusive gel in thin films). Malgré le fait que ces mesures intégratives moyennent pendant un mois des conditions biogéochimiques variables, les caractéristiques liées aux crues hivernales et au temps sec ont été bien observées. L'utilisation du Kd intégratif pourrait être intéressante dans la surveillance en routine des métaux dans les milieux aquatiques, car elle minimise l'investissement en échantillonnage et en analyse, tout en maximisant l'interprétation en termes de toxicité.

En ce qui concerne l'échantillonnage et la préparation des échantillons, il serait important de conserver l'état d'oxydation des matières dans les études de spéciation des métaux, même dans un milieu oxique tel que la Seine, tel que les rivières.Il s'avère que le sulfure de zinc est très présent dans l'aval de la Seine et que la conservation des échantillons est importante dans le cas d'étude très détaillée de la spéciation.

Cette thèse était la première étude dans le bassin de la Seine à étudier en parallèle la phase dissoute, labile et particulaire obtenues individuellement (et non pas par déduction « fraction totale »moins « fraction dissoute » ou obtenues par des modèle de spéciation). Ce suivi exhaustif a permis de suivre les évolutions spatiales et temporelles de ces différentes composantes afin d'avoir une idée globale de la dynamique des métaux particulaires. Elle avait un objectif plus général qui lui était de caractériser le plus finement possible les différentes phases porteuses de métaux dans l'espace et dans le temps. Visiblement, la Seine est un système très compliqué avec une multitude de phases porteuses et cette thèse a permis l'ouverture de différentes voies vers diverses possibilités de comprendre la mobilité et la toxicité des métaux dans le système fluvial. Si la compréhension a bien progressé sur le zinc, les processus d'échanges dissous – particulaires restent encore obscurs pour bon nombre de métaux.

L'un des résultats intéressant résultant de la collaboration interdisciplinaire au sein du projet Médisis a été le niveau significatif de contribution des métaux particulaires dans les MES dans la bio-accumulation des métaux dans la moule zébrée par rapport à des métaux totaux (labiles + particulaires) (Bourgeault et al. soumis). Des perspectives pendant cette collaboration ont été développées, les données de spéciation pouvant être ainsi intégrées à un modèle d'assimilation. Ce travail aura une continuité sous forme d'une thèse en collaboration (LSCE/Cemagref 2010 – 2012) sur la bio-disponibilité des métaux particulaires dans la Seine en utilisant la moule zebrée (*Dreissena polymorpha*) comme modèle biologique de la toxicité

des polluants. Il sera intéressant d'étudier spécifiquement l'impact du ZnS sur l'organisme indicateur. L'acidité de la plupart des systèmes digestives la moule zébrée et l'instabilité du ZnS dans un milieu acidique pourrait faire de ce ZnS une phase porteuse importante du Zn. Un essai d'extraction séquentielle dans une atmosphère inerte de N_2serait une manipulation lourde mais néanmoins intéressante afin de comparer les résultats avec la bio-accumulation du Zn porté par le ZnS.

Il serait également intéressant d'étudier la spéciation exacte des métaux particulaires dans la panache du déversoir pour regarder en détails le devenir du ZnS provenant du réseau d'assainissement et également du sédiment du fond. Dans le but de comprendre le devenir de ces espèces sensibles à l'oxydation, l'échantillonnage serait plus intéressant en se focalisant plus sur les périodes critiques telles que la crue hivernale vers décembre à février, le bloom algal vers le mois d'avril à juin, et la pluie estivale en période d'étiage vers le mois d'août.

Les analyses EXAFS et MEB étant faisables sur des filtres, il pourrait être envisageable de collecter un flacon de 1 à 2 litres d'eau brutes (au lieu de 20 L) pour pouvoir recueillir et traiter le plus d'échantillons possibles pour analyser la dynamique d'un phénomène qui dure relativement peu de temps comme la resuspension du sédiment liée à un changement de régime hydrique.

En dehors du sulfure de zinc, un regard préliminaire des spectres d'EXAFS par la décomposition linaire indique d'autres espèces porteuses de Zn identifiables, telles que la calcite sur laquelle le zinc est adsorbé, l'hydrotalcite de zinc, le zinc adsorbé sur la goethite (oxyde de fer) et un co-précipité de Zn et Fe avec les phosphates. D'autres spectres de référence doivent être acquis par la méthode EXAFS, surtout les divers oxydes de manganèse, afin de compléter la spéciation du Zn dans un milieu complexe qui est la rivière urbaine.

Annexe 1

Papier sous presse

dans « *Journal of Environmental Monitoring* »

« Silver and thallium historical trends in the Seine River basin »

Silver and thallium historical trends in the Seine River basin

Sophie Ayrault,* Cindy Rianti Priadi, Olivier Evrard, Irène Lefèvre and Philippe Bonté

Received 23rd April 2010, Accepted 25th August 2010
DOI: 10.1039/c0em00153h

Records on pollution by metals of minor economic importance (*e.g.* silver and thallium) but which prove to be toxic are rarely documented in river sediment. This study used two sediment cores collected downstream of the Seine River to describe the temporal evolution of Ag and Tl concentrations in an urban catchment. Radionuclide analysis (*i.e.* Cs-137 and Pb-210) allowed dating sediment deposition within the cores (1933–2003). Ag concentration reached maximum values of 14.3–24.6 mg kg^{-1} in the 1960s and 1970s, before gradually decreasing up to values which approximated 4 mg kg^{-1} in 2003. In contrast, Tl concentrations remained roughly constant throughout the core (median value of 0.86 mg kg^{-1}). Suspended solids was collected at upstream locations in the catchment to derive the background concentrations in Ag and Tl. Very high Ag concentrations were measured in the upstream Seine River sites (0.33–0.59 mg kg^{-1}), compared to the values reported in the literature (0.055 mg kg^{-1}). This suggests the presence of a widespread and ancient Ag pollution in the Seine River basin, as demonstrated by the very high Ag enrichment ratios recorded in the cores. Annual flux of particulate Ag in the Seine River was estimated at 1.7 t yr^{-1} in 2003. In contrast, Tl concentrations remained in the same order of magnitude as the natural background signal (0.3–0.5 mg kg^{-1}). This study suggests that the Seine River basin is free of Tl contamination. Future concerns should hence mostly rely on Ag contamination, in a context of increasing Ag uses and possible releases to the environment.

Introduction

The presence of metals in the environment is known to be harmful and dangerous for fauna, biota and even for human health.[1,2] So far, research effort has focused on the behaviour of economically important trace metals (Cr, Hg, Ni, Pb and Zn). Nevertheless, other metals such as silver (Ag) and thallium (Tl) are also particularly toxic. Silver and thallium were assigned to the highest toxicity class, together with cadmium and mercury. Still, the environmental impacts of Ag and Tl anthropogenic emissions are poorly documented, which is probably due to their low abundance in the environment.

Whereas silver and thallium are rather scarce in the crust (0.08 mg kg^{-1} for silver and 0.1–1.7 mg kg^{-1} for thallium[3]), they can concentrate in sediment and bio-accumulate in organisms (*e.g.* in benthic invertebrates).[4] Silver has been used by people and extracted from argentiferous lead ores since ancient times. People first considered it as a precious metal and used it to make currency coins and jewellery. Its use has now greatly diversified and Ag is found in photographic films, electrical devices, batteries, brazing alloys and electroplating, coins and metals.[5] In 1995, photographic manufacturing represented 50% of the US silver demand, whereas electrical contacts and conductors only accounted for 15% of the total demand. With the fast development of digital photography, silver applications in this domain sharply decreased (from 26% in 1999 to 12.5% in 2008[6]), whereas silver use in electronic components greatly increased. Overall, the annual world demand in Ag increased significantly, from 13 500 t yr^{-1} in 1995[7] to 24 500 t yr^{-1} in 2005.[8] These authors estimated the global emissions of silver to the environment at 13 420 t yr^{-1}, from which *ca.* 457 t yr^{-1} were dissipated to water between 1997–2000.

Contrary to Ag, thallium was only discovered in 1861 and it mainly served as a rat killer in the past. However, Tl has not been as widely used as Ag. It is for instance used to make

Laboratoire des Sciences du Climat et de l'Environnement (LSCE/IPSL), UMR 1572 (CEA/CNRS/UVSQ), Domaine du CNRS, Avenue de la Terrasse, bat 12, 91198 Gif-sur-Yvette, France. E-mail: sophie.ayrault@lsce.ipsl.fr; Tel: +33 (0)1 69 82 43 54

Environmental impact

This manuscript reports the temporal evolution of silver (Ag) and thallium (Tl) concentrations in sediment cores. These cores, issued from downstream Seine River floodplains, represent extraordinary archives of the sediments flowing across Paris conurbation. Ag and Tl are two toxic metals, released to the environment by human activities and scarcely documented in river sediment. The present work shows a huge Ag sediment contamination around 1960. In contrast, no contamination was registered for Tl. These findings increase the understanding of Ag and Tl environmental cycles in urban environments. In addition, the Ag and Tl geochemical background concentrations in the Seine River were documented. Ag concentrations were tenfold higher than the Ag background values reported for the upper continental crust. This emphasizes the need to increase the research efforts on silver and thallium that have been understudied in an environmental context, whereas the uses of Ag are dramatically increasing.

thermometers and photocells, and 60% of thallium is used by the US electronics industry. Tl world production reached only 30 t yr^{-1} in 1984.[7] Because of the volatile nature of Tl compounds, Tl is readily emitted to the atmosphere by coal combustion, cement production, metal smelting and refining, as well as waste incineration.[9] Furthermore, half of the environmental emission is released to water, as reported in the US Environmental Protection Agency consumer factsheet devoted to thallium in drinking water and its impacts on public health (see http://www.epa.gov/ogwdw000/contaminants/dw_contamfs/thallium.html).

The historical evolution of Ag and Tl atmospheric concentrations was documented by several studies carried out in the northern hemisphere. Analyses were carried out on snow and ice samples collected at the Mont Blanc;[10] ombrotrophic peat bog samples from Switzerland;[11] sediment cores from boreal and remote, Swedish lakes;[12] and Artic snow and ice cores.[13] These studies indicate a regional and long-range contamination of ecosystems by atmospheric deposition for both Ag and Tl.

In the case of the Swedish boreal and remote lakes, a contribution from the catchment geological background to the Ag concentration was not excluded.[12] The authors concluded to an Ag contamination of the recent sediment due to the atmospheric deposition that occurred after the Second World War. Furthermore, analyses of snow and ice collected at the French Alps indicate an increase in Ag atmospheric deposition after 1950.[10] This increase is related to the increase in Ag production extracted from argentiferous lead ores. In Artic snow and ice cores, a huge Ag peak was observed around 1960 and the authors associated it with the economic boom that occurred after the Second World War.[13] A huge Ag peak dating from 1967 was also registered in ombrotrophic peat bog samples from Switzerland.[11] Even though Ag concentration has continuously increased since the beginning of last century, the average concentration found in samples of Arctic snow and ice in recent times is in the same order of magnitude of the enrichments already observed during the Medieval, Roman and Greek/Phoenician periods.

Data on Tl historical trends are even scarcer than for Ag, and the conclusions are somewhat different from one study to another. Tl concentrations have been increasing since the mid-1800s, but the most prominent increase took place after the Second World War, as it is recorded in lake sediment cores.[12] This increase is consistent with the 1967 peak observed in peat bogs.[11] The highest Tl concentrations were observed for the years 1870 and 1920 in Artic ice core[13] but a similar peak as the one observed for Ag concentrations in the 1960s was not identified for Tl. Ag and Tl experienced hence different historical evolutions. A decrease in both Ag and Tl concentrations was nevertheless observed during the last decade.

Overall, the former studies observed the occurrence of a significant Ag and Tl contamination in the environment after the Second World War, and they related it to the industrialisation of Europe. Ag contamination was observed in ancient archives (8000-300 BP). A decrease in Ag and Tl environmental concentrations was only detected during the last decade in archives exhibiting the highest temporal resolution (*i.e.* ice cores). These studies suggest that Ag and Tl release to the environment is controlled by independent sources and/or processes.

The availability of techniques to detect Tl at very low concentrations is recent.[14] Data on Tl concentrations in lakes are rather alarming (*e.g.* at the Great Lakes[15]). However, similar data are scarce for rivers. Still, obtaining information on the historical evolution of Tl and Ag concentrations in urban catchments is crucial, given river water is used as a supply source for human consumption in densely urbanised areas. Furthermore, the secondary mobilisation of heavy metals from overbank sediment has been demonstrated.[16]

Ag is found to be mostly bound to sulfides and organic matter. It is strongly sorbed to suspended particles. In river systems, it is rapidly incorporated into sediment and most of the dissolved silver (<0.45 μm filtration) is associated with colloids.[17] This high affinity for suspended matter would explain why 90% of Ag is found in the solid phase once they reach the estuary because of dissolved Ag scavenging by organic matter.[18] In this context, analysis of sediment cores sampled in river floodplains can offer a solution to determine the concentrations in this metal. With respect to Tl, the partitioning between the dissolved and solid phases remains the subject of lively debate.[19] Nevertheless, it seems reasonable to hypothesise that the occurrence of a severe pollution in Tl would be recorded in sediment despite the dominance of the dissolved fraction. We propose hence to analyse two sediment cores collected in the Seine River basin, which is one of the most polluted areas in the world in terms of metal contamination.[20,21]

This study aims to derive the historical trends of Ag and Tl contamination in the Seine River basin. Ag and Tl concentrations in sediment will be compared to the natural geochemical background concentrations. Sediment samples collected at upstream sites considered as only slightly impacted by human activities will be analysed to define the local geochemical background level. Scandium (Sc) will be used as a reference element, because of its conservative behaviour, to evaluate the anthropogenic impact of Ag and Tl on river contamination.[11,13] Finally, the main sources of Ag and Tl delivery to the river will also be outlined.

Experimental

Study area and selection of the coring sites

Two cores were collected in the Seine River floodplain, about 100 km downstream of Paris and its main waste waster treatment plant (Seine—Aval waste water treatment plant at Achères). The sampling sites drain 96% of the Seine River basin and are located within the last major meander of the Seine River before it reaches its estuary.

The first site (*i.e.* Bouafles) is located just upstream of a dam, in 'Les Andelys' (Fig. 1), in an oxbow lake located on the right bank of the Seine River. It corresponds to a recent accretion area as indicated by the recent burial of trees. This undisturbed sampling area has remained under grassland for 30 years, and gradual sediment deposition has occurred. Local inhabitants confirmed indeed that the site has been flooded at least once each year until 2004. The analysis of eleven cores collected in the area between 2003 and 2008 demonstrated that they correspond to the sedimentation that occurred during the last 60 years (see ref. 21 for details).

The second site (*i.e.* Muids) is located in the same meander and on the same bank of the Seine River, but 12 km further on

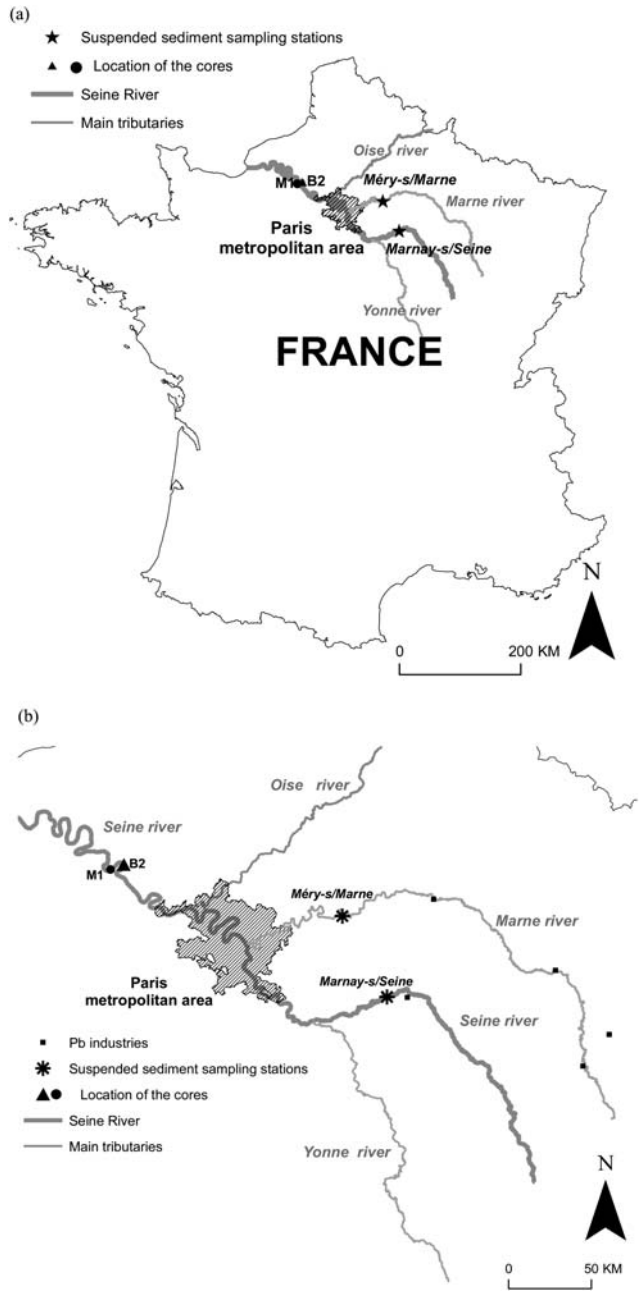

Fig. 1 (a) Location of the B2 and M1 sediment cores and the suspended sediment sampling sites (Marnay-sur-Seine and Méry-sur-Marne) in the Seine River basin. (b) Location of the currently operational Pb industries in the upstream part of the Seine catchment and in the Marne catchment (source: IREP, 2009).

downstream. This site is composed by four islands which experienced regular flooding during winter.

Core sampling

Three cores were sampled in each site on April 9, 2003 using an Eijkelkamp device equipped with a percussion drill bit (with 10 cm diameter and 1 m length). The soil corer could be opened laterally, which allowed an immediate transfer of the core into a PVC tube to prevent its contamination by metals.

Core dating

Dating of the sediment cores relied on the measurement of two radionuclides (*i.e.* Cs-137 and Pb-210) that strongly sorb to fine sediment.[22,23] Cs-137 was used as an event-tracer, whereas Pb-210 provided the sediment age.

Both radionuclides are γ emitters and they can be detected in small quantities of soil (*ca.* 50–100 g, typically) without any previous chemical treatment. Sediment was dried at 115 °C, sieved (<2 mm), ground to a fine powder and placed in airtight counting boxes. Counting was conducted during *ca.* 10^5 s using Germanium γ-ray detectors (Germanium hyperpure—GeHP, N-type, coaxial model) available at the *Laboratoire des Sciences du Climat et de l'Environnement* (Gif-sur-Yvette, France). Efficiencies and background of the detectors were periodically controlled with internal soil and sediment standards, pure KCl samples, and IAEA standards (*i.e.* Soil-6, -135 and -375). Activity decay was corrected taking account of the sediment collection period.

Cs-137 is an artificial radionuclide ($t_{1/2} = 30$ years) produced by the thermonuclear bomb testing conducted between the 1950s and the 1980s (with a maximum input in 1964) and the Chernobyl accident in 1986. Measurement of Cs-137 activity in sediment allowed determining the location of three events: the fallout due to the first significant input in the atmosphere in 1954, the maximum input in 1964 and the fallout due to the Chernobyl catastrophe in 1986. Cs-137 is now stored in soils, and this Cs-137 stock decreases by radioactive decay and by fine sediment transfer to the rivers. Cs-137 is easily identified in γ spectrometry by a peak at 661 keV. Uncertainty on measurements was *ca.* 0.5%, and the detection limits reached 0.3 Bq kg^{-1}.

Pb-210 is a natural radionuclide ($t_{1/2} = 22.3$ years) which is a decay product of U-238 ($t_{1/2} = 4.5 \times 10^9$ years). U-238 decays through a series of short-lived nuclides (*e.g.* Ra-226 and Rn-222). Rn-222 is a gas that partly remains *in situ*, forming "supported" Pb-210, and that partly escapes to the atmosphere, forming "excess" Pb-210, which reaches the soil surface by wet and dry fallout. It then strongly sorbs to soil particles. The activity in "excess" Pb-210 was calculated by subtracting the supported activity (determined using a U-238 daughter, *i.e.* Bi-214) from the total activity of Pb-210.[24] Uncertainty on measurements was thus higher than for Cs-137 (*ca.* 10%).

Suspended matter sampling

In order to determine the background values for Ag and Tl in the river, suspended matter (SM) was collected in the Seine and Marne rivers at upstream locations (*i.e.* at Marnay-sur-Seine and Méry-sur-Marne, Fig. 1a). At Méry-sur-Marne, water was collected on two field campaigns (April 2006 and January 2007) by grab sampling with PVC buckets from the riverbank. Twenty-litre samples were stored in PVC jerrycans thoroughly rinsed with alkaline detergent TFD-4®. SM was obtained by gravitational settling of the samples during several days. Uplying water was eliminated and approximately two litres of water were centrifuged at 3000 rpm. Finally, recovered SM was freeze-dried. At Marnay-sur-Seine, SM was collected in sediment traps from December 2008 to February 2009. These traps consisted in 1.5-litre PET water bottles.[25] They were emptied once a month, providing SM data at a monthly time step. Samples were

collected in polyethylene bottles thoroughly rinsed with 1 M HNO_3 for several days. Samples were then centrifuged at 14000 rpm and vacuum-dried.

Elemental analysis

Sc and Ag concentrations were measured using INAA (Instrumental Neutron Activation Analysis) analyses conducted on bulk sediment powder. Fifty milligram samples were irradiated during 30 minutes by a flux of 2.3×10^{13} neutrons cm^{-2} s^{-1} in the experimental reactor *Orphée* (*Commissariat à l'Energie Atomique*, Saclay, France), using the irradiation facilities of the *Laboratoire Pierre Süe*. Four successive γ spectrometry measurements were then conducted using Germanium γ-ray detectors (Germanium hyperpure—GeHP, N-type, coaxial model). Ag and Sc concentrations were determined using the 10 h counting after a 30 days decay.

Ag and Tl concentrations were measured using ICP-MS (Inductively Coupled Plasma-Mass Spectrometry) on totally digested samples. One hundred milligram samples were totally dissolved by successive additions of HNO_3 and HCl mixture, HF, and $HClO_4$ in Teflon vessels using a heating block (Digiprep, SCP Science). Ultra pure reagents were used (Normatom grade, VWR, France for HNO_3, and HCl, "for trace metal analyses", Baker, SODIPRO, France, for HF, and $HClO_4$). The solutions were evaporated to dryness, retaken 3 times in 2 mL of HNO_3 and then diluted with 50 mL of MilliQ water. The concentrations were determined by Inductively Coupled Plasma-Quadrupolar Mass Spectrometry ICP-QMS (X Series, ThermoElectron, France). To correct for instrumental drifts and plasma fluctuations, all solutions were spiked with rhodium (Rh) and rhenium (Re) standard solutions (SPEX, SCP Science, France) to a final concentration of 10 μg L^{-1} for Rh and 1 μg L^{-1} for Re. The solutions were weighted at each step of the dilution and spiking operations.

We only provide the Ag ICP-MS results for the suspended sediment collected at Méry-sur-Marne and Marnay-sur-Seine, because this technique offers lower detection limits than INAA (Table 1). The combined errors of the concentration measurements (Ag INAA, Sc INAA, Ag and Tl ICP-MS) were estimated to be in the order of 10%, 8% and 5%, respectively. The accuracy of the analytical data was checked by analysing the GXR-1 reference material (jasperoid, USGS) by both methods. The measured concentrations in GXR–1 agreed with the recommended Ag and Sc concentration values, and with the Tl provisional concentration value (Table 1).

The enrichment factors (EF) in both Ag and Tl were calculated based on the methodology developed by Wedepohl[26] (eqn (1)).

$$EF = ([M]/[Sc])_{sample}/([M]/[Sc])_{natural\ background} \quad (1)$$

where M represents Ag or Tl and using the natural background values of Ag/Sc (0.08) and Tl/Sc (0.10).[26]

Results and discussion

Dating of sediment cores

The cores (*i.e.* B2 for the Bouafles site and M1 for the Muids site) used in this study were selected because of their reliable record of sedimentation.

The depth profile of Cs-137 in the B2-core is shown in Fig. 2a. The events corresponding to the 1986 and 1964 fallout were clearly recorded. In depth, no Cs-137 was detected anymore, indicating that the core includes sediment deposited before 1954. Sedimentation rate derived from the excess Pb-210 profile appeared to be constant throughout the core, and the sedimentation rate derived from the chronology of the core reached 1.8 cm yr^{-1}.

With respect to the M1-core, sedimentation rates appeared to have varied throughout time (Fig. 2b). Chernobyl fallout is located at 14 cm depth, whereas the maximum Cs-fallout that occurred in 1964 is located at 43 cm depth (Fig. 2c). Calculated sedimentation rates sharply decreased throughout time, from 2.5 cm yr^{-1} before 1964 to 1.3 cm yr^{-1} between 1964 and 1986, and only 0.8 cm yr^{-1} between 1986 and 2003. This gradual decrease in sedimentation was due to the progressive burial of the riverbed by suspended matter deposition at this location.

Ag and Tl concentrations at upstream sites of the Seine River basin

Mean concentrations in Ag measured in the sediment collected at Marnay-sur-Seine (0.33 ± 0.15 mg kg^{-1}) and at Méry-sur-Marne (0.59 ± 0.01 mg kg^{-1}) are about tenfold higher than the Ag upper continental crust background values (0.055 mg kg^{-1}) (Table 2).[3,26]

Three explanations can be put forward to explain this difference. First, the high Ag concentrations measured in the Seine River could indicate that the geochemical background values are

Table 1 Analytical information. Instrumental detection limits (including digestion blanks for ICP-MS, mg kg^{-1}). Analysis of certified material GXR-1 (USGS). INAA: Instrumental Neutron Activation Analysis. ICP-MS: Inductively Coupled Plasma-Mass Spectrometry

	Quantification limits		Reference material		
				Measured value	Measured value
	INAA/mg kg^{-1}	ICP-MS/mg kg^{-1}	Certified value/mg kg^{-1}	INAA ($n = 3$)/mg kg^{-1}	ICP-MS ($n = 3$)/mg kg^{-1}
Sc	0.1	n.d.	1.58 ± 0.20	1.7 ± 0.1	n.d.
Ag	1	0.005	31 ± 4	33 ± 3	31 ± 3
Tl	n.d.	0.001	0.39 ± 0.20[a]	n.d.	0.40 ± 0.02

[a] Provisional concentration value, n.d. not determined.

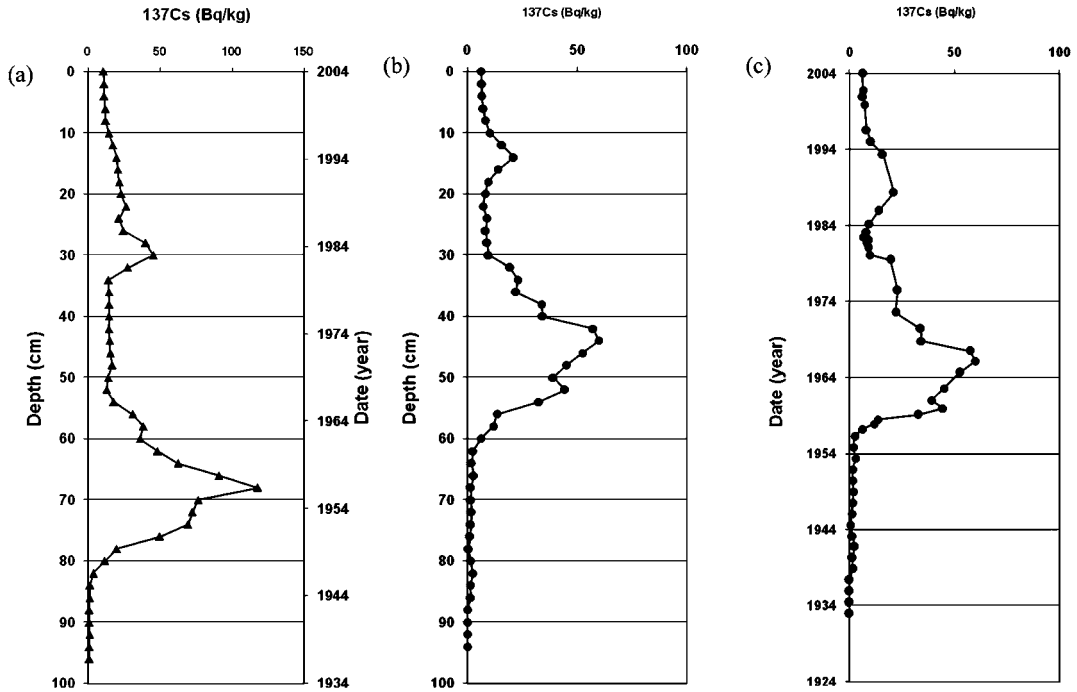

Fig. 2 Depth profiles of the Cs-137 activity. (a) (▲) B2 core (Bouafles); (b) (●) M1 core (Muids). (a) The chronology derived from the measured activities is indicated on the right axis of the graph for the B2 core. (c) Due to changes in the deposition rate along the depth profile of the M1 core, its chronological profile is shown in a separated graph.

exceptionally high in this river. However, we rule out this hypothesis, because of the dominant sedimentary origin of the rocks in the Seine River basin. Second, they could indicate that the Seine River basin underwent a general and very ancient pollution. This second hypothesis seems more likely. Such a large contamination by atmospheric deposition has also been observed in remote environmental archives.[13] Third, this contamination could be explained by Ag released by lead (Pb) industries present in the Upper Seine and the Marne catchments. Pb and Ag are indeed strongly associated in Pb-ores. Even though the activity of lead industrial facilities strongly decreased after 1970 in the Seine River basin,[27] there are still a dozen plants in activity in the Upper Seine and the Marne catchments (Fig. 1b).[28]

Overall, data are still too scarce to draw conclusions about the high Ag geochemical background signal in the Seine River basin. Sediment deposited before the proto-industrialisation in the region needs to be collected and analysed to derive this signal.

In contrast, thallium concentrations measured at Marnay-sur-Seine (0.30 mg kg^{-1}) and Méry-sur-Marne (0.45 mg kg^{-1}) (Table 2) are in good agreement with the median Tl concentration in European floodplain sediment.[29] They were even lower than the Tl geochemical background concentrations reported in the upper continental crust (0.75 mg kg^{-1}). The low Tl concentrations that we observed could be explained by the dilution of the geological Tl input by autochthonous calcite and/or organic matter. Scandium (Sc) concentrations were measured in all the samples. Normalising Tl concentrations to Sc allows taking account of this dilution effect. The Tl/Sc ratio for the reference geochemical background varies between 0.068 and 0.107. According to our data, the Tl/Sc ratio reached 0.046 ± 0.005 at Marnay-sur-Seine and 0.062 ± 0.001 at Méry-sur-Marne. These low Tl concentrations measured at upstream sites of the Seine River basin cannot be explained by a dilution effect. It is more reasonable to attribute these low concentrations to the sedimentary origin of

Table 2 Scandium (Sc), silver (Ag) and thallium (Tl) geochemical background values in the upper continental crust (literature) and in suspended sediment collected at upstream stations of the Seine River basin (mg kg^{-1})

		Sc	Ag	Tl
Upper continental crust				
Taylor and McLennan (1985)		11	0.050	0.75
Wedepohl (1995)		7	0.055	0.75
Local background stations				
Marnay-sur-Seine	Dec 08	6.6 [a]± 0.1	0.24 [b]± 0.01	0.32 [b]± 0.02
	Jan 09	6.6 [a]± 0.1	0.25 [b]± 0.01	0.31 [b]± 0.02
	Feb 09	6.7 [a]± 0.1	0.50 [b]± 0.02	0.27 [b]± 0.01
Méry-sur-Marne	Apr 06	7.0 [a]± 0.1	0.59 [b]± 0.03	0.43 [b]± 0.02
	Jan 07	7.6 [a]± 0.1	0.59 [b]± 0.03	0.48 [b]± 0.02

[a] INAA determinations. [b] ICP-MS determinations.

the rocks in the Seine River basin. Moreover, the Tl concentration observed at Marnay-sur-Seine lower than the Tl concentration at Méry-sur-Marne may be partly explained by a possible metal release from the suspended sediments trapped during one month periods at Marnay-sur-Seine.

Depth profiles of Ag and Tl concentrations

Sc, Ag and Tl concentrations measured along the sediment profiles of the B2 and M1 cores as well as the estimated chronology of deposition are shown in Tables 3 and 4.

The Ag concentration showed strong variations along the profile of the B2 core (from 4 to 25 mg kg^{-1}) (Table 3). The highest concentration (24.6 mg kg^{-1}) was recorded in 1960. The lowest concentration (3.8 mg kg^{-1}) was measured in the uppermost superficial layer which corresponds to the sediment deposited in 2003. Moreover, the peaks in Ag concentrations (observed in 1960 and, to a lesser extent, in 1994) correspond to similar peaks in Zn, Sb, Hg and Pb concentrations.[21] The 1960 peak probably reflects the industrial boom after the Second World War.

The depth profile of Ag concentration in the M1 core is similar to the one obtained in the other core, even though it is systematically characterised by slightly lower concentrations (Table 4). Similar observations can be made for Sc concentrations. This indicates the presence of a less abundant clay fraction in M1 compared to B2.

To document the influence of anthropogenic activities, temporal variations of the Ag and Tl enrichment factor (EF) ratios were calculated, taking account of the upper continental crust (UCC) concentrations as a reference (Table 5). The following EF values should be interpreted with some caution, keeping in mind the shortcomings of the EF approach, EF being calculated relative to the crust composition or to local background values.[30] Ag EF recorded in both B2 and M1 cores were extremely high. EF in Ag ranged between 51 and 300 in B2 and between 73 and 263 in M1, when using UCC concentrations as reference values. After normalising Ag concentrations to Sc, the Ag EF depth profiles were much more similar in both cores (Fig. 3). Ag EF obtained taking the concentrations measured at Marnay-sur-Seine as a reference ranged from 8 to 47 in the B2 core and from 12 to 39 in the M1 core. When using the concentrations at Méry-sur-Marne, Ag EF fluctuated similarly between 12 and 44 in the B2 core, and 12 and 26 in the M1 core. These results demonstrate a significant enrichment of sediment in Ag and Tl during its transfer from the upper catchment sites to the downstream sites. This enrichment is clearly associated with contemporary anthropogenic impacts, whereas the enrichment observed at the upstream sites was probably induced by more ancient human activities.

Given it is widely known that Pb-ores constitute an important Ag source,[31] it is particularly relevant to compare the Ag concentrations with the ones obtained for Pb.[21] Both profiles were found to be synchronous (results not shown). Examination of the Pb/Ag ratio can provide valuable insights about the dominant emission processes.[11] The Pb/Ag ratio decreased from

Table 3 Scandium (Sc), silver (Ag) and thallium (Tl) concentrations values in the B2 core (mg kg^{-1}) (n.d. not determined)

Year	Sc	Ag	Tl
2003	9.5 ± 0.8	3.8 ± 0.4	n.d.
1997	7.2 ± 0.6	7.9 ± 0.8	0.70 ± 0.04
1994	8.0 ± 0.6	13.1 ± 1.3	0.95 ± 0.05
1989	9.3 ± 0.7	10.7 ± 1.1	0.92 ± 0.05
1986	10.3 ± 0.8	7.4 ± 0.7	n.d.
1985	9.8 ± 0.8	9.2 ± 0.9	0.84 ± 0.04
1983	9.6 ± 0.8	10.5 ± 1.0	0.87 ± 0.04
1979	9.5 ± 0.8	11.3 ± 1.1	0.66 ± 0.03
1974	9.1 ± 0.7	15.5 ± 1.5	0.77 ± 0.04
1967	9.6 ± 0.8	22.4 ± 2.2	0.97 ± 0.05
1963	10.5 ± 0.8	24.6 ± 2.5	0.80 ± 0.04
1960	9.7 ± 0.8	20.8 ± 2.1	1.01 ± 0.05
1956	10.1 ± 0.8	20.4 ± 2.0	n.d
1949	9.0 ± 0.7	8.8 ± 0.9	n.d
1943	9.2 ± 0.7	9.9 ± 1.0	0.99 ± 0.05

Table 4 Scandium (Sc) and silver (Ag) concentrations values in the M1 core (mg kg^{-1}) (n.d. not determined)

Year	Sc	Ag	Tl
2002	7.7 ± 0.6	4.4 ± 0.4	0.54 ± 0.03
1995	6.0 ± 0.5	4.6 ± 0.5	0.50 ± 0.03
1988	6.9 ± 0.6	6.1 ± 0.6	0.56 ± 0.03
1986	6.7 ± 0.5	6.1 ± 0.6	n.d.
1983	5.7 ± 0.5	6.8 ± 0.7	0.49 ± 0.02
1980	5.7 ± 0.5	6.7 ± 0.7	n.d.
1970	6.9 ± 0.6	14.3 ± 1.4	0.64 ± 0.03
1968	6.4 ± 0.5	11.9 ± 1.2	0.49 ± 0.02
1961	8.0 ± 0.6	13.6 ± 1.4	0.64 ± 0.03
1957	8.9 ± 0.7	8.7 ± 0.9	0.68 ± 0.03
1951	7.4 ± 0.6	4.7 ± 0.5	n.d.
1943	9.0 ± 0.7	9.6 ± 1.0	1.36 ± 0.07
1936	8.6 ± 0.7	9.1 ± 0.9	n.d.
1933	7.5 ± 0.6	6.2 ± 0.6	0.67 ± 0.03

Table 5 Silver (Ag) and thallium (Tl) enrichment factors in the B2 and M1 cores, and in the upstream sites. Ref: upper continental crust reference concentrations used for the calculation of enrichment factors (Wedepohl, 1995). See text for details

B2 core			M1 core		
Year	Ag	Tl	Year	Ag	Tl
2003	51		2002	73	0.65
1997	140	0.91	1995	98	0.78
1994	208	1.11	1988	112	0.76
1989	146	0.93	1986	116	
1986	92		1983	152	0.79
1985	119	0.79	1980	151	
1983	139	0.84	1970	263	0.86
1979	153	0.65	1968	235	0.71
1974	217	0.79	1961	217	0.75
1967	296	0.94	1957	124	0.72
1963	300	0.72	1951	81	
1960	272	0.97	1943	136	1.41
1956	256		1936	135	
1949	124		1933	105	0.84
1943	137	1.01			
Marnay (Dec 08)	4.6	0.45			
Marnay (Jan 09)	4.9	0.45			
Marnay (Feb 09)	9.5	0.37			
Méry (Apr 06)	10.7	0.57			
Méry (Jan 07)	9.9	0.59			
Reflmg kg^{-1}	*0.055*	*0.75*		*0.055*	*0.75*

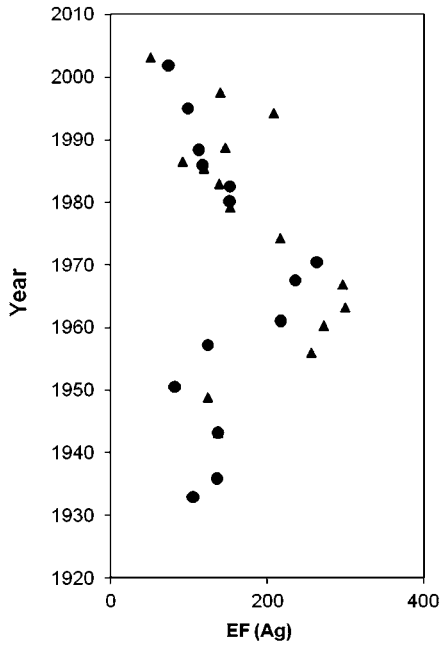

Fig. 3 Enrichment factor (EF) in Ag in the depth profiles of the two analysed cores: (▲) B2 core (Bouafles); (●) M1 core (Muids) using upper continental crust values as reference.

ca. 50 in sediment deposited in 1930, up to 20 in the 2003 sediment. The higher enrichment in Pb than in Ag observed in the Swiss peat bog[11] level corresponding to 1967 is not observed in the Seine River sediment. In addition, the Pb/Ag ratios observed in the Seine sediment cores are significantly lower than those observed in peat bog[11] and even lower than the Pb/Ag ratio reported in UCC (*i.e.* 400[3]). Overall, we can confidently state that the Seine River sediment is enriched in Ag compared to Pb.

Tl concentrations in the B2 core ranged between 0.66 and 1.01 mg kg^{-1}, with a median concentration of 0.86 ± 0.12 mg kg^{-1} all throughout the depth profile. No significant peak can be detected in the profile (Table 3). The lowest Tl concentration in sediment was measured in the sediment deposited in 1979. Furthermore, Tl EF mean values were close to 1 (0.9 in average) (Table 5) when taking the UCC concentrations as a reference, indicating an absence of enrichment. Tl EF calculated using concentrations measured at Marnay-sur-Seine and Méry-sur-Marne reached 2.1 and 1.5, respectively. The low but constant enrichment in Tl measured in the downstream sediment suggests the potential existence of a natural Tl source in the Seine River basin. We suspect that the Yonne River sediment could be responsible for this Seine sediment enrichment in Tl. The Yonne River flows indeed into the Seine River at a junction located downstream of Marnay-sur-Seine (Fig. 1a), after having flown across granites exposed in the Morvan region. Granites are known to be enriched in Tl.[7]

Thallium pollution records in the sediment cores

Atmospheric archives are characterised by an important Tl pollution, which is even more important than Ag pollution.[11–13] Our results clearly point out that the increase in Tl atmospheric source(s) measured in atmospheric archives did not impact the composition of the Seine River sediment. The geochemical behaviour of Tl is similar to the one of potassium and other alkali metal cations.[31,32] The lability of Tl may bring into question the relevance of a sediment core to record a Tl pollution signal. However, this issue remains the object of a lively debate in the literature. On the one hand, mobilisation of Tl from the solid phase to pore waters was observed in lacustrine sediment cores.[12,33] Laforte *et al.* (2005)[33] concluded that the significant post-depositional Tl mobility must be taken into account to interpret Tl profiles in sediment. On the other hand, it was also shown that Tl sorbed strongly on layered illitic and vermiculite clays.[19] Moreover, no Tl desorption was observed from clay-rich soils when adding NH_4^+ and K^+ competitive cations. Tl is even considered to be enough stable to allow its chronological evaluation.[34] The strong sorption of Tl from atmospheric origin on silty and silty-clay soils of France was demonstrated.[32] It was also showed that Tl present in the French soils had a pedological origin.

Consequently, it seems reasonable to conclude that, if a significant Tl contamination had affected the Seine River basin, it would have been recorded, at least partly, in the river sediment. Given the absence of any pollution signal in the B2 and M1 sediment cores, we can conclude to the absence of any significant Tl contamination in the Seine River sediment between the 1940s and today.

The need to further investigate the partitioning of Tl between the solid and dissolved phases in soils was outlined.[19] Future investigations could also usefully determine Tl partitioning between the sediment and the dissolved phase in rivers. Solid/dissolved partitioning of Tl is of primary importance because of the high toxicity of soluble Tl compounds. Moreover, obtaining this value would allow calculating the dissolved fluxes based on the particulate fluxes which are much easier to measure.

Potential sources of Ag to the river

Ag may be released by different sources to the environment. Thouvenin *et al.* (2005)[18] estimated the silver contribution of the Seine River to its estuary in 2003. Sediments were monthly sampled in Poses, which is the last dam before the estuary. In 2003, the Ag flux in Poses was estimated at 1.5 t yr^{-1}.[18] Based on the measurements obtained from the B2 sediment core sampled in 2003 at Bouafles, which is located 30 km upstream of Poses, we can propose a rough and comparative estimation of the Ag annual flux. The particulate output of the Seine was estimated at 450 000 t yr^{-1} in 2003.[18] Ag concentration in the uppermost layers of the B2 core reached 3.8 mg kg^{-1}, we can then estimate the particulate Ag output from the Seine River at 1.7 t yr^{-1}. Similar calculations applied to the M1 uppermost layer concentration result in an Ag particulate flux of 2.0 t yr^{-1}. Both estimations remain in good agreement with the ones obtained previously,[18] given that the concentrations in the uppermost layer of the core are only representative of the solids concentration reached during periods of high water level. Moreover, suspended sediment[18] and deposited sediment (this work) differ in terms of particle size and organic matter content. Still, these characteristics influence the metal concentration in sediment. Overall, our results suggest that the Ag export to the Seine River estuary (1.7–2.0 t yr^{-1}) is at least equivalent to the cadmium and mercury

fluxes at the river mouth (1.75 and 1.25 t yr^{-1}, respectively[27]). Given the high toxicity of Ag, Ag concentrations in the solid and the dissolved phases should be monitored to evaluate precisely the Ag particulate and dissolved fluxes from the river and to allow conducting further risk assessment studies.

It is necessary to determine the potential sources delivering Ag to the river in order to propose potential remediation regulations. Metal mining and smelting activities are known to constitute the major Ag contaminating sources to atmospheric and aquatic environments. However, there is no sulfide ore exploitation in the Seine River basin. In contrast, municipal waste incinerators could be an important source of Ag contamination in the Seine River. They incinerate domestic waste as well as electronic devices that were not sorted out for recycling. In the Seine River basin, more than 70% of the solid wastes are incinerated. 36% of discarded (not recycled) Ag in Europe is found in municipal solid wastes.[5] During the incineration process, silver ends up as bottom and fly ashes, and emissions to the atmosphere remain therefore limited.[17] Solid wastes issued from municipal waste incinerators contain the bulk of anthropogenic Ag.[5] Sewage sludge constitutes the second Ag source. Landfilling of solid wastes issued from thermal treatment incinerators and sewage sludge might constitute a delayed risk of Ag contamination if landfill contaminants were released to the environment by soil erosion.

Forty-five percents of the silver used in the film and photoproduction were not recycled and potentially exposed to the environment in 1997.[5] The film photography first developed at the end of the 19th century and became a mass-consumption product throughout the 20th century. This use may have induced a large part of the ancient sediment contamination, not only because of the lack of restrictive waste management regulations, but also because of the spreading of numerous photo-laboratories. The exponentially decreasing demand for this use could explain the decrease in Ag concentration measured in the contemporary sediment.

Ag content in domestic waste is likely to increase again in future. A recent study carried out in the Rhine River catchment showed that the production of goods using Ag nanoparticles will increase in future. This will amplify the Ag release to freshwater environments.[17] These products consist in plastics (medical catheters, sanitation tubes, computer keyboards, door handles, car steering wheels and mobile phones) and textiles benefiting from the biocide effect of Ag nanoparticles. The biocidal mechanism of silver-containing products results indeed from a long term release of silver ions (Ag^+) by oxidation of metallic silver (Ag^0) in contact with aqueous media. Up to 15% of the total silver emitted to water in Europe may be released from biocidal plastics and textiles in 2010.[17]

Conclusions

Very few records were available to document the contamination by metals of minor economic importance such as Ag and Tl in river catchments strongly modified by human activities. These metals prove nevertheless to be very toxic. This study demonstrated that the Seine River sediment was not contaminated by Tl during the last 60 years. However, the question of its partition between the solid and the dissolved phases remains a subject of lively debate. In contrast, the Seine River sediment was severely contaminated by Ag. Concentration in this metal started decreasing in the 1960s, but it is still present in the environment. Nowadays, the main source of Ag to the river sediment appears to originate from the waste incinerators. However, the sources of Ag may have changed throughout the last decades. Moreover, the increasing Ag demand and the growth of its uses demonstrate the necessity to understand the biogeochemical cycle of Ag, which can partly be investigated through the analysis of environmental archives.

Acknowledgements

We thank G. Varrault, B. Pernet-Coudrier and A. Bourgeault for their help for the collection of suspended sediment. M.-F. Le Cloarec and J.-M. Mouchel are thanked for their active participation to the sediment core collection and analysis. This work has been made possible thanks to funding from the Piren-Seine programme, the French National Research Agency (ANR) Biomet project and the EC2CO Medisis project. This is the LSCE contribution number 4097.

References

1 J. O. Nriagu, *Science*, 1996, **272**, 223–224.
2 R. P. Schwarzenbach, B. I. Escher, K. Fenner, T. B. Hofstetter, A. Johnson, U. von Gunten and B. Wehrli, *Science*, 2006, **313**, 1072–1077.
3 S. R. Taylor and S. M. McLennan, *The Continental Crust: its Composition and Evolution*, Blackwell Scientific, Oxford, 1985, 328p.
4 H. T. Ratte, *Environ. Toxicol. Chem.*, 1999, **18**, 89–108.
5 T. Lanzano, M. Bertram, M. De Palo, C. Wagner, K. Zyla and T. E. Graedel, *Resour., Conserv. Recycl.*, 2006, **46**, 27–43.
6 *World Silver Survey*, The Silver Institute and Gold Fields Mineral Services, Ltd., Washington, DC, 2009.
7 C. Reimann and P. De Caritat, *Chemical Elements in the Environment. Factsheets for the Geochemist and Environmental Scientist*, Springer-Verlag, Berlin, Heidelberg, New York, London, Paris, Tokyo, Hong Kong, 1999, 398p.
8 M. J. Eckelman and T. E. Graedel, *Environ. Sci. Technol.*, 2007, **41**, 6283–6289.
9 J. O. Nriagu and J. M. Pacyna, *Environ. Rev. (Ottawa, ON, Can.)*, 1988, **9**, 269–298.
10 K. Van de Velde, C. Barbante, G. Cozzi, I. Moret, T. Bellomi, C. Ferrari and C. Boutron, *Atmos. Environ.*, 2000, **34**, 3117–3127.
11 W. Shotyk and M. Krachler, *J. Environ. Monit.*, 2004, **6**, 427–433.
12 E. Grahn, S. Karlsson, U. Karlsson and A. Düker, *J. Environ. Monit.*, 2006, **8**, 732–744.
13 M. Krachler, J. Zheng, D. Fisher and W. Shotyk, *Sci. Total Environ.*, 2008, **399**, 78–89.
14 A. R. Flegal and C. C. Patterson, *Mar. Chem.*, 1985, **15**, 327–331.
15 T. S. Lin, J. Nriagu and X. Q. Wang, *Bull. Environ. Contam. Toxicol.*, 2001, **67**, 921–925.
16 V. Cappuyns and V. Swennen, *J. Environ. Monit.*, 2004, **6**, 434–440.
17 S. A. Blaser, M. Scheringer, M. MacLeod and K. Hungerbühler, *Sci. Total Environ.*, 2008, **390**, 396–409.
18 B. Thouvenin, B. Boutier, J.-F. Chiffoleau, J.-L. Gonzalez., D. Cossa, D. Auger, B. Averty, E. Rozuel-Chartier, D. Ménard, A. Santini and M. Olivier, Contribution à l'étude de la dynamique et de la spéciation des contaminants, Rapport d'activité 2004, Programme Seine Aval 3, 2005, 46p, http://seine-aval.crihan.fr/web.
19 A. R. Jacobson, M. B. McBride, P. Baveye and T. S. Steenhuis, *Sci. Total Environ.*, 2005, **345**, 191–205.
20 M. Meybeck, L. Lestel, P. Bonté, R. Moilleron, J.-L. Colin, O. Rousselot, D. Hervé, C. de Pontevès, C. Grosbois and D. R. Thévenot, *Sci. Total Environ.*, 2007, **375**(1–3), 204–231.
21 M.-F. Le Cloarec, P. Bonté, L. Lestel, I. Lefèvre and S. Ayrault, *Phys. Chem. Earth*, DOI: 10.1016/j.pce.2009.02.003.

22 K. Wang and R. J. Cornett, *J. Paleolimnol.*, 1993, **9**, 179–188.
23 C. Gil-García, A. Rigol and M. Vidal, *J. Environ. Radioact.*, 2009, **100**, 690–696.
24 P. Bonté, J.-M. Mouchel, A. Thomas, M.-F. Le Cloarec, J.-P. Dumoulin, S. Sogon and L. Tessier, *Acta Geol. Hisp.*, 2000, **35**, 339–355.
25 L. Tessier, Transport et caractérisation des matières en suspension dans le bassin de la Seine: identification de signatures naturelles et anthropiques, PhD thesis, Ecole Nationale des Ponts et Chaussée, France, 2003, 344p.
26 K. H. Wedepohl, *Geochim. Cosmochim. Acta*, 1985, **59**, 1217–1232.
27 D. R. Thévenot, R. Moilleron, L. Lestel, M.-C. Gromaire, V. Rocher, P. Cambier, P. Bonté, J.-L. Colin, C. de Pontevès and M. Meybeck, *Sci. Total Environ.*, 2007, **375**(1–3), 180–203.
28 Irep, *Registre Français des Émissions Polluantes [French Register on Contaminant Emissions]*, French Ministry of Ecology, Energy, Sustainable Development and Marine Affairs, Paris, 2009, http://www.pollutionsindustrielles.ecologie.gouv.fr/IREP/index.php.
29 R. Salminen, *Geochemical Atlas of Europe. Part 1-Background Information, Methodology and Maps*, Forum of European Geological Surveys (FOREGS), G.S. of Finland, Espoo, 2005, www.gsf.fi/publ/foregsatlas/index.php.
30 C. Reimann and P. De Caritat, *Sci. Total Environ.*, 2005, **337**, 91–107.
31 D. C. Adriano, *Trace Elements in Terrestrial Environments: Biogeochemistry, Bioavailability, and Risks of Metals*, Springer-Verlag, New York, 2nd edn, 2001, p. 867.
32 A. Tremel, P. Masson, T. Sterckeman, D. Baize and M. Mench, *Environ. Pollut.*, 1997, **95**(3), 293–302.
33 L. Laforte, A. Tessier, C. Gobeil and R. Carignan, *Geochim. Cosmochim. Acta*, 2005, **69**(22), 5295–5306.
34 Y. Gélinas, M. Lucotte and J.-P. Schmit, *Atmos. Environ.*, 2000, **34**, 1797–1810.

Annexe 2

Papier en cours de préparation pour une soumission à « *Aquatic Toxicology* »

« Bioavailability of particulate metal to zebra mussels: Biodynamic modeling shows that assimilation efficiencies are site-specific »

Bioavailability of particulate metal to zebra mussels: Biodynamic modeling shows that assimilation efficiencies are site-specific

Bourgeault Adeline[1, 2], *Gourlay-Francé Catherine*[1, 2 *], *Priadi Cindy*[3], *Ayrault Sophie*[3] *and Tusseau-Vuillemin Marie-Hélène*[4]

[1] Cemagref, Unité de recherche Hydrosystèmes et Biobrocédés, Parc de Tourvoie - BP 44, 92163 Antony, France.

[2] FIRE, FR-3020, 4 place Jussieu, 75005 Paris, France.

[3] LSCE/IPSL CEA-CNRS-UVSQ, avenue de la Terrasse 91198 Gif-sur-Yvette, France.

[4] IFREMER Technopolis 40, 155 rue Jean-Jacques Rousseau, 92138 Issy-Les-Moulineaux, France.

* Corresponding author:

Tel: +33 (0)1 40 96 61 63

Fax: +33 (0)1 40 96 61 99

e-mail address: catherine.gourlay@cemagref.fr

ABSTRACT. This study investigates the ability of the biodynamic model to predict the trophic bioaccumulation of Cd, Cr, Cu, Ni and Zn. Zebra mussels were transplanted to three sites along the Seine River, and collected monthly for 11 months. Monthly-average concentrations of dissolved labile and particulate metals in water were measured. Particles were collected in sediment traps and treated by chemical sequential extraction. Measurements of the mussels' metal body burdens were compared with the biodynamic model's predictions. The particles metal exchangeable fraction did not account for the bioavailability of particulate metals, since it did not capture the differences between sites. The Assimilation Efficiency (AE) parameter is necessary to take into account biotic factors influencing particulate metal bioavailability. The biodynamic model, applied with AEs from the literature, overestimated the measured concentrations in zebra mussels, the overestimation being site-specific. Therefore, for each site and metal, AEs were optimized over the first five months: site-specific AEs for Cr, Cd, Cu, Ni and Zn were respectively 0%, 1-26%, 2-27%, 3-14% and 0-5%. Using these optimized AEs, the biodynamic model succeeded in predicting the metal bioaccumulation of the next six months. This study highlights the need for site-specific biodynamic parameters and proposes an original methodology for *in situ* AE measurements.

KEYWORDS: bioaccumulation, active biomonitoring, bioavailability of particulate metals, assimilation efficiency, chemical sequential extration.

BRIEFS: The interpretation of metal bioaccumulation in transplanted zebra mussels with biodynamic modeling highlights the need for site-specific assimilation efficiencies of particulate metals.

Introduction

Most aquatic organisms are exposed to trace metals that are both dissolved in water and associated with suspended particles. The toxicokinetics-based biodynamic model is commonly employed to investigate quantitatively the metal bioaccumulation processes in aquatic invertebrates and to predict metal body burdens from environmental concentrations (Casado-Martinez et al., 2009; Luoma and Rainbow, 2005; Pan and Wang, 2008; Roditi et al., 2000). This model describes the metal concentration in invertebrates as follows:

$$\frac{dC_{org}}{dt} = k_u \cdot C_w + AE \cdot IR \cdot C_f - (k_e + g) \cdot C_{org} \quad (1)$$

where C_{org} is the metal concentration in the organism (µg.g^{-1}), t is the time of exposure (d), k_u is the uptake rate constant from the dissolved phase (L.g^{-1}.d^{-1}), C_w is the concentration of bioavailable metal in the dissolved phase (µg.L^{-1}), AE is the assimilation efficiency of ingested metal (%), IR is the ingestion rate (g.g^{-1}.d^{-1}), C_f is the metal concentration in the food (µg.g^{-1}), k_e is the efflux rate constant (d^{-1}) and g is the growth rate constant of the animal (d^{-1}).

Using the biodynamic model to predict metal bioaccumulation requires information on the metal concentration in water (both dissolved and particulate), but also kinetic and physiological parameters that are usually determined experimentally in the laboratory and then used in field conditions. Among the latter, the assimilation efficiency (AE) - that correspond to the fraction of ingested particulate metal that is actually retained in the tissue - , the ingestion rate (IR) and the metal concentration in particles (C_f) reflect dietborne bioaccumulationand are of great importance in bioaccumulation modeling, especially for filter-feeding organisms such as mussels, for which food can be the predominant source of metals (Roditi et al., 2000; Wang and Fisher, 1998). For mussels, the modeling can be complicated since they can select their food according to both its quality (i.e. its chemical composition) and its quantity (Arifin and Bendell-Young, 1997; Arifin and Bendell-Young, 2000). The food actually ingested by the organism can thus greatly vary from the suspended particles present in the water column and so measuring the right trophic parameters may be challenging.

Beyond the critical aspect of food selection, several studies have pointed out some limitations to using laboratory-determined AEs for the prediction of *in situ* dietborne bioaccumulation. For instance, the geochemical properties of each potential site and the speciation of particulate metals are not recreated in the laboratory (Griscom et al., 2000; Wang and Fisher, 1998; Wang et al., 2002). Indeed, freshly spiked metals are generally found in the more easily exchangeable phase, whereas native metals are usually distributed in more residual phases (Wang et al., 2002). However, up to now, no generalization of geochemical and biological effects on AE has been established.

Other authors have investigated whether the bioavailability of particulate metal could be assessed through the chemical characterisation of an exchangeable metal fraction in particles (Bryan and Langston, 1992; Griscom and Fisher, 2004; Luoma, 1989; Stecko and Bendell-Young, 2000). The operationally exchangeable metal fraction can be characterized by different protocols such as sequential extraction (Pueyo et al., 2001), digestive gut-fluid extraction (Mayer et al., 1996), HCl extraction (Luoma, 1989) or the Acid Volatile Sulfide / Simultaneously Extracted Metals (AVS/SEM) model (Di Toro et al., 1992). The AVS-based approach has lately been proposed as a regulatory tool to assess metal bioavailability in sediments (Ahlf et al., 2009), despite some reported exceptions (De Jonge et al., 2010; Griscom et al., 2000). The relationship between digestive gut-fluid or weak acid extractions and AE is also questionable: although a relationship has been established for Cd, the exchangeable metal fraction (whether evaluated by acids or gut juice) is unrelated to AE in the case of Cr and Zn (Fan and Wang, 2003; Wang et al., 2002).

The objective of the present study was to assess the actual bioavailability of particulate metals to zebra mussels in rivers, using a combination of biodynamic modeling and chemical analysis. Zebra mussels were transplanted for 11 months to three sites along the Seine River, and monitored monthly. Meanwhile, metal concentrations were also monitored in water and suspended particles. The mussels' metal body burdens as measured were compared with biodynamic model predictions. We first investigated whether – and if so, to what extent – chemical sequential extraction could mimic the bioavailability of particulate metals. We also tested the ability of the biodynamic model to do so when combined with laboratory-

90 determined parameters. This led us to propose an alternative metholodogy to estimate AE directly from
91 field measurements.
92
93

94 1 Materials and methods

95 *1.1 Study area and sampling*

96 Three sites were studied along the Seine River (France): Marnay-sur-Seine (Site1), Bougival (Site 2)
97 and Triel-sur-Seine (Site 3). Site 1 is located 200 km upstream from Paris while Sites 2 and 3 are situated
98 respectively 40 km and 80 km downstream from Paris. Site 2 and 3 are thus both subjected to diffuse
99 urban contamination (i.e. atmospheric fallout combined with sewer overflows). In addition to this, Site 3
100 is also subject to wastewater discharges (domestic and industrial sewage).
101 Zebra mussels were sampled in October 2008 in a reference site in the Meuse-Marne canal (France)
102 (48°45'33"N, 5°36'05"W), on the day before deployment. Mussels (20-22 mm in shell length) were
103 distributed in cages (25 mussels per cage) and then transplanted onto the three sites. One cage was
104 sampled each month over an 11-month period and brought back to the laboratory in field water within a
105 few hours.
106 On the same dates as mussels were sampled, water samples were collected monthly to monitor
107 physico-chemical parameters (i.e. dissolved and particulate organic carbon, chlorophyll, pheopigment,
108 total suspended solids (TSS), ash free dry weight (AFDW) which allows to assess the percentage of
109 carbon in particles, major ions, temperature, conductivity and pH).
110 The one-month integrative metal contamination was monitored using three Diffusive Gradient in Thin
111 film technique (DGT) to assess dissolved labile metals (Davison and Zhang, 1994; Tusseau-Vuillemin et
112 al., 2007) and using sediment traps for particulate metals. DGTs were composed by resin and restricted
113 diffusive gel of 0.8 mm thickness (DGT research, Landcaster, UK) covered with a 0.45 mm

polyethersulfone (PES) filter and a 0.4 µm polycarbonate filter (Tusseau-Vuillemin et al., 2007). The sediment trap consisted of a 2L polyethylene terephtalate (PET) bottle with two holes of a diameter of about 4 cm carved on both sides on the upper side of the bottle allowing water flow.

1.2 Filtration rate measurement

Once brought back to the laboratory, the mussels were used for field filtration rate (FR) estimations. For each site, in the laboratory, the apparent filtration rate (FR_{app}) was measured in filtered field water spiked with 1.10^6 cells.mL^{-1} of algae (*Selenastrum capricornutum*), as described in Bourgeault et al. (Bourgeault et al., 2010a). Indeed, the quantification of FR with controlled TSS is necessary to get reliable measurement of particle decrease. The algae addition corresponds to a TSS concentration of 20 mg.L^{-1} (TSS concentrations measured *in situ* during the whole campaign ranged from 4 to 45 mg.L^{-1}). Three replicates of 5 pooled mussels were placed on a nylon sieve in a 500 mL beaker. The medium was continuously homogenized using a magnetic stirrer (300 rpm) and the experiments were conducted in a thermostated room, adjusted to the site water's temperature.

The field filtration rate *FR* was deduced from FR_{app} by taking into account the actual TSS concentration in the field, based on the empirical relation obtained by Reeders and Bij de Vaate (1990):

$$FR = FR_{app} \cdot e^{-0.037 \cdot (TSS_{Field} - TSS_{Laboratory})} \quad (2)$$

1.3 Condition Index

The soft tissues of mussels were removed from the shell and byssus threads were cut off. Soft tissues and shells were weighed. The Condition Index (CI) was calculated as the ratio between the wet weight of soft tissues and the total weight of the mussel (including the shell).

1.4 Metal analysis

The mussels' tissues were then freeze-dried and weighed. The mussels' dried tissues were pooled for a given date and site and homogenized (MM 400 Retsch). The tissues (about 80mg) were digested for 1.5h in polypropylene tubes (Sarstedt) with 2mL of HNO_3 (65% suprapur Merck) using a heating block (DigiPREP, SCP Science) set at 95°C. After cooling, 0.8mL of H_2O_2 (30% suprapur Merck) were added and the sample was once again heated for 1.5h at 95°C. Finally, 17.2mL of ultrapure water (Elga) were added to the extract.

After retrieval, the chelex resins of DGTs were eluted in 1M nitric acid (Suprapur, Merck) in which the analysis was performed. The monthly average labile concentrations were determined as described by Tusseau-Vuillemin et al. (Tusseau-Vuillemin et al., 2007).

Particles collected by sediment traps were centrifuged, freeze dried and then subjected to Community Bureau of Reference (BCR) sequential extraction scheme, following a revised protocol (Pueyo et al., 2001). The digestion was performed with various acids in Teflon vessels using a heating block (Digiprep, SCP Science). Particulate metals were divided in exchangeable (Exch), reducible (Red), oxidizable (Oxy) and residual (Res) fractions. Methods and data are reported elsewhere (Priadi et al., In press). However, among the 11-month exposure, suspended particles were not sampled by sediment traps in November and December 2008 and in June and September 2009. These four missing values were therefore extrapolated, based on the others data of sequential extraction (since the percentage of metal in each fraction is constant during the exposure for a given site (Priadi et al., submitted.)) and the analysis of total metal concentration of particle which was performed for the entire 11-month exposure by Priadi et al (Priadi et al., submitted.). Total metal extraction from particles is described elsewhere (Priadi et al., submitted.). In the present study, only the exchangeable and the reducible fractions were considered since the metals liberated by the 2-step sequential extraction of oxidized particles (such as the suspended particles collected in the sediment traps) are expected to be broadly the same as those liberated by HCl extraction (Larner et al., 2008) recommended by Luoma et al. (Luoma, 1989) to roughly assess particulate metal bioavailability.

Internal standards (^{103}Rh, ^{115}In and ^{185}Re) were added to the samples prior to metal analysis. Metal concentrations were determined using an Inductively Coupled Plasma-Mass Spectrometer (ICP-MS ThermoFisher Scientific), checking the accuracy of the analytical procedure with a reference natural water sample (NIST 1640). The relative standard deviations were <15% for Cr, Ni, Cu and Cd, and <27% for Zn (*n*=5). A reference mussel material (Mussel Tissue ERM-CE 278) was also used to validate the acidic digestion. The deviation from certified values was <10% for Cr, Cd, Cu and Zn, except for one sample in the case of Cr, where the deviation reached 31% (*n*=4) – Ni concentration is not referenced in this mussel material. Metal body burden was expressed in µg of metal per g of dry tissue ($\mu g.g_{dry\ wt}^{-1}$). Since the samples were pooled, we assumed a 10% deviation for the metal analysis in mussel tissues, based on the results obtained by Bervoets *et al.* (Bervoets et al., 2004), who showed that a representative sample with an RSD lower than 10% was obtained with 15 pooled individuals. Our own measurements on the reference mussel material confirmed the RSD was lower than 10% (*n*=4). It is important to notice that this deviation reflects both biological and analytical variability.

1.5 Statistical analysis

All data was first tested for normality using the Shapiro-Wilkinson test. Significant differences in trace metal body burdens and filtration rates at different date and site were tested using the Kruskal-Wallis analysis. The normally-distributed Condition Indexes were compared using analyses of variance (ANOVA) followed by the Tukey HSD test. A probability level of 0.05 was considered to be statistically significant.

2 Bioaccumulation modeling

In order to apply the biodynamic model to monthly data, metal bioaccumulation in mussels was predicted from Equation 1, under the hypothesis that environmental variables (i.e. TSS concentration, C_w

and C_f), physiological parameter (IR= FR x TSS and g) are constant between t_{i-1} and t_i, but may vary from month to month. The metal concentration in mussel tissues is described by the following equation (details of the differential equation's resolution are reported in SI):

$$C_{org}(t_i) = C_{org}(t_{i-1}) \cdot e^{-(k_e+g)(t_i-t_{i-1})} + C_{org\_ss} \cdot (1 - e^{-(k_e+g)(t_i-t_{i-1})}) \quad (3)$$

where $$C_{org\_ss} = \frac{k_u \cdot C_w + AE \cdot TSS \cdot FR \cdot C_f}{k_e + g} \quad (4)$$

C_{org} being the metal concentration in the organism ($\mu g.g^{-1}$), C_w the bioavailable dissolved metal concentration between t_{i-1} and t_i ($\mu g.L^{-1}$), C_f the metal concentration of the particles collected by the sediment traps between t_{i-1} and t_i ($\mu g.g^{-1}$), k_u the uptake rate constant from the dissolved phase ($L.g^{-1}.d^{-1}$), *AE* the assimilation efficiency of ingested metal (%), *TSS* the Total Suspended Solid concentration obtained by averaging the values measured at t_{i-1} and t_i ($g.L^{-1}$), *FR* the filtration rate ($L.g^{-1}.d^{-1}$) measured as described in the M&M part and also obtained by averaging the values measured at t_{i-1} and t_i, k_e the efflux rate constant (d^{-1}) and *g* the growth rate constant (d^{-1}) between t_{i-1} and t_i.

The ingestion rate (IR) was expressed as the product of TSS concentration and FR in order to take into account the biological activity of mussels over sites and time. However, since mussels have the ability to select their food, the appropriate particles concentration in the model would be the concentration of particles actually ingested. As the measurement of this concentration is not reachable in the field, the default assumption made here is that the ingested particles are approximately similar to the partcles sampled in the water column. Moreover our estimate of the metal concentration in particles actually ingested is the concentration measured in particles collected in sediment traps at each sites even if it is not necessarily the same as ingested ones. The filtration rate (FR) of mussels was measured *ex situ* at the site temperature in filtrered field water spiked with a standard food (algae). Wherease this approach was selected because of its simplicity, the use of algae can induce a substantial difference between the *in situ* and the *ex situ* situations. However, other methods often result in disturbance of the mussels (isolation of siphons by a wall (Galstoff, 1928; Kryger and Riisgard, 1988) or anemometry method where the temperature of the water from the exhalant siphon is measured) and are obviously

inaproppriate for *in situ* measurement. The concentration of labile metal measured using DGT devices were used as C_w since DGT devices allow an integrative measurement which mimic the bioavailable metal fraction (Ferreira et al., 2008; Tusseau-Vuillemin et al., 2004). Initial metal concentration in mussels $C_{org}(t_0)$ is the measured concentration in mussels at the collection site. The growth rate g (d^{-1}) was calculated for each month from the evolution of the dry weight of the mussels' soft tissues between t_{i-1} and t_i. This parameter is equal to the gain or loss of body weight over a month divided by time and the initial weight of mussels at t_{i-1}. Let us point out that during spawning, the weight loss leads to a negative growth rate. Indeed, we inferred that spawning concentrates the metals in soft tissues since evacuated gametes have a low metal content compared to the other soft parts (Phillips, 1980).

The mean predicted metal accumulation was performed using the mean values of the biodynamic parameters summarized in Table 1. Parameters were obtained from several studies on zebra mussels (Bourgeault, 2010; Bourgeault et al., 2010a; Mersch et al., 1993; Roditi and Fisher, 1999), or marine mussels when not available for zebra mussels (Wang et al., 1996; Zaroogian and Johnson, 1984). We give priority to studies focusing on the determination of biodynamic parameters since some methodologies are quite specific (such as the determination of AE). Otherwise we extended to less specific studies focussing on dissolved metal accumulation or on elimination processes. As far as Cd and Cr are concerned, modeling was performed using biodynamic parameters determined for the zebra mussel by Roditi and Fisher (Roditi and Fisher, 1999) exept the uptake rate constants of Cd (k_u) which was determined in laboratory in a previous study and was expressed as a function of the filtration rate and confounding factors (i.e. Ca and Zn dissolved concentrations)(Bourgeault et al., 2010a). The uptake rate constant of Ni was also determined as a function of the filtration rate and confounding factors. It allows refining the parameters of dissolved accumulation by adapting them to water chemistry and biological activity of mussels. The accumulation of dissolved Cu was also studied in laboratory in a previous study algthout the effect of confounding factors were not assessed (unpublished data). Hence, for Cd and Ni, k_u varied from month to month and from sites whereas for Cu, Cr and Zn, k_u were constant over time and space. Cr speciation was not determined in the present study, that is why we used a mean of the

237 respective k_u of Cr(III) and Cr(VI) determined by Roditi and Fisher (Roditi and Fisher, 1999). As
238 biodynamic parameters were not determined for the zebra mussel for Zn we used the biodynamic
239 parameters determined for the mussel *M. edulis* (Wang et al., 1996). Assimilation efficiencies for Cu and
240 Ni were not available in the literature. However elimination rates k_e were obtained from Mersch et al.
241 (Mersch et al., 1993) and Zaroogian and Johnson (Zaroogian and Johnson, 1984) who studied the
242 elimination of metal from contaminated mussels. When several AEs were reported in the litterature, we
243 chose the one which had been determined from the natural seston (instead of food composed by algae or
244 diatoms only) that had characteristics the closest to the sites studied (i.e. TSS loads, particulate organic
245 carbon and chlorophyll concentrations).
246
247 In a first simulation, the ability of chemical sequential extractions to reflect the concentration of
248 bioavailable particulate metal was investigated. The measured metal concentrations in mussels were
249 compared to the predicted values with an AE equal to 100% and C_f as the concentration of particulate
250 metal measured in the different fractions of the chemical extraction.
251 In a subsequent simulation, we evaluated the predictive capacity of the biodynamic model to determine
252 the contamination of mussels with AE from the literature (Table 1). No simulations were made for Cu
253 and Ni, since no AEs were available for zebra mussels or other closely related bivalve species.
254 Finally, data from the first 5 months of exposure was used to optimize AE for each metal and each site,
255 using the least squares method in Microsoft Excel. The biodynamic model was applied with optimized
256 AEs to data from the last 6 months and predicted accumulation concentrations were compared to the
257 measured ones.
258

3 Results

3.1 Chemical Characterization

The different chemical parameters measured over the exposure indicated a gradient from upstream (Site 1) to downstream (Site 2 and 3) (Table 2). Indeed the DOC, POC and chlorophyll concentrations are significantly higher downstream ($p<0.05$), as well as the percentage of organic carbon in the TSS althought not statistically significant. A metal gradient was also observed since the labile and particulate metal concentrations were significantly higher at sites 2 and 3 compared to Site 1 for Cu, Zn and Cd ($p<0.05$, Kruskall Wallis analysis).

3.2 Biological activity of mussels

Condition index (CI) and filtration rate (FR) data is given in Figure 1 and 2.

Most mussels survived from October 2008 to July 2009, the mean mortality rate being <12%. In August the mortality rates were 27, 79 and 70% for Sites 1, 2 and 3 respectively and then reached 88, 88 and 92% in September.

The CI exhibited a seasonal trend, with an increase over the first 6 months, reaching a maximum at the end of March (0.45 ± 0.03 for Site 2) or April (0.40 ± 0.04 for Site 1 and 0.42 ± 0.06 for Site 3), followed by a decrease until September (0.19 ± 0.02, 0.25 ± 0.05 and 0.26 ± 0.08 for Sites 1, 2 and 3 respectively). Hence we infered that spawning occurred in April for Site 2 and in May for Sites 1 and 3.

The FRs sharply dropped at the 3 sites in December and increased steadily from January to August. The water temperature, which fell below 5°C in December, could partly explain the decrease of FR during the winter (Reeders and Bij de Vaate, 1990). The FR at Site 1 was generally higher than at both other sites, the difference being significant in February and March (Kruskal and Wallis analysis, $p<0.05$). This may be explained by a smaller food supply (Reeders and Bij de Vaate, 1990), since concentrations of dissolved and particulate organic matter were smaller at Site 1 (Priadi et al., submitted.).

3.3 Metal contamination in mussels

A significant difference in the metal contamination of water and suspended particules was observed between the upstream site on the one hand, and the two downstream sites on the other hand (a detailed description is provided elsewhere (Priadi et al., submitted.) and compiled data is reported in Table 2). Nevertheless, over the 11-month exposure, no significant difference in metal body burdens was observed between the sites (Figure 3) (Kruskall and Wallis analysis, $p>0.05$). The mean body burdens during exposure, all sites considered, were 0.8 ± 0.2 µg.g $_{dry\ wt}^{-1}$ for Cd, 1.0 ± 0.4 µg.g $_{dry\ wt}^{-1}$ for Cr, 11.5 ± 2.1 µg.g $_{dry\ wt}^{-1}$ for Cu, 7.4 ± 2.7 µg.g $_{dry\ wt}^{-1}$ for Ni and 106.7 ± 11.8 µg.g $_{dry\ wt}^{-1}$ for Zn. The metal concentrations in zebra mussels were similar to those previously obtained for transplanted mussels along an affluent of the Seine River (Bourgeault et al., 2010b). These concentrations were already similar to the metal contamination of mussels from reference sites in other studies (Camusso et al., 2001; De Lafontaine et al., 2000; Voets et al., 2006), even though the Seine River basin is subjected to very high anthropogenic pressure (Meybeck et al., 2007). This highlights the complexity of urbanized sites, which are undoubtedly contaminated, but with low levels of numerous substances and are therefore not strongly contrasted sites as regards one specific substance.

A decrease of Cd, Cr and Cu body burden is observed in April, as the same time as maximal weight of mussel – and consequentely maximum CI. It can thus be inferred that the mussels' growth had induced a biological dilution of metals (Bourgeault et al., 2010b). Conversely, metal body burdens increase in June presumably as a consequence of spawning (Phillips, 1980).

4 Discussion

The modelling of metal bioaccumulation performed using mean concentrations of metal in the particles (either measured in the 1, 2, 3 or 4 steps of the sequential extraction) and in the water in the Seine river

basin and biodynamic parameters reported in Table 1 showed that almost the total amount of Zn and Cd accumulated comes from the trophic pathway. This result is in agreement with a previous study of Cd uptake in the zebra mussels, which demonstrated that this organism accumulates in average 78% of the total Cd from food (Roditi et al., 2000). This result supports the fact that the key to better predict the bioaccumulation relies on the accurate determination of trophic exposure.

4.1 Does chemical sequential extraction mimic the bioavailability of particulate metals?

Assuming that the bioavailability of particulate metals would be properly assessed by a weak and selective extraction (Luoma, 1989), as performed in the first or the second steps of sequential extraction (Larner et al., 2008), a 100% AE combined with the concentration of particulate metals in selected fractions of the sequential extraction would be sufficient to adjust the modeled data to the measured one.

With these parameters, the model overestimated the metal contamination in the mussel tissues if the concentration of particulate metals is considered as the concentration measured in the Exchangeable and Reducible fractions (Figure 4). A better adjustment was obtained when considering the concentration of particulate metals as the concentration measured in the exchangeable fraction only (Figure 4), since the predicted values in the mussel tissues were then in the same order of magnitude as measured values. However, 35% of predicted values are more than 3 times higher than the measured values (comparisons over time for the 3 sites are given in SI). For example, Cr and Ni contamination is always overestimated, which suggests that metals in the exchangeable fraction are not fully bioavailable. Conversely, Cu in mussel tissue is well simulated for Site 1 and tends to be underestimated for Sites 2 and 3, which means that Cu in less exchangeable fractions is probably bioavailable at these sites. Hence, representing the bioavailability of particulate metals by the concentration in the exchangeable fraction only was not sufficient to accurately predict metal accumulation in organisms. Thus, in the present study the speciation

331 defined by the chemical extraction was found to be an unreliable predictor of the bioavailability of
332 particulate metals, independently from the site and the metal considered.

333 The simulations presented here are conditionned by the assumed accuracy of model constants, i.e. k_u
334 and k_e. This assumption seems realistic for the elimination constant, since it is generally low variable
335 (Roditi and Fisher, 1999), however k_u is largely conditioned by the environmental chemistry (DOC, Ca,
336 Zn ...) (Bourgeault et al., 2010a). These changes have not been fully taken into account in the
337 simulations, especially for Zn, Cu and Cr. Thus, we investigated whether a correction of the parameter k_u
338 could be sufficient to adjust the predicted values to measured ones. The results have shown that with
339 metal particulate concentration measured in the 2, 3 or 4 steps of the sequential extraction, even a lack of
340 dissolved accumulation (i.e. $k_u = 0$) did not improve model predictions. If now considering the particulate
341 metal concentration as the concentration measured in the first step of the sequential extraction, various
342 results were obtained depending on the metal and the site. As an example, for Site 3, a lack of dissolved
343 Ni and Cd accumulation (i.e., $k_u = 0$) did not improved the fit of the data (Figure 5). With regard to Zn
344 and Cr, a lack of dissolved accumulation improved the prediction since the model which initially
345 overestimated the accumulation respectively by a factor 2.4 and 3.7, finally overestimated the
346 accumulation by a factor 1.2 and 1.4. In the case of Cu, the constant accumulation by dissolved should be
347 multiplied by a 3-fold factor to adjust the predicted values with those measured. Given these results, we
348 have not considered appropriate to change the values of k_u without having a better basis.
349

350 ***4.2 Need for site-specific assimilation efficiencies in biodynamic modeling***

351 The inability of chemical speciation to properly evaluate the bioavailability of particulate metals
352 highlights the fundamental role of the AE parameter. Unfortunately, the application of the biodynamic
353 model with AEs from the literature leads to an overestimation of metal accumulation in organisms
354 (Figure 4). Moreover, this overestimation is greater at Sites 2 and 3 than at Site 1 (see details of the
355 simulation over time in SI). For example, Cd concentrations in mussels are overestimated on average by a

356 factor of 3, 13 and 6 at Sites 1, 2 and 3 respectively. It is important to notice that these variations from
357 one site to another do not result from an adapation of the metal (Cd and Ni) accumulation through the
358 dissolved pathway to the site's characteristics (Bourgeault, 2010; Bourgeault et al., 2010a). Indeed, the
359 fact that Zn and Ca competition were included in k_u estimation resulted in a reduced Cd uptake rate
360 constant at Sites 2 and 3, and yet bioaccumulation at Sites 2 and 3 are the most overestimated ones. The
361 properties of particles (i.g. binding characteristics of particles; concentrations of organic matter, sulfides
362 and metals) and the biological behavior of organisms, which probably differs between sites, may
363 presumably explain the differences in the model's accuracy between sites. We thus concluded that the
364 application of variable AEs between sites is necessary to get accurate predictions of the biodynamic
365 model.

366 Indeed the use of an optimized AE for each site and for each metal does lead to a good match between
367 predicted and measured concentrations (Figure 4). Indeed, 86% of the values predicted for the last 6
368 months of exposure were similar to the actual measured concentrations, within a 2-fold factor. AEs
369 optimized from the first 5 months of exposure are reported in Table 3. Optimized AEs were at least 3
370 times smaller than laboratory-determined AEs from the literature (Table 1). This confirms that the
371 assimilation of metals freshly spiked onto particles in the laboratory is higher than that of natural
372 particulate metals (Griscom et al., 2000). AEs at Site 1 were higher than those at the two downstream
373 sites, even though sequential extractions tend to show that metals were more labile downstream (Priadi et
374 al., In press). To determine the major driving factor of the different optimized AE, a statistical analysis
375 was performed on the data using XLstat software. A Partial Least Square (PLS) analysis was thus
376 performed between the response (i.e. optimized AE) and independent variables (i.e. FR, chlorophyll,
377 POC, DOC, TSS, pheopigment concentration, percentage of carbon in particles, temperature and pH).
378 Despite the upstream/downstream differences observed with both optimized AE and biological and
379 physico-chemical parameters, no correlation has been established. However, as regards the mussels at
380 Site 1, we can hypothesis that the lower trophic level at this site might result in a greater uptake of
381 carbon, and thus a higher uptake of metals (Reeders et al., 1989). Let us point out that, except for Cu at

Site 1 and Ni at Site 3, AEs optimized from the first 5 months of exposure are close to AEs obtained from the calibration data corresponding to 11 months of exposure or the last 5 months (Table 3). This indicates that the biological cycle of the organism, which strongly varies through the year, may have less influence on metal AEs than site-specific environmental conditions. Practically speaking, an exposure of just 6 months is sufficient to determine site-specific AEs.

Conclusion

This study highlights the problem with using generic biodynamic parameters and proposes an original methodology to determine site-specific AEs and provide a good fit between the biodynamic model's predictions and bioaccumulation measurements. This original methodology for estimating AE requires, above all, a robust biodynamic model with precisely determined kinetic constants (k_u, k_e and IR). Obtaining this robust model is not straightforward. Yet, this methodology enables the assessment of the actual assimilation efficiency of metals, taking into account both the effects of organism physiology and the geochemical variations in the speciation of particulate metals.

ACKNOWLEDGMENTS: The authors thank Emmanuelle Uher and Aurélie Germain for their support in field work and sample analysis, Julien Guieu for his linguistic support and the S.I.A.A.P. for providing access to Site 2 (Bougival). This work is part of the Piren-Seine research program and the MEDISIS (Métaux dissous en Seine) project, in the context of the EC2CO (Ecosphère Continentale et Côtière) program. A. Bourgeault acknowledges a PhD grant from the Ile-de-France Regional Council (R2DS program).

In Supporting Information are reported the concentrations of labile and particulate metals over the whole exposure period, as well as the percentage of metals in the exchangeable and the reducible fractions at the three sites. The different outputs of bioaccumulation simulations over time are also presented, as is the theoretical resolution of the differential equations used for these simulations.

409 **Tables**

410

411 Table 1: Biokinetic parameters used to model metal concentrations in zebra mussel tissues.

	AE (%)	k_u ($L.g^{-1}.d^{-1}$)	k_e (d^{-1})
Cd	26 ± 2 [a1]	$k_u = FR \cdot \left(\frac{0.134}{1+10^{3.5} \cdot [Ca]+10^{7.4} \cdot [Zn]} \right)^{b}$	0.012 ± 0.001 [a3]
Cr	1.5 ± 0.5 [a2]	1.15 [a]	0.015 ± 0.002 [a3]
Zn	32 ± 5 [c1]	1.047 [c2]	0.018 ± 0.004 [c3]
Ni	-	$k_u = FR \cdot \left(\frac{0.043}{1+10^{3.6} \cdot [Ca]} \right)^{b}$	0.019 [d]
Cu	-	0.163 [b]	0.022 [e]

412 [a] : (Roditi and Fisher, 1999)

413 [a1]: AE referring to natural seston identified as 'seston B' in the Roditi and Fisher study. This seston was
414 sampled from the Hudson River, which had a TSS concentration of 11 $mg.L^{-1}$. For a comparison
415 purpose, the average TSS concentration was respectively 12, 14 and 10 mg/L for Site 1, 2 and 3 over the
416 11-month exposure.

417 [a2]: Since the AE for Cr was not available for 'seston B' in the Roditi and Fisher study, we used AE
418 determined for a second natural seston identified as 'seston A'. This seston was sampled from the Hudson
419 River, which had a TSS concentration of 28 $mg.L^{-1}$.

420 [a3]: Mean of the respective k_e of Cr III and Cr VI, obtained as a result of mussel contamination through
421 the trophic and the dissolved pathways

422 [b] : values obtained from a previous laboratory study on zebra mussels ((Bourgeault, 2010; Bourgeault
423 et al., 2010a) and unpublished data for Cu)

424 [c] : (Wang et al., 1996)

425 [c1]: AE referring to the natural seston identified as seston of '11 March', which had physicochemical
426 characteristics closer to the characteristics measured at site 1, 2 and 3. Indeed the chlorophyll
427 concentration of the seston identified as '11 March' is 11,7 $\mu g.L^{-1}$ and its TSS concentration is 9.5 mg/L
428 compared to the average concentrations measured at sites 1, 2 and 3 over 11 months that were
429 respectively 1.3, 5.6 and 5.4 µg/L for chlorophyll and 12, 14 and 10 mg/L for TSS.

430 [c2]: Mean k_u

431 [c3]: Mean k_e obtained as a result of mussel contamination through the trophic and the dissolved routes

432 [d]: (Zaroogian and Johnson, 1984)

433 [e]: k_e estimated from bioaccumulation data after a depuration period (Mersch et al., 1993)

434 Table 2: Physico-chemical parameters and metal concentrations measured at Site 1, 2 and 3 expressed as

435 minimum – maximum and mediane in parenthesis.

	Site 1	Site 2	Site 3
Q (m^3/s)	25 - 89 (50)	92 - 324 (184)	198 - 550 (340)
pH	8.06 - 8.32 (8.18)	7.20 - 8.24 (7.91)	7.10 - 8.01 (7.73)
Temperature (°C)	5.6 - 23 (13.1)	4.5 - 22.8 (15.2)	4.9 - 22 (14.4)
Conductivity (µS/cm)	268 - 526 (479)	446 - 611 (527)	506 - 668 (619)
Alkalinity (mg/L)	152 - 287 (238)	182 - 281 (244)	189 - 281 (253)
DOC (mg/L)	1.62 - 2.68 (2.05)	2.56 - 4.34 (2.94)	3.42 - 5.45 (3.87)
TSS (mg/L)	4.0 - 33.4 (9.5)	6.4 - 44.1 (10.9)	4.2 - 21.9 (9.8)
C in TSS (%)	16 – 61 (28)	21 – 48 (32)	0 – 59 (34)
POC (mg/L)	0.05 - 1.9 (0.56)	0.38 - 3.92 (0.88)	0.04 - 2.47 (0.89)
Chlorophyll (µg/L)	0.5 - 3.5 (1.0)	0.4 - 15.1 (3.7)	0.3 - 16.4 (2.5)
Pheopigment (µg/L)	0.9 - 7.5 (1.3)	0.8 - 17.3 (1.7)	0.3 - 2.5 (1.4)
Labile metal concentration (µg/L)			
Cd	0 - 0.002 (0.001)	0 - 0.007 (0.003)	0 - 0.005 (0.004)
Cr	0 - 0.035 (0.020)	0 - 0.093 (0.028)	0 - 0.086 (0.031)
Zn	0 - 1.49 (0.44)	0 - 3.13 (1.83)	0 - 3.74 (2.68)
Ni	0 - 0.212 (0.173)	0 - 0.47 (0.322)	0 - 0.796 (0.543)
Cu	0 - 0.104 (0.074)	0 - 0.481 (0.253)	0 - 0.388 (0.251)
Particulate metal concentration measured in the Exchangeable and Reducible fractions (µg/g)			
Cd	0.20 - 0.32 (0.23)	0.65 - 2.90 (1.73)	0.70 - 2.90 (1.51)
Cr	0.27 - 1.43 (1.03)	6.57 - 10.56 (7.93)	2.00 - 10.02 (7.20)
Zn	141.56 - 277.20 (246.19)	236.55 - 377.07 (305.30)	141.56 - 277.20 (246.19)
Ni	2.21 - 4.86 (4.39)	6.01 - 9.88 (8.47)	3.40 - 8.10 (7.23)
Cu	2.08 - 7.68 (2.42)	16.70 - 61.22 (37.77)	9.04 - 38.89 (18.40)

436 Q: discharge, DOC: Dissolved Organic Carbon, TSS: Total Suspended Solids, POC: Particulate
437 Organic Carbon, C: carbon.

438

439

440

441

442 Table 3: Assimilation efficiencies (AE) obtained through the optimisation of predicted concentrations
443 with the measured ones over the first 5 months, the last 5 months and the whole 11 months of exposure.

	Optimisation over the first 5-month exposure			Optimisation from the last 5-month exposure			Optimisation from the 11-month exposure		
	Site 1	Site 2	Site 3	Site 1	Site 2	Site 3	Site 1	Site 2	Site 3
Cd	9%	1%	7%	11%	2%	2%	9%	2%	4%
Cr	0%	0%	0%	0%	0%	0%	0%	0%	0%
Zn	5%	0%	0%	0%	0%	0%	5%	0%	0%
Ni	13%	3%	14%	8%	4%	5%	13%	3%	14%
Cu	26%	2%	8%	9%	2%	3%	9%	2%	5%

444

445

446

447 **Figures**

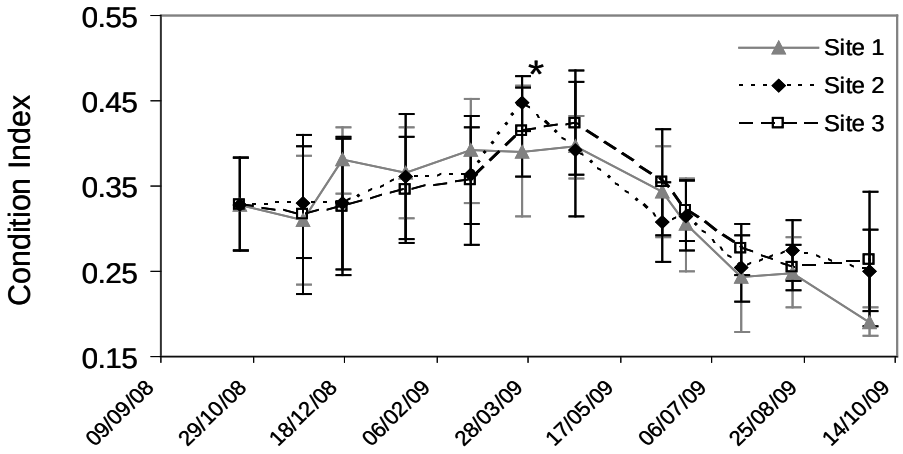

448

449 Figure 1: Condition Index (CI) of the mussels exposed at the three sites. Mean ± SD (*n*=15). * Maximal
450 values for each of the three sites are significantly different from the initial CI (except for Site 1) and from
451 the final CI (except for Site 3), Anova - TukeyHSD ($p<0.05$).

452

453

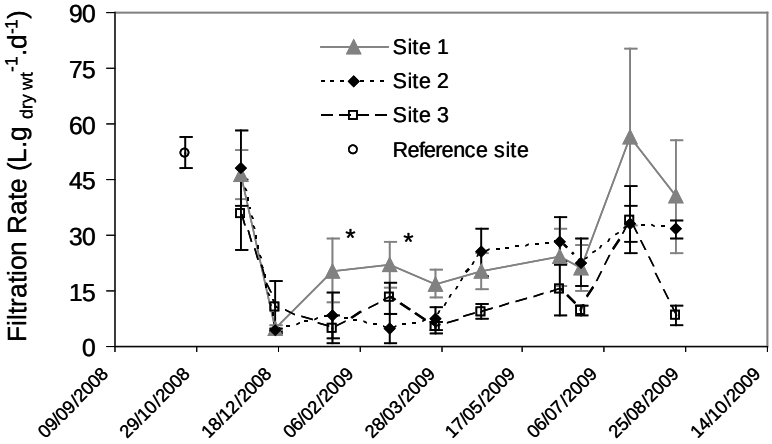

454

455 Figure 2: Filtration rate of the mussels exposed at the three sites ($L.g_{\text{dry wt}}^{-1}.d^{-1}$). Mean of three replicates
456 (each composed of 5 mussels) ± SD. The asterisks * indicate that the values are significantly different
457 between Site 1 and Site 3 in February and between Site 1 and Site 2 in March (Kruskal and Wallis
458 analysis, $p<0.05$).

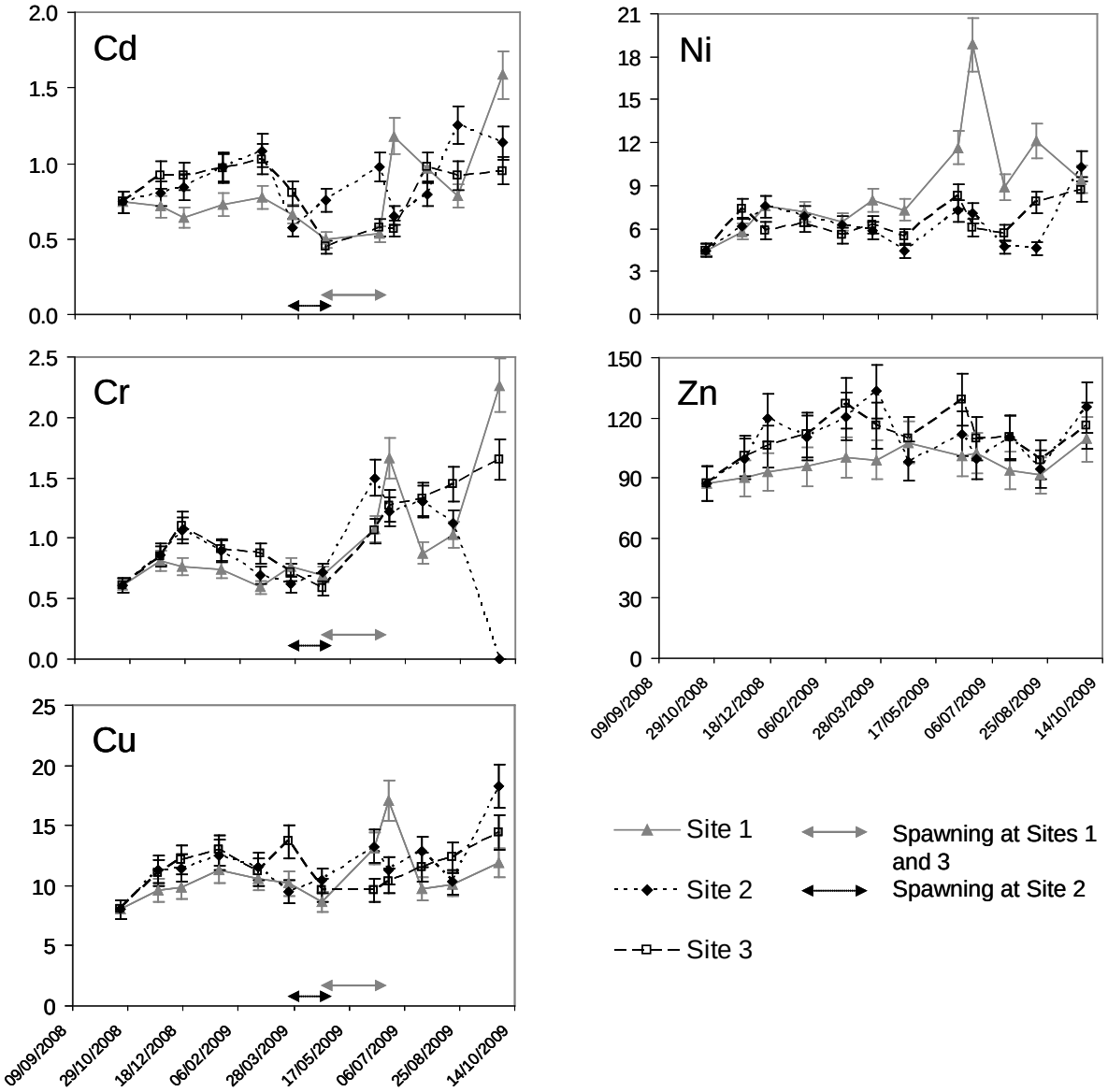

459

460 Figure 3: Metal concentrations in mussels (µg.g $_{\text{dry wt}}^{-1}$) over the 11-month exposure at Site 1 (Marnay-
461 sur-Seine), Site 2 (Bougival) and Site 3 (Triel-sur-Seine), and spawning period as indicated by a
462 decreased condition index.

463

464

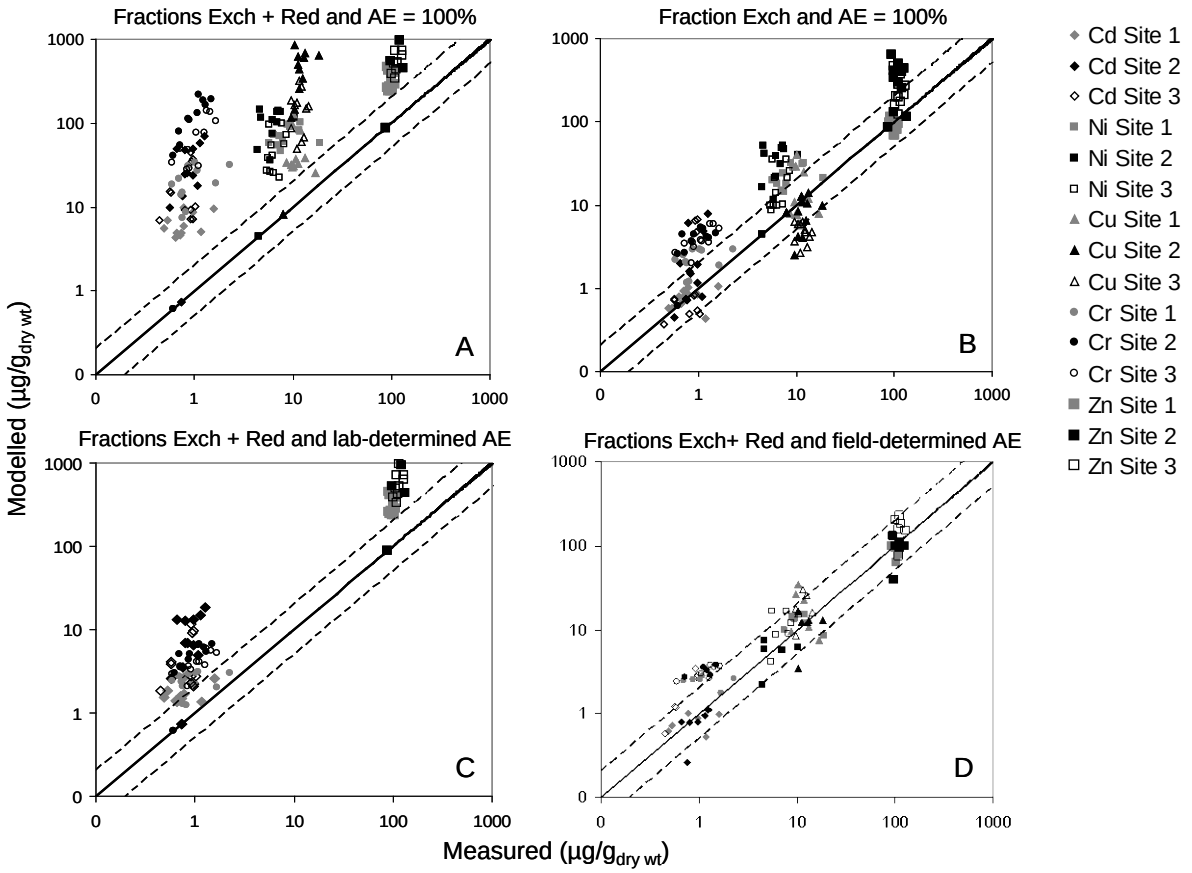

Figure 14: Measured and modeled metal concentrations in mussel tissues ($\mu g.g_{dry\ wt}^{-1}$) as a function of assimilation efficiency (AE) and concentration of particulate metals. The concentration of particulate metals is equal to the metal concentration measured in the different fractions of the chemical sequential extraction (Exchangeable: Exch., Reducible: Red). The assimilation efficiencies are 100%, the laboratory-determined AE from the literature or the field-determined AE from *in situ* data. The solid line represents a 1:1 ratio and the broken lines correspond to a deviation of 2 above or below this line.

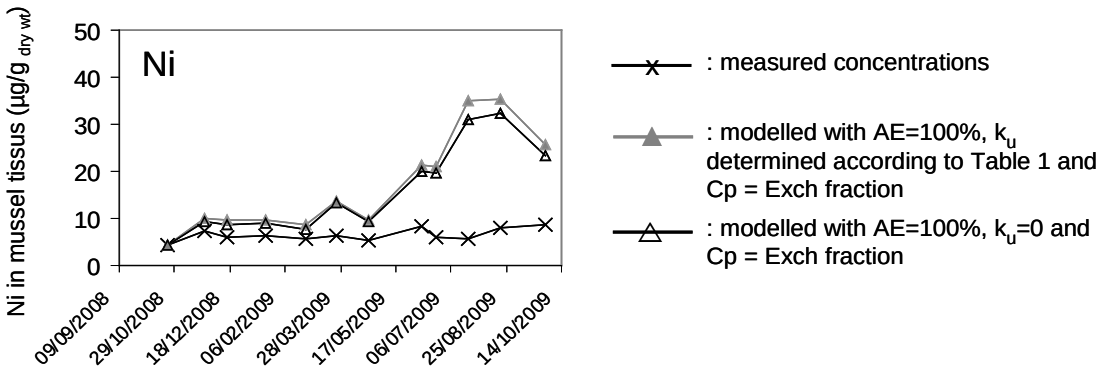

473

474 Figure 5: Measured and modelled Ni concentration in mussel tissue over the exposure at Site 3 ($\mu g.g^{-1}$)

475 and effect of the absence of dissolved route on the modelled values.

476

477

478

479

Literature Cited

Ahlf, W., Drost, W. and Heise, S. 2009. Incorporation of metal bioavailability into regulatory frameworks-metal exposure in water and sediment. Journal of Soils and Sediments 9(5):411-419.

Arifin, Z. and Bendell-Young, L.I. 1997. Feeding response and carbon assimilation by the blue mussel *Mytilus trossulus* exposed to environmentally relevant seston matrices. Marine Ecology Progress Series 160:241-253.

Arifin, Z. and Bendell-Young, L.I. 2000. Influence of a selective feeding behaviour by the blue mussel *Mytilus trossulus* on the assimilation of ^{109}Cd from environmentally relevant seston matrices. Marine Ecology Progress Series 192:181-193.

Bervoets, L., Voets, J., Chu, S., Covaci, A., Schepens, P. and Blust, R. 2004. Comparison of accumulation of micropollutants between indigenous and transplanted zebra mussels (*Dreissena polymorpha*). Environmental Toxicology and Chemistry 23(8):1973-1983.

Bourgeault, A. 2010. Bioaccumulation par Dreissena polymorpha: quel reflet de la contamination chimique du milieu ? Expérimentation - Observation - Modélisation. PhD dissertation. Paris, France: Université Pierre et Marie Curie

Bourgeault, A., Gourlay-Francé, C. and Tusseau-Vuillemin, M.H. 2010a. Modeling the effect of water chemistry on the bioaccumulation of waterborne Cd in zebra mussels. Environmental Toxicology and Chemistry 29(10):2182-2189.

Bourgeault, A., Gourlay-Francé, C., Vincent-Hubert, F., Palais, F., Geffard, A., Biagianti-Risbourg, S., Pain-Devin, S. and Tusseau-Vuillemin, M.-H. 2010b. Lessons from a transplantation of zebra mussels into a small urban river: An integrated ecotoxicological assessment Environmental Toxicology 25(5):468-478.

Bryan, G.W. and Langston, W.J. 1992. Bioavailability, accumulation and effects of heavy metals in sediments with special reference to United Kingdom estuaries. Environmental Pollution 76(2):89-131.

Camusso, M., Balestrini, R. and Binelli, A. 2001. Use of zebra mussel (*Dreissena polymorpha*) to assess trace metal contamination in the largest Italian subalpine lakes. Chemosphere 44(2):263-270.

Casado-Martinez, M.C., Smith, B.D., DelValls, T.A., Luoma, S.N. and Rainbow, P.S. 2009. Biodynamic modelling and the prediction of accumulated trace metal concentrations in the polychaete Arenicola marina. Environmental Pollution 157(10):2743-2750.

Davison, W. and Zhang, H. 1994. In situ speciation measurements of trace components in natural waters using thin-film gels. Nature 367(6463):546-548.

De Jonge, M., Blust, R. and Bervoets, L. 2010. The relation between Acid Volatile Sulfides (AVS) and metal accumulation in aquatic invertebrates: Implications of feeding behavior and ecology. Environmental Pollution 158(5):1381-1391.

De Lafontaine, Y., Gagné, F., Blaise, C., Costan, G., Gagnon, P. and Chan, H.M. 2000. Biomarkers in zebra mussels (*Dreissena polymorpha*) for the assessment and monitoring of water quality of the St Lawrence River (Canada). Aquatic Toxicology 50(1-2):51-71.

Di Toro, D.M., Mahony, J.D., Hansen, D.J., Scott, K.J., Carlson, A.R. and Ankley, G.T. 1992. Acid volatile sulfide predicts the acute toxicity of cadmium and nickel in sediments. Environmental Science and Technology 26(1):96-101.

Fan, W. and Wang, W.X. 2003. Extraction of spiked metals from contaminated coastal sediments: A comparison of different methods. Environ Toxicol Chem 22(11):2659-2666.

Ferreira, D., Tousset, N., Ridame, C. and Tusseau-Vuillemin, M.H. 2008. More than inorganic copper is bioavailable to aquatic mosses at environmentally relevant concentrations. Environmental Toxicology and Chemistry 27(10):2108-2116.

Galstoff, P.S. 1928. Experimental study of the function of the oyster gills and its bearing on the problems of oyster culture, and sanitary control of the oyster industry. Bulletin U.S. Bur. Fish. 44:1-39.

Griscom, S.B. and Fisher, N.S. 2004. Bioavailability of sediment-bound metals to marine bivalve molluscs: An overview. Estuaries 27(5):826-838.

Griscom, S.B., Fisher, N.S. and Luoma, S.N. 2000. Geochemical influences on assimilation of sediment-bound metals in clams and mussels. Environmental Science and Technology 34(1):91-99.

Kryger, J. and Riisgard, H.U. 1988. Filtration rate capacities in 6 species of European freshwater bivalves. Oecologia 77(1):34-38.

Larner, B.L., Palmer, A.S., Seen, A.J. and Townsend, A.T. 2008. A comparison of an optimised sequential extraction procedure and dilute acid leaching of elements in anoxic sediments, including the effects of oxidation on sediment metal partitioning. Analytica Chimica Acta 608(2):147-157.

Luoma, S.N. 1989. Can we determine the biological availability of sediment-bound trace elements? Hydrobiologia 176-177:379-396.

Luoma, S.N. and Rainbow, P.S. 2005. Why Is Metal Bioaccumulation So Variable? Biodynamics as a Unifying Concept. Environmental Science and Technology 39(7):1921-1931.

Mayer, L.M., Chen, Z., Findlay, R.H., Fang, J., Sampson, S., Self, R.F.L., Jumars, P.A., Quetel, C. and Donard, O.F.X. 1996. Bioavailability of sedimentary contaminants subject to deposit-feeder digestion. Environmental Science and Technology 30(8):2641-2645.

Mersch, J., Morhain, E. and Mouvet, C. 1993. Laboratory accumulation and depuration of copper and cadmium in the freshwater mussel *Dreissena polymorpha* and the aquatic moss *Rhynchostegium riparioides*. Chemosphere 27(8):1475-1485.

Meybeck, M., Lestel, L., Bonté, P., Moilleron, R., Colin, J.L., Rousselot, O., Hervé, D., de Pontevès, C., Grosbois, C. and Thévenot, D.R. 2007. Historical perspective of heavy metals contamination (Cd, Cr, Cu, Hg, Pb, Zn) in the Seine River basin (France) following a DPSIR approach (1950-2005). Science of the Total Environment 375(1-3):204-231.

Pan, K. and Wang, W.X. 2008. Validation of biokinetic model of metals in the scallop *Chlamys nobilis* in complex field environments. Environmental Science & Technology 42(16):6285-6290.

Phillips, D.J.H. 1980. Quantitative Aquatic Biological Indicators: Their Use to Monitor Trace Metal and Organochlorine Pollution. London: Applied Science Publishers Ltd.

Priadi, C., Ayrault, S., Pacini, S. and Bonte, P. In press. Urbanization impact of the Greater Paris Region on metal mobility in suspended sediments in the Seine River, France: Role of iron oxides International Journal of environmental Science and Technology.

Priadi, C., Bourgeault, A., Uher, E., Ayrault, S., Gourlay-Francé, C., Tusseau-Vuillemin, M.-H., Bonté, P. and Mouchel, J.M. submitted. Time-integrated metal partitioning using sediment traps and DGT samplers versus discrete metal partitioning: Comparison of spatial and temporal variability in an urban river. Journal of Environmental Monitoring.

Pueyo, M., Rauret, G., Lück, D., Yli-Halla, M., Muntau, H., Quevauviller, P. and Lopez-Sanchez, J.F. 2001. Certification of the extractable contents of Cd, Cr, Cu, Ni, Pb and Zn in a freshwater sediment following a collaboratively tested and optimised three-step sequential extraction procedure. Journal of Environmental Monitoring 3(2):243-250.

Reeders, H.H. and Bij de Vaate, A. 1990. Zebra mussels (*Dreissena polymorpha*): a new perspective for water quality management. Hydrobiologia 200-201(1):437-450.

Reeders, H.H., Bij De Vaate, A. and Slim, F.J. 1989. The filtration rate of *Dreissena polymorpha* (Bivalvia) in three Dutch lakes with reference to biological water quality management. Freshwater Biology 22(1):133-141.

Roditi, H.A. and Fisher, N.S. 1999. Rates and routes of trace element uptake in zebra mussels. Limnology and Oceanography 44(7):1730-1749.

Roditi, H.A., Fisher, N.S. and Sañudo-Wilhelmy, S.A. 2000. Field testing a metal bioaccumulation model for zebra mussels. Environmental Science and Technology 34(13):2817-2825.

Stecko, J.R.P. and Bendell-Young, L.I. 2000. Uptake of ^{109}Cd from sediments by the bivalves *Macoma balthica* and *Protothaca staminea*. Aquatic Toxicology 47(3-4):147-159.

Tusseau-Vuillemin, M.H., Gilbin, R., Bakkaus, E. and Garric, J. 2004. Performance of diffusion gradient in thin films to evaluate the toxic fraction of copper to *Daphnia magna*. Environmental Toxicology and Chemistry 23(9):2154-2161.

581 Tusseau-Vuillemin, M.H., Gourlay, C., Lorgeoux, C., Mouchel, J.M., Buzier, R., Gilbin, R., Seidel, J.L.
582 and Elbaz-Poulichet, F. 2007. Dissolved and bioavailable contaminants in the Seine river basin.
583 Science of the Total Environment 375(1-3):244-256.
584 Voets, J., Talloen, W., de Tender, T., van Dongen, S., Covaci, A., Blust, R. and Bervoets, L. 2006.
585 Microcontaminant accumulation, physiological condition and bilateral asymmetry in zebra mussels
586 (*Dreissena polymorpha*) from clean and contaminated surface waters. Aquatic Toxicology
587 79(3):213-225.
588 Wang, W.-X. and Fisher, N.S. 1998. Assimilation efficiencies of chemicals contaminants in aquatic
589 invertebrates: a synthesis. Environmental Toxicology and Chemistry 18(8):2034-2045.
590 Wang, W.X., Fisher, N.S. and Luoma, S.N. 1996. Kinetic determinations of trace element
591 bioaccumulation in the mussel *Mytilus edulis*. Marine Ecology Progress Series 140(1-3):91-113.
592 Wang, W.X., Yan, Q.L., Fan, W. and Xu, Y. 2002. Bioavailability of sedimentary metals from a
593 contaminated bay. Mar Ecol Prog Ser 240:27-38.
594 Zaroogian, G.E. and Johnson, M. 1984. Nickel uptake and loss in the bivalves *Crassostrea virginica* and
595 *Mytilus edulis*. Archives of Environmental Contamination and Toxicology 13(4):411-418.
596
597

Annexe 3

Information supplementaire du papier en cours de préparation pour une soumission à « *Aquatic Toxicology* »

« Bioavailability of particulate metal to zebra mussels: Biodynamic modeling shows that assimilation efficiencies are site-specific »

In situ bioavailability of particulate metals to zebra mussels: need for site-specific assimilation efficiencies in biodynamic modeling

Bourgeault Adeline, Gourlay-Francé Catherine, Priadi Cindy, Ayrault Sophie, and Tusseau-Vuillemin Marie-Hélène

Number of pages: 8

Number of Figures: 4

Number of Tables: 2

Table A.1: Concentrations of labile[a] and particulate[b] metals over the 11-month exposure at Marnay (Site 1), Bougival (Site 2) and Triel (Site 3).

An asterisk (*) indicates that the values were extrapolated as explained in the materials and methods section.

Date	Cd		Cr		Cu		Ni		Zn	
	labile (DGT) ($\mu g.L^{-1}$)	sediment trap ($\mu g.g^{-1}$) Exch+Red	labile (DGT) ($\mu g.L^{-1}$)	sediment trap ($\mu g.g^{-1}$) Exch+Red	labile (DGT) ($\mu g.L^{-1}$)	sediment trap ($\mu g.g^{-1}$) Exch+Red	labile (DGT) ($\mu g.L^{-1}$)	sediment trap ($\mu g.g^{-1}$) Exch+Red	labile (DGT) ($\mu g.L^{-1}$)	sediment trap ($\mu g.g^{-1}$) Exch+Red
Marnay (Site 1)										
25.11.08	0.0007 ± 0.0002	0.32*	0.0184 ± 0.0025	0.63*	0.0615 ± 0.0117	2.55*	0.1537 ± 0.0155	4.86*	0.4443 ± 0.0794	54.38*
16.12.08	0.0014 ± 0.0006	0.21*	0.0180 ± 0.0021	0.27*	0.0751 ± 0.0075	2.30*	0.2049 ± 0.0171	2.21*	1.4880 ± 0.3041	32.87*
19.01.09	0.0010 ± 0.0007	0.21	0.0352 ± 0.0062	1.03	0.0655 ± 0.0063	2.42	0.2021 ± 0.0274	3.64	0.9879 ± 0.6036	40.40
24.02.09	0.0012 ± 0.0001	0.22	0.0250 ± 0.0020	0.84	0.0748 ± 0.0077	2.24	0.2088 ± 0.0154	4.24	0.8363 ± 0.2054	48.53
24.03.09	0.0009 ± 0.0001	0.24	0.0249 ± 0.0038	0.80	0.0736 ± 0.0059	2.57	0.1949 ± 0.0178	4.41	0.1593 ± 0.2726	41.11
22.04.09	0.0004 ± 0.0004	0.25	0.0333 ± 0.0110	1.43	0.0970 ± 0.0096	2.45	0.2120 ± 0.0356	4.77	0.7561 ± 0.3556	52.91
09.06.09	0.0009 ± 0.0003	0.23	0.0214 ± 0.0033	1.13	0.0907 ± 0.0197	2.32	0.1730 ± 0.0370	4.44	0.6933 ± 0.1770	47.76
22.06.09	0.0011 ± 0.0005	0.20*	<QL ± 0.0000	1.06*	0.0852 ± 0.0086	2.08	0.1959 ± 0.0227	4.43	0.0000 ± 0.0000	53.07
22.07.09	0.0004 ± 0.0001	0.26	0.0178 ± 0.0027	0.93	0.0581 ± 0.0098	7.26	0.0954 ± 0.0082	4.23	0.3653 ± 0.2242	52.50
19.08.09	0.0006 ± 0.0001	0.29	0.0196 ± 0.0026	1.11	0.1038 ± 0.0123	7.68	0.1350 ± 0.0184	4.24	0.2743 ± 0.0185	55.47
24.09.09	0.0006 ± 0.0000	0.22*	0.0167 ± 0.0041	1.15*	0.0730 ± 0.0055	2.39*	0.1164 ± 0.0076	4.39*	0.1149 ± 0.0942	52.06*
Bougival (Site 2)										
25.11.08	0.0041 ± 0.0006	1.57*	0.0574 ± 0.0248	7.47*	0.2663 ± 0.0435	37.77*	0.3686 ± 0.0287	7.56*	2.6357 ± 0.3660	288.07*
16.12.08	0.0051 ± 0.0009	0.65*	0.0926 ± 0.0131	6.67*	0.2590 ± 0.0469	16.70*	0.4456 ± 0.0353	8.89*	3.1303 ± 0.4687	236.65*
19.01.09	0.0021 ± 0.0003	1.73	0.0270 ± 0.0060	7.93	0.1716 ± 0.0125	36.82	0.2971 ± 0.0523	8.47	1.7871 ± 0.3823	305.30
24.02.09	0.0022 ± 0.0002	1.38	0.0583 ± 0.0304	7.11	0.2181 ± 0.0760	42.79	0.3215 ± 0.0582	9.88	2.4681 ± 0.5169	325.97
24.03.09	0.0031 ± 0.0028	1.47	0.0353 ± 0.0033	7.23	0.1408 ± 0.0568	27.69	0.2284 ± 0.0982	8.45	0.4016 ± 0.7782	237.97
22.04.09	0.0016 ± 0.0006	1.80	0.0291 ± 0.0081	8.14	0.1649 ± 0.0290	27.55	0.1769 ± 0.0411	8.55	0.3518 ± 0.1285	247.44
09.06.09	0.0022 ± 0.0008	2.31	0.0244 ± 0.0065	10.06	0.1867 ± 0.0696	46.95	0.1846 ± 0.1641	8.10	1.5101 ± 0.8240	325.66
22.06.09	0.0041 ± 0.0028	1.48*	0.0024 ± 0.0035	6.57*	0.2981 ± 0.0485	24.69*	0.3244 ± 0.0534	6.01*	2.0656 ± 0.3286	239.23*
22.07.09	0.0054 ± 0.0009	2.90	0.0323 ± 0.0054	10.56	0.3864 ± 0.0328	61.22	0.4699 ± 0.0656	8.58	2.4936 ± 0.3778	377.07
19.08.09	0.0028 ± 0.0005	2.83	0.0277 ± 0.0033	9.33	0.2532 ± 0.0481	60.56	0.3210 ± 0.0857	7.50	1.6872 ± 0.8048	340.36
24.09.09	0.0066 ± 0.0024	2.88*	0.0211 ± 0.0024	9.43*	0.4257 ± 0.0726	53.95*	0.4194 ± 0.0478	8.70*	1.8259 ± 0.3294	362.45*
Triel (Site 3)										
25.11.08	0.0022 ± 0.0010	1.51*	0.0314 ± 0.0112	6.48*	0.1511 ± 0.0640	12.23*	0.1716 ± 0.1870	4.97*	1.4578 ± 0.7045	230.91*
16.12.08	0.0051 ± 0.0017	0.98*	0.0857 ± 0.0081	2.00*	0.2511 ±	9.04*	0.5448 ± 0.0412	3.40*	3.5673 ± 0.3334	157.00
19.01.09	0.0036 ± 0.0005	0.70	0.0284 ± 0.0035	4.81	0.1743 ± 0.0139	18.40	0.4651 ± 0.0440	5.37	2.7852 ± 0.4558	162.62
24.02.09	0.0027 ± 0.0004	1.42	0.0452 ± 0.0111	7.74	0.2095 ± 0.0158	38.89	0.4506 ± 0.0308	6.73	3.7381 ± 0.2701	277.20
24.03.09	0.0050 ± 0.0026	0.80	0.0415 ± 0.0144	6.02	0.2167 ± 0.0545	19.98	0.4265 ± 0.0927	6.30	1.4446 ± 0.2907	141.56
22.04.09	0.0021 ± 0.0009	1.52	0.0372 ± 0.0101	7.20	0.2406 ± 0.0707	24.58	0.4431 ± 0.1258	7.23	1.5454 ± 0.4717	192.39
09.06.09	0.0032 ± 0.0003	1.62	0.0243 ± 0.0031	10.02	0.2798 ± 0.0229	31.34	0.5783 ± 0.0451	8.06	2.8858 ± 0.2618	257.41
22.06.09	0.0045 ± 0.0005	1.65*	0.0083 ± 0.0069	8.73*	0.3004 ± 0.0216	14.11*	0.5425 ± 0.0446	7.33*	2.6829 ± 0.2066	246.19*
22.07.09	0.0051 ± 0.0004	2.90	0.0314 ± 0.0047	9.28	0.3878 ± 0.0299	31.97	0.7516 ± 0.0564	7.26	3.0716 ± 0.2291	260.48
19.08.09	0.0043 ± 0.0006	2.83	0.0256 ± 0.0026	6.77	0.3336 ± 0.0373	17.60	0.5643 ± 0.0534	7.68	2.4158 ± 0.1857	274.26
24.09.09	0.0050 ± 0.0007	1.14*	0.0319 ± 0.0165	8.61*	0.3628 ± 0.0444	14.78*	0.6810 ± 0.0707	8.10*	2.3656 ± 0.3861	253.71*

Table A.2: Percentage of metals in the exchangeable and the reducible fractions of total suspended solids (TSS) collected with sediment traps [1]. Mean over the exposure ± SD.

	Site 1	Site 2	Site 3
Cd	82 ± 6%	88 ± 1%	88 ± 6%
Cr	7 ± 1%	25 ± 2%	28 ± 5%
Zn	64 ± 5%	84 ± 1%	84 ± 4%
Ni	40 ± 4%	45 ± 3%	45 ± 5%
Cu	21 ± 12%	39 ± 3%	41 ± 9%

(1) Priadi, C.; Ayrault, S.; Pacini, S.; Bonte, P., Urbanization impact of the Greater Paris Region on metal mobility in suspended sediments in the Seine River, France: Role of iron oxides *International Journal of Environmental Science and Technology* **In press**.

Figures

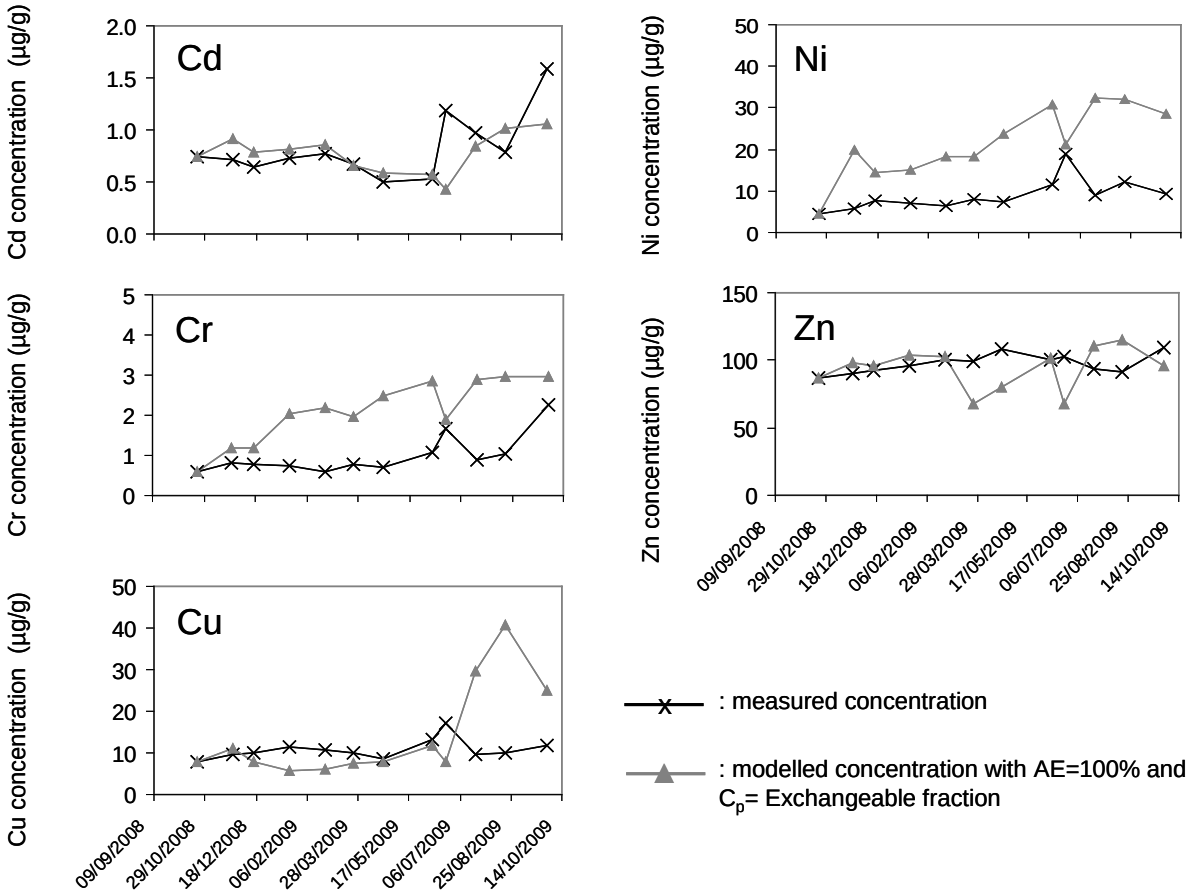

Figure A.1: Measured and modeled metal concentrations in mussel tissue ($\mu g.g_{dry\ wt}^{-1}$) at Site 1 with AE=100% and the metal contamination being considered as the concentration measured in the exchangeable fraction.

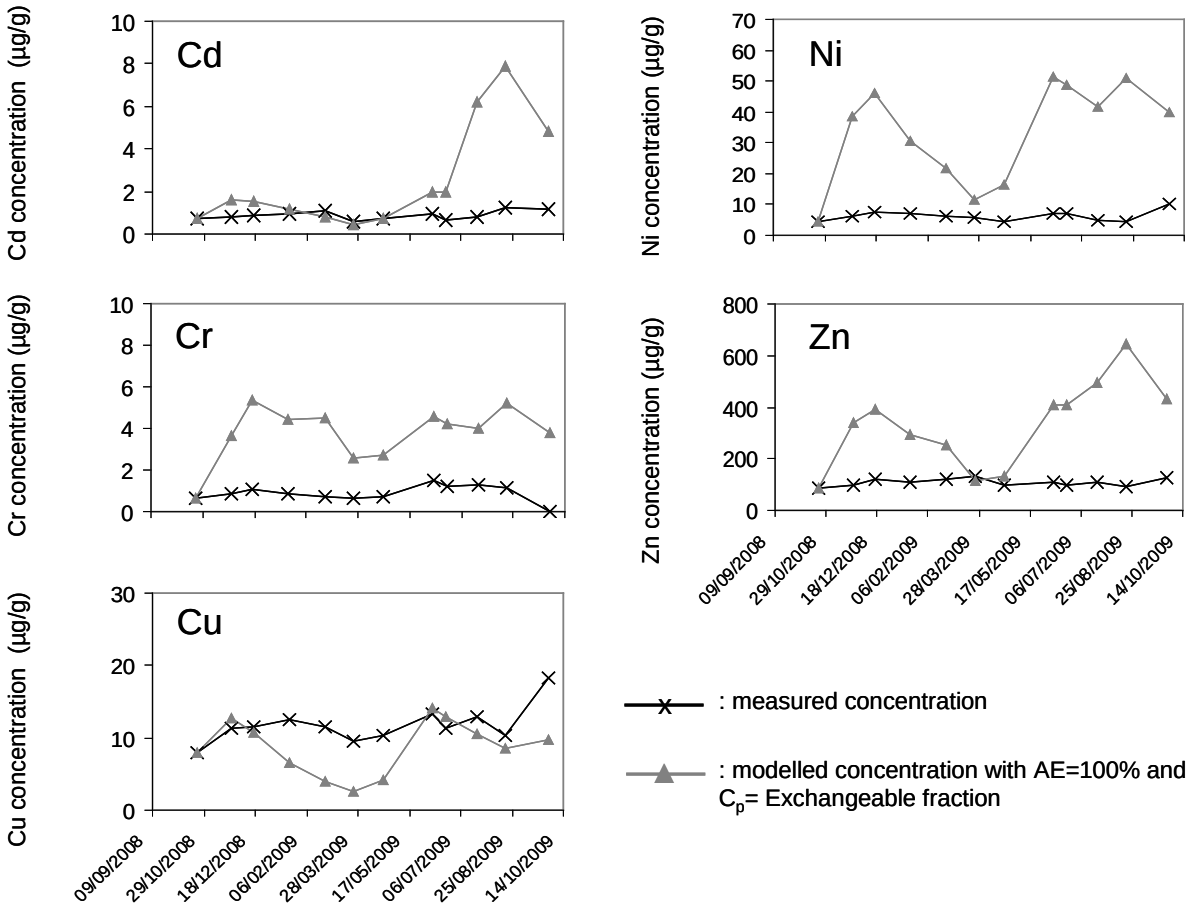

Figure A.2: Measured and modeled metal concentrations in mussel tissue ($\mu g.g_{dry\ wt}^{-1}$) at Site 2 with AE=100% and the metal contamination being considered as the concentration measured in the exchangeable fraction.

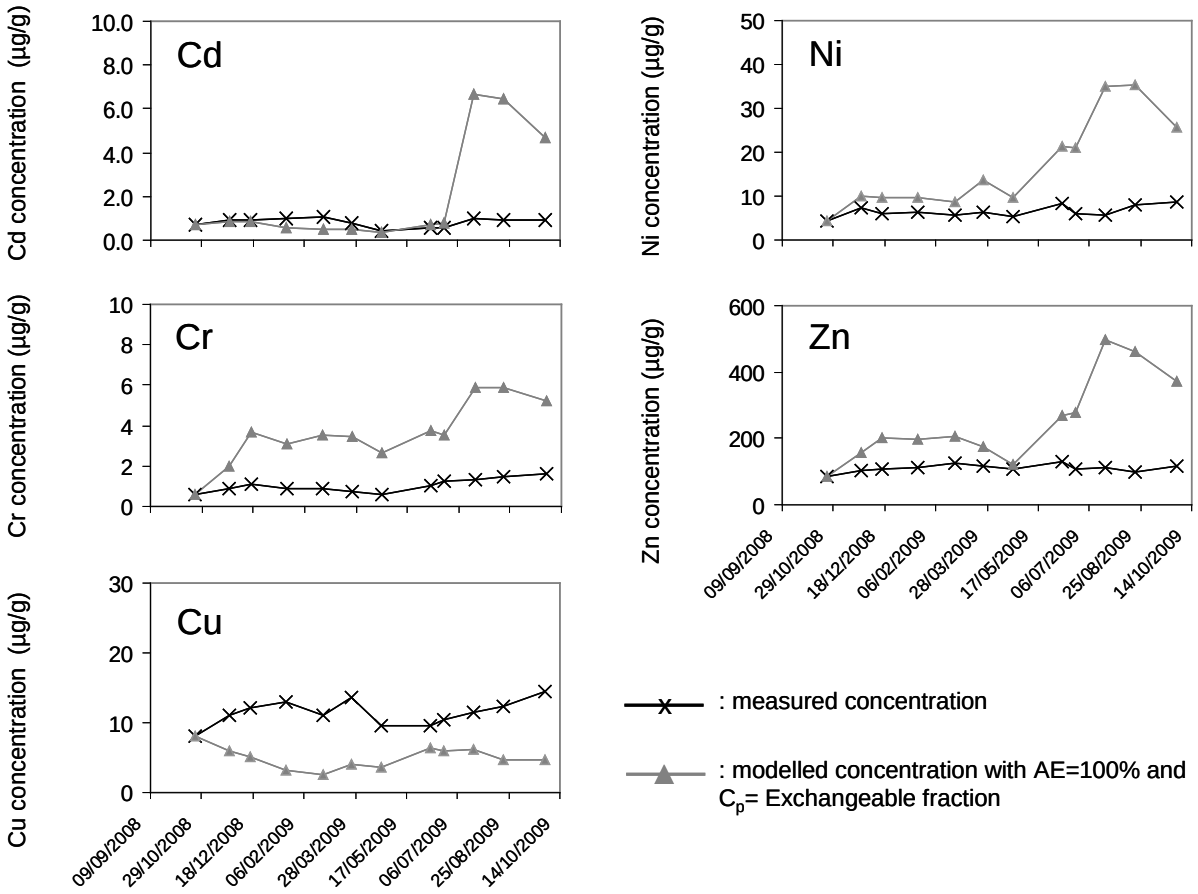

Figure A.3: Measured and modeled metal concentrations in mussel tissue ($\mu g.g_{dry\ wt}^{-1}$) at Site 3 with AE=100% and the metal contamination being considered as the concentration measured in the exchangeable fraction.

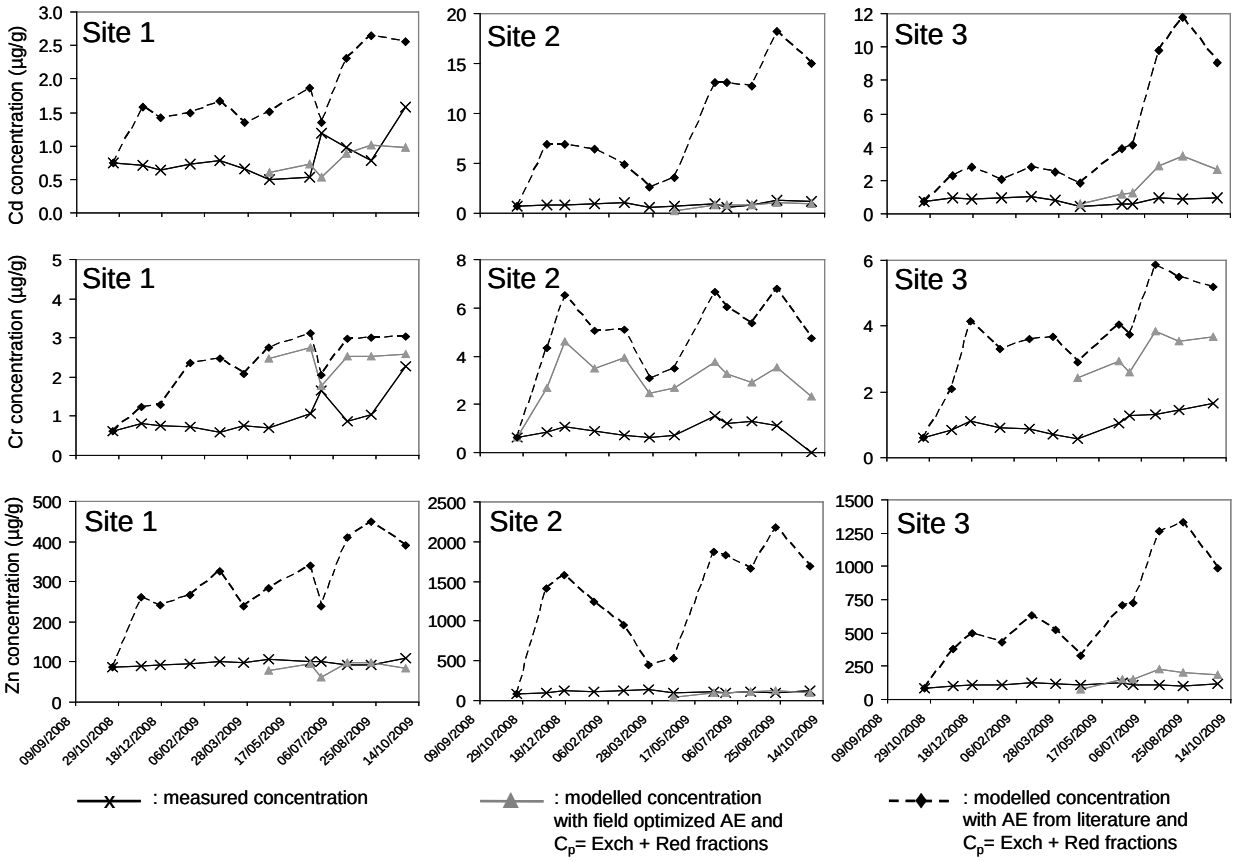

Figure A.4: Measured and modeled metal concentrations in mussel tissue ($\mu g.g_{dry\ wt}^{-1}$) with AE from the literature or from optimization of field data.

Resolution of the first order differential equation

The biodynamic differential equation is :

$$\frac{dC_m}{dt} = k_u \cdot C_w + AE \cdot IR \cdot C_f - (k_e + g) \cdot C_m \qquad \text{Eq. (A.1)}$$

It can be re-written as

$$\frac{dC_m}{dt} + (k_e + g) \cdot C_m = (k_e + g) \cdot C_{m\_ss} \qquad \text{Eq. (A.2)}$$

with $C_{m\_ss} = \frac{k_u \cdot C_w + AE \cdot IR \cdot C_f}{k_e + g}$ Eq. (A.3)

Since C_w and C_f are monthly-average concentrations, they are constant between two time-steps. Hence, between t_{i-1} and t_i, C_{m_ss} is a constant.

The generic solution of a differential equation of the $y'+ay=b$ type is $y = \alpha \cdot e^{-ax} + \frac{b}{a}$

Hence, between t_{i-1} and t_i, where C_{m-ss} is a constant, the solution of Equation (3) is:

$$C_m(t) = \alpha \cdot e^{-(k_e+g)t} + C_{m\_ss} \qquad \text{Eq. (A.4)}$$

At time t_{i-1} the concentration in mussels is given by

$$C_m(t_{i-1}) = \alpha \cdot e^{-(k_e+g)t_{i-1}} + C_{m\_ss} \qquad \text{Eq. (A.5)}$$

This enables the expression of α as a function of C_{m-ss} and $C_m(t_{i-1})$

$$\alpha \cdot = \frac{C_m(t_{i-1}) - C_{m\_ss}}{e^{-(k_e+g)t_{i-1}}} \qquad \text{Eq. (A.6)}$$

With a combination of Equation 5 and Equation 7, $C_m(t_i)$ can be expressed as

$$C_m(t) = \frac{C_m(t_{i-1}) - C_{m\_ss}}{e^{-(k_e+g)t_{i-1}}} \cdot e^{-(k_e+g)t} + C_{m\_ss} \qquad \text{Eq. (A.7)}$$

$$C_m(t_i) = (C_m(t_{i-1}) - C_{m\_ss}) \cdot e^{-(k_e+g)\cdot(t_i - t_{i-1})} + C_{m\_ss} \qquad \text{Eq. (A.8)}$$

Finally,

$$C_m(t_i) = C_m(t_{i-1}) \cdot e^{-(k_e+g)\cdot(t_i - t_{i-1})} + C_{m\_ss} \cdot (1 - e^{-(k_e+g)\cdot(t_i - t_{i-1})}) \qquad \text{Eq. (A.9)}$$

Annexe 4

Information supplementaire du Chapitre II

Méthodologie de la digestion chimique total de sédiment

S1: Sediment digestion protocol

SPM was digested completely during 3-4 weeks using various acids at different temperatures. The complete discrete SPM samples+filter (MF-Millipore cellulose ester filters) and 0.1 g of time-integrated SPM from sediment trap were digested in Teflon vessels under laminar flow hood using a heating block (Digiprep, SCP Science) using 3 solutions:

1. The first attack uses 15 mL *aqua regia* (HNO_3 65%: HCl 30%, 3:1) for 3 days at room temperature (vessel capped). Excess nitrogen dioxide was then evaporated at 90°C for 2 hours. This step assured the dissolution of Ca and Mg, abundant in the Seine River. Remaining liquid in vessels were pipetted (VWR, low density polyethylene) into a disposable tube (Falcon, polypropylene) and carefully avoiding pipetting the sediment. The remaining sediment was rinsed with 10 mL 0.5 N HNO_3 This was performed 3 times to ensure the evacuation of Ca and Mg, previously dissolved by *aqua regia*, and avoid re-precipitation of Ca and Mg fluorides in HF solution.
2. Digestion continued with 10 mL of a HF(48.9%) : HNO_3 (65%) mixture (1:1) to attack siliceous minerals during 24h at room temperature (vessels capped). Sample was then evaporated to near dryness at 100°C to eliminate hexafluorosilicic acid (3-5 days).
3. The solid residue was then attacked with 12 mL of a HNO_3 65% : $HClO_4$ 69- 72% (1:1) mixture heated at 120°C during 5 days (vessels capped). This step is aimed to oxidize organic matter. Final solutions were again evaporated to near dryness to eliminate perchloric acid. Pipetted solution recovered in separate tubes during the first step using *aqua regia* were re-introduced to the Teflon vessels and were again evaporated near to dryness. Afterwards, 1 mL 618 of 65% HNO_3 was added to the remaining solution and evaporated to near dryness. This step was repeated three times to ensure minimal residue of chloride ions. The solutions were then brought into a 50 mL 0.5 N HNO_3 solution for ICP-MS analysis. This method was adopted for total SPM digestion of the highly carbonated SPM of Seine River. All solutions were made from ultrapure reagents to minimize contamination (HNO_3 and HCl Normatom grade, VWR France, and HF and $HClO_4$ "for trace metal analyses", Baker, from Sodipro France). For each digestion, 0.1 g of a certified lake sediment reference material was also digested (SL1, International Atomic Energy Agency IAEA).

Annexe 5

Information supplementaire du Chapitre II

Données physico-chimique du campagne de projet Medisis

Date	[SPM] (mg/L)	Flowrate (m^3/s)	Conductivity (µS/cm)	dissolved oxygen (mg/L)	POC (mg/L)	DOC (mg/L)
Marnay						
22.10.08	4,0	59	395	nm	0,42	2,68
25.11.08	9,5	49	474	nm	0,61	1,83
16.12.08	33,4	73	495	nm	1,90	1,94
19.01.09	20,2	37	485	nm	1,20	1,62
24.02.09	19,4	89	nm	nm	0,88	1,95
24.03.09	10,8	50	509	nm	0,56	1,75
22.04.09	20,4	34	516	nm	0,90	2,57
09.06.09	7,0	27	490	nm	0,45	2,16
22.06.09	5,9	25	526	nm	0,05	2,05
22.07.09	11,4	54	402	nm	0,42	2,23
19.08.09	4,4	47	364	nm	0,29	1,73
24.09.09	5,7	52	268	nm	1,23	2,44
22.10.09	4,7	50	350	nm	0,34	2,38
Bougival						
22.10.08	10,9	187	446	9,5	0,88	2,94
25.11.08	11,1	221	490	10,5	0,94	2,79
16.12.08	44,1	295	501	12,2	1,06	3,51
19.01.09	21,2	215	557	12,8	3,92	2,77
24.02.09	15,7	324	nm	11,8	1,03	2,77
24.03.09	9,3	212	570	11,3	0,89	2,69
22.04.09	7,7	184	611	8,9	0,66	3,00
09.06.09	16,8	167	606	6,3	1,61	4,34
22.06.09	6,4	116	609	5,1	0,73	3,21
22.07.09	10,9	148	550	6,8	0,55	3,25
19.08.09	7,9	97	527	6,8	0,69	3,73
24.09.09	9,7	92	474	7,4	0,38	2,56
22.10.09	8,5	112	498	8,0	0,69	2,64
Triel						
22.10.08	7,8	334	538	7,5	0,04	4,16
25.11.08	4,1	391	506	9,1	0,72	3,87
16.12.08	14,1	495	513	12,5	0,93	4,14
19.01.09	14,3	383	612	12,1	2,47	3,97
24.02.09	21,9	550	nm	12,7	1,46	3,42
24.03.09	10,2	384	619	10,0	0,97	3,72
22.04.09	9,8	340	655	8,0	0,88	3,77
09.06.09	11,9	375	668	6,0	1,16	5,45
22.06.09	6,9	228	668	6,0	0,67	3,63
22.07.09	11,6	209	655	5,8	1,08	3,96
19.08.09	9,7	211	604	6,1	0,73	3,54
24.09.09	8,8	198	619	5,9	0,50	3,84
22.10.09	4,8	225	625	6,1	0,89	3,93

nm = non measured
<QL = lower than quantification limit

Date	Temperature (°C)	Chlorophyll (µg/L)	pH	Alcalinity (mg/L)	Sodium (mg/L)	Ammonium (mg/L)
Marnay						
22.10.08	11,20	0,50	8,14	226	20,3	0,6
25.11.08	6,50	0,70	8,28	287	7,9	<QL
16.12.08	5,60	nm	8,30	287	5,8	<QL
19.01.09	6,00	1,40	8,32	262	9,0	<QL
24.02.09	7,20	2,00	8,19	262	2,5	0,3
24.03.09	8,00	3,50	8,15	250	7,5	<QL
22.04.09	14,90	2,10	8,14	244	12,1	1,4
09.06.09	16,40	0,70	8,18	226	7,7	<QL
22.06.09	19,00	0,60	8,23	232	10,8	<QL
22.07.09	21,70	nm	8,06	195	6,2	<QL
19.08.09	23,00	1,24	8,30	171	5,7	<QL
24.09.09	16,40	1,02	8,07	153	9,0	<QL
22.10.09	nm	nm	8,13	nm	6,4	<QL
Bougival						
22.10.08	14,40	1,10	7,88	226	6,7	<QL
25.11.08	9,03	0,40	8,07	268	13,6	0,4
16.12.08	5,10	nm	8,24	281	9,9	0,1
19.01.09	4,50	9,50	7,76	256	16,9	<QL
24.02.09	7,00	3,30	8,11	268	8,6	0,1
24.03.09	10,40	6,60	8,09	250	12,6	<QL
22.04.09	16,00	3,70	7,91	250	14,5	0,8
09.06.09	19,80	2,10	7,20	238	16,1	2,9
22.06.09	20,70	3,20	7,71	232	16,3	0,5
22.07.09	22,80	11,36	7,77	220	14,9	<QL
19.08.09	20,30	15,05	7,93	182	16,1	<QL
24.09.09	19,50	5,64	7,71	207	17,7	<QL
22.10.09	nm	nm	8,10	nm	14,9	<QL
Triel						
22.10.08	13,90	0,90	7,59	250	13,6	0,3
25.11.08	8,90	0,30	7,83	281	16,1	1,3
16.12.08	5,20	nm	8,01	281	10,9	0,5
19.01.09	4,90	10,00	7,10	262	22,7	<QL
24.02.09	6,90	2,10	7,93	268	10,4	0,5
24.03.09	10,20	5,10	7,93	256	15,3	<QL
22.04.09	15,40	2,10	7,73	256	17,6	1,8
09.06.09	19,00	2,00	7,55	250	20,6	4,3
22.06.09	20,10	2,50	7,61	238	19,5	0,4
22.07.09	22,00	12,64	7,58	232	22,2	0,2
19.08.09	19,55	16,38	7,85	220	20,0	<QL
24.09.09	19,20	5,82	7,58	189	27,5	<QL
22.10.09	14,40	nm	7,81	nm	23,3	<QL

nm = non measured
<QL = lower than quantification limit

Date	Potassium (mg/L)	Magnesium (mg/L)	Calcium (mg/L)	Chloride (mg/L)	Nitrite (mg/L)	Nitrate (mg/L)
Marnay						
22.10.08	6,3	6,8	88,3	13,9	<QL	14,8
25.11.08	<QL	4,7	98,4	14,3	<QL	20,4
16.12.08	<QL	3,3	105,3	12,7	<QL	24,8
19.01.09	1,9	3,9	93,2	18,6	<QL	26,0
24.02.09	<QL	0,5	88,1	15,1	<QL	24,9
24.03.09	1,6	4,0	88,9	19,6	<QL	25,7
22.04.09	6,0	4,3	93,2	27,2	<QL	25,9
09.06.09	2,1	3,6	89,2	21,1	<QL	16,1
22.06.09	2,4	4,0	87,8	23,3	<QL	18,0
22.07.09	2,0	7,6	72,4	12,9	<QL	11,3
19.08.09	1,9	8,9	64,8	12,0	<QL	8,8
24.09.09	<QL	1,3	58,0	11,4	<QL	7,8
22.10.09	<QL	1,4	59,6	12,7	<QL	7,8
Bougival						
22.10.08	2,2	3,4	77,3	23,9	<QL	19,2
25.11.08	<QL	6,7	94,7	19,1	<QL	19,2
16.12.08	<QL	0,6	99,6	17,4	<QL	25,0
19.01.09	3,4	6,4	100,3	30,1	<QL	26,1
24.02.09	2,8	6,2	97,7	22,7	<QL	25,5
24.03.09	2,9	6,4	96,8	26,2	<QL	26,7
22.04.09	3,4	7,8	97,6	30,7	<QL	24,1
09.06.09	4,6	6,7	95,5	34,2	<QL	24,4
22.06.09	4,4	7,1	91,4	32,3	<QL	21,3
22.07.09	4,3	10,3	85,0	29,2	<QL	15,1
19.08.09	4,0	7,0	79,8	29,0	<QL	14,5
24.09.09	0,4	3,2	72,9	25,5	<QL	13,2
22.10.09	0,7	3,3	74,1	26,6	<QL	13,9
Triel						
22.10.08	3,9	5,4	77,5	34,7	1,2	27,9
25.11.08	<QL	7,9	98,7	<QL	26,4	20,2
16.12.08	<QL	0,7	98,6	19,9	<QL	28,5
19.01.09	4,3	7,3	102,4	41,3	0,8	28,2
24.02.09	3,2	7,0	108,8	25,7	0,8	28,3
24.03.09	3,7	7,3	101,8	31,9	<QL	35,2
22.04.09	4,0	8,1	101,8	35,5	0,9	31,9
09.06.09	5,7	7,9	101,4	41,9	<QL	33,7
22.06.09	5,3	8,6	95,5	38,3	<QL	29,5
22.07.09	6,0	8,6	94,1	41,1	<QL	31,3
19.08.09	5,4	8,6	89,1	35,6	<QL	22,1
24.09.09	1,5	5,8	84,6	40,3	2,2	28,7
22.10.09	9,2	5,5	86,3	41,6	3,2	25,3

nm = non measured
<QL = lower than quantification limit

Date	Sulfate (mg/L)	Cd			
		dissolved <0.45 µm (µg/L^{-1})	solid >0.45 µm (µg.g^{-1})	labile (DGT) (µg.L^{-1})	sediment trap (µg.g^{-1})
Marnay					
22.10.08	15,9	<QL	0,537	nm	nm
25.11.08	17,3	<QL	0,432	0,0007 ± 0,0002	nm
16.12.08	17,6	<QL	0,493	0,0014 ± 0,0006	0,336
19.01.09	18,8	<QL	0,677	0,0010 ± 0,0007	0,311
24.02.09	18,5	<QL	0,433	0,0012 ± 0,0001	0,444
24.03.09	20,0	<QL	1,046	0,0009 ± 0,0001	0,294
22.04.09	22,4	<QL	2,303	0,0004 ± 0,0004	0,269
09.06.09	16,8	<QL	nm	0,0009 ± 0,0003	0,273
22.06.09	19,0	<QL	4,420	0,0011 ± 0,0005	0,297
22.07.09	14,3	<QL	0,048	0,0004 ± 0,0001	0,339
19.08.09	14,2	<QL	1,643	0,0006 ± 0,0001	0,307
24.09.09	13,7	<QL	0,385	0,0006 ± 0,0000	0,320
22.10.09	14,3	<QL	0,846	0,0017 ± 0,0003	nm
Bougival					
22.10.08	31,1	0,0116	4,050	nm	nm
25.11.08	29,4	<QL	1,874	0,0041 ± 0,0006	nm
16.12.08	24,4	<QL	0,770	0,0051 ± 0,0009	nm
19.01.09	36,1	<QL	1,691	0,0021 ± 0,0003	2,017
24.02.09	30,3	<QL	1,675	0,0022 ± 0,0002	1,528
24.03.09	36,4	<QL	2,878	0,0031 ± 0,0028	1,562
22.04.09	42,6	0,0152	3,931	0,0016 ± 0,0006	1,790
09.06.09	44,6	0,0131	1,546	0,0022 ± 0,0008	8,065
22.06.09	43,1	0,0101	2,632	0,0041 ± 0,0028	nm
22.07.09	38,4	<QL	20,53	0,0054 ± 0,0009	4,092
19.08.09	38,1	0,0136	8,043	0,0028 ± 0,0005	3,401
24.09.09	33,4	0,0136	4,221	0,0066 ± 0,0024	3,292
22.10.09	35,0	<QL	2,473	0,0066 ± 0,0014	nm
Triel					
22.10.08	43,9	0,0151	1,188	nm	nm
25.11.08	<QL	0,0116	1,832	0,0022 ± 0,0010	nm
16.12.08	28,0	<QL	2,152	0,0051 ± 0,0017	0,853
19.01.09	44,7	0,0131	2,218	0,0036 ± 0,0005	1,233
24.02.09	35,4	<QL	0,657	0,0027 ± 0,0004	0,354
24.03.09	42,8	<QL	0,441	0,0050 ± 0,0026	0,724
22.04.09	46,8	0,0136	1,950	0,0021 ± 0,0009	1,175
09.06.09	51,5	0,0131	0,837	0,0032 ± 0,0003	1,778
22.06.09	49,8	0,0187	2,287	0,0045 ± 0,0005	1,865
22.07.09	50,2	0,0146	1,409	0,0051 ± 0,0004	3,029
19.08.09	46,1	0,0141	2,055	0,0043 ± 0,0006	2,546
24.09.09	47,8	0,0126	1,378	0,0050 ± 0,0007	nm
22.10.09	49,4	0,0121	0,878	0,0050 ± 0,0009	nm

nm = non measured
<QL = lower than quantification limit

Date	Cr			
	dissolved <0.45 µm ($\mu g/L^{-1}$)	solid >0.45 µm ($\mu g.g^{-1}$)	labile (DGT) ($\mu g.L^{-1}$)	sediment trap ($\mu g.g^{-1}$)
Marnay				
22.10.08	<QL	7,7	nm	nm
25.11.08	1,09	30,0	0,0184 ± 0,0025	nm
16.12.08	<QL	68,7	0,0180 ± 0,0021	53,7
19.01.09	<QL	41,9	0,0352 ± 0,0062	50,1
24.02.09	<QL	14,9	0,0250 ± 0,0020	42,1
24.03.09	<QL	57,2	0,0249 ± 0,0038	50,0
22.04.09	0,22	64,8	0,0333 ± 0,0110	50,8
09.06.09	<QL	50,2	0,0214 ± 0,0033	49,9
22.06.09	<QL	64,8	<QL ± 0,0000	50,2
22.07.09	<QL	46,0	0,0178 ± 0,0027	51,2
19.08.09	0,41	53,6	0,0196 ± 0,0026	51,4
24.09.09	<QL	65,3	0,0167 ± 0,0041	54,2
22.10.09	nm	101,7	0,0196 ± 0,0078	nm
Bougival				
22.10.08	0,54	88,9	nm	nm
25.11.08	1,04	73,0	0,0574 ± 0,0248	nm
16.12.08	<QL	65,2	0,0926 ± 0,0131	nm
19.01.09	<QL	46,3	0,0270 ± 0,0060	71,8
24.02.09	<QL	84,2	0,0583 ± 0,0304	83,0
24.03.09	0,60	102,0	0,0353 ± 0,0033	69,2
22.04.09	0,28	90,6	0,0291 ± 0,0081	70,0
09.06.09	<QL	75,5	0,0244 ± 0,0065	108,9
22.06.09	0,25	77,5	0,0024 ± 0,0035	nm
22.07.09	<QL	82,0	0,0323 ± 0,0054	109,3
19.08.09	0,51	102,4	0,0277 ± 0,0033	87,8
24.09.09	<QL	84,7	0,0211 ± 0,0024	92,2
22.10.09	<QL	85,4	0,0246 ± 0,0108	nm
Triel				
22.10.08	<QL	94,9	nm	nm
25.11.08	1,24	58,1	0,0314 ± 0,0112	nm
16.12.08	<QL	121,9	0,0857 ± 0,0081	61,0
19.01.09	0,23	65,6	0,0284 ± 0,0035	73,5
24.02.09	<QL	46,6	0,0452 ± 0,0111	56,4
24.03.09	0,39	35,9	0,0415 ± 0,0144	65,0
22.04.09	0,32	88,3	0,0372 ± 0,0101	71,7
09.06.09	<QL	69,1	0,0243 ± 0,0031	80,9
22.06.09	0,21	58,1	0,0083 ± 0,0069	78,3
22.07.09	0,21	88,1	0,0314 ± 0,0047	86,0
19.08.09	0,51	74,2	0,0256 ± 0,0026	86,7
24.09.09	<QL	77,3	0,0319 ± 0,0165	nm
22.10.09	0,32	60,5	0,0252 ± 0,0039	nm

nm = non measured
<QL = lower than quantification limit

Date	Co			
	dissolved <0.45 µm ($\mu g/L^{-1}$)	solid >0.45 µm ($\mu g.g^{-1}$)	labile (DGT) ($\mu g.L^{-1}$)	sediment trap ($\mu g.g^{-1}$)
Marnay				
22.10.08	0,16	7,39	nm	nm
25.11.08	0,18	7,61	0,0132 ± 0,0013	nm
16.12.08	0,11	8,62	0,0203 ± 0,0016	7,13
19.01.09	0,16	6,49	0,0218 ± 0,0021	6,78
24.02.09	0,10	2,48	0,0191 ± 0,0013	5,76
24.03.09	0,12	7,59	0,0193 ± 0,0019	6,63
22.04.09	0,18	8,52	0,0145 ± 0,0062	6,39
09.06.09	0,13	5,69	0,0099 ± 0,0016	6,21
22.06.09	0,14	9,2	0,0107 ± 0,0046	7,11
22.07.09	0,06	6,55	0,0044 ± 0,0004	6,73
19.08.09	0,09	5,12	0,0057 ± 0,0009	6,60
24.09.09	0,04	8,85	0,0039 ± 0,0007	6,90
22.10.09	0,05	8,48	0,0120 ± 0,0036	nm
Bougival				
22.10.08	0,22	12,70	nm	nm
25.11.08	0,25	10,75	0,0416 ± 0,0088	nm
16.12.08	0,15	11,23	0,0509 ± 0,0079	nm
19.01.09	0,21	6,42	0,0416 ± 0,0079	9,25
24.02.09	0,17	13,29	0,0503 ± 0,0154	11,37
24.03.09	0,17	38,40	0,0232 ± 0,0100	8,64
22.04.09	0,25	12,63	0,0162 ± 0,0019	8,25
09.06.09	0,24	11,51	0,0147 ± 0,0071	11,14
22.06.09	0,22	12,59	0,0319 ± 0,0057	nm
22.07.09	0,17	8,29	0,0164 ± 0,0012	11,81
19.08.09	0,23	11,05	0,0181 ± 0,0029	9,61
24.09.09	0,13	16,35	0,0143 ± 0,0010	9,97
22.10.09	0,13	11,69	0,0309 ± 0,0042	nm
Triel				
22.10.08	0,39	17,55	nm	nm
25.11.08	0,32	17,22	0,0347 ± 0,0137	nm
16.12.08	0,20	25,22	0,0729 ± 0,0080	8,10
19.01.09	0,32	13,85	0,0727 ± 0,0118	9,63
24.02.09	0,21	8,07	0,0780 ± 0,0062	7,69
24.03.09	0,26	5,95	0,0464 ± 0,0113	12,09
22.04.09	0,33	12,82	0,0376 ± 0,0091	9,00
09.06.09	0,31	15,37	0,0275 ± 0,0020	10,33
22.06.09	0,30	7,98	0,0435 ± 0,0031	10,96
22.07.09	0,38	17,99	0,0288 ± 0,0026	13,04
19.08.09	0,28	10,92	0,0294 ± 0,0027	11,76
24.09.09	0,21	20,30	0,0287 ± 0,0053	nm
22.10.09	0,29	14,01	0,0567 ± 0,0073	nm

nm = non measured
<QL = lower than quantification limit

Date	Cu					
	dissolved <0.45 µm (µg/L^{-1})	solid >0.45 µm (µg.g^{-1})	labile (DGT) (µg.L^{-1})			sediment trap (µg.g^{-1})
Marnay						
22.10.08	0,36	95,5		nm		nm
25.11.08	0,36	18,7	0,0615	±	0,0117	nm
16.12.08	0,34	18,8	0,0751	±	0,0075	18,1
19.01.09	0,37	25,0	0,0655	±	0,0063	17,5
24.02.09	0,35	5,7	0,0748	±	0,0077	13,5
24.03.09	0,38	19,4	0,0736	±	0,0059	16,4
22.04.09	0,57	21,8	0,0970	±	0,0096	14,9
09.06.09	0,60	14,0	0,0907	±	0,0197	15,7
22.06.09	0,67	69,2	0,0852	±	0,0086	15,2
22.07.09	0,46	18,8	0,0581	±	0,0098	16,1
19.08.09	0,42	18,2	0,1038	±	0,0123	16,0
24.09.09	0,27	28,0	0,0730	±	0,0055	17,5
22.10.09	0,29	34,5	0,0569	±	0,0443	nm
Bougival						
22.10.08	1,04	119,6		nm		nm
25.11.08	1,02	103,9	0,2663	±	0,0435	nm
16.12.08	0,89	45,9	0,2590	±	0,0469	nm
19.01.09	1,27	149,6	0,1716	±	0,0125	93,6
24.02.09	0,77	44,7	0,2181	±	0,0760	100,0
24.03.09	0,96	63,5	0,1408	±	0,0568	80,0
22.04.09	1,22	69,6	0,1649	±	0,0290	78,8
09.06.09	1,76	102,4	0,1867	±	0,0696	155,0
22.06.09	1,27	103,3	0,2981	±	0,0485	nm
22.07.09	1,12	116,1	0,3864	±	0,0328	185,3
19.08.09	1,42	154,1	0,2532	±	0,0481	143,4
24.09.09	1,28	146,6	0,4257	±	0,0726	148,4
22.10.09	1,02	169,3	0,4811	±	0,0683	nm
Triel						
22.10.08	1,38	72,2		nm		nm
25.11.08	1,22	79,0	0,1511	±	0,0640	nm
16.12.08	0,93	93,6	0,2511	±		56,0
19.01.09	1,52	130,3	0,1743	±	0,0139	81,8
24.02.09	0,80	24,7	0,2095	±	0,0158	54,1
24.03.09	1,03	21,1	0,2167	±	0,0545	53,4
22.04.09	1,21	56,2	0,2406	±	0,0707	58,2
09.06.09	1,39	58,7	0,2798	±	0,0229	83,9
22.06.09	1,56	54,1	0,3004	±	0,0216	91,1
22.07.09	1,56	66,5	0,3878	±	0,0299	88,9
19.08.09	1,45	84,3	0,3336	±	0,0373	96,8
24.09.09	1,12	95,5	0,3628	±	0,0444	nm
22.10.09	1,07	111,1	0,3074	±	0,0226	nm

nm = non measured
<QL = lower than quantification limit

Date	Mn					
	dissolved <0.45 µm (µg/L^{-1})	solid >0.45 µm (µg.g^{-1})	labile (DGT) (µg.L^{-1})			sediment trap (µg.g^{-1})
Marnay						
22.10.08	2,20	761		nm		nm
25.11.08	2,60	658	1,8876	±	0,1829	nm
16.12.08	1,51	593	2,3995	±	0,1779	441
19.01.09	2,73	444	3,2134	±	0,2852	425
24.02.09	1,64	130	2,2352	±	0,1809	334
24.03.09	2,55	417	2,2688	±	0,2095	311
22.04.09	3,19	793	1,1308	±	0,1065	282
09.06.09	2,45	422	0,6496	±	0,1857	268
22.06.09	3,01	394	0,7869	±	0,1181	527
22.07.09	1,82	343	0,3611	±	0,0277	456
19.08.09	2,43	379	0,4063	±	0,0335	436
24.09.09	1,44	798	0,2789	±	0,0755	464
22.10.09	1,81	910	1,1428	±	0,8756	nm
Bougival						
22.10.08	7,01	972		nm		nm
25.11.08	8,01	917	4,9943	±	1,1708	nm
16.12.08	3,07	1035	8,3243	±	1,0681	nm
19.01.09	8,68	514	7,1816	±	1,3119	532
24.02.09	6,97	1057	7,8177	±	2,2111	679
24.03.09	6,77	1282	3,7178	±	1,7581	372
22.04.09	7,40	1528	2,0570	±	0,3913	1825
09.06.09	10,75	817	1,9484	±	0,8829	281
22.06.09	17,39	1450	8,3785	±	1,2276	nm
22.07.09	13,46	665	2,6621	±	0,5720	633
19.08.09	13,13	797	3,4854	±	0,3507	642
24.09.09	8,30	1762	2,2697	±	0,3271	644
22.10.09	8,89	1186	6,5533	±	0,8238	nm
Triel						
22.10.08	17,67	1678		nm		nm
25.11.08	12,72	1911	3,4317	±	1,4363	nm
16.12.08	4,37	2209	9,8236	±	1,0832	594
19.01.09	13,18	1224	10,2302	±	1,7280	502
24.02.09	9,37	570	9,9251	±	0,7406	513
24.03.09	11,18	484	6,5585	±	1,4618	780
22.04.09	11,62	1329	4,5635	±	1,1724	437
09.06.09	17,59	1428	3,2379	±	0,2842	414
22.06.09	20,17	752	9,3822	±	0,6874	872
22.07.09	27,63	2314	4,6341	±	0,6337	966
19.08.09	22,06	1097	4,7103	±	0,3726	948
24.09.09	15,38	2208	4,4451	±	0,5543	nm
22.10.09	15,78	1667	9,6470	±	1,6696	nm

nm = non measured
<QL = lower than quantification limit

Date	Ni					
	dissolved <0.45 µm (µg/L^{-1})	solid >0.45 µm (µg.g^{-1})	labile (DGT) (µg.L^{-1})			sediment trap (µg.g^{-1})
Marnay						
22.10.08	1,39	83,5		nm		nm
25.11.08	1,77	23,7	0,1537	±	0,0155	nm
16.12.08	1,53	32,0	0,2049	±	0,0171	26,2
19.01.09	1,43	26,4	0,2021	±	0,0274	24,8
24.02.09	1,45	13,8	0,2088	±	0,0154	20,5
24.03.09	1,54	19,9	0,1949	±	0,0178	21,6
22.04.09	1,93	23,8	0,2120	±	0,0356	20,5
09.06.09	1,68	25,4	0,1730	±	0,0370	20,6
22.06.09	1,59	9,1	0,1959	±	0,0227	21,6
22.07.09	0,61	20,5	0,0954	±	0,0082	21,1
19.08.09	0,80	33,8	0,1350	±	0,0184	20,6
24.09.09	0,51	28,5	0,1164	±	0,0076	21,4
22.10.09	0,48	35,2	0,1662	±	0,0444	nm
Bougival						
22.10.08	1,76	36,7		nm		nm
25.11.08	2,15	27,3	0,3686	±	0,0287	nm
16.12.08	1,66	32,1	0,4456	±	0,0353	nm
19.01.09	1,95	20,9	0,2971	±	0,0523	31,2
24.02.09	1,79	36,0	0,3215	±	0,0582	38,8
24.03.09	1,76	33,9	0,2284	±	0,0982	27,8
22.04.09	2,25	30,3	0,1769	±	0,0411	26,2
09.06.09	2,12	26,3	0,1846	±	0,1641	40,2
22.06.09	1,98	27,3	0,3244	±	0,0534	nm
22.07.09	1,21	26,2	0,4699	±	0,0656	37,0
19.08.09	1,48	38,5	0,3210	±	0,0857	28,7
24.09.09	1,07	32,7	0,4194	±	0,0478	31,4
22.10.09	0,94	40,5	0,4583	±	0,0420	nm
Triel						
22.10.08	2,74	47,8		nm		nm
25.11.08	2,43	18,4	0,1716	±	0,1870	nm
16.12.08	1,96	59,5	0,5448	±	0,0412	28,0
19.01.09	2,21	30,2	0,4651	±	0,0440	30,5
24.02.09	2,04	21,5	0,4506	±	0,0308	21,2
24.03.09	2,11	12,9	0,4265	±	0,0927	23,6
22.04.09	2,59	30,1	0,4431	±	0,1258	25,2
09.06.09	2,34	29,3	0,5783	±	0,0451	27,7
22.06.09	2,36	20,6	0,5425	±	0,0446	27,2
22.07.09	2,17	39,5	0,7516	±	0,0564	30,7
19.08.09	1,79	38,5	0,5643	±	0,0534	29,3
24.09.09	1,49	30,0	0,6810	±	0,0707	nm
22.10.09	1,96	41,5	0,7961	±	0,0550	nm

nm = non measured
<QL = lower than quantification limit

Date	Zn			
	dissolved <0.45 µm (µg/L^{-1})	solid >0.45 µm (µg.g^{-1})	labile (DGT) (µg.L^{-1})	sediment trap (µg.g^{-1})
Marnay				
22.10.08	0,00	45	nm	nm
25.11.08	2,67	128	0,4443 ± 0,0794	nm
16.12.08	0,00	171	1,4880 ± 0,3041	149
19.01.09	9,77	188	0,9879 ± 0,6036	141
24.02.09	0,00	71	0,8363 ± 0,2054	126
24.03.09	3,94	395	0,1593 ± 0,2726	106
22.04.09	2,26	451	0,7561 ± 0,3556	108
09.06.09	2,61	140	0,6933 ± 0,1770	109
22.06.09	2,53	134	0,0000 ± 0,0000	125
22.07.09	1,82	185	0,3653 ± 0,2242	117
19.08.09	1,24	713	0,2743 ± 0,0185	113
24.09.09	0,00	219	0,1149 ± 0,0942	122
22.10.09	2,43	417	0,5778 ± 0,1292	nm
Bougival				
22.10.08	6,68	465	nm	nm
25.11.08	24,11	410	2,6357 ± 0,3660	nm
16.12.08	7,35	336	3,1303 ± 0,4687	nm
19.01.09	15,05	642	1,7871 ± 0,3823	439
24.02.09	4,39	480	2,4681 ± 0,5169	506
24.03.09	6,02	567	0,4016 ± 0,7782	307
22.04.09	6,28	645	0,3518 ± 0,1285	307
09.06.09	9,76	380	1,5101 ± 0,8240	694
22.06.09	6,22	409	2,0656 ± 0,3286	nm
22.07.09	3,55	383	2,4936 ± 0,3778	629
19.08.09	4,77	671	1,6872 ± 0,8048	505
24.09.09	3,28	542	1,8259 ± 0,3294	515
22.10.09	3,65	508	2,3360 ± 0,3841	nm
Triel				
22.10.08	7,08	351	nm	nm
25.11.08	14,58	363	1,4578 ± 0,7045	nm
16.12.08	3,90	1402	3,5673 ± 0,3334	299
19.01.09	14,60	608	2,7852 ± 0,4558	408
24.02.09	3,47	232	3,7381 ± 0,2701	226
24.03.09	4,72	135	1,4446 ± 0,2907	225
22.04.09	6,15	434	1,5454 ± 0,4717	249
09.06.09	7,88	302	2,8858 ± 0,2618	342
22.06.09	9,45	43	2,6829 ± 0,2066	387
22.07.09	6,72	350	3,0716 ± 0,2291	395
19.08.09	4,53	522	2,4158 ± 0,1857	415
24.09.09	4,10	399	2,3656 ± 0,3861	nm
22.10.09	9,00	256	3,0642 ± 0,3981	nm

nm = non measured
<QL = lower than quantification limit

Date	Pb			
	dissolved <0.45 µm (µg/L^{-1})	solid >0.45 µm (µg.g^{-1})	labile (DGT) (µg.L-1)	sediment trap (µg.g^{-1})
Marnay				
22.10.08	0,00	36	nm	nm
25.11.08	0,00	29	0,0022 ± 0,0014	nm
16.12.08	0,00	29	0,0285 ± 0,0080	23
19.01.09	0,00	42	0,0308 ± 0,0099	22
24.02.09	0,00	11	0,0039 ± 0,0030	20
24.03.09	0,00	33	0,0067 ± 0,0025	20
22.04.09	0,00	46	0,0093 ± 0,0045	19
09.06.09	0,00	<QL	0,0099 ± 0,0028	19
22.06.09	0,07	47	0,0136 ± 0,0011	20
22.07.09	0,00	25	0,0047 ± 0,0008	20
19.08.09	0,00	67	0,0058 ± 0,0009	20
24.09.09	0,00	66	0,0041 ± 0,0022	23
22.10.09	0,00	69	0,0108 ± 0,0016	nm
Bougival				
22.10.08	0,23	157	nm	nm
25.11.08	0,15	135	0,1612 ± 0,0711	nm
16.12.08	0,08	71	0,1425 ± 0,0648	nm
19.01.09	0,17	118	0,0171 ± 0,0088	105
24.02.09	0,08	77	0,0227 ± 0,0142	95
24.03.09	0,14	125	0,0239 ± 0,0031	80
22.04.09	0,15	149	0,0323 ± 0,0126	87
09.06.09	0,24	139	0,0249 ± 0,0139	245
22.06.09	0,25	159	0,0868 ± 0,0307	nm
22.07.09	0,23	307	0,0378 ± 0,0080	177
19.08.09	0,25	245	0,0302 ± 0,0088	141
24.09.09	0,19	181	0,0348 ± 0,0121	148
22.10.09	0,22	161	0,0578 ± 0,0313	nm
Triel				
22.10.08	0,20	115	nm	nm
25.11.08	0,15	112	0,0272 ± 0,0219	nm
16.12.08	0,00	145	0,0393 ± 0,0225	59
19.01.09	0,16	119	0,0124 ± 0,0023	82
24.02.09	0,00	40	0,0197 ± 0,0075	55
24.03.09	0,11	34	0,0225 ± 0,0136	51
22.04.09	0,14	88	0,0194 ± 0,0127	64
09.06.09	0,16	82	0,0088 ± 0,0012	84
22.06.09	0,33	71	0,0180 ± 0,0034	83
22.07.09	0,20	111	0,0176 ± 0,0036	90
19.08.09	0,16	109	0,0176 ± 0,0034	99
24.09.09	0,21	119	0,0339 ± 0,0216	nm
22.10.09	0,24	109	0,0199 ± 0,0051	nm

nm = non measured
<QL = lower than quantification limit

Annexe 6

Papier sous presse du Chapitre III dans « *International Journal of Environmental Science and Technology* »

« Urbanization impact on metal mobility in riverine suspended sediment: Role of metal oxides »

Int. J. Environ. Sci. Tech., 8 (1), 1-18, Winter 2011
ISSN: 1735-1472

Urbanization impact on metals mobility in riverine suspended sediment: Role of metal oxides

C. Priadi; S. Ayrault; S. Pacini; P. Bonte

Laboratoire des Sciences du Climat et de l'Environnement (LSCE/IPSL, CEA-CNRS-UVSQ) avenue de la terrasse, 91198 Gif sur Yvette cedex, France

Received 22 June 2010; revised 4 October 2010; accepted 25 November 2010

ABSTRACT: Spatial and temporal fractionation of trace metals and major elements in suspended particulate matter in the Seine River was investigated to study the impact of the increasing urbanization in the Greater Paris Region. Suspended sediments in the Seine River were collected between December 2008 to August 2009 upstream and downstream of Paris. They were subjected to total digestion and sequential extraction procedure certified by the Bureau Communautaire de Référence and trace metals along with major elements were analyzed with inductively coupled plasma mass spectroscopy. Metal enrichment factors increased up to eight folds after the Seine River downstream of the Greater Paris Region showing a significant contribution of urbanization. Enrichment of copper, lead and zinc downstream of Paris are followed by the increase of their reducible fraction of at least 10% implicating an increase in metals associated with iron oxides. The exchangeable fraction, which includes the carbonate-associated metals, is only significant for cadmium, nickel and zinc (more than 2 %) while the oxidisable fraction accounts for less than 20 % for the anthropogenic metals downstream except for copper. The metals can be divided to (a) "reducible" group including cadmium, lead, and zinc, associated with more than 60 % of the total Bureau Communautaire de Référence extractable metals to the reducible fraction containing mostly iron oxide phases for the downstream sites. (b) A "distributed" group including chromium, copper, and nickel that are associated to at least 3 different phase-groups: (1) oxides, (2) organic matter and sulphides and (3) mineral phases.

Keywords: *Carbonate; Enrichment factor; Pollution; Reducible fraction; Sequential extraction*

INTRODUCTION

In the last decade, metal contamination in urban continental aquatic system has been a growing concern (Sekabira *et al.*, 2010; Mohiuddin *et al.*, 2010). Impacts of anthropogenic activities on metal contamination in a watershed are far from being insignificant (Horowitz *et al.*, 1999; Davis *et al.*, 2001; Taylor and Owens, 2009; Igbinosa and Okoh, 2009). They are known to generate a considerable amount of metal to the environment through various pathways including atmospheric particles (Azimi *et al.*, 2005; Zhu *et al.*, 2009), urban runoff (Gromaire-Mertz *et al.*, 1999; Igwe *et al.*, 2008), industrial and wastewater effluents (Buzier *et al.*, 2006; Nwuche, 2008; Shah *et al.*, 2009). Urbanization impacts on metal contamination concern watersheds inhabiting more than 50 % of the world population (Meybeck, 2003). The Seine River watershed is home to 25-30 % of French industries, 23 % of French constantly increasing urban and agricultural activities contribute to metallic aquatic contamination. In the last two decades, many institutions carried out actions in the Seine River to understand pollutant behaviour with parallel decontamination. Since then, the concentration of trace elements such as the Cd, Cr, Cu, Ni, Pb, and Zn showed a significant decline measured in dated sediment cores (Le Cloarec *et al.*, 2009). Nevertheless, due to very high anthropogenic pressures and very limited dilution power, the Seine River downstream of Greater Paris is still among the world's most contaminated rivers (Meybeck *et al.*, 2007). Despite the decreasing concentrations in the solid phases, Elbaz-Poulichet *et al.* (2006) still found moderate contamination of dissolved metals in the water column of the Marne and Seine Rivers. Various studies contributed to the understanding of metal behaviour in different compartments due to the dynamic metal distribution between different phases in the water column. In the

*Corresponding Author Email: *cindy.priadi@lsce.ipsl.fr*
Tel.: +33 16982 4362; Fax: +33 1698 24362

Seine River, the value and dynamics of dissolved Mn, Cu, Cd and Mo were partly attributed to variation in redox condition (Elbaz-Poulichet *et al.*, 2006). Short-time extreme variation of dissolved Zn is also observed using high-definition sampling (Pepe *et al.*, 2008). Depending on the element, the solid fraction holds 50-90 % of the anthropogenic metal stock (Cd, Cu, Cr, Zn, and Pb) in the Seine River water column (Thévenot *et al.*, 2007). Furthermore, floodplain and bed sediments contain a large stock of historical deposit and contamination. Therefore, this solid fraction plays an important role in metal contamination as it may release heavy metal to the water column, as well as scavenging them. It is then necessary to understand the behaviour and distribution of trace elements in the different solid phases and their mobility towards the dissolved fraction. The latter, more specifically the labile fraction, represent the bio-available fraction. Moreover, the solid fraction may hold evidences of metal sources and formation processes. The study of metal speciation in the solid fraction may therefore help us understand the contribution of different sources and biogeochemical processes in the formation and mobility of metal in the solid phase.

Metal speciation studies such as the sequential extraction are often performed on mining-impacted rivers (Da Silva *et al.*, 2002; Galan *et al.*, 2003; Audry *et al.*, 2006; Lesven *et al.*, 2009) but rarely on non-mining urban watershed even though urban anthropogenic activities can generate a specific characteristic of metal speciation in a water course (Garnaud, 1999; Dali-Youcef *et al.*, 2004; Carter *et al.*, 2006; Sutherland and Tack, 2007). Interpretation are also rarely compared by simultaneous extraction of major elements originating from the metal-bearing particles including Ca, Fe, Mn, and Mg, except for a few studies (Gagnon *et al.*, 2009; Li *et al.*, 2009; Vieira *et al.*, 2009). Tongtavee *et al.* (2005) have shown that the analysis of extracted major elements is of great interest to understand lead speciation in soils affected by mining activities.

Despite the Seine River basin's great economic importance and the many articles published on contents and behaviour in dissolved and labile fraction of trace metals in the Seine River (Elbaz-Poulichet *et al.*, 2006; Tusseau-Vuillemin *et al.*, 2007; Chen *et al.*, 2009; Jouvin *et al.*, 2009), trace metal speciation on solid fraction were only conducted on average suspended matter from 3 sites (Taconet, 1996) and urban source-related samples (Garnaud, 1999). According to these studies, metal mobility can be ranked as follows: Cu<<Cd<Pb<Zn. Nevertheless, these studies do not detail the temporal variation of the metal distribution, and spatial variation was concluded from only one sampling in three sites.

This study is therefore aimed to investigate anthropogenic impact on the temporal and spatial variability of metal speciation and understand heavy metal mobility in the Seine River suspended particulate matter (SPM) through the BCR sequential extraction with preliminary study focusing on efforts on reducing working weight. A one-year study was conducted in three characteristic sites of the Seine River. The solid speciation of six metals (Cd, Cr, Cu, Ni, Pb and Zn) along with nine major elements was determined.

MATERIALS AND METHODS

Location

Seven monthly samplings from December 2008 August 2009 were conducted in the 3 study sites along the Seine River (Fig. 1). The sampling scheme aims to distinguish the impacts of two sources of anthropogenic influence to the Seine River which have previously been observed. First source is the area of Greater Paris, including the most urbanised area in the region with more than 3700 habitants/km^2. Second is the wastewater treatment plant WWTP Paris-Aval (formerly known as Achères) treating around 1.7 million m^3 per day (SIAAP, 2007). The first sampling site is located at Marnay-sur-Seine, situated in far upstream of the Seine River. It was chosen to represent a relatively pristine site non-affected by the Greater Paris region, where the Seine is a 6 Strahler order river. The second site is the Seine at Bougival, a Strahler order 7 River situated 40 km downstream of Paris. It was chosen to represent the impact of Paris without the influence of the WWTP Paris-Aval. Another 40 km further downstream, Triel-sur-Seine was selected to represent the impact of Paris along with the Paris-Aval after the confluent of the Seine River with the Oise River, making it a Strahler order 8. The Seine River is affected mainly by the sedimentary basin mostly containing carbonate rocks (Meybeck *et al.*, 1999). The flow regime is low from July to September and high flows are observed from January to March (Fig. 2).

Sampling and sample treatment

Materials and sample handling were done in a systematic clean method. All bottles and containers were soaked in 2 N HNO_3 during at least 3 days. Afterwards they were rinsed thoroughly 3 times with

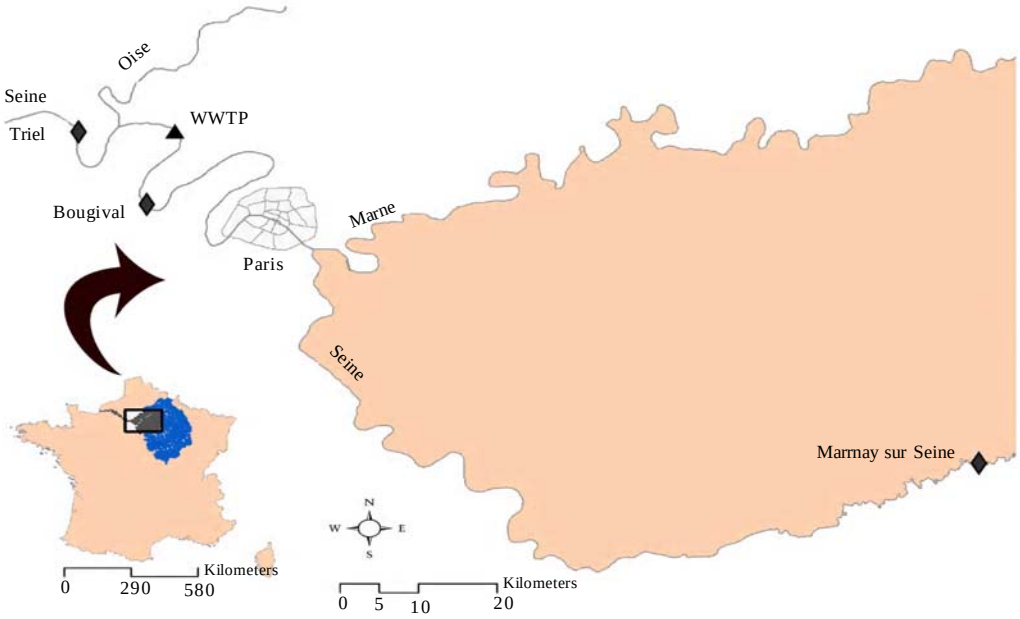

Fig. 1: Sampling sites marked with diamonds; from upstream to downstream: Marnay sur Seine, Bougival, and Triel. Black triangle indicates Seine-Aval waste water treatment plant

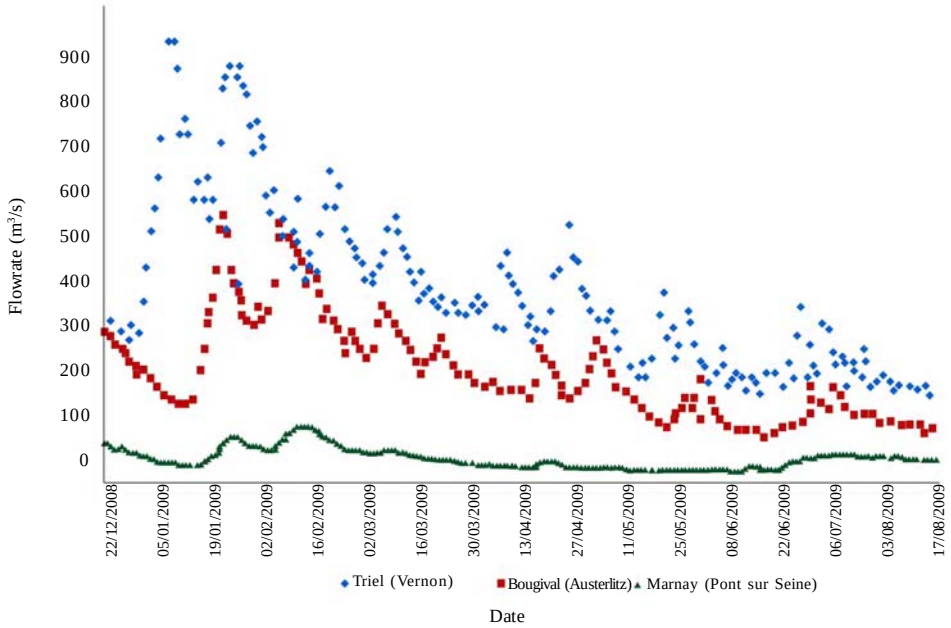

Fig. 2: Evolution of daily flow measured at 3 sites similar to the study sites of this paper measured by the Syndicat Intercommunal d'Assainisement de l'Agglomération Parisienne (SIAAP)

de-ionised water. All bottles and containers were rinsed 3 times with river water before handling the samples.

To obtain enough SPM for sequential extraction purposes, a sediment trap was installed in each site. It consisted of a 2 L PVC water bottle hanged from at least 1 m from the river bank at mid-depth. Two holes of a diameter of around 4 cm were carved on two sides on the upper side of the bottle with the two holes posed creating a parallel axe to the river flow. This method was previously successfully used by Tessier and Bonté (2002) to collect the Seine SPM. SPM from sediment trap was emptied in a polyethylene bottle on field along with uplying water. Samples were transported and stored in the dark at 4 °C before analysis. Storage duration ranged from 2 days to one month before sample treatment.

Samples were then centrifuged in the laboratory at 3500 rpm for 20 min for several cycles until all the water are centrifuged and all the SPM are recovered. It was then freeze-dried for at least 48 h and homogenized with agate mortar. Samples were then stored in acid-cleaned glass jars in the dark before analysis.

Solid phase analyses

Bulk digestion

To obtain total metal contents, 0.1 g of SPM was digested in Teflon vessels under laminar flow hood using a heating block (Digiprep, SCP Science). The first attack uses 10 mL *aqua regia* (HNO_3 65 %: HCl 30 %, 3:1) for 3 days at room temperature. Excess nitrate and chloride were evaporated at 90°C and underlying liquid was separated ensuring the least quantity of HCl remaining in the vessels through rinsing 3 times with 10 mL 0.5 N HNO_3. Digestion continued with 10 mL of a HF 48.9 %: HNO_3 65 % mixture (1:1) to attack siliceous minerals during 24h at room temperature. Sample was evaporated to dryness at 100°C to eliminate hexafluorosilicic acid. The solid residue was then attacked with 12 mL of a HNO_3 65 % : $HClO_4$ 69-72 % (1:1) mixture heated at 120 °C during 5 days. Final solutions were evaporated near to dryness. 1 mL of 65 % HNO_3 was added to the remaining solution that was then evaporated near dryness. This step was repeated three times. The solutions were then brought into a 50 mL 0.5 N HNO_3 solution. This method was adapted for the Seine River carbonated SPM, and allows complete SPM digestion. The 3 day a*qua regia* step allowed dissolution of the abundant amount of carbonates in samples. Afterwards, underlying liquid was separated to avoid re-precipitation of the Ca and Mg fluorides in HF solution. All solutions were ultrapure reagents to assure minimum contamination (HNO_3 and HCl Normatom grade, VWR France, and HF and $HClO_4$ "for trace metal analyses", Baker, from Sodipro France).

BCR sequential extraction

Each BCR sequential extraction was performed on duplicates of 0.25 g of sediment following Revised BCR with extra rinsing to overcome the difficulty due to the smaller amount of extracting solution used. Extraction protocol is summarized in Table 1. Due to a lack of end-to-end shaker, shaking was performed using a platform orbital shaker during 16 h at 300 rpm (Heidolph vibramax 100). The speed was chosen to keep the samples well in suspension without shaking excessively to avoid over-extraction. Due to the relatively low quantity of samples used, separating the extracted solution without removing the sample was a difficult task. A second rinsing was applied using half the normal volume of the same extracting solution before rinsing samples with water. Each extraction batch was accompanied by a duplicate of the BCR 701 (Bureau Communautaire de Recherches, Gent, Belgium) certified lake sediment for sequential extraction.

Analytical procedure

Major and trace metal concentration were determined in total and sequential extraction samples using Inductively Coupled Plasma Quadrupolar Mass Spectrometry (ICP-QMS) (X-Series, CCT II+ ThermoElectron, France). ICP-QMS spectrometer was calibrated using standard solutions and checked for with certified river water (SRM 1640, National Institute for Science and Technology, Gaithersburg, USA) routinely during analysis, at least once per day of analysis and once for every 20 samples at the most. Instrumental drifts and plasma fluctuations were corrected using internal standards (Re, Rh, and In (SPEX, SCP Science, France)) for all the metals studied, and Ge for major elements including Ca, Al, and Mg. To minimise interferences, analysis with the Collision Cell Technology (CCT) introducing a supplementary gas mixture of H_2 (7 %) and He (93 %) was applied for Fe, Mn, and the 6 metals studied (Cd, Cr, Cu, Ni, Pb, Zn). Major elemental bulk analysis including Ca, Si, Al, Fe, Mg, S, K, P, and Ti were performed with micro (50 µm) X-ray fluorescence (XRF) (Microfocus x-ray source IFG X-1) through measurements of pressed pellets (diameter 0.5 cm,

Table 1 : Summary of the BCR sequential extraction protocol after Pueyo *et al.* (2001) except step 4 with *aqua regia*, added to complete protocol

	Reagent	Operationally defined fraction	Nominal target phase	experimental condition
step 1	0.11 mol/L CH_3COOH	exchangeable	soluble and exchangeable cations and carbonates	room temperature, constant shaking 16 h
step 2	0.5 mol/L $NH_2OH.HCl$ at pH 1.5	reducible	Fe-Mn oxyhydroxides	room temperature, constant shaking 16 h
step 3	H_2O_2 (85°C) then 1.0 mol/L CH_3COONH_4	oxidisable	organic matter and sulfides	room temperature 1h, occasional shaking, then agitation 85°C, 1h room temperature, constant shaking 16 h
step 4	aqua regia	residual		room temperature, constant shaking 16 h

average weight 0.02 g). Measurements were calibrated with at least 5 reference materials (USGS Mn Nodule A1, USGS Marine mud MAG-1, USGS jasperoid GXR-1, IAEA lake sediment SL1 and IAEA Soil-7) and sample analysis was done in duplicate to compensate for possible sample heterogeneity. Particulate organic carbon (POC) and nitrogen (PON) contents were measured in 0.25 mg samples previously decarbonated by 3.4 mL of 1 N HCl. Decarbonation comprises of 4 cycles of addition of HCl solution, 20 mn of 300 rpm orbital shaking, 3000 rpm centrifugation, solution separation. Samples were weighed precisely and analysed through a Carbon Hydrogen and Nitrogen (CHN) analyser (Thermoflash EA 1112 series).

Enrichment factors

Enrichment factors (EF) were calculated by normalizing concentrations to Al and using local background values established for the Seine river watershed by (Thévenot *et al.*, 2002) through measurements of selected river mouth values based on an Al content of 33000 mg/kg. Assembled background values are shown on Table 2 and formulae is shown in Equation 1. The EF values should be evaluated keeping in mind the shortcomings of this approach (Reimann and de Caritat, 2005; Karbassi *et al.*, 2008). Here, local background values were preferred to continental crust concentrations, due to the specificity of the carbonaceous Seine River basin geology.

$$EF = \frac{[Me]_{sample} / [Al]_{sample}}{[Me]_{background} / [Al]_{background}}$$

Where EF where $[Me]_{sample}$ = metal concentration in sample, $[Al]_{sample}$ = aluminum concentration in sample, $[Me]_{background}$ = metal concentration in background value and $[Al]_{background}$ = aluminum concentration in sample.

Scanning electron microscopy analyses

Cartography of suspended sediment were collected at 6-7 kV using in backscattered electrons imaging mode on a Zeiss ULTRA scanning electron microscopy (SEM) coupled with field emission gun (FEG) at the IMPMC, Paris, France. Energy Dispersive X-ray Spectroscopy (EDXS) data were collected at the same electron beam-voltage using a BRUKER AXS Si-drift detector. A supplementary image coupled with its EDS spectrum is also demonstrated. This latter image was obtained with JEOL JSM 840 SEM coupled to an X-ray microanalysis system from Princeton Gamma Tech (PGT) at LSCE.

RESULTS AND DISCUSSION

Extraction recoveries, analytical uncertainties and limit of detection

Extraction and analytical processes were validated using various standard materials. Extraction recovery (recovery in Table 4) was calculated by comparing the average concentration of our BCR sequential extraction on 0.25 g (n=4) with the BCR certified values comprising of Zn, Cd, Pb, Cr, Ni and Cu in the exchangeable, reducible and oxidisable fraction. Recovery value is accompanied with standard deviation (SD in Table 4). Analytical detection limits (DL in Table 4) are two times the blank value of sample that went to the same preparation, extraction, and analytical treatment. Speciation values were also validated by comparing the sum of the 4 extracted fractions with

Table 2: Background concentration (mg/kg) in selected river mouth values (Poses estuary) established by Thévenot *et al.* (2002)

	Zn	Cd	Pb	Cr	Ni	Cu	Fe	Al
Background in Poses (mg/kg)	60 ± 10	0.22 ± 0.05	20 ± 3	40 ± 5	16 ± 2	15 ± 5	15000	33000

Table 3: Concentration of average major element contents of suspended particulate matter collected monthly in the sediment trap from December 2008 to August 2009 (n=7)

	POC (%)	PON (%)	Ca (%)	Si (%)	Al (%)	Fe(%)
Marnay	7.6 ± 0.9	0.8 ± 0.1	26.5 ± 1.0	10.9 ± 0.7	3.4 ± 0.2	2.1 ± 0.2
Bougival	10.0 ± 1.9	0.9 ± 0.2	18.5 ± 1.4	17.4 ± 0.8	4.8 ± 0.5	3.3 ± 0.7
Triel	7.7 ± 1.7	0.9 ± 0.2	15.4 ± 1.7	20.6 ± 1.5	4.9 ± 0.4	3.4 ± 0.5

	Mg (mg/kg)	P (mg/kg)	S (mg/kg)	Mn (mg/kg)	K (mg/kg)	Ti (mg/kg)
Marnay	5845 ± 1288	1582 ± 340	1337 ± 328	442 ± 70.7	8300 ± 643	1696 ± 299
Bougival	10506 ± 1877	4071 ± 723	4148 ± 798	609 ± 133	12040 ± 1278	3923 ± 1048
Triel	10771 ± 2097	4790 ± 901	3966 ± 1094	721 ± 172	13311 ± 1565	3378 ± 1926

Table 4: Average recovery and its standard deviation (Recovery and SD in %) of BCR sequential extraction in this study performed on the BCR-701 sediment compared with concentration of trace elements, certified by the BCR (n=4). Analytical detection limits (DL in mg/kg) are calculated through 2 times the average blank values.

	Zn		Cd		Pb		Cr		Ni		Cu	
	recovery±SD	DL	recovery±SD	DL	recovery±SD	DL	recovery±SD	DL	recovery±SD	DL	recovery±SD	DL
Exchangeable fraction	98 ± 3	0.5	104 ± 6	53	121 ± 7	3.7	118 ± 9	32	95 ± 9	0.5	115 ± 5	20
Reducible fraction	93 ± 8	904	82 ± 9	26	99 ± 2	46	91 ± 6	394	96 ± 7	208	92 ± 7	149
Oxidisable fraction	82 ± 11	368	86 ± 26	185	58 ± 23	53	90 ± 4	115	81 ± 10	100	81 ± 7	56

Table 5: Average recovery and standard deviation (Recovery SD in %). Recovery compares the total extracted metals in the four fractions with the BCR sequential extraction procedure compared to metal concentration obtained by total digestion (n=7)

	Zn	Cd	Pb	Cr	Ni	Cu
	recovery±SD	recovery±SD	recovery±SD	recovery±SD	recovery±SD	recovery±SD
Marnay	65 ± 6	98 ± 13	79 ± 8	29 ± 4	51 ± 2	88 ± 13
Bougival	84 ± 10	99 ± 12	103 ± 10	41 ± 5	62 ± 6	97 ± 11
Triel	77 ± 13	93 ± 19	104 ± 12	36 ± 3	58 ± 6	40 ± 5
	Mn	Fe	Ca	Mg	Al	
	recovery±SD	recovery±SD	recovery±SD	recovery±SD	recovery±SD	
Marnay	60 ± 9	46 ± 10	81 ± 8	25 ± 4	9 ± 3	
Bougival	87 ± 17	70 ± 23	86 ± 8	41 ± 6	15 ± 1	
Triel	91 ± 21	72 ± 13	119 ± 30	35 ± 4	14 ± 1	

the total digestion results (Table 5). For the trace elements, SD values showed that Cd and Cu shows a low reproducibility with SD ranging from 13-19 % for Cd and 13-16 % for Cu. Cd concentrations are relatively low, which may be prone to contamination during the extraction. This is reflected in our recovery levels which are higher than total digestion values in downstream sites, 99±12 and 93+19 at Bougival and Triel, respectively. Ca presented difficulties as it is present in extremely high quantity in the exchangeable fraction and may often pose difficult analytical problems.

Nevertheless, the recovery level between the 4 extraction phases of the BCR and our total bulk extraction depends on the metal's properties and the site's location. For most cases, more than 90 % of Cd and Pb are extracted by the BCR extraction, except for Pb in Marnay which has a slightly lower recovery, at 79+7 %. More than 80 % of Cu, Zn, and Ca are extracted with the BCR sequential extraction except for Zn at Marnay where recovery compared to the total digestion is relatively lower, 65+6 %. Zn, Pb, Cr, Ni and Al extracted by the BCR are significantly higher at Bougival than at Marnay. This shows that Zn, Pb, Cr, and Ni could be

from natural sources, associated to Al which would be more resistant to chemical extraction. Cr and Ni are probably found in the crystalline phases because they are only half extracted by the BCR extraction, 52+2, 62+6, 58+5 for Ni, and even lower for Cr 29+3 41+5 37+3 at Marnay, Bougival and Triel, respectively. For Cd, Cr, Cu, Ni, Pb and Zn, these results agree with most studies using the BCR sequential extraction, although none specified the uncertainty and detection limits for each extraction phase and each element. Larner *et al*. (2008) stated an extraction efficiency of 70-115 %. Nevertheless, these values were incomparable with those from other studies because our total digestion protocol attacks almost 100% of the bulk sediment. Our recovery would then be underestimated compared to recoveries values in other studies where pseudo-total digestion were performed (i.e. Larner *et al*., 2008). The major elements showed different extractability by the BCR extraction compared to the total bulk digestion, reflecting the different mineral forms in which the major element take form. The order of extractability from the element less extracted by the BCR to the most extracted is Al< Mg < Fe < Mn < Ca.

Enrichment factors

Enrichment factors (EF) of the 7 values at each site were averaged and shown on Fig. 3. Values showed significant increase in downstream samples for Zn, Cd, Pb and Cu. On the other hand, Cr and Ni show no spatial increase in EF, keeping a relatively steady value of around 2 from Marnay to Bougival and Triel. These two

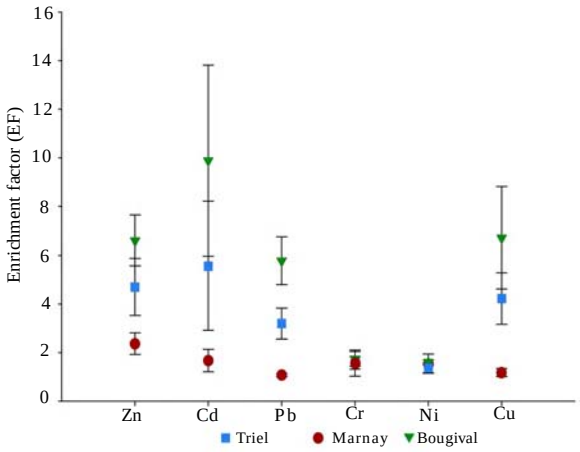

Fig. 3: Average enrichment factors during December 2008 until August 2009 for six metals (Cd, Cu, Cr, Ni, Pb, Zn) at the 3 studied sites (Marnay, Bougival, Triel) n=7

elements represent metals with the solid phase non-enriched by urban activities. In the case of the Seine River, the evolution of the concentration of the trace elements is also accompanied by an increase in most of the major elements (Table 3). The trend of metal enrichment in suspended sediments is similar with recent studies of metals in the Seine River through analysis of sediment cores and estuarine mussels (Meybeck *et al*., 2007; Le Cloarec *et al*., 2009). This shows that SPM collected in this study are representative to the Seine watershed and that these four metals represent metals affected by anthropogenic sources. Urban activities may increase EF in two or even seven folds in the downstream sites, depending on the metals. In average, Cd is the metal most enriched while Zn, Pb and Cu present EF of 6-7. Metal concentrations at Bougival were not found to be lower than at Triel (Mann-Whitney, $p = 0.983$), despite of the Seine Aval WWTP outlet situated between the two sites. Considering the possible contribution of the WWTP outgoing flow to the metal contamination in the water column, one could have expected that metal concentrations in SPM would be higher at Triel than at Bougival. In 2002, Thévenot et al. (2002) calculated that particulate flux of Cd, Cu and Pb from the Seine-Aval WWTP contributed from 2-6 % in the river mouth despite of the relatively low SPM concentration in the WWTP outlet water of 28-49 mg/L ((Estebe *et al*., 1998; Meybeck *et al*., 1998; Thévenot *et al*., 2007). Through calculations of influx, WWTP treatment efficiency and sludge recovery, Thévenot *et al*. (2007) established an outflux of 26, 25.5 and 90 $t.y^{-1}$ for Cu, Pb, and Zn respectively. Buzier *et al*., (2006) also found that WWTP outflux may have a significant impact on the labile metal flux downstream of the outlet in low flow conditions. Ever since these studies were published, an effort was made through construction of numerous WWTP to distribute and relieve the wastewater load of Seine Aval. This finding indicates that improved WWTP are efficient in reducing incoming metal load to the Seine River. The analysis of the major elements is an important aspect in the interpretation of sequential extraction data as these major phases are likely to be the carrier phase of the trace elements. In order to confirm whether our extraction corresponds to the operationally-defined fraction, the extracted major elements for each step are presented (Fig. 4). At Bougival and Triel, Ca is more than 90 % extracted on the exchangeable fraction, leaving less than 10 % extracted in the reducible step and almost no Ca is found in the oxidisable and residual

phase. Upstream, the Seine shows a slightly different behaviour where more Ca is found in the reducible fraction. Unlike Ca, Fe and Al that varies between the three sites, there is no significant difference in the distribution of Mg and Mn at the three sites. Mn takes on a slightly similar behaviour to Ca where around 70 % are found in the exchangeable form while Mg contains more oxidisable and residual form. Even though Fe and Mn exist as oxides, the distribution of the two elements is significantly different. Fe is not released in the exchangeable fraction but rather during reducible and residual extraction for Bougival and Triel and mostly in the residual fraction for Marnay. The domination of Ca at Marnay with an average of 26.5 % reflects the geological condition of the Seine watershed where 95 % being underlain by carbonate rocks (Meybeck *et al.*, 1999). Further downstream, Ca concentration decreases to an average of 18.5 % and 15.4 % for Bougival and Triel, respectively, and replaced by the general increase of other major elements such as Si, Fe, Mg, P, S, Mn, K and Ti. For example, Si concentration increases from 10.9 % at Marnay to 17.4 % and 20.6 %, Fe average concentration increases from 2.1 % to 3.3 % in the downstream sites. A dramatic increase is observed for P and S concentrations at Bougival and Triel compared to Marnay. The impacts of anthropogenic activities on P and S are less well documented but some studies mentioned sources mostly coming from wastewater (Houhou *et al.*, 2009). The increase of P and S may be due to the increase of organic matter. Even though on the average, there is no significant difference between POC at Marnay, Bougival and Triel, but on a monthly basis, Bougival contains higher POC than Marnay and Triel (Mann Whitney Test for 7 months of samples $\alpha = 0.05$).

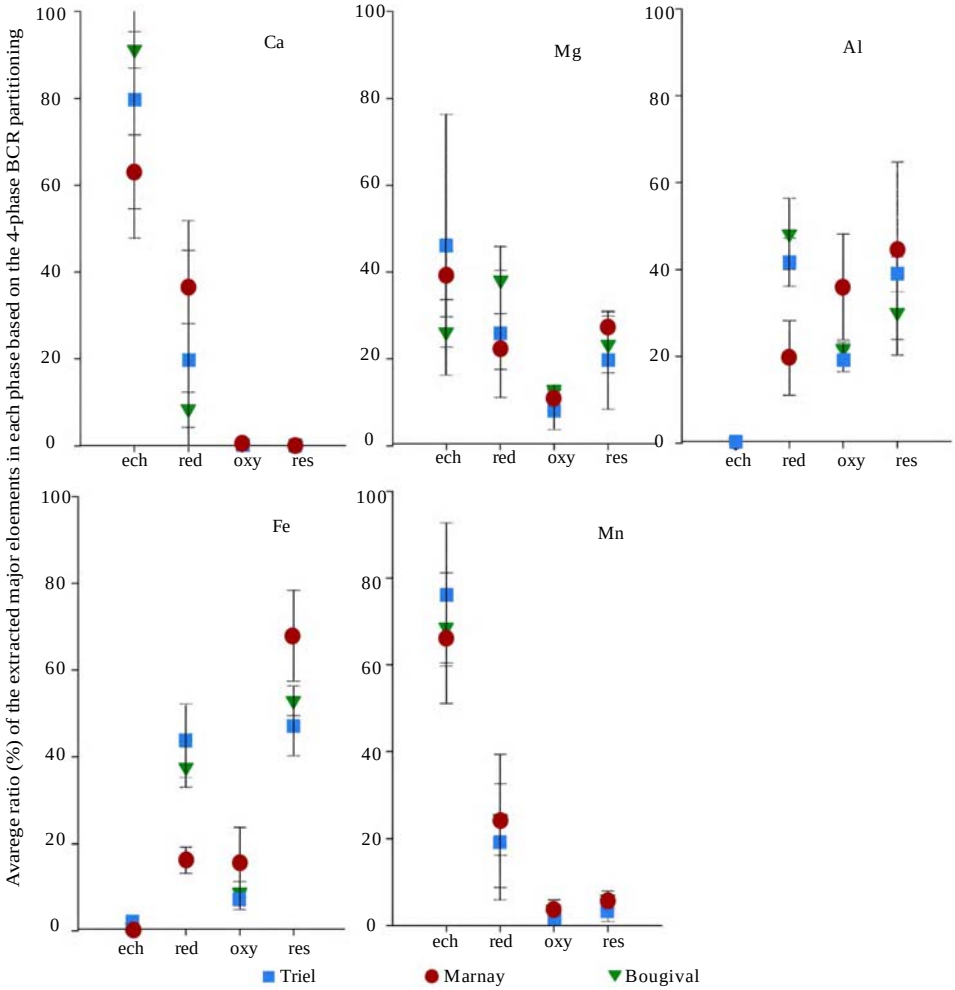

Fig. 4 : Average ratios of extracted major elements for each BCR sequential extraction phase at the 3 sites (Marnay, Bougival, Triel) (n=7)

Nevertheless, it is also possible that P and S increase is due to increasing phosphate, sulfate or sulfide species. The evolution of Al concentrations in the 3 sites underlines the importance of also interpreting data normalized with Al through enrichment factor.

Speciation

The average distribution for the 7 monthly sampling of the 6 metals is shown in Fig. 5. The distribution is different for each metal and site. Detailed speciation of the environmentally relevant trace metals are presented in Fig. 6. Sediment traps integrate one month of SPM during which the sample may be subjected to evolution of speciation. In the course of a month, SPM sedimenting on the bottom of sediment trap may create reducing conditions, favourizing the oxidation of organic matter and the formation of reduced forms. This possibility is to be taken into account during the lecture and interpretation of data. A spatial evolution in the Al speciation is also observable mostly for the reducible phase. This evolution of Al would mean that there is an increase of allochthonous Al coming from the Greater Paris Region. This is also the case for Fe where the reducible proportion increases in the downstream sites. The similarity of Fe and Al where both elements tend to be present mostly in the reducible fraction at Bougival and Triel may mean a similar anthropogenic source. Indeed, Fe and Al are the two most abundant metals (Luoma and Rainbow, 2008) thus becoming the two mostly utilized metals worldwide (USGS, 2010). In 2004, 1370 kt of Al were used in France, mostly in the transportation, construction and packaging sector (AFA). Nevertheless, this anthropogenic Al possibly present in the reducible fraction only accounts for 30-40 % of total BCR extractable Al (Fig. 4), which in turn only contributes to 14-15 % of the total Al in Seine SPM (Online Resource Table 2). This small proportion of reducible and possibly anthropogenic Al would only be around 6 % of the total Al and with this uncertainty it is still considered safe to calculate enrichment factors through normalization by Al. As a whole, an evolution from upstream to downstream is significant enough while the difference between Bougival and Triel is less pronounced (Mann Whitney, p= 59 %, 49 % 85 % between Marnay to Bougival, Marnay to Triel and Bougival and Triel, respectively, with H_0 hypothesis is proportion $_{site\ 1}$ = proportion $_{site\ 2}$). Regarding temporal variation, the distribution at a given site is relatively stable with deviation of around 5 % for most metal in certain fractions (n=7), and with a maximum of 10-15 % for some metals. Speciation evolution from Marnay to Bougival and Triel was observed for Zn, Cd, Pb and Cu but not for Cr and Ni. Moreover, these four metals are those demonstrating a significantly higher EF downstream. This implicates that anthropogenic contamination is likely to bring in material with different metal distribution and that variation in the physico-chemical condition downstream leads to a different type of speciation. The general observation allows us to divide the six metals into 2 distinct groups. The first group constituting of Zn, Cd, and Pb, averages more than 60 % in the reducible fraction and even reaching up to 90 %. The reducible fraction for these three elements is always significantly higher than the 3 other fractions (t test, α=0.05). These metals are known to be preferably associated with iron oxy-hydroxides (Luoma and Bryan, 1981) which would explain the high proportion found in the reducible fraction. The increasing proportion of these reducible metals rises significantly from upstream to downstream, marking a possible anthropogenic impact. This idea is also supported with the increasing EF as the water reaches Bougival and Triel. The increase in EF is accompanied with the increase in the reducible fraction for Zn, Pb and Cu but in a lesser extent for Cd which shows that for this metal, the metal physico-chemical properties also play an important role in determining the distribution. The second group consists of Cr, Ni, and Cu with higher fractions of the residual phase than the first group, averaging around 35 %. Compared to the first group, the metals in the second group are distributed relatively equal where no fraction holds more than 60 % for a given metal, except for residual Cu at Marnay. While in a first approach, the metals can be divided into two groups, each metal shows a typically different behaviour and it will be interesting to discuss the distribution of each particular metal. From the first group, Zn seems to stand out from Cd and Pb in terms of association to the exchangeable fraction (Fig. 5). The proportion of Zn associated to this phase remains around 20 % from Marnay to Triel. Despite the stability in its proportion, this means an increase of 4-6 folds in concentration going from an average of 9 mg/kg at Marnay to an average of 63 and 45 mg/kg at Bougival and Triel respectively. Moreover, the relative stability of the proportion of Zn associated to the exchangeable phase is seen in a smaller proportion for oxidisable Zn. The proportion remains around 10 % while the concentration increases 2-4 folds in most cases. Except for July 2009, the average proportion of exchangeable and oxidisable Zn is relatively stable from Marnay to

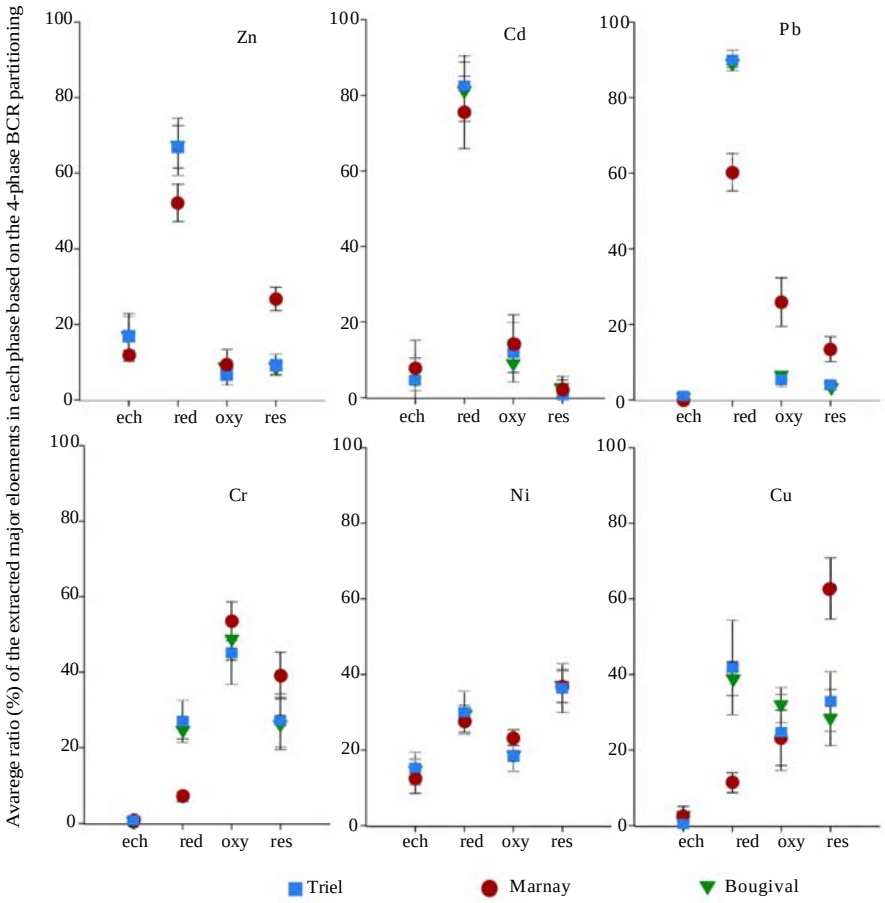

Fig. 5 : Average ratios of extracted trace elements for each BCR sequential extraction phase of the 3 sites (Marnay, Bougival, Triel) (n=7)

Triel. Distinct changes are observable with Zn associated to the reducible phase (student test confidence interval 99 % between Marnay and the two downstream sites). Average reducible Zn increased from upstream to downstream with 52+9 % at Marnay to 67+6 % at Bougival and 67+8 % at Triel. This is the result of a 4 to 7 time increase of concentration from Marnay to Bougival and Triel. Consequently, the reducible fraction accounts for at least 50 % of BCR extractable Zn at Marnay and up to 75 % for Bougival and Triel. Garnaud *et al.* (1999) also found a majority of reducible and exchangeable Zn particularly in SPM sampled during a rain period in the le Marais catchment outlet of the Seine River. A weak increase of Zn in the residual form from upstream to downstream also marks a relatively steady amount of residual Zn transported in the Seine River which could originate from the Seine's geological background. It is difficult to compare Seine Zn distribution with other urban river studies because Zn in the Seine river watershed is particular compared to other urban rivers in the world. Unlike most watersheds, roof runoff constitutes one of the major sources of Zn contamination in the Greater Paris Region, where it reaches roughly 40 % of all roofing surfaces (Robert-Sainte *et al.*, 2009). 85-100 % of Zn washed from roof surfaces are in its ionic form (Heijerick *et al.*, 2002). Zn has a high affinity for solid particles and so it is easily adsorbed mostly to carbonates, hydrous iron oxide and silicate minerals (Fujiyoshi *et al.*, 1994). Nevertheless, these Zn-bearing particles undergo physico-chemical evolution and once found in the sewer system, 70 % of Zn is found to be associated with organic matter and biofilm (Rocher *et al.*, 2004). However, our analysis showed that Zn in the SPM is far more likely to be associated with the reducible form, with an average of more than two thirds of the total

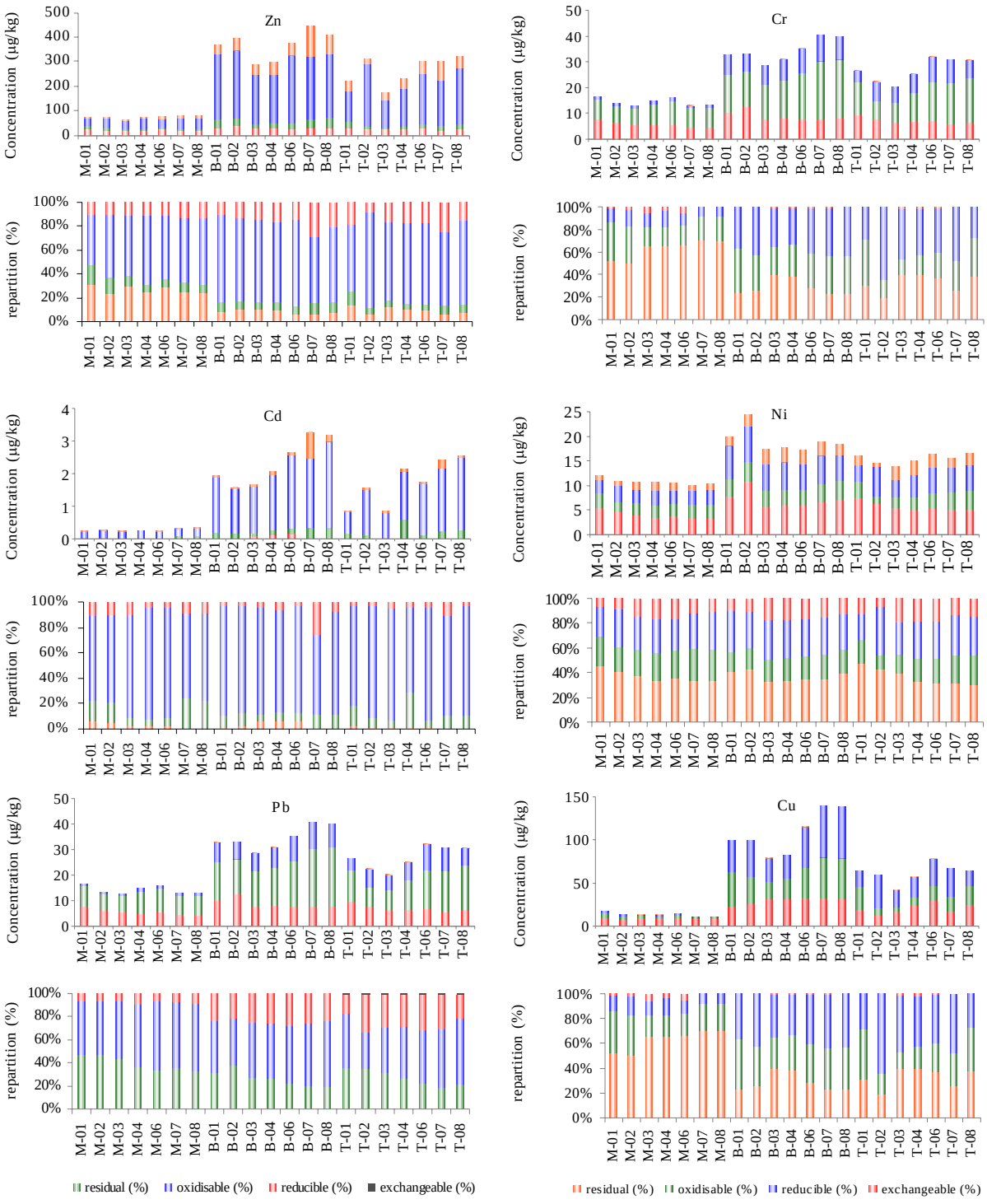

Fig. 6 : Distribution of Zn, Cd, Pb, Cr, Ni, and Cu in the 4 different fractions of the BCR defined phases both in concentration (mg/kg) and relative concentration (%) with axis X indicating M for Marnay, B for Bougival and T for Triel sites accompanied by numbers representing the month when the sediment trap was collected (01 = January 2009 until 08 = August 2009)).

BCR extractable Zn for Bougival and Triel. This means that the sediment undergoes further transformation until reaching the water body. Our result is comparable to the lower median percentage of acid-soluble Zn found in the urban streams of Prague (Hnatukova *et al.*, 2009). The dominating reducible phase of Zn is to a further extent similar for Cd. Cd is found to be associated up to 80 % with the reducible phase increasing the concentration to 10 folds going from 200 µg/kg of Cd to around 2000 µg/kg from upstream to downstream. Although the relative distribution of the 4 phases remains relatively stable, the absolute concentration increases to 4-6 times from Marnay to Triel, and increasing more labile Cd in the exchangeable and reducible fraction simultaneously. The exchangeable proportion is higher in Bougival and Triel, in the 5-10 % range. Nevertheless, along with Zn and Ni, Cd still represents one of the metals with the highest proportion associated to the exchangeable phase making it relatively more mobile to the environment than other metals, because the exchangeable phase is the phase most likely to go into the dissolved phase thus becoming more available to the environment. The high proportion of reducible Cd and Zn in the Seine River SPM differs from previous urban river studies which showed mostly acid-soluble fraction. Hnatukova *et al.*, (2009) found 38-64 and 15-43 % acid-soluble Cd and Zn, respectively, in the urban streams of Prague as opposed to the acid-soluble Cd and Zn in Seine measuring at 3-11 % and 8-28 % respectively. This makes Cd one of the most mobile element compared to the 6 studied elements showing the highest proportion associated to the mobile phase (exchangeable+ reducible+ oxidisable), with an average of 2 % associated to the residual phase. Comparing the six studied metals, Cd shows the highest EF increase from upstream to downstream, increasing 3 to 5 folds compared to an average EF increase of 2 to 3 folds for Zn and Pb in the downstream sites. This significant Cd increase in the bulk concentration is not accompanied with an evolution of the average distribution from upstream to downstream (Fig. 5). This is not the case for two urban watersheds, the St Lawrence River, Canada (Gagnon *et al.*, 2009)and the Loura River, Spain (Filgueiras *et al.*, 2004) which exhibited significant spatial variation of Cd solid speciation. Evolution for the Seine River solid SPM is only observable once comparing monthly variations when the proportion of exchangeable Cd along with exchangeable Zn increases in July 2009. This phenomenon could be attributed to the low flow occurring during the SPM accumulation for this sample (22 June to 22 July, 2009), illustrated in Fig. 2, but also the transport of first flush runoff from the storm rain taking place between the 16 and 17 July increasing the river flow rate from 126 to 189 m^3/s. This runoff discharge may consist of particles with different speciation as opposed to the low flow-particles which would explain the abrupt increase of exchangeable Cd and Zn. The high EF of Cd and the relatively high proportion of Cd in the mobile fraction make Cd an important element to monitor in the environment. Nevertheless, despite of this high enrichment of the Cd downstream of the Seine River, Cd shows a stable distribution in the 4 fractions from upstream to downstream. The speciation of Cd found downstream is not similar to Cd speciation of solid matters collected in the basin such as traffic aerosols containing 75 % of exchangeable Cd (Lebreton and Thevenot, 1992)or road dusts containing more than 30 % of oxidisable Cd (Thévenot *et al.*, 2002). This implies that urban Cd would be mobile and solid Cd entering the river would be directly remobilized to its preferable fractions in the solid phase, despite of its original form. This would make speciation-based source tracing in the solid form unadoptable for Cd in the Seine River. Pb showed the highest increase of the reducible fraction relative content from upstream to downstream (20-30 %) and a 10-15 fold the concentration increase. This is by far the highest spatial increase of the reducible fraction compared to Zn and Cd. Compared to Zn and Cd, there does not seem to be a significant proportion of exchangeable Pb compared to the four other fractions. In the downstream sites, the three remaining fractions, exchangeable, oxidisable and residual only makes up 10 % of the total extractable Pb. This means that further studies on Pb contamination has to be focused on the reducible fraction, containing mostly Pb associated with iron and manganese oxides. Nevertheless, our results remain similar to other studies of metal fractionation in urban watersheds. The preference of Pb for the reducible phase is also observed by Sutherland and Tack (2007) and Carter *et al.* (2006). They found a high association of Pb with the Mn oxide and to a lesser extent with the Fe oxide. Hnatukova *et al.* (2009) also found Pb to be mainly bound to the reducible fraction. Jain *et al.* (2008) also found only 1-3 % of exchangeable Pb in the sediments of the River Narmada, India. The weak association of Pb with the exchangeable fraction is equally observed in

the study by Carter *et al*. (2006). Nevertheless, the Seine oxidisable Pb proportion seems to be underestimated compared to their study as fractionation of Pb is mainly dominated by the reducible fraction. The study of Hassellov and von der Kammer (2008) strongly suggests that iron-oxide Pb bearing particles are in the form of nano-colloids. Consequently, Pb may be efficiently transported to the estuary. The Seine River is located in a carbonated basin. Consequently, SPM contains abundant carbonates onto which the metals could be adsorbed. Nevertheless, this is not the case for the Seine River where the absence of exchangeable Cu, along with Cr and Pb, is notably similar to the distribution in the Aire River (Carter *et al*., 2006). The predominant species in the range of pH of the Seine River measured during the campaign (between 7.5-8.3) would be $CuCO_3$(aq) and $Cu(CO_3)_2^{2-}$ (Stumm and Morgan, 1981)which means that $CuCO_3$(s) is not present even with abundant $CaCO_3$ in the system. Along with Zn, Cu seems to be the element with a mobile phase evolving considerably from upstream to downstream, where its proportion could reduce 20 % the proportion of the residual phase. This would mean a higher mobility downstream, and it would also mean a high anthropogenic contribution. Similar to Cd, Ni is distributed steadily from Marnay to Triel, around 15, 20, 30, and 40 % for the exchangeable, oxidisable, reducible and residual phases respectively. Ni displays a minimum spatial increase in absolute concentration from upstream to downstream, reflected by the values of Ni EF. These two evidences may mean that Ni sources mostly originate from lithogenic sources rather than anthropogenic contamination. Ni seems to be the metal containing in average the highest metal proportion in the residual fraction ranging around 31-47 %. The relatively steady proportion of the residual Ni from upstream to downstream would signify the steady contribution of lithogenic background, reflected by the steady values of enrichment factor from upstream to downstream. The relatively high exchangeable Ni is somehow comparable to that of Zn but while reducible and residual Zn varies considerably from upstream to downstream, reducible and residual Ni remain stable and do not show significant spatial variation. Therefore, the high exchangeable Ni cannot be contributed to anthropogenic sources, but more to the typical geochemistry of Ni to the solid phase. Among the elements found in the second group, Ni shows the highest exchangeable phase, which is not the case for other fractions. Similarly to Cd and Zn, Ni is found to be already significantly associated with the exchangeable phase beginning from the upstream site. The presence of a significant exchangeable phase in Ni, Cd and Zn is not at all apparent in Pb, Cr, and Cu. The grouping of Ni, Cd, and Zn was observed by (Tusseau-Vuillemin *et al*., 2005)on Seine River SPM. Based on a multi-elementary study, they found a correlation between the ratio of the dissolved and solid fraction (K_d) of Ni, Cd and Zn. This would indicate similar adsorption-desorption behaviour for Ni, Cd and Zn. As mentioned above, a recent study observed a high variation of dissolved Zn in the Seine. Zn similar behaviour with Ni and Cd would imply that pulsating concentration of dissolved Ni and Cd could also be a problem in the Seine River. This should be further investigated as Cd and Ni are considered even a more toxic element and regulated by the European Water Directive. Similar to Ni, Cr displays a constant EF for the 3 sites. Nevertheless, what distinguishes Cr from Ni is that Cr seems to even be less mobile with relatively no exchangeable phase present. This is also supported by the low BCR-extractability of Cr, representing more than 60 % associated with the non-extractable phase indicated by the difference of the total Cr of the four BCR extracted fractions and the total Cr obtained by the bulk extraction. This would indicate as Cr being mostly incorporated in mineral particles, relatively difficult to extract. Chromite is regularly found in the Seine SPM through analysis by Scanning Electron Microscopy (SEM) (unpublished work) and this may be a possible mineral form of Cr. This is an evidence of the importance of completing total digestion with metal speciation study to understand its mobility to the environment. Compared to the 5 other elements, Cr seems to be an element that is mostly associated with the oxidisable phase, averaging about 40-50 %. The strong preference of Cr with organic matter was mostly observed in an anoxic estuary (Du Laing et al. 2009). The high capacity of Cr complexation with the organic matter is also observed in bed sediments (Lin and Chen, 1998).This would mean that Cr could be ingested by organisms consuming the organic matter. Despite the stable enrichment factor from upstream to downstream indicating possible lithogenic origin of Cr, a shift of distribution, is apparent from Marnay towards Bougival and Triel. There is a 10 % decrease of Cr in the residual phase, replaced by an increase in the reducible form. This shows that Cr evolves more considerably than Ni inside the solid phase and is more labile to physico-chemical changes. The abundance in the oxidisable phase is also apparent at a lesser extent for

Cu. The oxidisable Cu represents 30 % as compared to Cr going up to 50 %. A concentration increase of 5-20 times is observed, the highest upstream-downstream increase of oxidisable Cu compared to other metals. Luoma and Rainbow (2008) noted the strong affinity of Cu to organic ligands. More recently, various studies in the Seine River also noted this characteristic which would be due to the presence of urban dissolved organic matter. It presents different complexing capacity as compared to the natural organic matter, thus creating a higher affinity for the dissolved copper (Pernet-Coudrier *et al.*, 2008). Such colloidal organic matters could possibly be collected in a monthly trap. The formation of bio-film inside the trap could also be an equally important Cu-collecting mechanism. As for Zn and Pb, reducible Cu also shows an increase in proportion going from 12 % at Marnay to 30-40 % at Bougival and Triel. This abrupt apparition of reducible Cu could be attributed to a source related phenomenon where average EF increases 3-5 folds from Marnay to Bougival and Triel. Cu introduced to the river could be associated with the reducible fraction, especially the iron and Mn oxides. Luoma and Bryan (1981) noted Cu preference to iron oxy-hydroxides, although in our cases, the proportion of reducible Cu is relatively low as compared to reducible Zn, Cd and Pb ranging about 40 %. A higher reducible fraction is observed at Triel on February 2009 where it reaches up to 70 %. This sudden increase of reducible Cu on February 2009 coincides with the increase of reducible Zn, Cd, and Pb for the same period. During this period, the Seine River flow rate at Bougival more than tripled in 11 days from 157 to 528 m^3/s. The flow decreased by an average of 200 m^3/s during the next 9 days and re-increased to 505 m^3/s in 7 days. These increasing flow rate episodes due to rain runoff would include urban runoff with specific source-related characteristics. As during this period, a significant increase in reducible Zn, Cd, Pb and Cu is observed, the 2 rain episodes were likely to transport urban pollutants associated in the reducible fraction, mostly iron oxides. Images of the Triel August 2008 suspended sediment sample using the SEM-FEG demonstrated iron oxide as a cluster with a geometrical crystal structure (Fig. 7a inset). The Ca detected behind the iron oxide cluster could indicate a calcite-hosted iron-oxide growth as suggested by the elemental cartography (Fig. 7a). The similar composition of iron oxide with Ca was also observed by SEM-EDS on bed sediment collected on 2001 (Tessier and Bonté, 2002). Iron oxide particles were found as cohesive particles and proved to be an effective metal scavenger (Hochella and White, 1990; Morin *et al.*, 2009; Sekabira *et al.*, 2010) found to be associated with Cu, Pb, Sb and Zn.

Sulfidic species

The grouping of Zn, Cd, and Pb along with relatively mobile Cu would support the hypothesis of possible sulfidic forms in the samples. These four elements are known as chalcophile elements in the Geochemical Classification of Goldschmidt and preferably bond with sulphur rather than oxygen. Indeed, according to Larner *et al.* (2008), sequential extraction of samples containing sulfidic phases in oxic conditions would lead to redistribution of Cd, Zn, Cu and Pb to a lesser extent from the oxidisable to the reducible phase. This study explained that during the exchangeable extraction, sulfidic phases may be oxidised and redistributed to the reducible phase. No previous studies showed a significant amount of sulfidic phases in oxic riverine SPM non-affected by mining activities (Taylor and Owens, 2009). Therefore no special care was taken in preserving oxidation state during the sequential extraction procedure. This study showed that with the minor oxidisable phase, and the extremely high reducible fraction, a considerable amount of the studied metals could be associated with the sulfidic phases.

Urban impacts on metal speciation

The proportion of the reducible fraction seems to reflect the enrichment factor of the metal. Metals affected by anthropogenic activities having a relatively high enrichment factor (EF>3), seems to prefer association with the reducible form. Obviously, the proportion of the residual fraction reflects the contribution of the background. The oxidisable fraction also seems to show, to a lesser extent, contribution by natural sources as it is exceptionally high for Cr, reaching up to 50 % compared to the other fractions. Ni, a non-enriched metal in the Seine River, also contains a relatively high oxidisable fraction, ranging around 23 % at Marnay, and 11-23 % at the downstream sites. It seems that the immediate mobility is minimized for most of the metals, reflected by their small proportion in the exchangeable form. Two downstream sites were chosen in order to measure impacts of Greater Paris at Bougival and of the wastewater treatment plant (WWTP) Seine Aval at Triel. Even though at Bougival the metal concentrations are

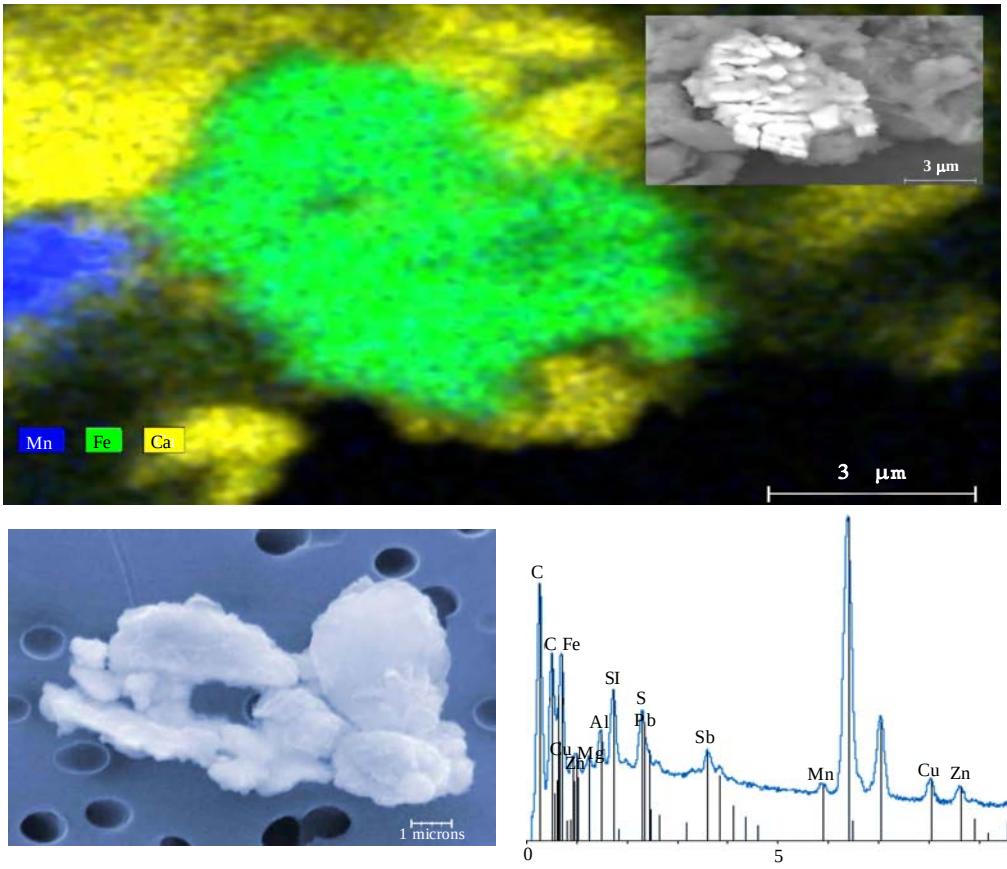

Fig. 7: (a) Cartography from energy dispersive spectroscopy (EDS) and Scanning electron microscopic image (inset) and of iron-manganese oxide growth on calcium carbonate mineral analyzed with MEB-FEG at IMPMC, Paris ; Bottom : SEM image (b) and EDS spectrum (c) of a cluster of particles indication metal bearing iron oxide associated with antimony, copper, lead, and zinc analyzed with MEB-EDS at LSCE, Gif sur Yvette

significantly higher than at Triel, no significant difference is remarkable in their distribution between the four phases for any of the six metals. The addition of numerous WWTP and the redistribution of incoming wastewater to other plants in the course of the Seine River may prove to be effective in reducing the metal load flowing in the Seine River at Bougival. Nevertheless, the issue of reducing the metal load is still important for Greater Paris where enrichment from Marnay to Bougival remains considerably high.

CONCLUSION

In this study, applying the BCR sequential extraction to suspended particulate matter sampled monthly in the Seine River, a river impacted by human activities, the highly urban Greater Paris Region is found to modify not only metal concentration but also metal speciation as observed in speciation evolution between Marnay vs Bougival and Triel. As Cd, Cu, Pb and Zn are enriched in the suspended matter, their reducible fraction is found to greatly increase. Based on the speciation behaviour, the analysed metals can be divided into two groups; the first group contains the anthropogenic metals, Cd, Pb, and Zn, in which the reducible fraction accounts for more than 60 % of the total BCR extractable metals for the downstream Paris sites. The second group includes Cr, Cu, and Ni that are associated with at least 15 % in three of the four defined BCR fraction in the downstream Paris sites. Exchangeable fraction is only significant for Cd, Ni and Zn while the oxidisable fraction accounts for less than 20 % for the anthropogenic metals downstream except for Cu. The enrichment of Zn, Pb and Cu by the Greater Paris Region seen at Bougival and Triel is accompanied by the increasing distribution of metals on more mobile phases including the exchangeable and reducible phases. This

fraction is more mobile as the metals can be released to the dissolved phase easily with pH variation, thus making the metal more bio-available. Temporal variation in the speciation is found to be related with discharge variations. No impact from the waste water treatment plant was observed, neither on the trace metal concentration, enrichment factors nor speciation.

This study suggests that a considerable amount of the metal studied could be associated with sulfidic phases which will be investigated in further studies. Nevertheless, the possible formation of sulfidic phases in the SPM accumulating during one month in the trap must be considered.

ACKNOWLEDGEMENTS

The authors would like to thank A. Bourgeault and the HBAN team in Cemagref Antony for sampling assistance, E. Robin for XRF analysis, N. Tisnerat-Laborde for decarbonatation discussion, C. Gautier and C. Hatté for POC and PON measurements, E. Douville for ICP-MS assistance, D. Thévenot for advice and corrections and J.-M. Mouchel, G. Morin and C. Quantin for helpful discussions. The Marnay-sur-Seine botanical garden and the SIAAP are thanked for giving access to the sampling sites located on their ground. For the acquisition of SEM data, we would like to thank A. Elmaleh and I. Estève at IMPMC and E. Robin at LSCE. We are also grateful to R. Hochreutener (MSc student) and to her research advisor G. Morin (IMPMC) as for organizing and preparing SEM analysis. The study is a contribution of the interdisciplinary research program on the environment PIREN-Seine and was also funded by the the Continental and Coastal Ecosphere French research program (EC2CO – INSU). Cindy Priadi acknowledges the French Foreign Affairs Ministry and PIREN Seine for her PhD scholarship. This is LSCE contribution number 4055.

REFERENCES

Afa, A. F. D. L. A., Les utilisations: Les marchés; http://www.Aluminium-info.Com/fr/utilisations/marches. [Accessed 27-Apr 2010].

Audry, S.; Blanc, G.; Schäfer, J., (2006). Solid state partitioning of trace metals in suspended particulate matter from a river system affected by smelting-waste drainage Sci. Total. Environ., 363 (1-3), 216-236 **(21 pages)**.

Azimi, S.; Rocher, V.; Garnaud, S.; Varrault, G.; Thevenot, D. R., (2005). Decrease of atmospheric deposition of heavy metals in an urban area from 1994 to 2002 (Paris, France). Chemosphere, 61 (5), 645-651 **(7 pages)**.

Buzier, R.; Tusseau-Vuillemin, M. H.; Dit Meriadec, C. M.; Rousselot, O.; Mouchel, J. M., (2006). Trace metal speciation and fluxes within a major French wastewater treatment plant: Impact of the successive treatments stages. Chemosphere, 65 (11), 2419-2426 **(8 pages)**.

Carter, J.; Walling, D. E.; Owens, D. P. N.; Leeks, G. J. L., (2006). Spatial and temporal variability in the concentration and speciation of metals in suspended sediment transported by the River Aire, Yorkshire, UK. Hydrolog. Process., 20, 3007-3027 **(21 pages)**.

Chen, J.; Gaillardet, J.; Louvat, P.; Huon, S., (2009). Zn isotopes in the suspended load of the Seine River, France: Isotopic variations and source determination. Geochimica et Cosmochimica Acta, 73 (14), 4060-4076 **(18 pages)**.

Da Silva, I. S.; Abate, G.; Lichtig, J.; Masini, J. C., (2002). Heavy metal distribution in recent sediments of the Tietê-Pinheiros river system in São Paulo state, Brazil. Appl. Geochem., 17 (2), 105-116 **(12 pages)**.

Dali-Youcef, N.; Ouddane, B.; Derriche, Z., (2004). Metal partitioning in calcareous sediment of the Tafna river and its estuary (Algeria). Fresen. Environ. Bull., 13 (12B), 1500-1508 **(9 pages)**.

Davis, A. P.; Shokouhian, M.; Ni, S., (2001). Loading estimates of lead, copper, cadmium, and zinc in urban runoff from specific sources. Chemosphere, 44 (5), 997-1009 **(13 pages)**.

Du Laing, G.; Van de Moortel, A.; Moors, W.; De Grauwe, P.; Meers, E.; Tack, F.; Verloo, M., (2009). Factors affecting metal concentrations in reed plants (*Phragmites australis*) of intertidal marshes in the Scheldt estuary, Ecol. Eng. 35, 310–318 (**9 pages**).

Elbaz-Poulichet, F.; Seidel, J. L.; Casiot, C.; Tusseau-Vuillemin, M. H., (2006). Short-term variability of dissolved trace element concentrations in the Marne and Seine rivers near Paris. Sci. Total. Environ., 367 (1), 278-287 **(10 pages)**.

Estebe, A.; Mouchel, J. M.; Thevenot, D. R., (1998). Urban runoff impacts on particulate metal concentrations in river Seine. Water Air Soil Pollut., 108 (1-2), 83-105 **(23 pages)**.

Filgueiras, A. V.; Lavilla, I.; Bendicho, C., (2004). Evaluation of distribution, mobility and binding behaviour of heavy metals in surficial sediments of Louro river (Galicia, Spain) usingchemometric analysis: A case study. Sci. Total. Environ., 330 (1-3), 115-129 **(15 pages)**.

Fujiyoshi, R.; Okamoto, T.; Katayama, M., (1994). Behavior of radionuclides in the environment . 2. Application of sequential extraction to Zn (II) sorption studies. Appl. Radiat. Isotopes, 45 (2), 165-170 **(6 pages)**.

Gagnon, C.; Turcotte, P.; Vigneault, B., (2009). Comparative study of the fate and mobility of metals discharged in mining and urban effluents using sequential extractions on suspended solids. Environ. Geochem. Health, 31 (6), 657-671 **(15 pages)**.

Galan, E.; Gomez-Ariza, J. L.; Gonzalez, I.; Fernandez-Caliani, J. C.; Morales, E.; Giraldez, I., (2003). Heavy metal partitioning in river sediments severely polluted by acid mine drainage in the Iberian Pyrite Belt. Appl. Geochem., 18 (3), 409-421 **(13 pages)**.

Garnaud, S., (1999). Transfert et évolution géochimique de la pollution métallique en bassin versant urbain. Université Paris XII-Val de Marne, Créteil.

Gromaire-Mertz, M. C.; Garnaud, S.; Gonzalez, A.; Chebbo, G., (1999). Characterisation of urban runoff pollution in Paris. Water Sci. Tech. 39, 1-8 **(8 pages)**.

Hassellov, M.; Von Der Kammer, F., (2008). Iron oxides as geochemical nanovectors for metal transport in soil-river systems. Elements, 4 (6), 401-406 **(6 pages)**.

Heijerick, D. G.; Janssen, C. R.; Karlen, C.; Wallinder, I. O.; Leygraf, C., (2002). Bioavailability of zinc in runoff water from roofing materials. Chemosphere, 47 (10), 1073-1080 **(8 pages)**.

Hnatukova, P.; Benesova, L.; Kominkova, D., (2009). Impact of urban drainage on metal distribution in sediments of urban streams. Water Sci. Tech, 59 (6), 1237-1246 **(10 pages)**.

Hochella, M. F.; White, A. F., (1990). Mineral-water interface geochemistry - an overview. Rev. Mineral. Geochem., 23 (1), 1-16 **(16 pages)**.

Horowitz, A. J.; Meybeck, M.; Idlafkih, Z.; Biger, E., (1999). Variations in trace element geochemistry in the Seine River basin based on floodplain deposits and bed sediments. Hydrol. Process., 13 (9), 1329-1340 **(12 pages)**.

Houhou, J.; Lartiges, B. S.; Hofmann, A.; Frappier, G.; Ghanbaja, J.; Temgoua, A., (2009). Phosphate dynamics in an urban sewer: A case study of Nancy, France. Water Res., 43 (4), 1088-1100 **(13 pages)**.

Igbinosa, E. O.; Okoh, A. I., (2009). Impact of discharge wastewater effluents on the physico-chemical qualities of a receiving watershed in a typical rural community. Int. J. Environ. Sci. Tech., 6 (2), 175-182 (**8 pages**)

Igwe, J. C.; Abia, A. A.; Ibeh, C. A., (2008). Adsorption kinetics and intraparticulate diffusivities of Hg, As and Pb ions on unmodified and thiolated coconut fiber. Int. J. Environ. Sci. Tech, 5 (1), 83-92 (**10 pages**)

Jain, C. K.; Gupta, H.; Chakrapani, G. J., (2008). Enrichment and fractionation of heavy metals in bed sediments of River Narmada, India. Environ. Monit. Assess., 141 (1-3), 35-47 **(13 pages)**.

Jouvin, D.; Louvat, P.; Juillot, F.; Marechal, C. N.; Benedetti, M. F., (2009). Zinc isotopic fractionation: Why organic matters. Environ. Sci. Tech., 43 (15), 5747-5754 **(8 pages)**.

Karbassi, A. R.; Monavari, S. M.; Bidhendi, G. R. N.; Nouri, J.; Nematpour, K., (2008). Metal pollution assessment of sediment and water in the Shur River. Environ. Monit. Assess., 147 (1-3), 107-116 **(10 pages)**.

Larner, B. L.; Palmer, A. S.; Seen, A. J.; Townsend, A. T., (2008). A comparison of an optimised sequential extraction procedure and dilute acid leaching of elements in anoxic sediments, including the effects of oxidation on sediment metal partitioning. Anal. Chem. Acta., 608 (2), 147-157 **(11 pages)**.

Le Cloarec, M. F.; Bonte, P. H.; Lestel, L.; Lefèvre, I.; Ayrault, S., (2009). Sedimentary record of metal contamination in the Seine River during the last century. Phys. Chem. Earth.parts A/B/C.

Lebreton, L.; Thevenot, D. R., (1992). Metal pollution release by road aerosols. Environ. Tech., 13 (1), 35-44 **(10 pages)**.

Lesven, L.; Lourino-Cabana, B.; Billon, G.; Proix, N.; Recourt, P.; Ouddane, B.; Fischer, J.; Boughriet, A., (2009). Water-quality diagnosis and metal distribution in a strongly polluted zone of Deûle River (Northern France). Water. Air. Soil. Pollut., 198 (1), 31-44 **(14 pages)**.

Li, Y.; Wang, X. L.; Huang, G. H.; Zhang, B. Y.;Guo, S. H., (2009). Adsorption of Cu and Zn onto Mn/Fe oxides and organic materials in the extractable fractions of river surficial sediments. Soil Sed. Contam.: Int. J., 18 (1), 87 – 101 **(15 pages)**.

Lin, J. G.; Chen, S. Y., (1998). The relationship between adsorption of heavy metal and organic matter in river sediments. Environ. Int., 24 (3), 345-352 **(8 pages)**.

Luoma, S. N.; Bryan, G. W., (1981). A statistical assessment of the form of trace-metals in oxidized estuarine sediments employing chemical extractants. Sci. Total. Environ., 17 (2), 165-196 **(30 pages)**.

Luoma, S. N.; Rainbow, P. S., (2008). Metal Contamination in Aquatic Environments. Cambridge: Cambridge University Press. 573

Meybeck, A., (2003). Global analysis of river systems: From earth system controls to anthropocene syndromes. Philos Trans R. Soc. Lond. B. Biol. Sci., 358 (1440), 1935-1955 **(21 pages)**.

Meybeck, M.; De Marsily, G.; Fustec, E., (1998). La Seine en Son Bassin: Fonctionnement Ecologique d'un Système Fluvial Anthropisé. Elsevier. 752

Meybeck, M.; Idlafkih, Z.; Fauchon, N.; Andreassian, V., (1999). Spatial and temporal variability of total suspended solids in the Seine basin. Hydrobiologia, 410, 295-306 **(12 pages)**.

Meybeck, M.; Lestel, L.; Bonte, P.; Moilleron, R.; Colin, J. L.; Rousselot, O.; Herve, D.; De Ponteves, C.; Grosbois, C.; Thevenot, D. R., (2007). Historical perspective of heavy metals contamination (Cd, Cr, Cu, Hg, Pb, Zn) in the Seine River basin (France) following a DPSIR approach (1950-2005). Sci. Total. Environ., 375 (1-3), 204-231 **(28 pages)**.

Mohiuddin, K. M.; Zakir, H. M.; Otomo, K.; Sharmin, S.; Shikazono, N., (2010) Geochemical distribution of trace metal pollutants in water and sediments of downstream of an urban river. Int. J. Environ. Sci. Tech , 7 (1), 17-28 (**12 pages**).

Morin, G.; Wang, Y. H.; Ona-Nguema, G.; Juillot, F.; Calas, G.; Menguy, N.; Aubry, E.; Bargar, J. R.; Brown, G. E., (2009). EXAFS and HRTEM evidence for As (III)-containing surface precipitates on nanocrystalline magnetite: Implications for as sequestration. Langmuir, 25 (16), 9119-9128 **(10 pages)**.

Nwuche, C. O.; Ugoji, E. O., (2008). Effects of heavy metal pollution on the soil microbial activity. Int. J. Environ. Sci. Tech , 5 (3), 409-414 (**6 pages**).

Pepe, M.; Gaillard, A.; Harrault, L.; Groleau, A.; Benedetti, M. F., (2008). Les métaux dissous en Seine à paris. Paris.

Pernet-Coudrier, B.; Clouzot, L.; Varrault, G.; Tusseau-Vuillemin, M. H.; Verger, A.; Mouchel, J. M., (2008). Dissolved organic matter from treated effluent of a major wastewater treatment plant: Characterization and influence on copper toxicity. Chemosphere, 73 (4), 593-599 **(8 pages)**.

Reimann, C.; De Caritat, P., (2005). Distinguishing between natural and anthropogenic sources for elements in the environment: Regional geochemical surveys versus enrichment factors. Sci. Total. Environ., 337 (1-3), 91-107 **(17 pages)**.

Robert-Sainte, P.; Gromaire, M. C.; De Gouvello, B.; Saad, M.; Chebbo, G., (2009). Annual metallic flows in roof runoff from different materials: Test-bed scale in Paris conurbation. Environ. Sci. Tech., 43 (15), 5612-5618 **(7 pages)**.

Rocher, V.; Azimi, S.; Moilleron, R.; Chebbo, G., (2004). Hydrocarbons and heavy metals in the different sewer deposits in the 'Le Marais' catchment (Paris, France): Stocks, distributions and origins. Sci. Total Environ., 323 (1-3), 107-122 **(16 pages)**.

Sekabira, K.; Oryem Origa, H.; Basamba, T. A.; Mutumba, G.; E., K., (2010). Assessment of heavy metal pollution in the urban stream sediments and its tributaries. Int. J. Environ. Sci. Tech., 7 (3), 435-446 **(12 pages)**.

Sekabira, K.; Oryem Origa, H.; Basamba, T. A.; Mutumba, G.; E., K., (2010). Heavy metal assessment and water quality values in urban stream and rain water. Int. J. Environ. Sci. Tech., 7 (4), 759-770 (**12 pages**).

Shah, B. A.; Shah, A. V.; Sigh, R. R., (2009). Sorption isotherms and kinetics of chromium uptake from wastewater using natural sorbent material, Int. J. Environ. Sci. Tech., 6 (1) , 77-90 (**14 pages**)

Siaap, (2007). Dossier du maitre d'ouvrage [online]. http://www.debatpublic-station-epuration-seineaval.org/docs/pdf/dossier-mo/doc-synthese-2.pdf.

Stumm, W.; Morgan, J. J., (1981). Aquatic Chemistry, 2ed. Toronto: Wiley-Interscience.780

Sutherland, R.; Tack, F., (2007). Sequential extraction of lead from grain size fractionated river sediments using the optimized BCR procedure. Water Air Soil Pollut., 184 (1), 269-284 **(16 pages)**.

Taconet, J., (1996). Métaux fixés sur les matières en suspension dans le bassin de la Seine : Évolution des teneurs et des mobilités. DEA Sciences et Techniques de l'Environnement. MSc. Thesis Université Paris XII: Val de Marne Créteil.

Taylor, K. G.; Owens, P. N., (2009). Sediments in urban river basins: A review of sediment-contaminant dynamics in an environmental system conditioned by human activities. J. Soils. Sediments, 9 (4), 281-303 **(23 pages)**.

Tessier, L.; Bonté, P., (2002). Suspended sediment transfer in Seine River watershed, France: A strategy using fingerprinting from trace elements. Science for Water Policy: The implications of the Water Framework Directive, Norwich, 79-99 **(21 pages)**.

Thévenot, D.; Meybeck, M.; Lestel, L., (2002). Métaux lords: Des bilans en mutation. Paris.

Thévenot, D. R.; Moilleron, R.; Lestel, L.; Gromaire, M. C.; Rocher, V.; Cambier, P.; Bonté, P.; Colin, J. L.; De Pontevès, C.; Meybeck, M., (2007). Critical budget of metal sources and pathways in the Seine River basin (1994-2003) for Cd, Cr, Cu, Hg, Ni, Pb and Zn. Sci. Total Environ., 375 (1-3), 180-203 **(24 pages)**.

Tongtavee, N.; Shiowatana, J.; Mclaren, R. G., (2005). Fractionation of lead in soils affected by smelter activities using a continuous-flow sequential extraction system. Int. J. Environ. Anal. Chem., 85 (8), 567-583 **(17 pages)**.

Tusseau-Vuillemin, M. H.; Buzier, R.; Meriadec, C. D.; Chardon, I.; Elbaz-Poulichet, F.; Seidel, J. L.; Mouchel, J. M.; Varrault, G., 2005. Du réseau à la rivière et de la Marne à Andrésy : Métaux labiles, dissous et particulaires. Paris.

Tusseau-Vuillemin, M. H.; Gourlay, C.; Lorgeoux, C.; Mouchel, J. M.; Buzier, R.; Gilbin, R.; Seidel, J. L.; Elbaz-Poulichet, F., (2007). Dissolved and bioavailable contaminants in the Seine River basin. Sci. Total Environ., 375 (1-3), 244-256 **(13 pages)**.

USGS, (2010). Aluminum: Statistics and information.

Vieira, J. S.; Botelho, C. L. M. S.;Boaventura, R. A. R., (2009). Trace metal fractionation by the sequential extraction method in sediments from the Lis river (Portugal). Soil Sed. Contam.: Int. J., 18 (1), 102 – 119 **(18 page)**.

Zhu, T.; Li, J.; Jin, Y. Q.; Liang, Y. H.; Ma, G. D., (2009) Gaseous phase benzene decomposition by non-thermal plasma coupled with nano titania catalyst. Int. J. Environ. Sci. Tech, 6 (1),141-148 (**8 pages**).

AUTHOR (S) BIOSKETCHES

Priadi, C., is a PhD scholar in Environmental geosciences at the Laboratoire des Sciences du Climat et de l'Environnement (LSCE/IPSL, CEA-CNRS-UVSQ). Email : *cindy.priadi@lsce.ipsl.fr*

Ayrault, S., is a researcher in trace element environmental cycles at the Laboratoire des Sciences du Climat et de l'Environnement (LSCE/IPSL, CEA-CNRS-UVSQ). Email : *sophie.ayrault@lsce.ipsl.fr*

Pacini, S., (MSc) performed her 3rd year engineering internship at the Laboratoire des Sciences du Climat et de l'Environnement (LSCE/IPSL, CEA-CNRS-UVSQ). Email: *stephanie.pacini@gmail.com*

Bonté, P., is a retired senior scientist in soil erosion and particles transfer in river at the Laboratoire des Sciences du Climat et de l'Environnement (LSCE/IPSL, CEA-CNRS-UVSQ). Email : *bonté@lsce.ipsl.fr*

How to cite this article: (Harvard style)

Priadi, C.; Ayrault, S. ; Pacini, S. ; Bonte, P. (2011). Urbanization impact on metals mobility in riverine suspended sediment: Role of metal oxides. Int. J. Environ. Sci. Tech., 8 (1), 1-18.

Annexe 7

Information supplementaire du chapitre IV

Données du campagne du temps de pluie 2008

	Teneur solide (µg/g)							
type	**nom**	**MES**	**Mg**	**Al**	**K**	**Ca**	**Ti**	**V**
panache	Seine A surface	0,017	9296	38013	9442	12,08	2793	32,6
panache	Seine A bottom	0,019	10313	40247	11531	9,34	2924	<LQ
panache	Seine B surface	0,075	7699	32463	8814	9,59	2693	32,7
panache	Seine B bottom	0,026	7214	32186	9321	12,03	2720	43
panache	Seine C surface	0,007	17515	69059	17783	21,88	4424	36,4
panache	Seine C bottom	0,009	6184	35983	9119	11,48	2559	51,7
panache	Seine D surface	0,01	8344	34261	8950	9,68	2416	29,8
panache	Seine D bottom	0,014	7550	36255	9271	12,02	2702	<LQ
collecteur	coll 1	0,829	5819	15442	4551	7,41	1981	21,7
collecteur	coll 2	0,287	5110	13540	3947	8,41	1871	23,3
collecteur	coll 3	0,158	4476	13641	4150	9,32	2052	24,5
collecteur	coll 4	0,157	4362	12026	4400	7,64	1400	19
collecteur	coll 5	0,201	4626	12517	4980	6,73	2603	20,7
collecteur	coll 6	0,148	5780	9398	3481	6,23	1248	16,1
collecteur	coll 7	0,109	4074	10881	4470	6,18	1781	28,1
collecteur	coll 8	0,111	5292	15855	5251	7,65	2105	22,4
collecteur	coll 9	0,117	5677	17547	5796	8,65	3213	26,6
collecteur	coll 10	0,073	6150	17502	5879	7,58	2528	26
collecteur	coll 11	0,097	6111	17056	5987	8,56	2382	34,9
collecteur	coll 12	0,107	1711	18754	1537	5,69	656	8,1
collecteur	theoritical coll moyen	0,21	8010	16075	5411	7,57	2139	8,7
sediment	Tolbiac270907	NM	3513	30873	8255	15,04	2169	38,9
sediment	Suresnes270907	NM	3954	36144	13745	16,88	2033	37,1
sediment	Sartrouville240708	NM	3541	29358	8659	16,5	2062	36
sediment	SuresnesAmont050809	NM	2630	24885	8203	11,81	1548	27,5
sediment	Colombes050809	NM	4828	31580	7875	15,69	1428	44
sediment	Clichy050809	NM	4023	33906	8553	14,38	2273	47
sediment	Sartrouville030909	NM	3571	30370	8074	14,18	2172	44,9

	Teneur solide (µg/g)							
type	**nom**	**Cr**	**Mn**	**Fe**	**Co**	**Ni**	**Cu**	**Zn**
panache	Seine A surface	74	746	41700	10,8	18	280	863
panache	Seine A bottom	61	939	47800	11,5	0	254	1080
panache	Seine B surface	96	500	38700	9,5	25	300	4319
panache	Seine B bottom	77	539	40100	10,1	21	363	1914
panache	Seine C surface	58	599	68600	8,8	10	151	708
panache	Seine C bottom	70	665	39700	11,1	24	199	916
panache	Seine D surface	69	773	39600	2,4	19	205	1163
panache	Seine D bottom	96	762	41500	11,6	9	264	1206
collecteur	coll 1	91	213	20900	6,6	20	507	2308
collecteur	coll 2	70	262	28600	6,9	25	382	3245
collecteur	coll 3	79	269	29800	8,7	19	341	3856
collecteur	coll 4	46	209	25100	6,6	16	372	2707
collecteur	coll 5	47	202	35100	7,1	18	440	3392
collecteur	coll 6	39	183	22400	5,2	22	1353	3033
collecteur	coll 7	54	195	25600	5,6	17	355	3614
collecteur	coll 8	80	258	30100	7,5	25	694	4256
collecteur	coll 9	77	295	32500	8,6	23	495	3649
collecteur	coll 10	87	290	30700	8,3	28	512	3959
collecteur	coll 11	63	278	29400	7,9	21	544	1204
collecteur	coll 12	86	102	14600	7	17	515	2920
collecteur	theoritical coll moyen	74	246	26000	7,6	27	533	4091
sediment	Tolbiac270907	58,7	487	20100	7,23	22,6	76,9	299
sediment	Suresnes270907	51,2	426	20100	8,29	23,2	61,8	290
sediment	Sartrouville240708	58,7	439	19400	7,21	23,6	78	312
sediment	SuresnesAmont050809	37,8	374	15400	6,59	18,6	51,1	198
sediment	Colombes050809	109,9	401	19100	9,76	40,3	181,7	654
sediment	Clichy050809	62,1	390	21900	8,39	25,1	77,3	293
sediment	Sartrouville030909	69,7	385	21100	7,86	25,6	88,8	401

	Teneur solide (µg/g)							
type	**nom**	**Ag**	**Cd**	**Sb**	**Ba**	**Tl**	**Pb**	**COP**
panache	Seine A surface	3,94	2,73	13,71	363	0,8	226	20,93
panache	Seine A bottom	4,97	3,47	8,22	309	0,9	200	12,02
panache	Seine B surface	19,23	3,67	22,08	391	0,6	316	14,96
panache	Seine B bottom	9,35	3,92	14,18	433	0,7	407	19,7
panache	Seine C surface	4,24	1,99	5,81	675	0,6	175	20,64
panache	Seine C bottom	5,27	2,62	7,25	341	0,8	223	19,54
panache	Seine D surface	6,76	3,9	6,56	353	0,7	238	17,46
panache	Seine D bottom	6,73	3,5	12,99	338	0,7	261	16,78
collecteur	coll 1	18,78	3,59	10,22	470	0,5	461	41,85
collecteur	coll 2	9,76	2,57	8,93	1507	0,4	560	25,4
collecteur	coll 3	7,81	3,5	12,39	864	0,4	801	17,72
collecteur	coll 4	4,92	2,92	9,84	361	0,4	452	25,26
collecteur	coll 5	9,98	5,43	9,85	691	0,4	515	24,81
collecteur	coll 6	6,47	2,93	7,36	388	0,3	566	24,58
collecteur	coll 7	8,97	3,39	12,63	716	0,4	478	28,37
collecteur	coll 8	14,85	5,51	20,14	587	0,4	948	27,78
collecteur	coll 9	8,61	5,55	18,54	593	0,4	588	28,29
collecteur	coll 10	19,87	5,01	17,48	574	0,4	684	27,64
collecteur	coll 11	4,81	5,15	9,98	520	0,4	656	32,2
collecteur	coll 12	12,3	3,15	12,31	476	0,2	605	39,05
collecteur	theoritical coll moyen	12,82	4,68	16,14	500	0,5	717	26,71
sediment	Tolbiac270907	2,3	1,54	2,11	319	0,46	99,7	NM
sediment	Suresnes270907	1,57	1,14	1,67	306	0,711	75,2	3,27
sediment	Sartrouville240708	2,51	2,21	1,39	321	0,582	93,8	4,02
sediment	SuresnesAmont050809	0,87	0,7	0,98	281	0,478	74	2,42
sediment	Colombes050809	13,08	7,38	0,67	495	0,586	281,7	3,96
sediment	Clichy050809	1,78	1,06	1,62	299	0,553	95,5	4,34
sediment	Sartrouville030909	2,89	2,76	1,58	328	0,614	108,5	5,75

Annexe 8

Information supplementaire du chapitre IV

Langage de R utilisée dans la modélisation de trois sources

S1 – Least Square Fitting programming language used in R statistical computing to quantify contribution of CSO, the Seine River and the bed sediment in overflow plume

µ

```
refcoll = subset(toto.nom=="calculated coll moyen")

refsed = subset(toto.type=="bed sediment")
refsed = rbind(refsed.0)
refsed$nom=as.character(refsed$nom)
refsed$nom[7]="moyen"
refsed$type[7]="sediment"
for (i in 3:27)
  {refsed[[i]][7] = mean(refsed[[i]][1:6].na.rm=TRUE)}
refsed = subset(refsed.nom=="moyen")

refriver = subset(toto.type=="river pre-CSO")

# Calcul des r√©f√©rences rapport√©es √† l'aluminium

refcollAl = refcoll[3:27]
refcollAl = refcollAl/as.numeric(refcollAl[3])

refsedAl = refsed[3:27]
refsedAl = refsedAl/as.numeric(refsedAl[3])

refriverAl = refriver[3:27]
refriverAl = refriverAl/as.numeric(refriverAl[3])

# Un exemple de d√©finition des poids de diff√©rents √©l√©ments
# pour l'estimation de la r√©partition

poids = refriverAl
poids[1:25] = 0
poids$Mg = 1
poids$K = 1
poids$Ca = 1
poids$Ti = 1
poids$Fe = 1
poids$COP = 1

objo = function(x.data.poids=poids)
  {
    coriv = x[1]
    cocoll = x[2]
    cosed = 1
    total = coriv+cocoll+cosed
    coriv = coriv/total
    cocoll = cocoll/total
    cosed = cosed/total
    expected =as.numeric(refriverAl)*coriv+
      as.numeric(refsedAl)*cosed+
      as.numeric(refcollAl)*cocoll
    dataAl = data[3:27]
```

```
    dataAl = dataAl/as.numeric(dataAl[3])
    distance = ((expected-as.numeric(dataAl))/as.numeric(dataAl))^2*poids
    distance = sum(distance[poids!=0])
    objo = distance
  }

objo2 = function(x.data.poids=poids)
  {
    alpha = x[1]
    beta = x[2]
    gamma = x[3]
    expected = as.numeric(refcoll)*alpha +
      (as.numeric(refriver)*beta+
      as.numeric(refsed)*(1-beta))*gamma
    distance                                =                                ((expected[3:27]-
as.numeric(data[3:27]))/as.numeric(data[3:27]))^2*poids
    distance = sum(distance[poids!=0])
    objo2 = distance
  }

datapanache = subset(toto.type=="CSO plume")


calcule.repartition2 = function(poids=poids)
  {
# Initialisation de results
    results = subset(datapanache.select=nom)
    results$riv=0
    results$coll=0
    results$sed=0
    results$conv=0
    results$objo=0
    nam = names(datapanache)
    for (j in 3:27)
      {
        results[nam[j]]=0
      }

# Boucle de calcul sur toutes les lignes de datapanache
    for (i in 1:8)
      {
        initial = c(0.5.0.5.1)
        uu = nlminb(initial.objo2.lower=c(0.0.0.1).upper=c(1.1.10).
          poids=poids.
          data=subset(datapanache.as.numeric(rownames(datapanache))==i))
        alpha = uu$par[1]
        beta = uu$par[2]
        gamma = uu$par[3]
        results$riv[i] = gamma*beta
        results$coll[i] = alpha
        results$sed[i] = gamma*(1-beta)
        results$conv[i] = uu$convergence
```

```
        results$objo[i] = uu$objective
        for (j in 3:27)
          {
            bip=nam[j]
            results[bip][i.] = refcoll[bip][1]*alpha +
              (refriver[bip][1]*beta +
               refsed[bip][1]*(1-beta))*gamma
          }
      }
    results
  }


# Graphe des rapports/Al. des estim√©s versus mesur√©s dans le panache


drawres2 = function(results)
  {
    nam = names(datapanache)
    for (j in 4:27)
      {
        y = results[[nam[j]]]
# pour √©viter des graphes avec des NA
        if (prod(is.na(y)) == 0)
          {
            x = as.vector(datapanache[[nam[j]]])
            plot(y.x.
                 ylab=paste(nam[j]." dans le panache").
                 xlab=paste(nam[j]." estim√©").
                 xlim=range(c(0.x.y)).ylim=range(c(0.x.y)))
            mm = max(range(0.x.y))
            lines(c(0.mm).c(0.mm))
            locator(type="o")
          }
      }
  }
```

Annexe 9

Information supplementaire du chapitre IV

Sortie du model de trois sources

nom	riv	coll	sed	conv	objo	Mg / Al	Al / Al	K / Al
Seine A surf	0.438	0.045	0.516	0.000	0.522	0.15115	1	0.25627
Seine A fond	0.741	0.015	0.243	0.000	0.383	0.15649	1	0.22879
Seine B surf	0.258	0.132	0.609	0.000	0.722	0.16617	1	0.27588
Seine B fond	0.231	0.210	0.559	0.000	0.578	0.18539	1	0.28192
Seine C surf	0.000	0.000	1.000	0.000	2.145	0.12003	1	0.29184
Seine C fond	0.393	0.054	0.553	0.000	0.551	0.15135	1	0.26053
Seine D surf	0.000	0.000	1.000	0.000	9.824	0.12003	1	0.29184
Seine D fond	0.496	0.078	0.426	0.000	0.367	0.1622	1	0.25285

nom	Ca / Al	Ti / Al	Cr / Al	Mn / Al	Fe / Al	Co / Al	Ni / Al	COP / Al
Seine A surf	0.0004	0.06708	0.00219	0.024749	7.24E-05	0.0003	0.000817	0.00021
Seine A fond	0.0003	0.06463	0.00212	0.032373	6.99E-05	0.00032	0.000768	0.00026
Seine B surf	0.00044	0.07443	0.00242	0.020479	8.39E-05	0.00031	0.000895	0.00018
Seine B fond	0.00045	0.08104	0.00263	0.020073	9.49E-05	0.00033	0.000953	0.00018
Seine C surf	0.00048	0.06303	0.00206	0.013366	6.31E-05	0.00025	0.000824	0.00013
Seine C fond	0.00041	0.06776	0.00221	0.02363	7.33E-05	0.0003	0.000827	0.0002
Seine D surf	0.00048	0.06303	0.00206	0.013366	6.31E-05	0.00025	0.000824	0.00013
Seine D fond	0.00039	0.06987	0.00228	0.026343	7.74E-05	0.00032	0.000835	0.00022

nom	Cu / Al	Zn / Al	Ag / Al	Cd / Al	Sb / Al	Ba / Al	Tl / Al	Pb / Al
Seine A surf	0.00451	0.0217	0.00014	8.41E-05	6.10E-05	0.01065	1.68E-05	0.00585
Seine A fond	0.00337	0.01464	0.00012	7.56E-05	2.02E-05	0.00808	1.51E-05	0.00478
Seine B surf	0.00778	0.04198	0.00019	1.04E-04	1.43E-04	0.01497	1.85E-05	0.00929
Seine B fond	0.01069	0.06003	0.00024	1.20E-04	2.09E-04	0.01821	1.94E-05	0.01241
Seine C surf	0.00284	0.01127	0.00012	7.73E-05	4.62E-05	0.01082	1.83E-05	0.00382
Seine C fond	0.00482	0.02363	0.00014	8.61E-05	7.02E-05	0.01119	1.71E-05	0.00617
Seine D surf	0.00284	0.01127	0.00012	7.73E-05	4.62E-05	0.01082	1.83E-05	0.00382
Seine D fond	0.00572	0.02923	0.00016	9.06E-05	8.50E-05	0.0117	1.68E-05	0.00719

Annexe 10

Information supplementaire du Chapitre V

Spectres d'EXAFS et calcul de fit du premier voisin des matières en suspension collectées dans le trappe à sédiment en Décembre 2008 et Juin 2009

Supporting Information

EXAFS and SEM evidence for zinc sulfide solid phases in suspended matter from the Seine River, France

Cindy Priadi[1], Guillaume Morin[2] *, Sophie Ayrault[1], Fabien Maillot[2], Farid Juillot[2], Isabelle Llorens[3], Denis Testemale[4], Olivier Proux[5], Gordon E. Brown Jr[6,7].

[1]Laboratoire des Sciences du Climat et de l'Environnement (LSCE/IPSL), UMR 1572 (CEA/CNRS/UVSQ), Domaine du CNRS, Avenue de la Terrasse, bat 12, 91198 Gif-sur-Yvette, France

[2] *Institut de Minéralogie et de Physique des Milieux Condensés (IMPMC), UMR 7590, CNRS, UPMC – Université Paris 7 - IPGP, case 115, 4 Place Jussieu, 75252 Paris, Cedex 05, France.

[3] CEA INAC/SP2M/NRS, 17 rue des Martyrs, 38054 Grenoble Cedex 9, France.

[4]Institut Néel MCMF, CNRS, 38042, Grenoble France.

[5]Observatoire des Sciences de l'Univers de Grenoble, LGIT, BP 53, 38041 Grenoble, Cedex 9, France.

[6]Surface & Aqueous Geochemistry Group, Department of Geological and Environmental Sciences, Stanford University, Stanford, CA, 94305-2115, USA.

[7]Stanford Synchrotron Radiation Lightsource, SLAC National Accelerator Laboratory, 2575 Sand Hill Road, MS 69, Menlo Park, CA, 94025, USA.

EXAFS data and first neighbor fits of samples whose SEM images are shown in **Figure SI2**. Samples consisted of sediments collected in a sediment trap in December 2008 and June 2009 which were dried under an inert N_2 atmosphere (complete procedure of sampling procedure and sample treatment are reported in (*23*).

Figure S1. Zn-K edge EXAFS of sediment from the Seine River collected in sediment trap in December 2008 and in June 2009, and dried under inert N_2 atmosphere. Left : Experimental unfiltered $k^3\chi(k)$ data (solid lines). Right : Fourier-filtered experimental data (dotted lines) within the 0.6-2.4 Å *R*-range were fit *k*-space (solid lines). Middle : Corresponding Fourier transforms are reported. Model compounds data are presented for comparison and include : amorphous ZnS, crystalline ZnS (sphalerite), both with Zn four-fold coordinated to sulfur, and Zn/Al LDH with Zn six-fold coordinated to oxygen.

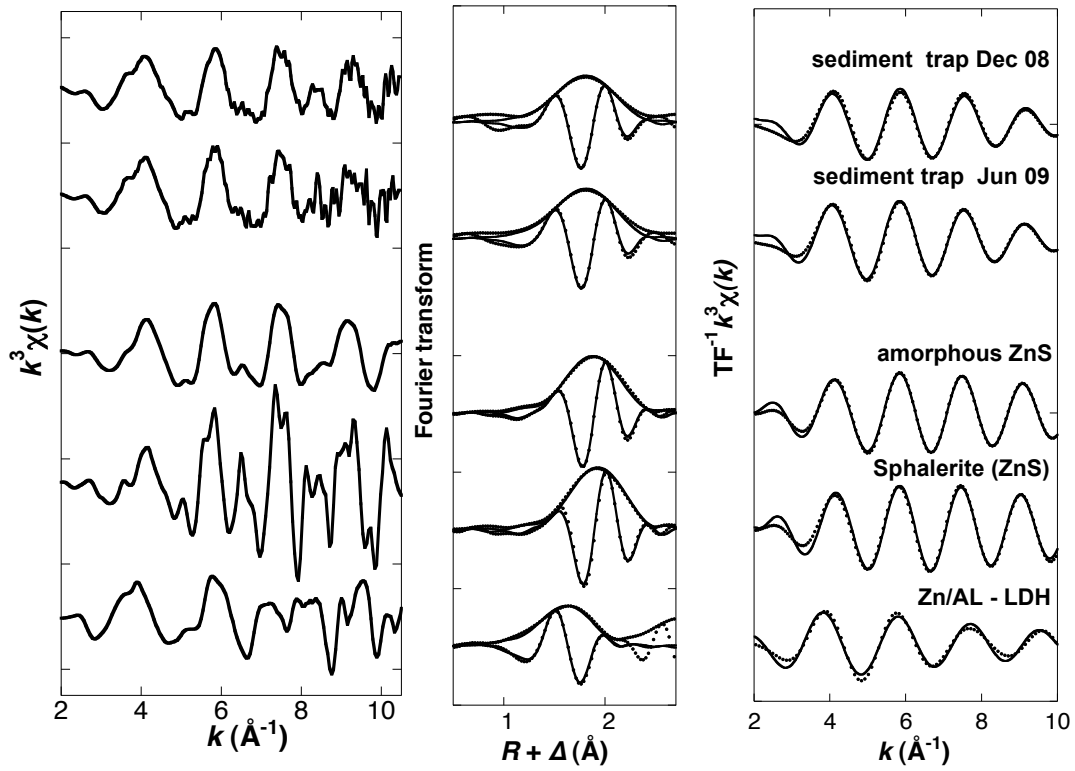

Table S1. Fitting results for the Fourier Filtered $k^3c(k)$ first coordination shell. Standard deviations on the interatomic distances R(Å) were estimated to ±0.05Å from the fit of the model compounds by varying the energy shift ΔE0(eV) of ±3eV. Other fitting parameters are *N*: number of neighbors, σ(Å): Debye-Waller parameter, and χ^2 FT : goodness of fit (see text).

	Zn-O			Zn-S				
	R(Å)	*N*	σ(Å)	*R*(Å)	N	σ(Å)	ΔE0(eV)	χ^2 FT
Sediment trap Dec 2008 N_2 dried	2.07	1.7	0.06	2.35	1.9	0.07	10.3	0.89
Sediment trap June 2009 N_2 dried	2.06	1.8	0.07	2.34	2.5	0.08	9.1	1.00
Amorphous ZnS	-	-		2.34	7.3	0.09	10.6	0.04
Sphalerite (ZnS)	-	-		2.35	3.8	0.07	10.5	0.01
Zn-LDH	2.07	4.2	0.07	-	-	-	6.5	0.30